The Development of Pulsed Dendritic Cell Therapeutic Vaccine Strategies for the Treatment of Paediatric Solid Tumours and Leukaemias

Stephen Ralph Nabarro
Ph.D. Child Health
Institute of Child Health, University College London

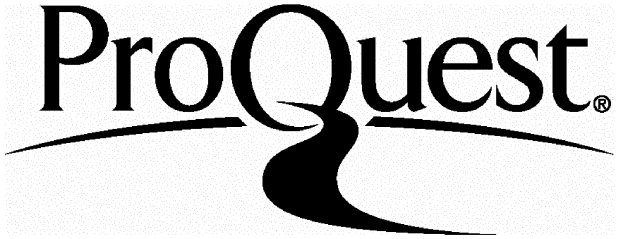

Thesis Abstract

Anti-tumour immune responses are a balance between host immunosurveillance and immune escape mechanisms developed by the tumour. In this thesis, I have attempted to explore the nature of this balance in two cancer types, which are potentially susceptible to immune attack, in order to develop immunotherapeutic strategies for the treatment of these disorders.

Alveolar rhabdomyosarcoma (ARMS) is an aggressive paediatric solid tumour associated with the translocation t(2;13)(q35;q14). The resultant PAX3-FKHR fusion protein is a desirable target antigen for directed anti-tumour immunotherapy. We have explored the use of dendritic cells (DCs) loaded with PAX3-FKHR antigen as a cellular vaccine for the treatment of ARMS patients. We developed a murine ARMS model by stably transfecting a mouse rhabdomyosarcoma cell line (76-9) with *PAX3-FKHR* cDNA (clones called C23 and C24). We found that immunisation with C23 tumour lysate-pulsed DCs or non-pulsed DCs protected C57BL/6 mice from a subsequent C23 tumour challenge. The small tumours that did form in DC-immunised mice were shown to contain large numbers of infiltrating $CD8^+$ and $CD4^+$ T lymphocytes. However, ELISpot assays revealed that the DC vaccines were unable to initiate PAX3-FKHR-specific immune responses. We identified one peptide, derived from the N-terminal PAX3 portion of PAX3-FKHR, that binds with intermediate affinity to human leukocyte antigen (HLA)-A*0201, and could be loaded onto DCs as an alternative immunotherapeutic approach. In another project, we attempted to identify the target genes of PAX3-FKHR by comparing the global mRNA profile of C23 and C24 cells with empty vector transfected 76-9 cells, using oligonucleotide microarray expression profiling. We found that PAX3-FKHR up-regulated 31 genes and down-regulated 69 genes, by more than 2 fold. Interestingly, a large proportion of the genes repressed by PAX3-FKHR are known to be stimulated by interferon (IFN)-γ (21 out of the 44 genes with known function), including the major histocompatability complex (MHC) class I genes *H2-K* and *H2-D1*, and plasminogen activator inhibitor-1. Results from flow cytometric and Western blot analyses suggest that PAX3-FKHR exerts some of its effect on the ARMS phenotype, including the down-regulation of MHC class I which might act as an immune escape mechanism, by negatively interfering with IFN-γ signalling.

In a separate study using patient blood samples, we assessed the feasibility of developing an immunotherapeutic strategy for the treatment of juvenile myelomonocytic leukaemia (JMML). Using granulocyte macrophage-colony stimulating factor and interleukin-4, we successfully differentiated JMML cells *in vitro* into immunostimulatory DCs. A cytotoxicity assay revealed that the leukaemic DCs were able to activate allogeneic T lymphocytes that specifically lysed leukaemic targets. Our novel findings suggest that JMML-derived DCs could be used for the *in vivo* or *ex vivo* generation of anti-leukaemia immune responses.

Our findings suggest that DC-based immunotherapeutic approaches can be used to manipulate the balance between host immunosurveillance and tumour immune escape, resulting in effective anti-tumour immunity.

Table of Contents

Acknowledgements

During the course of my PhD I have received assistance and advice from numerous people. Firstly, I need to thank my principal supervisor John Anderson for all his help. John was always available to teach me new laboratory techniques and to discuss my work. I am also grateful for his assistance performing animal experiments, where four pairs of hands were often needed. Finally, I have to thank John for letting me win our ski race in Lake Louise. My secondary supervisor Adrian Thrasher was a great source of ideas and was always able to answer my questions on the immunological aspects of the projects.

I need to thank the juvenile myelomonocytic leukaemia patients and healthy donors who provided blood samples, as well as Dr P. Veys, Dr D. Webb, Netty Hewitt and Helen Rees for sample collection. Persis Amrolia kindly taught me how to expand cytotoxic T lymphocytes *in vitro*, while Helena Kempski guided me through the flourescence *in situ* hybridisation experimental procedure.

I am grateful to Antigoni Papanastasiou for all her help in the laboratory. Additionally, she has now taken over the microarray project (Chapter 2), and is performing the experiments required to enable us to publish the work. I also have to thank Jo Buddle for all her assistance with designing and performing FACS analyses. Danielle Fletcher kindly aided me with the microarray experiments and analyses. I am also indebted to Sofia DeNoronha and Siobhan Burns, who showed me how to culture mouse and human dendritic cells, respectively. Katy Newton taught me how to use the enzyme-linked immunospot plate reader and BioSys analysis software. Finally, I need to thank numerous work colleagues and my football teammates for being good drinking partners, and my girlfriend Alaine for keeping me sane.

This work was supported by the Research into Childhood Cancer (RICC), Gibraltar, and REACH (fund for research and education to advance the understanding of cancer and haematological disorders in childhood).

List of Abbreviations

AD: Activation domain.
ALL: Acute lymphoblastic leukaemia.
AML: Acute myeloid leukaemia.
ATRA: All-trans-Retinoic acid.
ARMS: Alveolar rhabdomyosarcoma.
ADCC: Antibody-dependent cellular cytotoxicity.
APC: Antigen presenting cell.
5-Aza dC: 5-Aza-2'-deoxycytidine.
BCG: Bacillus Calmette Guerin.
β-gal: Beta-galactosidase.
BMT: Bone marrow transplantation.
BSA: Bovine serum albumin.
CD40L: CD40 ligand.
CRABP: Cellular retinoic acid binding protein.
CEF: Chicken embryo fibroblast.
CAT: Chloramphenicol acetyl transferase.
CML: Chronic myeloid leukaemia.
COL: Collagen.
CLP: Common lymphoid progenitor.
CMP: Common myeloid progenitor.
HF1: Complement factor H.
CXCR4: CXC chemokine receptor 4.
CASTing: Cyclic amplification and selection of targets.
CpG ODN: Cytosine-guanosine-dinucleotide-containing oligonucleotides.
CMV: Cytomegalovirus.
CTL: Cytotoxic T lymphocyte.
CTLA4: Cytotoxic T lymphocyte antigen 4.
DBE: DAF-16 family protein-binding element.
DTH: Delayed-type hypersensitivity.
DC: Dendritic cell.
AdDC: Dendritic cell transfected with an adenoviral vector.
DMSO: Dimethyl sulphoxide.
DTT: Dithiothreitol.
DLI: Donor lymphocyte infusion.
DMEM: Dulbecco's Modified Eagle's Medium.
EMSA: Electrophoretic mobility shift assay.
ERMS: Embryonal rhabdomyosarcoma.
ERV: endogenous retrovirus.
ER: Endoplasmic reticulum.
ELISA: Enzyme-linked immunosorbent assay.
ELISpot: Enzyme-linked immunospot.
EST: Expressed sequence tag.
ECM: Extra cellular matrix.
FCS: Fetal calf serum.
FMP: Flu matrix peptide.
FACS: Fluorescence activated cell sorter.
FISH: Fluorescence *in situ* hybridisation.
FITC: Fluoroscein isothiocyanate.
FKHR: Forkhead.
FD: Forkhead DNA-binding domain.
FSC: Forwards scatter.
GVL: Graft versus leukaemia.
GVHD: Graft-versus-host disease.
GM-CSF: Granulocyte macrophage-colony stimulating factor.
GFP: Green fluorescent protein.
GTP: Guanosine triphosphate.
HBSS: Hank's balanced salt solution.
HA: Hemagglutinin.
HGF/SF: Hepatocyte growth factor/scatter factor.
HD: Homeodomain.
HRP: Horse radish peroxidase.
Her2: Human epidermal growth factor receptor 2.
HLA: Human leukocyte antigen.
IVT: *In vitro* transcription-translation.
IGF: Insulin like growth factor.
IGFBP: insulin like growth factor binding protein.
IFN: Interferon.
IL: Interleukin.
JAK: Janus tyrosine kinase.
JMML: Juvenile myelomonocytic leukaemia.
KLH: Keyhole limpet haemocyanin.
KIR: Killer-cell immunoglobulin-like receptor.
LDH: Lactate dehydrogenase.
Lin 1: Lineage cocktail 1.
LPS: Lipopolysaccharide.
LOI: Loss of imprinting.
LB: Luria-Bertani.
MHC: Major histocompatability complex.

MFI: Mean fluorescence intensity.
MIC: MHC class I polypeptide-related.
MITF: Microphthalmia-associated transcription factor.
mHag: Minor histocompatability antigen
MAPK: Mitogen-activated protein kinase.
MoDC: Monocyte-derived dendritic cell.
MPD: Myeloproliferative disorder.
MTS: 3-(4,5-dimethylthiazol-2-yl)-5-(3-carboxymethoxyphenyl)-2-(4-sulfophenyl)-2H-tetrazolium.
MYOG: Myogenin.
NCBI: National Center for Biotechnology Information.
NK cell: Natural killer cell.
NKT cell: Natural killer T cell.
NCAM: Neural cell adhesion molecule.
NF1: Neurofibromatosis type 1.
OTT (gene name): Ovary testis described.
PB: Paired box.
PFA: Paraformaldehyde.
PAMP: Pathogen-associated molecular pattern.
PRR: Pattern recognition receptor.
PerCP: Peridinin chlorophyll protein.
PBMCs: Peripheral blood mononuclear cells.
PMS: Phenazine methosulfate.
Ph^+: Philadelphia chromosome positive.
PBS: Phosphate buffered saline.
PI3K: Phosphatidylinositol 3'-kinase.
PLA2: Phospholipase A2.
PE: Phycoerythrin.
PAI-1: Plasminogen activator inhibitor-1.
PDGFαR: Platelet-derived growth factor alpha receptor.
TERT: Polypeptide component of telomerase.
PI: Propidium iodide.
PSA: Prostate-specific antigen.
RhuGM-CSF: Recombinant human GM-CSF.
RA: Retinoic acid.
RT-PCR: Reverse transcription-polymerase chain reaction.
RMS: Rhabdomyosarcoma.
RPMI: Roswell Park Memorial Institute.
SEREX: Serological identification of antigens by recombinant expression cloning.
SSC: Side scatter.
STAT: Signal transducers and activators of transcription.
S.D.: Standard deviation.
S.E.M.: Standard error of the mean.
SDF-1: Stromal-derived factor-1.
TCR: T cell receptor.
TPA: 12-O-tetradecanoyl phorbol-13-acetate.
Th cell: T helper cell.
TLC: Thin layer chromatography.
TLR: Toll-like receptor.
TAP: Transporter associated with antigen processing.
TC: Tri-colour.
TEA: Tris acetate EDTA.
TGF: Tumour growth factor.
TIL: Tumour infiltrating lymphocyte.
TNF: Tumour necrosis factor.
TRAIL: Tumour necrosis factor-related apoptosis-inducing ligand.
TRP-1: tyrosinase-related protein-1.
uPA: Urokinase-type plasminogen activator.
VEGF: Vascular endothelial growth factor.
WS: Waardenburg syndrome.
XMR (gene name): Xlr-related, meiosis regulated.

List of Figures

the myogenic-specific *c-MET* promoter in the 76-9-derived cell lines. **B** Transactivation of the *MITF* promoter in 76-9-derived cell lines.

- **Table 3. Genes significantly up-regulated more than 2 fold by PAX3-FKHR.**
- **Table 4. Genes significantly down-regulated more than 2 fold by PAX3-FKHR.**
- **Figure 11. RT-PCR showing the expression of *PAX3-FKHR* mRNA in 76-9 cells stably transfected with pBK-CMV-P3F.**
- **Figure 12. Northern blot analysis to verify the microarray results.**
- **Figure 13. Northern blot analysis to examine the expression of *PAX3*, *PAX3-FKHR*, and two PAX3-FKHR target genes in several human RMS cell lines.**
- **Figure 14. Sensitivity of 76-9 cells expressing empty vector (CMV) and PAX3-FKHR (C23) to ATRA-induced cell death. A** Viability of CMV and C23 cells cultured in the presence of 1×10^{-5}M and 1×10^{-4}M ATRA for up to 72 hours. **B** Viability of CMV and C23 cells cultured for 24 hours in the presence of $1\text{-}8\times10^{-5}$M ATRA.
- **Figure 15. A** PAX3-FKHR down-regulates H2-D^b and H2-K^b expression on the surface of the mouse RMS 76-9 cell line. **B** MHC class I expression in several human RMS cell lines.
- **Figure 16. PAX3-FKHR protein function in RD-derived cell lines.**
- **Figure 17. MHC class I expression on the surface of RD-derived cell lines. A** PAX3-FKHR down-regulates MHC class I expression in the human ERMS cell line RD. **B** PAX3-FKHR causes a partial block in IFN-γ induced up-regulation of MHC class I. **C** Comparison of MHC class I expression on RD empty cells and RDP3F#6 cells when both cell lines are cultured in the presence of 20ng/ml IFN-γ for 48 hours.
- **Figure 18. Expression of PAI-1 in human RMS cell lines. A** Western blot analysis examining PAI-1 protein expression in several human RMS cell lines. **B** Western blot analysis examining PAI-1 protein expression in RD cells stably transfected with pBK-CMV empty vector (RD Empty) and pBK-CMV-P3F (termed RDP3F).
- **Figure 19. Western blot analysis revealing that PAX3-FKHR renders RD cells partially unresponsive to IFN-γ induced up-regulation of PAI-1.**
- **Figure 20. Effect of TPA on the viability of RD-derived cell lines. A** Schematic summarising the putative effect of TPA on RD cells. **B** Comparative *in vitro* proliferation assay, examining TPA-induced growth arrest in RD cells.
- **Figure 21. PAX3-FKHR up-regulates CXCR4 expression in human RMS cell lines.**
- **Figure 22. Western blot analysis examining the effect of AG490 treatment on PAI-1 levels in RD-derived cell lines.**
- **Figure 23. PAX3-FKHR does not down-regulate BIM expression in RD cells. A** Western blot analysis showing BIM protein levels in RD Empty and RDP3F cells, following treatment with 20ng/ml IFN-γ and diluted PBS (delivery vehicle for IFN-γ) for 48 hours. **B** Bar graph showing the normalised levels of BIM protein in the Western blot depicted in A. **C** Luciferase assay measuring the activation of BIM-luciferase and mutant BIM-luciferase reporter genes in transiently transfected RD-derived cell lines.
- **Figure 24. Luciferase assay demonstrating that PAX3-FKHR does not effect the level of *IGFBP-1* promoter activation in RD cells.**
- **Figure 25. Levels of phospho-Akt in RD-derived cell lines. A** A potential pathway for PAX3-FKHR-mediated down-regulation of PAI-1. **B** Western blot analysis of phospho-Akt expression in wild type RD, RD transfected with empty vector, and 4 clones of RD transfected with PAX3-FKHR.

4. Discussion

- **Figure 26. The anti-tumourigenic and pro-tumourigenic effects of PAI-1.**

Appendices

- **Appendix Table 1. The complete list of 35 sequences (derived from 31 different genes) significantly up-regulated by more than 2 fold in C23 and C24 cells relative to CMV.**
- **Appendix Table 2. The complete list of 69 sequences significantly down-regulated by more than 2 fold in C23 and C24 cells relative to CMV.**

Chapter 3:
The Use of Pulsed Dendritic Cell Vaccine Strategies to Target PAX3-FKHR-Expressing Alveolar Rhabdomyosarcoma Cells

1. Introduction

- **Figure 1. Use of pulsed DC vaccines for the induction of anti-tumour immunity.**

3. Results

- **Figure 2. Immunophenotype of a representative DC culture.**
- **Figure 3. Immunisation with C23 lysate-pulsed DCs or non-pulsed DCs protects C57BL/6 mice from a subsequent C23 tumour challenge.** **A** Schematic of the experimental plan. **B** Tumour volumes following C23 tumour challenge. **C** Survival curve analysis of data from B.
- **Figure 4. ELISpot assay measuring IFN-γ secretion by splenic T lymphocytes cultured *in vitro* in the presence or absence of KLH.**
- **Figure 5. IFN-γ secretion by splenic T lymphocytes cultured *in vitro* with CMV (PAX3-FKHR^{-ve}) or C23 (PAX3-FKHR^{+ve}) RMS target cells.**
- **Figure 6. Immunisation with C23 lysate-pulsed DCs protects mice from a subsequent challenge with C23 or CMV RMS cells.** **A** Schematic of the experimental plan. **B** Tumour volumes following C23 or CMV tumour challenge. **C** Combined data from two DC vaccine experiments (marked *3.1.3.* and *3.1.4.*).
- **Figure 7. Flow cytometric analysis of tumour infiltrating lymphocytes (from the pulsed DC vaccine experiment marked *3.1.4.*).** **A** Size and granulatiry of splenocytes, C23 cells and disaggregated tumour cells isolated from a DC-immunised mouse. **B** The immunophenotype of lymphocytes isolated from a representative small, hard, fibrous tumour excised from C57BL/6 mice immunised with C23 lysate-pulsed DCs or non-pulsed DCs. **C** The immunophenotype of cells with a FSC and SSC typical of lymphocytes, isolated from a representative large, soft tumour excised from a C57BL/6 mouse that received the C23 challenge alone.
- **Figure 8. Flow cytometric analysis of tumour infiltrating lymphocytes (from the pulsed DC vaccine experiment marked *3.1.4.*).**
- **Figure 9. IFN-γ secretion by splenic T cells cultured *in vitro* with CMV (PAX3-FKHR^{-ve}) or C23 (PAX3-FKHR^{+ve}) RMS target cells.**
- **Figure 10. Immunisation with C23 lysate-pulsed DCs or non-pulsed DCs protects beige C57BL/6 mice from a subsequent C23 tumour challenge.** **A** Schematic of the experimental plan. **B** C23 tumour lysate-pulsed DC vaccine experiment in beige C57BL/6 mice. **C** Comparing the tumour volumes in wild type C57BL/6 mice and beige C57BL/6 mice that received the C23 challenge alone.
- **Figure 11. Flow cytometric analysis of tumour infiltrating lymphocytes from NK-deficient beige C57BL/6 mice (pulsed DC experiment marked *3.1.5.*).**
- **Figure 12. IFN-γ secretion of beige mouse splenocytes cultured *in vitro* with CMV (PAX3-FKHR^{-ve}) or C23 (PAX3-FKHR^{+ve}) RMS target cells.**
- **Table 1. Screening the PAX3 amino acid sequence present in mixed murine/human PAX3-FKHR for the presence of potential H2-K^b and H2-D^b**

binding motifs. A Theoretical H2-K^b binding peptide sequences derived from the N-terminal PAX3 region of the synthetic mixed murine/human PAX3-FKHR protein. **B** Theoretical H2-D^b binding peptide sequences derived from the N-terminal PAX3 region of the synthetic mixed murine/human PAX3-FKHR protein.

- **Figure 13. Mouse RMA-S peptide binding assays. A** Binding of peptides derived from mixed murine/human PAX3-FKHR protein to mouse H2-K^b. **B** Binding of peptides derived from mixed murine/human PAX3-FKHR protein to mouse H2-D^b.
- **Table 2. Screening the human PAX3-FKHR amino acid sequence for the presence of potential HLA-A*0201 binding motifs. A** The predicted HLA-A*0201 binding affinities of nonamers spanning the breakpoint region of human PAX3-FKHR. **B** The theoretical HLA-A*0201 binding affinities of peptides derived from the PAX3 amino acid sequence present in human PAX3-FKHR.
- **Figure 14. Up-regulation of HLA-A*0201 expression on T2 cells after incubation with the PAX3 peptide KLT. A** and **B** are two representative experiments.
- **Figure 15. Transfection of the human RD cell line with *in vitro* transcribed *GFP* mRNA. A** *In vitro* transcription and translation (IVT) of GFP protein from the pGEM4Z/GFP/A64 plasmid, using the TNT coupled reticulocyte lysate system. **B** GFP protein expression in human RD cells after transfection with *GFP* mRNA (+ 5′ cap) using TransMessenger Reagent.
- **Figure 16. A** GFP protein expression in immature mouse DCs after transfection with *in vitro* transcribed *GFP* RNA (+ 5′ cap), using TransMessenger Reagent. **B** *In vitro* transcription and translation of mixed murine/human PAX3-FKHR protein from the pBK-CMV-P3F plasmid, using the TNT Coupled Reticulocyte Lysate System.

Appendices

- **Appendix 1. Tumour volumes (in mm^3) from the initial C23 lysate-pulsed DC vaccine experiment in wild type C57BL/6 mice.**
- **Appendix 2. IFN-γ secretion of splenocytes cultured *in vitro* with CMV or C23 RMS target cells.**
- **Appendix 3. Tumour volumes (in mm^3) from the repeat C23 lysate-pulsed DC vaccine experiment in wild type C57BL/6 mice.**
- **Appendix 4. Tumour volumes (in mm^3) from the C23 lysate-pulsed DC vaccine experiment in beige C57BL/6 mice.**

Chapter 4:
Generation of Immunostimulatory Dendritic Cells from the Malignant Clone in Patients with Juvenile Myelomonocytic Leukaemia

1. Introduction

- **Figure 1. RAS signalling pathway.**
- **Figure 2. Proposed DC-based therapy for JMML.**

2. Methods and Materials

- **Table 1. Clinical and laboratory data for the 3 JMML patients in the current study.**

3. Results

- **Figure 3. Immunophenotype of DCs cultured *in vitro* from normal donor and JMML-1 PBMCs.**

- **Figure 4. Immunophenotype of DCs cultured *in vitro* from normal donor and JMML-2 PBMCs.**
- **Figure 5. Immunophenotype of DCs cultured *in vitro* from normal donor and JMML-3 PBMCs.**
- **Figure 6. Interphase FISH showing monosomy 7 in the nuclei of DCs cultured *in vitro* from JMML-2 PBMCs.**
- **Figure 7. Interphase FISH showing monosomy 7 in the nuclei of DCs cultured *in vitro* from JMML-3 PBMCs. A** Purified $CD86^+$ DCs cultured *in vitro* from JMML-3 PBMCs. **B** $CD86^+$ DCs cultured *in vitro* from a normal control. **C** Purified $CD14^+$ cells from JMML-3 PBMCs.
- **Figure 8. IL-12 secretion profile of DCs cultured *in vitro* from normal donor, JMML-2, and JMML-3 PBMCs.**
- **Figure 9. IFN-γ secretion, as a marker of T cell activation, following stimulation with *in vitro* cultured mature DCs. A** Graph depicting the IFN-γ ELISpot results from the MLR. **B** Pictures of representative ELISpot wells.
- **Figure 10. Cytotoxicity of T cells (derived from JMML-1 BMT donor PBMCs post engraftment) stimulated with JMML-1-derived leukaemic DCs.**
- **Figure 11. The number of DCs found in normal donor and JMML-2 peripheral blood.**

Chapter 1:

Function of Dendritic Cells in Anti-Tumour Immunity

1. History of cancer immunotherapy:

The development of vaccines is arguably the most successful contribution of the field of immunology to improving human health. Preventative vaccines have eradicated small pox, and have been used to protect countless people from infectious diseases such as polio, tetanus, and measles. However, in spite of two centuries of vaccine development, immunotherapy of cancer is yet to be of widespread clinical use.

The first recognised form of cancer vaccination was carried out in 1893 by the American surgeon William Coley. Coley extracted soluble toxins from *Streptococcus* and *Serratia*, and used the toxins ('Coley's toxins' as they became known) to treat more than 800 cancer patients between 1893 and 1936. Approximately half of the patients showed a beneficial clinical response, however the results have proven to be non-reproducible (Starnes, 1992).

Burnett (1967) postulated that lymphocytes continually patrol around the body and eliminate malignant cells, presumably via recognition of tumour-associated antigens. Burnett coined the phrase 'immunosurveillance' to describe this phenomenon. One of the first experiments to demonstrate the existence of tumour-associated antigens was performed by Foley (1953), who found that immunisation of mice with a syngeneic methylcholanthrene-induced sarcoma provided protection against a subsequent challenge with the same sarcoma.

The concept of immunosurveillance has been a contentious issue for immunologists throughout the last 35 years. There are several lines of evidence supporting Burnett's immunosurveillance hypothesis. Firstly, several immunodeficient mouse strains (such as $RAG^{-/-}$, $STAT1^{-/-}$, IFN-$\gamma^{-/-}$) have a higher incidence of carcinogen-induced tumours than syngeneic wild type mice (Kaplan *et al*, 1998; Shankaran *et al*, 2001). Secondly, Fenton and Longo (1995) demonstrated that tumour cells are genetically very unstable, creating numerous novel tumour-defined antigens that can potentially be recognised by the host immune system. Finally, the critical role of dendritic cells (DCs) at initiating anti-tumour immune responses has become better understood. Preliminary clinical trials have demonstrated that tumour antigen-pulsed DC vaccines induce beneficial clinical responses in some patients (Hsu *et al*, 1996; Nestle *et al*, 1998). The current view is that immunosurveillance definitely occurs, however tumours often develop immune evasion mechanisms (Parish, 2003).

2. Identification of tumour-rejection antigens:

Tumours are derived from normal host cells; hence tumour immunity is comparable to beneficial autoimmunity. In the early 1930s, the prevailing view was that tumours are not sufficiently distinct from normal tissues to activate the immune system. This led Woglom (1929) to state that 'it would be as difficult to reject the right ear and leave the left ear intact as it is to immunise against cancer'. However, the search for potential tumour-rejection antigens has been very successful in recent years. Tumour-rejection antigens can be divided into two main categories: tumour-specific antigens that are uniquely expressed in tumour cells, and tumour-associated antigens that are expressed at elevated levels in tumour cells but also present in normal cells.

Methods for identifying tumour antigens that are suitable candidates for vaccination therapy have improved with technological advances. One strategy is to isolate tumour-reactive T lymphocytes from cancer patients and use them to screen autologous target cells transfected with a tumour cDNA expression library (Boon *et al*, 1994). A serological identification of antigens by recombinant expression cloning (SEREX) approach has been used to screen tumour-derived expression libraries for tumour antigens that are detected by antibodies present in cancer patient sera. Antigens identified by SEREX are then examined for the presence of antigenic peptides that can be recognised by tumour-specific T lymphocytes (Pfreundschuh, 2000). Gene array studies allow determination of which genes are expressed in tumour tissue versus normal tissue, and tumour-defined antigens can then be tested for immunogenicity (see Chapter 2). Computer algorithms are now widely used to predict peptide sequences, derived from newly identified tumour antigens, that can bind to specific human leukocyte antigens (McKenzie *et al*, 2003). An alternative approach to identify tumour-specific peptide epitopes involves eluting the peptides bound to major histocompatibility complex (MHC) molecules on the surface of tumour cells (Slingluff *et al*, 1994).

Tumour-specific antigens are ideal targets for immunotherapy because antigen-specific immune responses should eradicate tumour cells, whilst importantly avoiding autoimmunity. Additionally, T cells in the host's immune repertoire that are specific for such antigens are unlikely to have been rendered inactive by immunological tolerance mechanisms.

Examples of tumour-specific antigens include idiotypes of B and T cell lymphomas (Lynch *et al*, 1979), the products of mutated genes (such as the break point region of BCR-ABL fusion protein in chronic myeloid leukaemia; Choudhury *et al*, 1997), and virus-encoded proteins (such as Epstein-Barr virus in Burkitt lymphoma; Rickinson and Moss, 1997). Immunotherapeutic strategies targeting such tumour-specific antigens have been shown to induce beneficial clinical responses in a proportion of patients (Hsu *et al*, 1996).

A rapidly growing number of tumour-associated antigens have been discovered. Briefly, the antigens fall into three main categories: over-expressed tumour antigens (e.g.: PRAME), tissue-specific differentiation antigens (e.g.: tyrosinase, and carcino-embryonic-antigen), and activated expression of silent genes (MAGE-1, MAGE-3, and Wilms tumour antigen 1). The majority of tumour-associated antigens identified to date are over-expressed in melanomas (Rosenberg, 1997), however tumour-rejection antigens have also been discovered for other cancer types. Autologous DCs pulsed *ex vivo* with tumour-associated antigens have been used as vaccines, and in some patients successfully induce anti-tumour immunity (several examples described in Chapter 3, **1.4.**). It is important to note that tumour antigens recognised by $CD4^+$ T cells have been identified, as well as tumour antigens that elicit $CD8^+$ T cell responses.

A model tumour-rejection antigen should have several properties. The most crucial being that the tumour antigen activates cytotoxic T lymphocytes (CTLs) that bind with high avidity to tumour targets. Zeh and colleagues (1999) found that only high avidity CTLs exert biological function *in vivo*. Ideally the antigen should be tumour-specific, expressed in malignant but not normal cell types, thus avoiding any potential autoimmunity. Additionally, the tumour antigen should be vital for the growth and survival of the tumour. This minimises the risk that the tumour will down-regulate expression of the tumour antigen to evade the immune system. Finally, if the tumour antigen is shared by many patients, rather than being a patient-specific antigen, then therapy targeting the tumour antigen will be widely applicable (Gilboa, 1999).

3. Types of cancer immunotherapy:

Cancer immunotherapeutic strategies can be either active or passive, and specific or non-specific (Davis, 2000). Interestingly, some passive and non-specific active vaccines have been shown to be effective at generating beneficial anti-tumour immune responses

in a clinical setting. The aim of active specific vaccination is to harness the power and specificity of the immune system to target antigens expressed by malignant cells, resulting in the induction of long lasting anti-tumour immunity. Therapeutic vaccinations against cancer have two major problems to overcome: the majority of tumour antigens are only weakly immunogenic (Yu *et al*, 2004); and, anti-tumour immune responses might have to be generated in the setting of immune tolerance (Goodnow, 1997; Colella *et al*, 2000). A variety of immunotherapeutic approaches, which target different antigens and induce different effector mechanisms, are currently being tested in preclinical studies and clinical trials.

3.1. Monoclonal antibodies:

The use of monoclonal antibodies for passive specific cancer immunotherapy is a rapidly evolving field that is beginning to realise its promise. The aim of this strategy is to administer antibodies that are specific for antigens expressed on the surface of tumour cells. These antibody-based approaches have utilised protein-engineering technology that allows the production of 'humanised' monoclonal antibodies, which overcomes the limitation of murine antibodies that can initiate detrimental human anti-mouse antibody responses (Winter and Harris, 1993).

Several monoclonal antibodies are now approved for clinical use. Trastuzumab (Herceptin™; Genentech, USA) is a recombinant monoclonal antibody against human epidermal growth factor receptor 2 (Her2), which is over-expressed in approximately 30 percent of breast cancers (Slamon *et al*, 1987). In a phase 3 clinical trial, Slamon and colleagues (2001) treated metastatic breast cancer patients with conventional chemotherapy alone or with a combination of chemotherapy plus trastuzumab. The investigators found that the addition of trastuzumab significantly extended the time to disease progression and significantly increased the rate of objective response. Slamon *et al* (2001) concluded that trastuzumab augments the clinical benefit of chemotherapy in metastatic breast cancers that over-express Her2.

Rituximab (MabThera™; Roche, Switzerland) is a chimeric monoclonal antibody specific for the CD20 B-cell antigen and has been used in clinical trials to treat B-cell non-Hodgkin's lymphoma. Coiffier and colleagues (2002) found that rituximab, when added to standard chemotherapy, can improve the complete response rate of B-cell non-Hodgkin's lymphoma patients. Given as a single agent, rituximab shows moderate

beneficial clinical activity. However, when rituximab is conjugated to a yttrium-90 radioisotope, the antibody provided additionally efficacy compared to unconjugated rituximab alone (Witzig, 2004).

B cell malignancies are attractive immunotherapy targets because the monoclonal tumour cells express the same unique idiotypic immunoglobulin receptor, which is truly tumour-specific. Treatment with anti-idiotype antibodies induced a complete response in approximately one fifth of non-Hodgkin's lymphoma patients (Davis *et al*, 1998). The main disadvantages of this strategy are that each patient's idiotypic immunoglobulin is different, and it is expensive to produce anti-idiotype antibodies.

Recent studies have addressed how passively administered monoclonal antibodies mediate their anti-tumour effect. Therapeutic antibodies can use a wide range of effector mechanisms *in vivo*, including the activation of complement (Teeling *et al*, 2004), antibody-dependent cellular cytotoxicity (ADCC; Cartron *et al*, 2002), and direct induction of apoptosis (Byrd *et al*, 2002; Mineo *et al*, 2004).

3.2. Non-specific activators of anti-tumour immunity:

The injection of cancer patients with 'Coley's toxins' was an early form of non-specific active cancer vaccination, and there is currently renewed interest in the development of non-specific strategies to activate anti-tumour immunity.

The *mycobacterium* Bacillus Calmette Guerin (BCG) is currently used to treat patients with superficial bladder cancer and can enhance the development of anti-tumour immunity (Bassi, 2002). BCG contains unmethylated cytosine-guanosine-dinucleotide-containing oligonucleotides (CpG ODN), which acts as a potent activator of B lymphocytes and certain cell types of the innate immune system (Krieg *et al*, 1995; Chace *et al*, 1997; Jakob *et al*, 1998; Bauer *et al*, 1999). A more refined strategy is to inject CpG ODN, which have been shown to have therapeutic activity in murine models of cancer (Hafner *et al*, 2001; Krieg, 2002). CpG ODN can be used as a single agent, or as an adjuvant for vaccination against specific tumour antigens (Davis *et al*, 1998; Liu *et al*, 1998).

CpG ODN is not the only adjuvant that has been used to try to enhance anti-tumour immunity. Chemical adjuvants, such as incomplete Freund's adjuvant and keyhole

limpet haemocyanin have been used for the treatment of various cancer types (Salgaller *et al*, 1996; Caspar *et al*, 1997). Cytokines, such as interleukin (IL)-2, IL-12, and granulocyte macrophage-colony stimulating factor (GM-CSF), have been studied as adjuvants for cancer immunotherapy, however high cytokine doses can cause toxicity (Salgaller and Lodge, 1998; Cebon *et al*, 2003; Woodson *et al*, 2004). Complexing tumour antigens to heat shock proteins represents a potential vaccine candidate, with evidence suggesting that the heat shock proteins target antigen presenting cells (APCs) and mediate cross-presentation of the complexed antigen (Castelli *et al*, 2004; SenGupta *et al*, 2004).

3.3. Active vaccines using tumour-defined proteins or peptides:

The identification of a multitude of candidate tumour antigens (see **2.**) has allowed the development of active vaccine strategies that involve the treatment of cancer patients with tumour-defined proteins or peptides. In a pilot clinical trial, Atanackovic and colleagues (2004) vaccinated non-small cell lung cancer patients with recombinant MAGE-3 protein and the adjuvant AS02B. The vaccinations induced antigen-specific antibody and cellular immune responses in a large proportion of patients, however the clinical benefit of the MAGE-3 protein vaccine is yet to be demonstrated.

Numerous tumour antigen-derived peptide sequences have been identified that bind to specific human leukocyte antigen (HLA) class I and class II molecules. Immunodominant peptides derived from several melanoma-associated antigens have been used in clinical trials for the treatment of metastatic melanoma. However, beneficial clinical responses have been observed in only a very small percentage of patients, even when the peptide is administered with an adjuvant (Marchand *et al*, 1995; Cebon *et al*, 2003; Rosenberg *et al*, 2004).

Combination immunotherapy strategies have been employed in an attempt to increase the therapeutic potency of the cancer vaccine (reviewed by Pardoll and Allison, 2004). Phan and colleagues (2003) treated melanoma patients with peptides derived from the melanoma-associated antigen gp100, in conjunction with a monoclonal antibody that blocks the negative co-stimulatory molecule cytotoxic T lymphocyte-associated antigen 4 (CTLA4). The combination immunotherapy approach caused cancer regression in 21% of the patients, however CTLA4 blockage caused clinical autoimmunity in 43% of the patients. Strategies targeting molecules that influence T cell activation and effector

functions are currently being investigated for their ability to improve the anti-tumour immunity induced by cancer vaccinations (Pardoll and Allison, 2004).

DCs are the subject of clinical interest as vehicles to deliver tumour rejection antigens to the patient immune system. As an alternative strategy, tumour peptide or protein antigens have been loaded onto DCs *ex vivo*, and the pulsed DCs adoptively transferred to the patient. This approach has shown promise in clinical trials (Hsu *et al*, 1996; Nestle *et al*, 1998) and is reviewed in Chapter 3 (**1.4.**).

3.4. Adoptive T cell therapy:

Another well-studied form of cancer immunotherapy is the adoptive transfer of tumour-reactive T lymphocytes. In pilot clinical studies conducted nearly two decades ago, several groups attempted to isolate tumour infiltrating lymphocytes (TILs) from tumour biopsies, expand the TILs *ex vivo* in the presence of IL-2, and adoptively transfer the expanded TILs back into the patient as a form of passive cancer immunotherapy (Topalian *et al*, 1988; Rosenberg *et al*, 1988). Rosenburg and colleagues (1988) treated 20 metastatic melanoma patients with TILs, and reported objective tumour regression in over a third of the patients. More recently, Yee and colleagues (2002) isolated patient PBMCs and expanded melanoma-specific $CD8^+$ T cell clones *ex vivo* using DCs loaded with melanoma defined peptides as stimulator cells. Adoptive transfer of the *ex vivo* expanded T cell clones resulted in a favourable clinical response in the majority of melanoma patients tested. These clinical findings provide evidence that cancer patients possess tumour-specific T cells that are capable of mediating anti-tumour immunity *in vivo* (Pardoll and Allison, 2004). However, the adoptive transfer of T lymphocytes specific for tumour-associated antigens, that are non-mutated self proteins, can lead to the development of autoimmunity (Dudley *et al*, 2002).

High avidity CTLs are required for *in vivo* anti-tumour efficacy (Alexander-Miller *et al*, 1996; Zeh *et al*, 1999). However, the majority of tumour associated antigens are expressed at low levels in normal tissues, and as a result high avidity CTLs are often absent or tolerised in cancer patients. Several investigators have studied the retroviral transfer of tumour-specific T cell receptor (TCR) genes into patient T lymphocytes as an attempt to generate high avidity CTLs capable of killing tumour cells *in vivo* (reviewed by Kessels *et al*, 2001; Morris *et al*, 2003).

The adoptive transfer of allogeneic T cells has curative potential for the treatment for myeloid leukaemias (reviewed in Chapter 4, *1.3.3.*). The current treatment for chronic myeloid leukaemia (CML) and acute myeloid leukaemia (AML) patients is high-dose chemotherapy followed by allogeneic bone marrow transplantation. Several investigators have demonstrated that the allogeneic T lymphocytes are able to eliminate the residual leukaemic cells in the host, and this has been described as the graft versus leukaemia (GVL) effect (Marmont *et al*, 1991). Donor lymphocyte infusions (DLIs) are now routinely used to treat relapsed CML patients, and have been shown to induce prolonged remission (Kolb *et al*, 1995). However, the success of DLIs at inducing a GVL effect is limited by the morbidity and mortality associated with the accompanying graft versus host disease (GVHD). The challenge for immunologists is to isolate the beneficial GVL effect from the damaging GVHD.

3.5. DNA vaccines:

Researchers have identified a vast array of tumour antigens and their encoding genes. Hence DNA vaccination is a suitable strategy for a large number of cancer types. Delivery of tumour antigens by injection of the encoding DNA allows *in vivo* transfection of host cells and endogenous antigen production. DNA vaccines have been shown to induce long-term humoral and cellular immune responses *in vivo* (Gurunathan *et al*, 2000).

As an alternative to generating anti-idiotype antibodies for each B-cell lymphoma patient, Spellerberg and colleagues (1997) generated DNA plasmids containing the variable (V) region genes (V_H and V_L), which encode the idiotypic determinant, assembled as a single chain Fv (scFv) sequence. The investigators found that injection of these scFv DNA vaccines into mice induced low anti-idiotypic antibody responses and provided poor protection against lymphoma (King *et al*, 1998). To increase the immunogenicity of DNA vaccines, the tumour antigen sequence can be fused to a gene encoding an immunoenhancing protein (reviewed by Stevenson *et al*, 2004a). Spellerberg *et al* (1997) chose to fuse the scFv sequence to a non-toxic component of the tetanus toxin called fragment C (FrC), and found that injection of this plasmid was able to induce potent anti-idiotype responses and provided strong protection from B-cell lymphoma. Following the encouraging findings of the preclinical studies, the investigators have conducted pilot clinical trials injecting the scFv-FrC fusion gene intramuscularly to treat follicular lymphoma. The preliminary findings are promising,

with cellular responses against the idiotype observed in a large proportion of the patients (Stevenson *et al*, 2004b).

A wide range of other immunoenhancer elements have also been tested. Ye and colleagues (2004) found that using a DNA fusion gene vaccine containing the MAGE-1 gene linked to the heat shock protein 70 sequence was superior to a MAGE-1 DNA vaccine at expanding CTLs specific for the melanoma associated antigen. Similarly, the fusion of various cytokine genes to the Her2 DNA plasmid improved the efficacy of the DNA vaccine against Her2 expressing tumours (Chang *et al*, 2004). It shall be interesting to observe whether the success of the DNA vaccines in mouse models translates into anti-tumour efficacy in a clinical setting.

Several groups have demonstrated that the bulk of the immune response induced by an injected DNA vaccine requires the transfer of the tumour antigen from transfected host cells to professional APCs that subsequently cross-present the tumour antigen (Corr *et al*, 1996; Corr *et al*, 1999; see *4.3.*). Additionally, the hypomethylated CpG ODN in the backbone of the bacterial plasmid can activate host innate immune responses (Krieg, 2002). One major aim of DNA fusion genes is to activate $CD4^+$ Th cells, which have been shown to aid humoral responses, licence $CD8^+$ CTL responses, and are important for the generation of immunological memory (see *5.1.2*). Fusion of the tumour antigen sequence to a microbial gene, such as tetanus toxin FrC, allows the activation of a $CD4^+$ T cell response from a large, non-tolerised anti-microbial repertoire (Zhu and Stevenson, 2002). The induction of Th responses specific for the FrC immunoenhancer protein is vital for the priming of tumour-specific antibody and CTL responses, and Stevenson and colleagues (2004b) suggest that FrC-specific Th cells 'licence' professional APCs to prime CTLs specific for tumour epitopes.

One advantage of DNA fusion gene vaccination is that the immunoenhancer sequence can be selected in order to induce the most relevant effector function. As described in **2.**, the majority of known tumour associated antigens are intracellular proteins and presented on the cell surface as peptides bound by MHC class I molecules. In this situation, a DNA vaccine that is tailored for the development of $CD8^+$ CTL responses would be advantageous. For the induction of $CD8^+$ CTL responses, Rice and colleagues (2002) modified the FrC gene to remove immunodominant tetanus toxin-derived epitopes and improve presentation of epitopes from the fused tumour antigen sequence.

Using the CT26 colon carcinoma mouse model that expresses a known immunodominant epitope (AH1), the authors investigated the effectiveness of a fusion DNA vaccine consisting of the modified FrC gene fused to the AH1 sequence. The modified FrC-AH1 DNA vaccine induced a strong AH1-specific CTL response that protected against tumour growth (Rice *et al*, 2002).

In this Ph.D. project, I have investigated the use of DC-based immunotherapeutic strategies for the treatment of alveolar rhabdomyosarcoma and juvenile myelomonocytic leukaemia. I shall now proceed to review the function of DCs *in vivo* and their potential use in a clinical setting.

4. The role of DCs in tumour immunosurveillance:

DCs are a family of professional APCs, uniquely capable of stimulating naïve T lymphocytes and initiating primary immune responses (Steinman, 1991). This led Steinman (1991) to describe DCs as 'nature's adjuvant'.

4.1. DC subsets:

DCs follow various haematopoietic pathways of differentiation. DCs are derived from bone marrow progenitors, with DC development driven mainly by Fms-like tyrosine kinase 3 ligand and GM-CSF (Pulendran *et al*, 2001). $CD34^+$ pluripotent bone marrow progenitors differentiate into common myeloid progenitors (CMPs) and common lymphoid progenitors (CLPs). CMPs can subsequently differentiate into myeloid $CD11c^+$ tissue DCs that express high levels of CD1a (epidermal langerhans cells) or low levels of CD1a (interstitial DCs; Ito *et al*, 1999). $CD123^+$ $CD11c^-$ plasmacytoid DCs are differentiated from CLPs (Spits *et al*, 2000; reviewed by Liu, 2001). In some instances, blood monocytes ($CD11c^+$ $CD14^+$) differentiate into DCs (Romani *et al*, 1994). The different DC subsets display similar yet subtly different functions, which might influence the type of immune response they induce (Liu, 2001).

4.2. The life cycle of DCs:

Newly generated immature DCs typically circulate through the blood and non-lymphoid peripheral tissues (Banchereau *et al*, 2000; Liu, 2001). Immature DCs are found at the interface of potential pathogen entry sites in most tissues, acting as sentinels for signs of pathogen invasion (Steinman, 1991). The immature DCs are highly phagocytic,

continually internalising soluble and particulate antigens, which are subsequently processed for presentation to T lymphocytes at a later time point (Banchereau and Steinman, 1998). Immature DCs are able to take up exogenous antigens by phagocytosis (Inaba *et al*, 1993; Reis e Sousa *et al*, 1993), macropinocytosis, and receptor-mediated endocytosis (Sallusto *et al*, 1995). Once captured, the DCs process the exogenous antigen in two distinct pathways. Firstly, the internalised protein is processed via the endocytic pathway and peptides loaded onto newly synthesized MHC class II molecules (Cella *et al*, 1997). Additionally, the captured antigen is processed and loaded onto MHC class I molecules, via a non-conventional MHC class I processing pathway (Albert *et al*, 1998). This allows DCs to present antigenic peptides to both $CD4^+$ and $CD8^+$ T cells (see *4.3.*on cross-priming). Unlike macrophages, the primary role of DCs is not to clear incoming pathogens, but to alert the immune system (Rescigno *et al*, 1999).

Having captured antigen that is perceived to be associated with a dangerous situation, the DCs undergo maturation (see *4.4.*). During this transitional stage, the early activated DCs secrete chemokines and pro-inflammatory cytokines that recruit effector cells of the innate immune system, such as macrophages and natural killer (NK) cells, to the site of inflammation (Rescigno *et al*, 1999). During DC maturation, the antigen capture capacity declines, motility increases, and expression of the chemokine receptor CCR7 increases. CCR7 expression directs the migration of maturing DCs, via the afferent lymph or the blood stream, into the T cell dependent areas of secondary lymphoid tissues, such as the spleen or lymph nodes (Saeki *et al*, 1999; Sallusto *et al*, 1999).

DCs are a reservoir of immunogens from the periphery, and establish a physical link between the periphery and lymphoid organs. Upon arrival in lymphoid tissues, the role of mature DCs is to activate the effector cells of the adaptive immune system. Mature DCs present immunodominant peptides to circulating antigen-specific $CD8^+$ and $CD4^+$ T lymphocytes, in conjunction with the co-stimulatory signals required to initiate primary immune responses (Harding *et al*, 1992; Acuto and Michel, 2003). Mature DCs derive their stimulatory capacity from their expression of elevated levels of MHC class I and class II molecules on their surface, along with co-stimulatory molecules, including CD80 and CD86, and adhesion molecules, such as ICAM-1 (Banchereau and Steinman, 1998). Mature DCs are potent T cell stimulators, and induce a mixed leukocyte reaction *in vitro*. It is important to note that, in addition to initiating primary $CD8^+$ CTL

responses, DCs also play a crucial role in establishing immunological memory, and polarising the type of T cell response towards $CD4^+$ T helper (Th) cells (Banchereau *et al*, 2000). It has been suggested that DCs also interact with regulatory T cells, possibly by providing IL-2, in order to maintain peripheral tolerance to self antigens (Granucci *et al*, 2003). Following interaction with lymphocytes, the irreversibly mature DCs die by apoptosis inside the lymphoid organ, restoring homeostasis of the immune system (Banchereau and Steinman, 1998).

4.3. Ability of DCs to cross-prime CTL responses against tumour antigens:
The main source of antigen entering the MHC class II pathway is exogenous protein that has been endocytosed by professional APCs. Upon endosomal processing, protein-derived peptides are loaded onto MHC class II molecules, which travel to the cell surface and are presented to $CD4^+$ Th cells (Cella *et al*, 1997). In contrast, MHC class I molecules usually present peptides derived from intracellular proteins (Braciale *et al*, 1987). In the classical MHC class I pathway, cytosolic proteins are degraded by the proteasome (Kloetzel, 2004), and peptides are transported to the endoplasmic reticulum (ER) by transporter associated with antigen processing (TAP) molecules (Lankat-Buttgereit and Tampe, 2002), where they can bind to newly synthesised MHC class I molecules. Peptide:MHC class I complexes are transported to the cell surface and recognised by $CD8^+$ CTLs (Germain and Margulies, 1993).

However, there is evidence for a specialised non-classical pathway that allows the presentation of exogenous antigens in the context of MHC class I molecules (termed cross-presentation; Bevan, 1976). The ability to cross-present exogenous antigen is restricted to bone marrow-derived professional APCs (Huang *et al*, 1994). Den Haan and colleagues (2000) demonstrated that the lymphoid $CD8\alpha^+$ DCs, but not $CD8\alpha^-$ myeloid DCs, are responsible for the cross-presentation of ovalbumin peptides *in vivo*.

Cross-presentation might occur by several pathways. Gagnon and colleagues (2002) showed that the ER is involved in macrophage phagocytosis, with the ER membrane fusing with the macrophage plasmalemma during phagosome formation. Ackerman and Cresswell (2004) suggest that the presence of ER-based proteins in phagosomes makes these compartments suitable for the cross-presentation of exogenous antigen in the context of MHC class I molecules, and discuss two potential models of cross-presentation. In the first model, the exogenous antigen is captured by ER-mediated

phagocytosis and then 'retrotranslocated' from the phagosome into the cytosol, where it is cleaved by proteasomes into peptides that are transported back into the phagosome by TAP molecules. The peptide:MHC class I complexes are delivered from the phagosome to the cell surface for recognition by $CD8^+$ CTLs. In the second model, the exogenous antigen is captured by ER-mediated phagocytosis, then directed into the ER lumen and processed for presentation on MHC class I molecules (Ackerman and Cresswell, 2004). In an alternative pathway, internalised MHC class I molecules enter MHC class II compartments, where bound MHC class I peptides can be exchanged for peptides derived from degraded exogenous antigens (Gromme *et al*, 1999; Chefalo and Harding, 2001). Additional pathways have been described for peptide-heat shock protein complexes (Arnold *et al*, 1995; Noessner *et al*, 2002).

The outcome of cross-presentation is dependent on the maturation status of the cross-presenting APC. DCs that cross-present antigen and have also received a strong activation signal are able to stimulate $CT8^+$ CTL responses (termed cross-priming; reviewed by Melief, 2003). Several studies have provided evidence for the cross-priming of CTL responses against tumour-defined antigens (Berard *et al*, 2000; Thomas *et al*, 2004). In the absence of adequate DC activation, the outcome of cross-presentation will be cross-tolerance of $CT8^+$ CTL responses (Steinman *et al*, 2003).

The primary function of DCs is to alert the immune system of environmentally acquired antigens, not the presentation of endogenously expressed proteins, and the cross-presentation ability of DCs appears to be very efficient. Storni and Bachmann (2004) found that DCs require only marginally more exogenous virus-like particles to cross-prime CTL responses than to prime Th responses via the classical MHC class II pathway.

4.4. Danger model of APC-mediated lymphocyte activation:

Burnett (1967) championed the view that during immunosurveillance lymphocytes discriminate between self and non-self. The binding of the T cell receptor to peptide-MHC complexes on the surface of APCs provides the antigen-specificity of the T cell-APC interaction (referred to as signal 1). Incorporating self-non-self discrimination, a '2-signal' model of lymphocyte activation was proposed in the 1970s, recognising firstly that lymphocytes require an additional signal ('help'; Bretscher and Cohn, 1970), and that lymphocytes receive the secondary signal (termed 'co-stimulation') from APCs

(Lafferty and Cunningham, 1975). According to the 2-signal model, the presentation of foreign antigen to an antigen-specific T cell (signal 1), in the absence of co-stimulation (signal 2), results in inactivation of the T cell. The major concern voiced by immunologists was that the APCs must ultimately decide whether to induce tolerance or initiate an immune response, yet APCs are not able to discriminate between self and non-self. Janeway (1992) proposed an improved self-non-self model, whereby APCs recognise evolutionarily conserved microbial products as non-self. According to this 'infectious non-self' model, APCs only provide the co-stimulation signal if they are activated as a result of their pattern recognition receptors (PRRs) recognising pathogen-associated molecular patterns (PAMPs). PAMPs are conserved microbial structures not found in mammalian cells, and act as a signature of micro-organisms (Medzhitov, 2001). DCs express a repertoire of PRRs including toll-like receptors (TLRs) and C-type lectins (Biragyn *et al*, 2002; Underhill and Ozinsky, 2002; reviewed by van Kooyk and Geijtenbeek, 2003). The PAMPs recognised by several of the TLRs have been identified, and include the TLR4 ligand lipopolysaccharide (LPS; Poltorak *et al*, 1998), and the TLR3 ligand double-stranded RNA (Alexopoulou *et al*, 2001).

However, the infectious non-self model was clearly incomplete, unable to explain several key findings, such as how alloreactivity occurs under microbe-free conditions. Matzinger (1994) proposed the 'danger model' whereby APCs do not discriminate between self and non-self, instead APCs are activated by antigenic danger signals from injured/distressed cells. The danger signals stimulate APCs to mature so that they can present antigens in conjunction with co-stimulation to antigen-specific T lymphocytes. Similar to the original 2-signal hypothesis, signal 1 in the absence of co-stimulation results in lymphocyte anergy or paralysis (immunological tolerance). An important principle is that the danger signal must not be provided by healthy cell or cells undergoing programmed cell death. Examples of alarm signals that activate APCs include intracellular proteins released by necrotic cells, and distressed cells expressing heat shock proteins on their surface (Gallucci and Matzinger, 2001). Recently, Shi and colleagues (2003) found that injured cells release uric acid, which acts as an endogenous danger signal, able to stimulate DC maturation. Bacterial and viral products such as LPS and double-stranded RNA would represent alarm signals and activate APCs, hence the danger model incorporates Janeway's infectious non-self model. Third party cells, such as activated NK cells, might also be able to convey danger signals to DCs (Piccioli *et al*, 2002).

5. Effector cells that participate in anti-tumour immunity:

5.1. T lymphocyte responses:

DCs, that capture antigens secreted by tumour cells or released during tumour cell lysis, are able to initiate tumour-specific T cell responses (Smyth *et al*, 2001). As mentioned in *3.3.*, T cell activation requires 2 signals. Signal 1 is delivered through the T cell receptor after engagement by a peptide-MHC complex (Figure 1) (Germain and Margulies, 1993). Whilst numerous co-stimulatory molecules have been identified (Liu and Linsley, 1992; Watts and DeBenedette, 1999), CD80 (B7.1) and CD86 (B7.2) are the prototypic co-stimulatory molecules expressed on APCs. Co-stimulation (signal 2) results from the interaction of these molecules with an activating receptor, such as CD28, on the surface of T cells (Harding *et al*, 1992). In contrast, binding of CD80 or CD86 to the inhibitory receptor cytotoxic T lymphocyte antigen 4 (CTLA4) does not provide a co-stimulatory signal (Acuto and Michel, 2003). Some investigators postulate that in addition to expressing MHC and co-stimulatory molecules, APCs need to secrete immunostimulatory cytokines, such as IL-2, IL-12, and IL-18, to activate naïve T cells (Schmidt and Mescher, 2002). This is often referred to as 'signal 3' of T cell activation (Figure 1).

5.1.1. $CD8^+$ T cells:

$CD8^+$ T cells recognise antigenic peptides that are presented on target cells by MHC class I molecules (Germain and Margulies, 1993). Activated antigen-specific $CD8^+$ T cells undergo clonal expansion and differentiate into CTLs, capable of lysing tumour cells. CTLs can utilize both the perforin system and the Fas ligand-Fas system to lyse targets (Kagi *et al*, 1994).

In cancer immunotherapy studies, both tumour lysate-pulsed DC immunisations and tumour peptide-pulsed DC immunisations have been shown to elicit antigen-specific CTL responses that lead to tumour regression (Nestle *et al*, 1998; Banchereau *et al*, 2001a; see Chapter 3, **1.4.** for review). Encouraged by these findings, several current clinical trials are attempting to use pulsed DC vaccinations to stimulate tumour-reactive CTL responses.

5.1.2. $CD4^+$ T cells:

The T cell receptors of $CD4^+$ T cells recognise antigen as a peptide-MHC class II complex (Germain and Margulies, 1993). It is well known that $CD4^+$ T cells help B

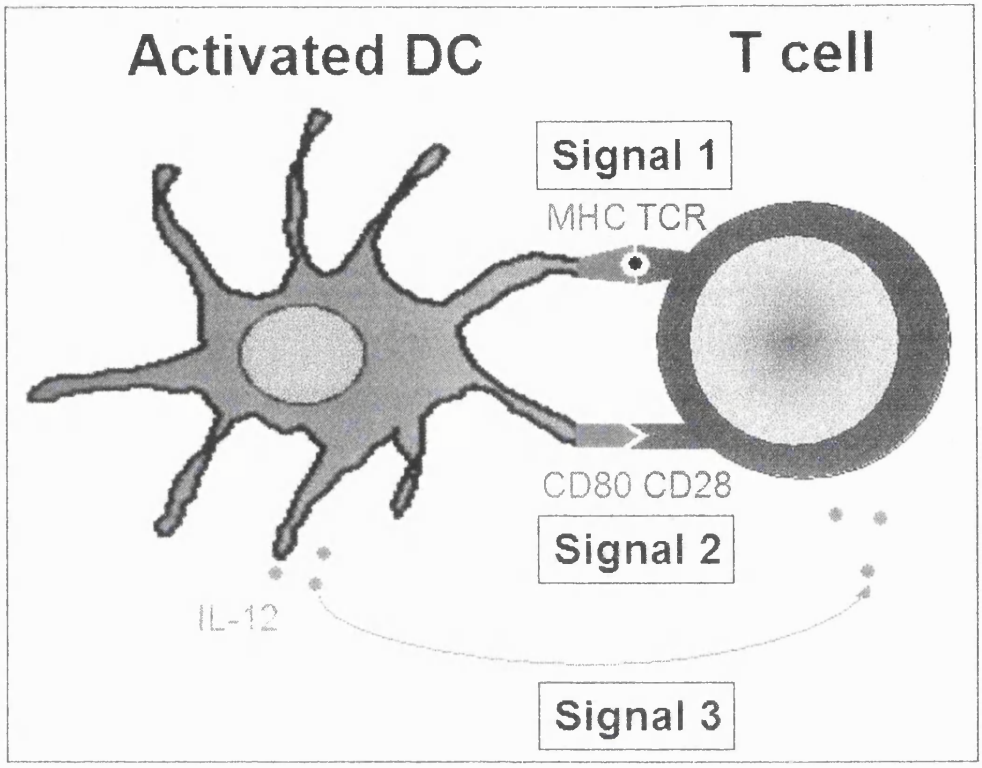

Figure 1. DC activation of an antigen-specific T cell. Signal 1 is provided by the T cell receptor (TCR) binding peptide-MHC complex. The binding of co-stimulatory molecules on the surface of APCs, including CD80 and CD86, to T cell activating receptors, such as CD28, provides signal 2 (co-stimulation). Immunostimulatory cytokines, such as IL-2, IL-2, and IL-18, are secreted by the APC and are described by some investigators as signal 3 of T cell activation. This figure is a compilation of the results derived from the studies discussed throughout the text.

cells to produce antibody. Another major function of $CD4^+$ T cells is to license CTL killing of tumour cells (referred to as $CD4^+$ T cell help). Help for CTL responses does not require direct $CD4^+$ T cell-$CD8^+$ T cell contact, instead it is provided in a cognate manner with both $CD4^+$ and $CD8^+$ T cells recognising antigen presented on the same DC. Interaction of CD40 ligand (CD40L) on $CD4^+$ T cell with CD40 on DC conditions the DC, which then becomes capable of priming effective CTL responses (Bennett *et al*, 1998; Ridge *et al*, 1998). Additionally, $CD4^+$ T cell-derived cytokines, such as IL-2, can amplify and sustain $CD8^+$ T cell responses (Wodarz and Jansen, 2001).

Furthermore, $CD4^+$ T cells can eliminate tumour cells *in vivo* in the absence of $CD8^+$ T cells. Activated $CD4^+$ T cells can migrate to the site of local tumour growth and directly lyse tumour cells that express MHC class II complexes (via the Fas ligand-Fas system; Hahn *et al*, 1995; Jiang *et al*, 1996). Primed $CD4^+$ T cells found at the tumour site also secrete cytokines, such as interferon (IFN)-γ and IL-4, which can direct macrophages and eosinophils to kill the tumour cells (Hung *et al*, 1998; Mumberg *et al*, 1999). Recent studies have found that effective and long lasting anti-tumour immunity requires the priming of both $CD4^+$ and $CD8^+$ T cells (Banchereau *et al*, 2001b;Goldszmid *et al*, 2003).

5.2. NK and natural killer T (NKT) cell responses:

A lot of work has focused on the role of DCs initiating adaptive CTL immunity to tumours. However, effector cells of the innate immune system play a vital role as the first line of defence against certain microbial infections and tumours.

NK cells are a lymphocyte subtype that mediates innate immunity. Numerous investigators have reported that NK cells can spontaneously lyse MHC class I negative tumour cells *in vivo* (Karre *et al*, 1986; Whiteside and Herberman, 1995). Following the interaction of NK cell receptors with their specific cellular ligands, NK cells mediate cytotoxicity by releasing perforin. Activated NK cells can also secrete a variety of cytokines, including IFN-γ and tumour necrosis factor, as well as chemokines, such as CCL4 and CCL5 (Cooper *et al*, 2001; Robertson, 2002). NK cell effector functions are regulated by a balance between the signals transmitted by inhibitory and activating receptors.

NK cell inhibitory receptors include killer-cell immunoglobulin-like receptors (KIRs), that are specific for MHC class I molecules, and prevent unwanted NK cell responses against self cells expressing normal levels of MHC class I molecules on their surface (Long, 1999). Importantly, the KIRs enable NK cells to attack self cells that have selectively down-regulated or lost MHC class I expression, as often found on transformed or infected cells (Garrido *et al*, 1997). NK cell activating receptors have only recently been identified (Bauer *et al*, 1999). In humans, a lectin-like NKG2D homodimer is expressed on killer cells of the innate immune system, including NK cells, NKT cells, and γδ-T cells, and also on $CD8^+$ T cells. The NKG2D receptor can bind to the MHC class I polypeptide-related (MIC) glycoproteins MICA and MICB (Bauer *et al*, 1999; Diefenbach *et al*, 2000). Distressed and transformed cells often over-express the stress-inducible MICA and MICB molecules, making them susceptible to NK cell attack (Groh *et al*, 1999). Interestingly, there is accumulating evidence that NK immunity might have some adaptive features, such as the requirement of co-stimulation for NK cell effector function (Gao *et al*, 2003).

Interactions between NK cells and DCs are able to amplify NK cell-mediated responses (reviewed by Moretta, 2002). Early activated DCs in injured tissues or sites of inflammation are able to recruit innate effector cells, including NK cells, by secreting chemokines such as CCL3 and CXCL8 (Sallusto *et al*, 2000). Activated mouse DCs secrete IL-12, which is known to play an essential role in activating NK cells (Trinchieri, 2003). Direct contact between activated DCs and NK cells at the site of inflammation can result in NK cell-maturation, which potentiates NK cell-mediated cytotoxicity (Nishioka *et al*, 2001; Gerosa *et al*, 2002). Fernandez and colleagues (1999) reported that adoptively transferred DCs are able to promote NK cell responses against mouse MHC class I-deficient tumours. The DC-NK cell cross-talk is bidirectional, as IL-2 activated NK cells are able to induce DC maturation (Piccioli *et al*, 2002). Additionally, activated NK cells have been shown to kill immature DCs (Wilson *et al*, 1999; Ferlazzo *et al*, 2002).

A subpopulation of T lymphocytes has recently been discovered that express both NK and T cell markers, and are referred to as NKT cells (Ballas and Rasmussen, 1990; MacDonald, 1995). NKT cells do not express a normal T cell receptor repertoire; instead they possess an invariant T cell receptor that specifically recognises the non-classical MHC class I-like molecule CD1d presenting glycolipid antigens (Bendelac *et*

al, 1995). Activated NKT cells secrete large amounts of Th1 and Th2 cytokines, and kill target cells by a perforin-dependent mechanism equivalent to that of NK and T cells (reviewed by Brutkiewicz and Sriram, 2002). Activated NKT cells have been shown to interact with DCs via a CD40L, inducing DC production of IL-12 (Kitamura *et al*, 1999). The DC-derived IL-12 can then stimulate NKT cytotoxic effector functions. Cui and colleagues (1997) reported that NKT cells are important in IL-12-mediated anti-tumour immunity.

5.3. B lymphocyte responses:

DCs have been shown to directly regulate B cell responses (Banchereau *et al*, 2000). Wykes and colleagues (1998) reported that DCs can transfer unprocessed captured antigen to naïve B cells to initiate antigen-specific responses. B lymphocytes have a limited role in anti-tumour immunity *in vivo*. Nonetheless, antibodies can recognise some tumour-associated surface antigens, and antibodies bound to tumour cells can stimulate important immune responses, such as the activation of the complement cascade and the initiation of ADCC. Important ADCC-mediating effector cells include NK cells and macrophages (Robertson and Ritz, 1990; Parihar *et al*, 2002). Another important function of tumour-specific antibodies is opsinization of tumour cells to promote their uptake by APCs (Finn, 2003).

B cell malignancies are interesting because the monoclonal tumour cells express a unique idiotypic immunoglobulin receptor that is truly tumour-specific. Hsu and colleagues (1996) treated follicular B cell lymphoma patients with autologous DCs pulsed *ex vivo* with idiotypic protein. The patients developed anti-idiotype cellular and humoral immune responses, and clinical responses were detected in three quarters of the patients. Administration of tumour-specific antibodies to patients has resulted in the induction of anti-tumour effects, in breast cancer (Vogel *et al*, 2001) and colon cancer (Riethmuller *et al*, 1994; reviewed by Kennedy and Shearer, 2003).

5.4. DCs are potential effector cells in anti-tumour immunity:

In addition to regulating anti-tumour responses from various effector cells of the innate and adaptive immune systems, DCs can lyse targets directly. Fanger and colleagues (1999) reported that human DCs can directly kill tumour cells via expression of the TNF-related apoptosis-inducing ligand (TRAIL) death receptor. Chapoval *et al* (2000) demonstrated that activated DCs can inhibit the growth of tumour cell lines.

6. Immune escape mechanisms of tumours:

Despite the potent immunostimulatory capacity of DCs, the existence of numerous tumour-associated antigens, and the huge armoury of effector cells able to target tumour cells, the immune system does not appear to be very efficient at rejecting tumours. There are several potential explanations for this. Firstly, the DCs that encounter tumours might not recognise them as 'dangerous', as the tumour cells initially grow as healthy cells and do not produce any alarm signals (Matzinger, 1994). Hence, the DCs may not be sufficiently activated to express the co-stimulatory molecules required to prime T lymphocytes specific for tumour-associated antigens. Consequently, these potentially tumour-reactive T cells might be tolerised, reducing the capacity of the immune system to eliminate tumours (Gallucci *et al*, 1999). It is possible that the DCs are only alerted to the danger once the tumour has reached an advanced stage, where uncontrolled tumour proliferation is associated with damage to the normal tissue, tumour cell necrosis, and the release of pro-inflammatory signals. By this point it is likely that the rapidly proliferating and metastatic tumour can not be controlled by a late developing DC-initiated adaptive immune response. Surprisingly, established tumours primarily induce immune tolerance, rather than immune activation, suggesting that tumours develop mechanisms that hinder the sensing of danger signals (Pardoll, 2003). Secondly, the tumour cells might protect themselves from specific immune reactions by down-regulating MHC expression or tumour-associated antigen expression on the cell surface (Ferrone and Marincola, 1995; Garrido *et al*, 1997). The loss of expression of various tumour antigens or MHC molecules by the tumour cells suggests that the host's immune system has attempted to eradicate the tumour. Finally, Elgert and colleagues (1998) suggested that some tumours release immunosuppressive cytokines, such as IL-10 and transforming growth factor-β, to dampen down anti-tumour adaptive immune responses (Elgert *et al*, 1998; Garcia-Hernandez *et al*, 2002; Lin *et al*, 2002). These cytokines could suppress tumour-specific immune response by acting on the $CD4^+$ T cells, $CD8^+$ T cells, or APCs (Mizoguchi *et al*, 1992; Finke *et al*, 1999).

It is important to investigate these tumour-induced immunosuppressive effects, in order to develop effective immunotherapeutic strategies. Encouraging reports, from phase I clinical trials of refractory prostate cancer patients, suggest that it might be possible to overcome tumour-induced immune tolerance by *ex vivo* stimulation of CTLs with antigen-loaded DCs expressing optimal co-stimulatory signals (Small *et al*, 2000).

7. Use of DC vaccines in the clinic:

Our detailed understanding of DC function, coupled with the clear evidence for the existence of tumour-associated antigens, has raised hopes that the antigen presenting capacity of DCs can be exploited for cancer immunotherapy. The ability of DC-based approaches targeting novel tumour-defined antigens to reject tumours *in vivo* requires testing in biologically relevant animal models. It is now possible to generate DCs *ex vivo* from monocytes using clinically approved methodology, and there are numerous clinical trials currently underway that are attempting to use DC-based vaccines to manipulate immune responses *in vivo* in order to control cancer.

Chapter 2:

Expression Profiling Suggests a Role for PAX3-FKHR Fusion Oncoprotein in the Inhibition of Interferon-Gamma Signalling in Rhabdomyosarcoma Cells

Abstract

Alveolar rhabdomyosarcoma (ARMS) is an aggressive paediatric solid tumour with a characteristic t(2;13)(q35;q14) translocation. The resultant chimeric PAX3-FKHR transcription factor is oncogenic due to enhanced transcriptional activation and has been shown to activate a myogenic transcription program. To investigate the oncogenic role of PAX3-FKHR in ARMS, we have stably transfected the mouse rhabdomyosarcoma (RMS) cell line 76-9 with a PAX3-FKHR expression construct. A matrigel invasion assay revealed that PAX3-FKHR significantly increased the invasive ability of 76-9 cells *in vitro* (student *t*-test; $p<0.01$). To determine the target genes of PAX3-FKHR in 76-9 cells, we compared the global mRNA profile of cells transfected with empty vector with two independent clones transfected with PAX3-FKHR, using oligonucleotide microarray expression profiling. We found that PAX3-FKHR up-regulated 31 genes and down-regulated 69 genes, by more than 2 fold. This result is in variance with a model of PAX3-FKHR as solely a transcriptional activator. Consistent with published findings, PAX3-FKHR induced expression of insulin like growth factor 2. Interestingly, a large proportion of the genes down-regulated by PAX3-FKHR are interferon (IFN)-γ stimulated genes (21 out of the 44 genes with known function), including the major histocompatibility complex (MHC) class I genes *H2-K* and *H2-D1*. Another gene repressed by PAX3-FKHR is plasminogen activator inhibitor-1 (*PAI-1*), which we discovered is stimulated by IFN-γ in the RD human embryonal RMS cell line. Northern blot analysis of representative target genes verified the microarray results. Follow up studies demonstrated that ectopically expressed PAX3-FKHR down-regulated MHC class I and PAI-1 expression at the protein level in RD cells. Moreover, PAX3-FKHR rendered RD cells partially resistant to IFN-γ induced up-regulation of MHC class I and PAI-1. Published data suggests that the down-regulation of MHC class I by PAX3-FKHR might aid immune escape of ARMS cells, and diminished PAI-1 levels might result in increased metastatic ability of ARMS cells. The transfection of RD cells with PAX3-FKHR resulted in the induction of CXC chemokine receptor 4 (CXCR4) protein expression. CXCR4 is known to be inhibited by IFN-γ, and this result is consistent with a role for PAX3-FKHR as an inhibitor of IFN-γ transcription. PAX3-FKHR did not repress transcription of the FKHR target genes *BIM* (Western blot analysis) and *IGFBP-1* (reporter assay using IGFBP-1-luciferase construct) in RD cells. Moreover, there was no increase in the levels of phosphorylated Akt in PAX3-FKHR-transfected RD cells. These results suggest that PAX3-FKHR did not repress the known FKHR

target PAI-1 by interfering with FKHR transcription either directly or indirectly via the PI3K-Akt pathway. Taken together our findings suggest that PAX3-FKHR exerts some of its effect on the ARMS phenotype by negatively interfering with normal IFN-γ induced transcription.

1. Introduction

1.1. Frequency, origins, and treatment of RMS:

RMS is the most common soft-tissue sarcoma of childhood, accounting for approximately 10% of all paediatric solid tumours (Pappo *et al*, 1995). RMS originates from undifferentiated mesenchymal cells and resembles developing skeletal muscle, expressing the myogenic transcription factor MyoD and the skeletal muscle structural proteins α-actin and myosin heavy chain (Fisher, 1990; Fletcher, 1995).

The recent advances made in multimodal therapy (chemotherapy, radiotherapy, and surgery) have increased the long-term survival rate in RMS to more than 70% (Pappo *et al*, 1995). However, metastatic RMS has an event free survival of only 20-30% despite aggressive treatment (Anderson *et al*, 1999a). The development of alternative therapeutic approaches is urgently required for the treatment of metastatic ARMS.

1.2. Histological, clinical, and cytogenetic features of the two RMS subtypes:

RMS can be broadly divided into two histopathological subtypes, embryonal RMS (ERMS) and alveolar RMS (ARMS) (Tsokos *et al*, 1992; Newton, 1995). The defining histological features of ARMS are small round cells, with abundant eosinophilic cytoplasm containing hyperchromatic nuclei. The cellular architecture of the ARMS histological subtype is characterised by the presence of alveolar-like spaces (Pappo *et al*, 1995). Giant cells are common in ARMS and may be the result of cell fusion, as seen in myotube formation (Anderson *et al*, 1999a). Tsokos and colleagues (1992) refined the classification, placing compact round-cell RMS in the ARMS subtype (referred to as solid alveolar RMS). This was based on the typical alveolar cytologic features observed in solid alveloar RMS, despite their lack of alveolar architecture. ERMS histology includes evenly distributed chromatin, and varying degrees of cytoplasmic myogenic differentiation. Spindle cell and botryoid variants of ERMS have been described in the literature (Newton, 1995; Pappo *et al*, 1995) (Table 1).

ERMS is the more frequent subtype and typically presents in young children. ERMS is commonly located in sites where skeletal muscle in not normally found, such as the head and neck region. ERMS is associated with a favourable prognosis (Newton *et al*, 1995; Barr, 2001). ARMS is the rarer subtype, and develops mainly in adolescents and young adults. ARMS is most frequently found in sites of abundant skeletal muscle,

especially the limbs. ARMS is associated with a poorer prognosis, partly because ARMS is metastatic at presentation. ARMS most commonly metastasises to the bone marrow and lymph nodes (Pappo *et al*, 1995; Barr, 2001) (Table 1).

At the cytogenetic level, ARMS is associated with minor genetic changes. These include the specific chromosomal translocations t(2;13)(q35;q14) and t(1;13)(p36;q14) (Turc-Carel *et al*, 1986; Galili *et al*, 1993), as well as genomic amplification of genes such as *MDM2* (Forus *et al*, 1993), *MYCN* (Driman *et al*, 1994; Gil-Benso *et al*, 2003) and *CDK4* (Berner *et al*, 1996). In contrast, ERMSs frequently contain whole chromosome alterations. Gain of chromosomes 2, 8, 12, and 13 have all been observed in ERMS (Weber-Hall *et al*, 1996). ERMS is often associated with loss of heterozygosity of 11p15.5 and presumably loss of the tumour suppressor gene located there (Gil-Benso *et al*, 2003). Lu and colleagues (2001) performed reverse transcription-polymerase chain reaction (RT-PCR) analysis of the *MYCN* locus (2p24) in numerous RMS patients and found that 66% of ERMS and 88% of ARMS patient samples over-expressed *MYCN*. The investigators speculated that *MYCN* provides an important survival signal to the RMS cells (Table 2).

The tumour suppressor activity of p53 is lost in roughly half of all human cancers, through mutations in p53 and alteration of upstream and downstream components of the p53 pathway (Steele *et al*, 1998). The p53 pathway regulates the induction of cell cycle arrest and apoptosis in cells, and the loss of p53 activity is generally associated with aggressive tumours. Some Li-Fraumeni families carry mutations in the *p53* gene and are predisposed to tumours, including RMS (Strong *et al*, 1992). MDM2 protein has been shown to ubiquitinate p53, resulting in the degradation of p53. The *MDM2* gene is amplified in a large proportion of RMS cases (Forus *et al*, 1993). Keleti and colleagues (1996) inferred that the majority of RMS cases have a disruption in the p53 pathway.

1.3. ARMS-specific chromosomal translocations:

ARMS is characterised in 70% of cases by the translocation t(2;13)(q35;q14) that juxtaposes a truncated *PAX3* gene on chromosome 2 with the 3′ sequences of the forkhead (*FKHR*) gene on chromosome 13 (Turc-Carel *et al*, 1986; Galili *et al*, 1993; Shapiro *et al*, 1993). This hybrid gene codes for a novel chimeric transcription factor that retains the paired box (PB) and homeodomain (HD) DNA-binding domains of the

Table 1. The histological and clinical features of the two RMS subtypes. The data is taken from Pappo *et al* (1995), Anderson *et al* (1999), and Barr (2001).

	Embryonal RMS	Alveolar RMS
Histology:	- Spindle cell and botryoid variants. - Uniform chromatin distribution.	- Hyperchromatic nuclei. - Cellular architecture resembling alveolar spaces in the lungs. - Recently described solid alveolar variant form.
Prognosis:	More favourable prognosis.	Poor prognosis, in part due to being more metastatic at presentation.
Age of patients:	Typically presents in children less than 10 years old.	Presents in adolescents and young adults.

Table 2. The cytogenetic features of the two RMS subtypes. The data is taken from Anderson *et al* (1999), Gil-Benso *et al* (2003) and Tiffin *et al* (2003).

	Embryonal RMS	Alveolar RMS
Major chromosome alterations:	- Whole chromosome gains/losses. - Loss of heterozygosity at 11p15.5.	- Chromosome translocations. - Genomic amplification.
Wild type *PAX3* expression:	~ 50%	~ 50%
***PAX-FKHR* fusions:**	-	- 70% PAX3-FKHR t(2;13)(q35;q14;) - 10-20% PAX7-FKHR t(1;13)(p36;q14)
p53 mutation/ *MDM2* amplification	+	+
***MYCN* amplification:**	+	+

PAX3 protein fused in frame to the bisected DNA-binding domain and intact transactivation domain of FKHR (Figure 1) (Galili *et al*, 1993; Shapiro *et al*, 1993).

A variant translocation, t(1;13)(p36;q14), has also been detected in a small subset (9-20%) of ARMS (Douglass *et al*, 1991). In these cases, the N-terminal PAX7 DNA-binding domains are fused to the C-terminus of FKHR (Biegel *et al*, 1991; Davis *et al*, 1994). ARMS associated with t(1;13) is typically less aggressive and has a better prognosis than the t(2;13) ARMS subset (Kelly *et al*, 1997; Sorensen *et al*, 2002).

The ARMS-specific chromosomal translocations are somatic genetic events. The cancer cell is heterozygous for the translocation, so also codes for wild type PAX3/7 and FKHR proteins.

1.4. Tumour-specific chromosome translocations:

Chromosomal translocations are seen frequently in human cancers. There are many examples of translocations in leukaemias (the prototype example is the BCR-ABL fusion associated with the t(9;22) Philadelphia chromosome of chronic myeloid leukaemia) (Rabbitts, 1994). Translocations are also seen in paediatric sarcomas, including the EWS/FLI-1 fusion protein found in Ewing's sarcoma (May *et al*, 1993), and the PAX3-FKHR fusion protein which is a hallmark of ARMS (Turc-Carel *et al*, 1986; Shapiro *et al*, 1993).

Chromosome translocations lead to tumourigenesis via two main mechanisms: (i) inserted activation, where the translocated gene is placed under the control of an active expression element of another gene. This results in the activation of protooncogenes; and more commonly (ii) gene fusion, where the translocation juxtaposes portions of two unrelated genes, generating a novel tumour-specific fusion protein (Rabbitts, 1994). Tumour-specific chromosome translocations that encode chimeric transcription factors (such as EWS/FLI-1 and PAX3-FKHR) are examples of the latter mechanism, and are thought to exert their oncogenic effects through the dysregulation of gene expression (Barr, 1998). For example, the chimeric EWS/FLI-1 transcription factor is oncogenic through a gain of function. EWS/FLI-1 is able to transform cells in culture and is a more potent transcriptional activator than FLI-1 (May *et al*, 1993).

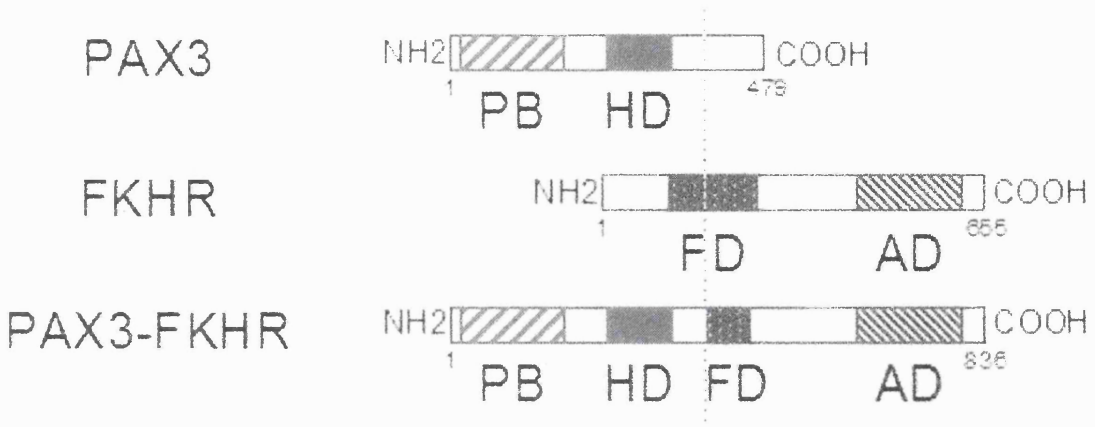

Figure 1. The structure of PAX3, FKHR, PAX3-FKHR proteins. The wild type PAX3 protein contains paired box (PB) and homeodomain (HD) DNA-binding domains separated by an octapeptide motif. Wild type FKHR contains a forkhead DNA-binding domain (FD) and a transcriptional activation domain (AD). The PAX3-FKHR fusion protein contains the N-terminal PAX3 DNA-binding motifs fused to the bisected FD and intact AD of FKHR.

It is important to note that peptide sequences derived from the rearrangement site of fusion proteins generated by chromosomal translocations are tumour-specific. Such unique tumour antigens are potential targets for immunotherapeutic strategies (Rabbitts, 1994).

1.5. PAX3:

1.5.1. Paired Box gene family:

PAX3 and PAX7 are members of the paired box (PAX) family of transcription factors. All 9 human PAX family proteins contain a PB DNA-binding domain and play fundamental roles during early embryogenesis as basic pattern forming genes (Goulding *et al*, 1991). PAX3, 6 and 7 are grouped into a subfamily, all containing a HD in addition to the PB (reviewed by Read, 1995; Stuart and Gruss, 1995).

When aberrantly expressed, most *PAX* genes have oncogenic potential. Maulbecker and Gruss (1993) reported that over-expression of PAX family proteins in transfected mouse NIH 3T3 fibroblasts leads to transformation in culture and tumour formation in mice. Furthermore, aberrant expression of a number of *PAX* genes has been correlated with different human tumours. For instance, PAX2, PAX3, and PAX5 have been found at high levels in Wilms tumour (Dressler and Douglass, 1992), RMS (Schafer *et al*, 1994; Tiffin *et al*, 2003), astrocytoma (Stuart *et al*, 1995), respectively.

Several of the *PAX* genes have a role in Mendelian syndromes. For instance, the human condition Waardenburg syndrome (WS) is due to a loss of function mutation in *PAX3* (Baldwin *et al*, 1992; Tassabehji *et al*, 1993; Baldwin *et al*, 1995), and aniridia is caused by a loss of function mutation in *PAX6* (Axton *et al*, 1997).

1.5.2. The role of PAX3 in embryogenesis:

PAX3 is normally expressed during early embryogenesis, primarily in early neurogenesis within the neural crest cell lineage, as well as in muscle precursors in the dermomyotome of the somites (Goulding *et al*, 1991; Bober *et al*, 1994). PAX3 plays an important role in the migration of myogenic progenitor cells during embryonic development and is therefore required for the development of proper limb musculature (Daston *et al*, 1996). Expression of PAX3 is tightly regulated, first expressed at embryonic day 8.5, and down-regulated by embryonic day 14.5, following muscle cell differentiation (Bober *et al*, 1994).

1.5.3. PAX3 mutations in splotch mice and human Waardenburg syndrome:

Homozygous 'splotch' mice have a loss of function mutation in *PAX3*, and do not synthesize normal PAX3 protein (Goulding *et al*, 1993). The splotch mice exhibit neural tube defects and fail to develop normal limb musculature as a result of impaired myogenic precursor migration (Epstein *et al*, 1991; Bober *et al*, 1994). In humans, *PAX3* mutations are responsible for WS type I and type III (Baldwin *et al*, 1995). WS is an autosomal dominant trait, characterised by a combination of deafness, dystopia canthorum (a minor facial malformation), musculoskeletal abnormalities, and pigmentation disturbances of the skin, eye or hair (Baldwin *et al*, 1992; Tassabehji *et al*, 1993; Baldwin *et al*, 1995). Some of these symptoms are the result of faulty migration or differentiation of PAX3-expressing precursors derived from the neural crest during development (Tassabehji *et al*, 1993).

1.6. FKHR:

FKHR (FOXO1) is a member of the mammalian FKHR family of transcription factors (recently renamed forkhead box, class O; FOXO*)* that also includes FKHRL1 (FOXO3a) and AFX (FOXO4). The mammalian FKHR family are homologous to the DAF-16 FKHR-type transcription factor found in *Caenorhabditis elegans*, and are characterised by a conserved FKHR DNA-binding domain, termed a winged helix (reviewed by Burgering and Kops, 2002). Members of the FKHR transcription family are widely expressed in mouse embryo and adult tissues (Furuyama *et al*, 2000). The FKHR family, like the PAX family, plays an important role during embryogenesis (Weigel *et al*, 1989; Hromas and Costa, 1995).

FKHR family members regulate the expression of insulin responsive genes. Guo and colleagues (1999) noted that FKHR transactivates insulin like growth factor binding protein1 (*IGFBP-1*) through binding to the insulin response sequence (IRS) in the *IGFBP-1* promoter. Furuyama *et al* (2000) found that mammalian FKHR family transcription factors are able to bind target genes containing DAF-16 family protein-binding elements (DBEs) with a stronger affinity than they bind to IRSs. FKHR transcription factors have been shown to play a role in promoting growth arrest and apoptosis (Dijkers *et al*, 2000; Schmidt *et al*, 2002; Gilley *et al*, 2003). The transcriptional activity of FKHR members is regulated by the serine/threonine kinase Akt (protein kinase B) (Brunet *et al*, 1999; Del Peso *et al*, 1999; Kops *et al*, 1999). Del Peso and colleagues (1999) showed that Akt inhibits the transcriptional activity of

FKHR via phosphorylation. The investigators infer that Akt-directed phosphorylation of FKHR retains the transcription factor in the cytoplasm, thereby repressing its ability to target DNA sequences (which are located in the nucleus).

1.7. The role of PAX3-FKHR in the pathological progression of ARMS:

1.7.1. The oncogenic potential of PAX3-FKHR:

Several investigators have provided evidence that the chimeric PAX3-FKHR transcription factor has oncogenic properties.

Davis and Barr (1997) demonstrated that PAX3-FKHR and PAX7-FKHR fusion proteins are over-expressed (relative to wild type PAX3/7 levels), in t(2;13) and t(1;13) subsets of ARMS, respectively. Interestingly, the two chimeric transcription factors are over-expressed by independent mechanisms. PAX7-FKHR over-expression is a result of gene fusion amplification, whereas PAX3-FKHR over-expression is copy number independent, instead resulting from increased transcription. The investigators concluded that expression of PAX3-FKHR and PAX7-FKHR above a threshold level is critical for the fusion proteins to have oncogenic effects.

Bernasconi and colleagues (1996) reported that specific down-regulation of the PAX3-FKHR fusion protein in the ARMS cell line RH30 using anti-sense oligonucleotides triggers the induction of apoptosis. The ERMS cell line RD does not express the PAX3-FKHR fusion protein but does have elevated levels of wild type *PAX3* mRNA in comparison to primary human myoblasts. The treatment of RD cells with anti-sense oligonucleotides targeting *PAX3* resulted in reduced cellular viability. The investigators concluded that both PAX3 and PAX3-FKHR provide a vital cell survival signal in RMS cells. In subsequent studies, Margue *et al* (2000) demonstrated that PAX3 and PAX3-FKHR stimulate transcription of endogenous *BCL-XL* mRNA in RMS cells. BCL-XL is a prominent anti-apoptotic protein, inferring that PAX3 and PAX3-FKHR proteins protect RMS cells from apoptosis, at least in part, through direct transcriptional activation of *BCL-XL.*

Ayyanathan and colleagues (2000) repressed the transcription of PAX3 and PAX3-FKHR target genes by generating and using a conditional PAX3 repressor. To engineer this, they fused the PAX3 DNA-binding elements to the KRAB repressor domain and the hormone binding domain of the oestrogen receptor. The KRAB domain represses

transcription by recruiting the KAP-1 co-repressor. Attaching the PAX3-KRAB repressor to the hormone-binding domain of the oestrogen receptor allows the repressor to be in an active form only in the presence of the ligand tamoxifen. The investigators stably transfected the ARMS cell line RH30, which expresses endogenous PAX3 and PAX3-FKHR, with the conditional PAX3 repressor and demonstrated that it inhibited the transcription of PAX3 targets in a tamoxifen-dependent manner. *In vitro* growth assays revealed that repression of PAX3 and PAX3-FKHR in RH30 results in reduced cellular viability in low serum conditions. The RH30 cells stably transfected with the conditional PAX3 repressor were then used in tumour xenograft experiments. SCID mice were injected with these RH30 cells, and after a 10 day period to establish tumour growth, half the mice were treated with tamoxifen. In the presence of tamoxifen, the active PAX3-KRAB repressor caused a significant reduction in tumour size relative to mice not receiving tamoxifen. These results clearly demonstrate that PAX3-KRAB expression repressed transcription of PAX3 and PAX3-FKHR targets, resulting in the suppression of RH30 cell tumourigenesis *in vivo*. The results found using the conditional PAX3-KRAB repressor corroborate the results found when repressing PAX3 and PAX3-FKHR with antisense oligonucleotides.

Scheidler and colleagues (1996) showed that *PAX3-FKHR* transforms chicken embryo fibroblasts (CEFs), with the cells acquiring the ability of anchorage-independent growth *in vitro*. However, when injected into the wingweb of newly hatched chickens, the PAX3-FKHR-expressing retrovirus did not lead to the formation of tumours *in vivo*. This suggests that additional genetic changes are required for tumour induction. In contrast, *PAX3* is unable to transform cells in culture, under identical conditions (Scheidler *et al*, 1996; Lam *et al*, 1999).

1.7.2. Comparing PAX3-FKHR and wild type PAX3 protein functions:

A lot of information on the tumourigenic role of the PAX3-FKHR fusion protein has come from experiments comparing the functional properties of PAX3-FKHR and wild type PAX3 proteins, since the bisected FKHR DNA-binding domain in PAX3-FKHR would not be predicted to contribute to target gene recognition (Sublett *et al*, 1995).

PAX3 contains both PB and HD DNA-binding elements, which bind DNA in a sequence-specific manner. It has been shown that PAX3 can specifically bind to the DNA sequence e5, found in the promoter of the *EVE* gene of *Drosophila melanogaster*

(Goulding *et al*, 1991), which contains adjacent PB domain (GTTCC) and HD (ATTA) consensus binding sites. Binding to the e5 target sequence serves as a useful indicator of the functional DNA-binding properties of PAX proteins. Fredericks and colleagues (1995) performed electrophoretic mobility shift assays (EMSAs) to compare the DNA-binding potential of PAX3-FKHR and PAX3 proteins to the e5 DNA sequence. PAX3-FKHR retains the PAX3-derived PB and HD motifs, and was found to bind e5 target sequences. However, wild type PAX3 bound to e5 with an affinity three times stronger than PAX3-FKHR. The authors speculate that the reduced binding affinity is a result of the N-terminal FKHR region interfering with the binding of the PAX3-derived HD. In subsequent transient co-transfection experiments, the investigators measured the ability of PAX3-FKHR and wild type PAX3 to activate transcription of an e5 target sequence-driven CAT reporter gene. They found that PAX3-FKHR is a far more potent transcriptional activator than wild type PAX3, despite having impaired DNA-binding affinity. Fredericks and colleagues (1995) postulate that the chimeric PAX3-FKHR transcription factor might be oncogenic as a result of excessive activation of normal PAX3 target genes.

Similarly, Bennicelli and colleagues (1996) performed transient co-transfection experiments in three different cell lines, using various expression constructs, to examine the transactivation potency of PAX3 and PAX3-FKHR proteins. PAX3-FKHR was approximately 100 fold more potent than PAX3 at activating the e5 target sequence-specific reporter construct and the PRS9 DNA-binding site reporter construct (containing 6 direct repeats of the PB and HD consensus recognition sequences) in NIH 3T3 murine fibroblasts. The authors suggest that this PAX3-FKHR gain of function results from switching the C-terminal PAX3 activation domain for the structurally distinct C-terminal FKHR-derived activation domain, which is relatively insensitive to the inhibitory effects of N-terminal PAX3 domains.

Lam and colleagues (1999) retrovirally infected NIH 3T3 fibroblasts with PAX3, PAX3-FKHR and specific mutant derivatives to determine the domains vital for PAX3-FKHR-mediated oncogenicity. The PAX3-derived HD and FKHR-derived transactivation domain were absolutely required for cellular transformation, with specific mutants lacking these domains unable to transform 3T3 cells. Lam *et al* (1999) further demonstrated that retroviral expression of the FKHR portion of PAX3-FKHR in 3T3 fibroblasts does not cause cellular transformation. Surprisingly, retroviral

expression of PAX3-FKHR mutants, with impaired PB-mediated DNA binding ability, retain their cellular transformation properties promoting anchorage independent cell growth. This clearly demonstrates that DNA binding through the PAX3-derived PB is not required for PAX3-FKHR-mediated cellular transformation.

Overall, several studies (Fredericks *et al*, 1995; Bennicelli *et al*, 1996) suggest that the chimeric PAX3-FKHR transcription factor exerts its oncogenic role in ARMS through the dysregulation of normal PAX3 target genes. However, more recently Epstein *et al* (1998) discovered that PAX3-FKHR can directly induce transcription of the platelet-derived growth factor alpha receptor (PDGFαR) gene, while PAX3 can not do so under identical conditions. Co-transfection experiments with mutant *PAX3-FKHR* DNA constructs demonstrated that the HD is the only PAX3-FKHR-derived DNA-binding domain vital for transactivation of the PDGFαR promoter constructs. Several explanations have been proposed for how PAX3-FKHR is able to transactivate PDGFαR whilst wild type PAX3 can not do so, despite possessing exactly the same HD DNA-binding motif. Epstein *et al* (1998) speculate that PAX3-FKHR and PAX3 have equal DNA-binding abilities, but PAX3-FKHR has superior ability to transactivate the PDGFαR gene once bound, possibly due to a different structural configuration of the fusion protein or an inability of PAX3-FKHR to bind an unknown PAX3 repressive cofactor. The authors infer that the oncogenicity of PAX3-FKHR is dependent on both protein-DNA and protein-protein interactions mediated through the PAX3 HD recognition helix. Cao and Wang (2000) postulate that in wild type PAX3, the PB and HD are functionally interdependent, requiring binding of both DNA-binding domains to target DNA sequences to facilitate transcriptional activation. However, there is an uncoupling of the PB and HD interdependency in PAX3-FKHR. This is the result of interchanging the PAX3 transactivation domain for a FKHR transactivation domain, removing the inhibitory actions of the PAX3 transactivation domain.

The discovery that PAX3-FKHR can activate a gene not normally activated by wild type PAX3 is evidence that that the oncogenic role of PAX3-FKHR is more complex than previously thought. Hollenbach and colleagues (1999) investigated the interaction of PAX3 and PAX3-FKHR proteins with the transcriptional repressor DAXX. Co-immunoprecipitation experiments of COS1 cells over-expressing PAX3 and DAXX proteins revealed that DAXX can interact with PAX3 *in vivo*. PAX3 deletion mutant experiments revealed that the PAX3 HD recognition helix and octapeptide domain are

required for the interaction with DAXX. DAXX was found to inhibit the ability of PAX3 to transactivate the PRS9-CAT reporter gene by roughly 80%. Whilst DAXX was found to interact with PAX3-FKHR *in vivo*, it only exerted a minimal repressive action on the transcriptional activity of the fusion protein (less than 25% inhibition). The authors propose the following two potential mechanisms to explain how PAX3-FKHR is unresponsive to the repressive action of DAXX: (i) the fusion protein contains a potent FKHR transactivation domain that is able to recruit transcriptional machinery and drive transcription of target genes, overriding the repressive efforts of DAXX; (ii) the FKHR domain may cause steric hindrance of DAXX. This hindrance does not prevent the interaction of PAX3-FKHR with DAXX, but may prevent the recruitment of other factors required for DAXX-mediated transcriptional repression.

1.7.3. Additional experiments investigating the effects of PAX3-FKHR on cell phenotype:

Epstein *et al* (1995) reported that PAX3 and PAX3-FKHR expression in cultured myoblast cells inhibits myogenic differentiation. Culturing the C2C12 myoblast cell line in low serum condition induces differentiation in approximately 90% of cells, as assessed by myosin expression. However, a lower percentage of C2C12 cells stably transfected with *PAX3* and *PAX3-FKHR* undergo myogenic differentiation after exposure to low serum (only 43% and 27% of cells express myosin, respectively). Furthermore, the introduction of a WS mutation into the PB of PAX3 abrogates the inhibition of myogenesis. C2C12 cells transfected with PAX2, which does not contain an intact HD, differentiate when cultured in low serum conditions. These assays suggest that intact PB and HD DNA-binding elements are required for the PAX3 and PAX3-FKHR anti-myogenic effect (Epstein *et al*, 1995). This inhibition of myogenic differentiation may be an important part of the RMS phenotype, maintaining the cells in a permanent primitive myoblastic state with proliferative potential (Khan *et al*, 1999). Anderson *et al* (2001a) reported that ectopic expression of PAX3-FKHR in the PAX3-expressing ERMS cell line RD results in increased growth rate in serum-starved conditions, *in vitro*. The RD cells stably transfected with *PAX3-FKHR* or empty vector were next examined in tumour xenograft experiments. Tumours derived from RD cells stably transfected with *PAX3-FKHR* were found to grow faster and be more locally invasive than tumours derived from RD cells transfected with empty vector. The authors concluded that PAX3-FKHR is directly responsible for the more aggressive tumour phenotype associated with ARMS.

Zhang and Wang (2003) similarly observed an elevated proliferative rate of fibroblasts ectopically expressing PAX3-FKHR. The investigators went on to examine the mechanisms involved in altering the cell cycle pathway that lead to elevated growth rate in PAX3-FKHR-expressing cells. They found that over-expression of PAX3-FKHR accelerates the G_0/G_1 to S cell cycle transition by degrading $p27^{Kip1}$ protein, an important cell cycle inhibitor, via the ubiquitin-dependent 26S proteasome pathway. Restoring $p27^{Kip1}$ expression to normal levels abolishes the hyperproliferative properties of the PAX3-FKHR-transformed fibroblasts, demonstrating that destabilization of $p27^{Kip1}$ protein is an active mechanism in PAX3-FKHR-mediated transformation.

Anderson *et al* (2001b) generated transgenic mice expressing the PAX3-FKHR fusion protein under the control of a *PAX3* promoter. They found that expression of PAX3-FKHR fusion protein in the mouse embryo interfered with the normal PAX3 functions, such as neural crest migration, and competed with PAX3 for transcriptional targets *in vitro*. However, PAX3-FKHR expression did not lead to tumour formation *in vivo*, suggesting that PAX3-FKHR expression is not sufficient for tumourigenesis. In contrast, similar translocations found in leukaemias do not require additional genetic changes to elicit tumourigenesis (Rabbitts, 1994). Anderson and colleagues (2001b) postulate that PAX3-FKHR disrupts normal PAX3 developmental functions as a prelude to transformation. Lagutina *et al* (2002) generated PAX3-FKHR knock-in mice by homologous recombination of PAX3-FKHR into the mouse *PAX3* locus. Consistent with data from PAX3-FKHR transgenic mice, the newborn heterozygous and parental chimeric PAX3-FKHR knock-in mice did not form muscle tumours. Despite the low level of expression of PAX3-FKHR, the chimeric knock-in mice and their heterozygous offspring showed phenotypic abnormlities, such as cardiac and respiratory failure, which were very different from those detected in splotch mice (Goulding *et al*, 1993; Bober, 1994). Lagutina *et al* (2002) concluded that the PAX3-FKHR knock-in allele caused lethal development defects that could be explained by a dominant negative effect of PAX3-FKHR on PAX3 function in cardiac neural crest-derived cells.

The t(2;13)(q35;q14) product is under the control of the 5′ *PAX3* promoter, yet does not appear to be expressed in a PAX3 regulated manner, as PAX3 is not expressed beyond embryonic day 14.5. The 3′ *FKHR* sequences might promote transcription of the hybrid gene, though little data is published on this subject.

1.7.4.Nuclear localisation of PAX3-FKHR:

In all reports to date, PAX3-FKHR has been found exclusively in the nucleus of cells. For instance, retroviral expression of PAX3-FKHR protein in CEFs and NIH 3T3 murine fibroblasts results in PAX3-FKHR localisation in the nucleus (Scheidler *et al*, 1996; Lam *et al*, 1999). Fredericks *et al* (1995) detected PAX3-FKHR fusion protein solely in the nuclear extract of RH30 cells, a human ARMS cell line with the translocation t(2;13)(q35;q14). Akt has been shown to phosphorylate FKHR, resulting in the localisation of FKHR in the cytoplasm where FKHR is unable to bind nuclear partners and target DNA sequences. Two of the three phosphorylation sites found in the FKHR protein are retained in the PAX3-FKHR fusion protein. Nonetheless, Akt is unable to prevent the nuclear localisation of PAX3-FKHR (Del Peso *et al*, 1999). The constitutive nuclear localisation of PAX3-FKHR might contribute to the oncogenic potential of the chimeric transcription factor.

It is important to note that the t(2;13)(q35;q14) is a reciprocal translocation. The above studies suggest that the PAX3-FKHR fusion protein has oncogenic activity. In contrast, the reciprocal FKHR-PAX3 fusion protein is assumed to have no functional properties because the fusion protein has no intact DNA-binding domain. Furthermore, FKHR-PAX3 is expressed in only a small proportion of RMS cases.

1.8. Target genes of wild type PAX3 and the chimeric PAX3-FKHR fusion protein:

1.8.1. PAX3 target genes:

The PAX3 PB and HD DNA-binding consensus sequences have been found in the 5′ promoter region of numerous genes. EMSAs and transient transfection experiments using target gene promoter-luciferase reporter constructs have confirmed the induction of several genes by PAX3, including microphthalmia-associated transcription factor (*MITF*) (Watanabe *et al*, 1998), the gene encoding the tyrosinase-related protein-1 (TRP-1) (Galibert *et al*, 1999), neural cell adhesion molecule (*NCAM*) (Watanabe *et al*, 1998; Mayanil *et al*, 2000), *STX* (Mayanil *et al*, 2001), and *BCL-XL* (Margue *et al*, 2000).

The receptor for hepatocyte growth factor (HGF)/scatter factor (SF) is encoded by the protooncogene *c-MET*, and has been shown to be required for limb muscle development during embryogenesis (Bottaro *et al*, 1991; Bladt *et al*, 1995). Epstein and colleagues (1996) reported that expression of the product of the *c-MET* protooncogene is abolished

in the limb muscle progenitor cells of PAX3-deficient splotch mice embryos. Transfection of *PAX3* into C2C12 myoblasts has been shown to up-regulate the expression of *c-MET*, and 4 out of 5 tested human RMS cell lines expressed detectable levels of *c-MET*. Co-transfection assays revealed that PAX3 transactivates a luciferase reporter gene under the control of the *c-MET* promoter. Epstein *et al* (1996) concluded that *c-MET* is a direct target of PAX3 during limb muscle development and in RMS. Whether PAX3-FKHR also up-regulates *c-MET* is contentious (Khan *et al*, 1999).

MyoD and MYF-5, two myogenic basic-helix-loop-helix transcription factors, regulate skeletal muscle lineage determination in vertebrates (Molkentin and Olson, 1996; Kucharczuk *et al*, 1999). *PAX3* and *MYF-5* double knock out mice fail to activate *MyoD* and lack trunk and limb musculature (Tajbakhsh *et al*, 1997). In contrast, *PAX3* and *MYF-5* single knock out mice are able to activate *MyoD* during development and exhibit normal muscle phenotype. These findings suggest that PAX3 and MYF-5 function in parallel pathways upstream of MyoD during myogenesis.

1.8.2. PAX3-FKHR target genes:

cDNA microarray analysis is a relatively new technology that provides a unique opportunity to examine the expression of thousands of genes (DeRisi *et al*, 1996; DeRisi *et al*, 1997). Gene expression profiling of human cancers has the potential to reveal genes highly expressed in certain cancers, which might be used for diagnostic purposes or as therapeutic targets, and also to elucidate the role of oncogenes in tumourigenesis (DeRisi *et al*, 1996).

Khan *et al* (1998) used cDNA microarray analysis to examine global gene expression in ARMS, comparing RNA collected from 7 ARMS cell lines, all endogenously expressing PAX3-FKHR, to several reference cell lines. They identified 37 genes expressed at elevated levels in 4 or more of the 7 ARMS cell lines relative to control cell lines. Three of the genes had previously been shown to be elevated in ARMS, namely *PAX3-FKHR* (Galili *et al*, 1993; Davis and Barr, 1997), *MYCN* (Driman *et al*, 1994; Lu *et al*, 2001) and *CDK4* (Berner *et al*, 1996). Numerous genes that Khan and colleagues (1998) found to be highly expressed in ARMS are involved in cellular proliferation, with genes such as the cyclin *CDC2* reported to be over-expressed in other cancer types (Keyomarsi and Pardee, 1993). The authors concluded that cDNA microarray analysis identified a gene expression pattern common to ARMS.

To investigate the role of the chimeric PAX3-FKHR transcription factor in oncogenesis, Khan and colleagues (1999) introduced *PAX3* and *PAX3-FKHR* into mouse NIH 3T3 fibroblasts by retroviral transduction and examined the gene expression changes by cDNA microarray analysis. They found that PAX3-FKHR, but not PAX3, had the ability to activate a myogenic transcription program, significantly up-regulating expression of the myogenic transcription factor genes *Myogenin* and *SIX1*, as well as numerous other muscle-related genes, such as insulin like growth factor 2 (*IGF2*) and its binding protein *IGFBP-5*. The investigators proposed a model whereby PAX3-FKHR contributes to the phenotype of ARMS by maintaining cells in a permanent primitive myoblastic state with proliferative potential, and a subsequent secondary genetic event leads to ARMS. This hypothesis is supported by data showing that the over-expression of PAX3 or PAX3-FKHR in cultured myoblast cells inhibits myogenic differentiation (Epstein *et al*, 1995).

1.9. Current mouse models of ARMS:

There are currently no mouse models that closely resemble ARMS. Takayama and colleagues (1997) generated transgenic mice expressing *HGF/SF* under the control of a metallothionein promoter to target *HGF/SF* expression to a wide variety of tissues. The forced mis-expression of HGF/SF induced aberrant development and the formation of a variety of tumour types, derived from both mesenchymal and epithelial origin. However, crossing these transgenic mice with $INK4a^{-/-}$ mice resulted in a very high incidence of RMS (Sharp *et al*, 2002).

Anderson *et al* (2001b) generated transgenic mice expressing a *PAX3-FKHR* transgene driven by the mouse *PAX3* promoter. However, the mice did not form tumours. Capecchi and colleagues (2003) have recently generated a conditional PAX3-FKHR knock-in mouse. Within one year, the mice reportedly develop muscle tumours that closely resemble human ARMS. Knock-in mice expressing *PAX3-FKHR* under the control of a *PAX3* promoter do not form muscle tumours (Lagutina *et al*, 2002), so investigating PAX3-FKHR expression in this new conditional PAX3-FKHR knock-in mouse model will shed light on the oncogenic role of the chimeric transcription factor in ARMS. Unfortunately, there is currently no published data about this conditional PAX3-FKHR knock-in mouse model.

1.10. Experimental aims:

There are three main aims of this project:

- Firstly, to generate a mouse RMS cell line that expresses elevated levels of PAX3-FKHR and forms tumours when injected into syngeneic mice. We hope to use this cell line to test the ability of tumour antigen-pulsed dendritic cells to specifically target and eliminate PAX3-FKHR-expressing tumour cells *in vivo* (described in Chapter 3).
- Secondly, comparing mouse RMS cells expressing PAX3-FKHR to mouse RMS cells expressing empty vector, we hope to identify genes that are up-regulated by PAX3-FKHR and can be targeted using directed immunotherapy for the treatment of ARMS.
- Finally, to investigate the oncogenic actions of PAX3-FKHR in RMS cells by comparing mouse RMS cells expressing PAX3-FKHR to mouse RMS cells expressing empty vector.

We chose to examine the target genes of PAX3-FKHR in the mouse RMS cell line called 76-9 for two reasons. Firstly, ectopic expression of PAX3-FKHR in 76-9 cells results in increased local invasive ability, a characteristic of the highly metastatic ARMS subtype (Anderson *et al*, 1999a). Secondly, a large proportion of ARMSs also express elevated levels of wild type PAX3 or PAX7 (Tiffin *et al*, 2003), and stimulation of a myogenic pathway might not be a physiologically important role of PAX3-FKHR.

We generated clones of 76-9 RMS cells stably transfected with a *PAX3-FKHR* expression construct. A matrigel invasion assay demonstrated that PAX3-FKHR significantly increased the invasive ability of 76-9 cells. Sub-cutaneous injection of PAX3-FKHR-expressing 76-9 cells into syngeneic mice resulted in the formation of tumours that express *PAX3-FKHR* mRNA. This is therefore a suitable mouse model of ARMS for testing immunotherapeutic strategies. The target genes of PAX3-FKHR in 76-9 cells were determined by comparing the global mRNA profile of cells transfected with empty vector with two independent clones transfected with PAX3-FKHR, using oligonucleotide microarray expression profiling. We found that PAX3-FKHR significantly up-regulated 31 genes and down-regulated 69 genes, by more than 2 fold. Published data suggests that none of the genes significantly induced by PAX3-FKHR are putative tumour-specific antigens suitable for directed immunotherapy. Nonetheless, several of the regulated genes, including the known PAX3-FKHR target *IGF2*, have

putative roles in cell proliferation, angiogenesis and metastagenesis. Moreover, a large proportion of the identified genes were found to be known IFN-γ targets. Our findings suggest that PAX3-FKHR negatively interferes with IFN-γ induced transcription in human and mouse RMS cells. We have shown for the first time that an oncogenic fusion protein interferes with basal IFN-γ signalling, and we propose that this contributes to the ARMS phenotype.

2. Methods and Materials

2.1. Cloning and expression constructs:

2.1.1 Expression plasmids:

A *PAX3-FKHR* mixed murine/human cDNA, which uses the second ATG start site of *PAX3*, was a gift from J. Epstein (University of Pennsylvania, USA). J. Anderson had previously inserted the *PAX3-FKHR* cDNA fragment into the pBK-CMV vector (Stratagene, USA), to give high level *PAX3-FKHR* expression under the control of the cytomegalovirus (CMV) immediate early gene promoter (Anderson *et al*, 2001a). This construct is called pBK-CMV-P3F (Figure 2). To generate an alternative expression construct, Anderson *et al* (2001a) inserted the 7 Kb MyoD enhancer sequence (Kucharczuk *et al*, 1999) upstream of *PAX3-FKHR* in the pBK-CMV plasmid. This vector is called pBK-MyoD-P3F.

The PRS9-chloramphenicol acetyl transferase (PRS9-CAT) plasmid was a gift from J. Bennicelli (University of Pennsylvannia, USA), and contains six direct repeats of the *PAX3* PB and HD consensus binding sequences upstream of a CAT reporter gene. The PRS9-CAT reporter construct was used in transient transfection experiments to determine the level of activity of PAX3 and PAX3-FKHR protein in our RMS cell lines.

The IGFBP-1-luciferase construct was a kind gift from T. Unterman (University of Illinois, USA) and contains the human *IGFBP-1* promoter upstream of a luciferase reporter gene (Guo *et al*, 1999). Two BIM reporter constructs were kindly donated by J. Gilley. The BIM-luciferase reporter consists of the 5.2 Kb region 5′ to the *BIM* initiation codon inserted upstream of a luciferase reporter gene. The mutant BIM-luciferase reporter contains mutations in both the FKHR binding sites of the BIM-luciferase reporter, which completely abrogates FKHR binding to the mutant *BIM* promoter (Gilley *et al*, 2003). The *c-MET* promoter-luciferase reporter gene was a gift from P. Scambler (Institute of Child Health, UK), and M. Tachibana (National Institutes of Health, USA) donated the *MITF* promoter-luciferase reporter construct.

To normalise for transfection efficiency, pGL3-Control luciferase and pSV-β-galactosidase control vectors (both from Promega, USA) were used. To allow selection for transfected cells in a mixed population, the cell lines were co-transfected with the

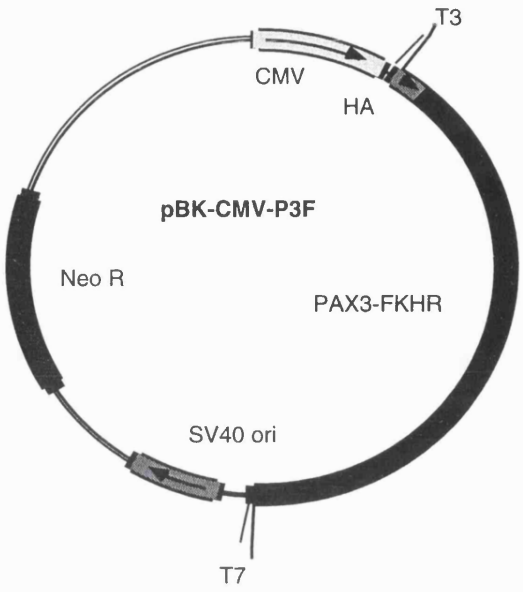

Figure 2. Map of the pBK-CMV-P3F phagemid vector. The PAX3-FKHR mixed murine/human cDNA, containing a hemagglutinin (HA) tag at its 5′ terminus, was cloned into the multiple cloning site of the pBK-CMV phagemid vector (Stratagene). In this vector, eukaryotic expression of PAX3-FKHR is driven by the CMV early gene promoter, and a SV40 polyadenylation cassette provides the signal required for the termination of transcription and polyadenylation. The presence of the neomycin resisitance gene allows cells stably transfected with the vector to be selected for their resistance to G418. The vector is also suitable for *in vitro* transcription of the PAX3-FKHR sequence with T3 and T7 RNA polymerase.

pCMS-EGFP vector (Clontech, USA) that contains a SV40 promoter/enhancer upstream of the green fluorescent protein (GFP) gene.

2.1.2. Growing up large quantities of plasmid DNA:

Large amounts (20µg-1mg) of the above listed DNA constructs were grown up in JM109 Competent *Escherichia coli* Cells (Promega). To transform JM109 Competent Cells with the plasmids, a standard transformation protocol was followed: approximately 50ng of DNA was added to 100µl of thawed competent cells and incubated at 4°C for 10-30 minutes. The cells were heat shocked for 30 seconds in a water bath at 42°C, and then immediately placed on ice for 2 minutes. Subsequently, 300µl of Luria-Bertani (LB) broth (without antibiotics) was added to the cells and incubated at 37°C with shaking (approximately 225 rpm) for 1 hour. Various volumes (20-200µl) of the cells were streaked out onto LB antibiotic plates, and incubated at 37°C overnight.

Up to 20 independent colonies were picked using sterile cloning loops, and each colony was used to inoculate 2ml of LB broth (containing the appropriate antibiotic: 100µg/ml of ampicillin, or 50µg/ml of kanamycin). For small scale preparations of DNA, the cells were incubated in 2ml of LB broth at 37°C with shaking overnight. For large scale preparations, the cells were incubated in 2ml LB broth for 3-4 hours at 37°C with shaking. This starter culture was then added to 200ml of LB broth (plus antibiotics) and incubated at 37°C with shaking for a further 24 hours. The bacteria cells were pelleted and the plasmid DNA extracted using QIAprep Spin Miniprep or HiSpeed Plasmid Maxi kits (both from Qiagen, UK), following the recommended protocols.

Finally, digestion of the miniprep or maxiprep plasmid DNA was performed to confirm that the correct plasmid was grown up and that no genetic rearrangements had occurred. Approximately 2-5µg of plasmid DNA was digested in a 30µl reaction, containing more than 1 unit of restriction enzyme per µg of DNA, 1× restriction enzyme specific buffer, and 1× bovine serum albumin (BSA) (all from Promega). The digestion reaction was incubated at 37°C for 1-3 hours and an aliquot electrophoresed on a TAE (Tris acetate EDTA)-agarose-ethidium bromide gel alongside a ladder of known DNA sizes (1 Kb Plus Ladder; Invitrogen, USA).

All standard laboratory chemicals were obtained from Sigma (UK) and all standard solutions were from BDH Laboratories (UK), unless stated otherwise.

2.2. Preparation of RNA, Northern blots, and RT-PCR:

2.2.1. Isolation of total RNA:

The RMS cell lines were harvested during their exponential phase of growth, at approximately 50-75% confluency. The cells were trypsinised and washed in phosphate buffered saline (PBS; Gibco, UK) (see *2.4.1.* for detailed methodology). 2×10^7 cells were pelleted by centrifugation at 130g for 5 minutes, dried throroughly and snap frozen to -70°C in dry ice-methanol freezing solution.

Total RNA was isolated from the frozen cells and mouse tissues using Trizol Reagent (Gibco), following the manufacturer's protocol. Briefly, 2×10^7 frozen cells were lysed in 3ml of Trizol Reagent by vigorous pipetting, whereas tissues isolated from C57BL/6 mice were homogenized in 1ml of Trizol Reagent per 100mg of tissue using a glass-Teflon homogeniser. The samples were incubated at room temperature for 5 minutes, then mixed with 0.2ml of chloroform per ml of Trizol Reagent, and incubated at room temperature for a further 2 minutes. The samples were centrifuged at 1,750g for 25 minutes at 4°C. The aqueous phase containing the RNA was transferred to a fresh tube, and mixed with 0.5ml of isopropanol per ml of Trizol Reagent, to precipitate the RNA. Following incubation at room temperature for 10 minutes, the samples were centrifuged at 1,750g for 30 minutes at 4°C. The supernatant was removed and the RNA pellet washed with 75% ethanol and centrifuged at 1,750g for 15 minutes at 4°C. The supernatant was removed and the RNA air dried, dissolved in RNase free water, quantified, and stored at -70°C.

Prior to use in Northern blots and RT-PCR reactions, the total RNA was treated with DNase I (Roche, USA) to remove residual genomic DNA. This was performed following the standard protocol (Sambrook *et al*, 1989). Briefly, 10µl of 0.1M Dithiothreitol (DTT), 20µl of 25mM $MgCl_2$, 3.3µl of 3M $NaC_2H_3O_2$ (pH 5.3), 0.5µl of RNasin RNase inhibitor (Promega), and 1µl of DNase I (Roche) were mixed, and added to 75µl of total RNA solution. The samples were mixed, and incubated at 37°C for 15-30 minutes. Next, the RNA was extracted twice with 100µl of Phenol:Chloroform:Isoamyl alcohol (25:24:1) (Sigma) and once with 100µl of

Chloroform, collecting the aqueous layer into a fresh tube after each phase separation (centrifugation at 15,800g for 2 minutes at 4°C). The RNA in the final aqueous layer was added to a new eppendorf tube and precipitated by adding 10µl of 3M $NaC_2H_3O_2$ (pH 5.3) and 250µl of 100% ethanol. The samples were mixed and incubated at -20°C for more than 30 minutes. The samples were centrifuged at 15,800g for 15 minutes at 4°C, washed in 75% ethanol, air dried, and resuspended in RNase free water.

The double distilled water used in all RNA experiments was RNase treated with diethyl pyrocarbonate (Sigma), and all equipment was treated with Rnase ZAP (Sigma) to remove trace RNases.

2.2.2. Northern blot analysis:

Total RNA was denatured in 2.2M formaldehyde and 50% formamide at 55°C for 15 minutes. After denaturation, the RNA was electrophoresed on 1% formaldehyde agarose gels, and transferred to Hybond N+ nylon membranes (Amersham Biosciences, UK) by capillary blotting. Following UV crosslinking, the membranes were prehybridised in Ultrahyb solution (Ambion, UK) with 0.1% denatured salmon testes DNA (Invitrogen), at 42°C for 30 minutes. The relevant denatured radioactively labelled DNA probe (see *2.2.2.1.*) was added to the prehybridisation solution and hybridised to the membrane overnight at 42°C. The blots were initially washed in a low stringency buffer, consisting of 2×SSC and 0.1% SDS, at 65°C for 30 minutes. If required, the membranes were subsequently washed in a high stringency buffer (0.2×SSC and 0.1% SDS) at 70°C. The membranes were then autoradiographed by exposing the membrane for 24-72 hours to X-ray film (BIOMAX MS film; Kodak, UK) at –70°C, or exposed on a phosphoimager screen overnight. The intensities of the bands were measured on the phosphoimager (Molecular Dynamics, UK), using ImageQuant software (Molecular Dynamics).

The membranes were stripped and re-probed a maximum of 3 times. The stripping protocol consisted of adding boiling 0.1% SDS to the membrane in a sealed container and incubating at room temperature until cooled. Following a rinse in 2×SSC, the removal of the probe was checked using a Geiger counter and by autoradiography. The stripped membrane was then prehybridised and hybridised with a different radio-labelled probe, as described earlier.

2.2.2.1. Radioactive labelling of the DNA probes:

The $^{\alpha 32}$P-labelled DNA probes were generated from RT-PCR amplified RNA templates. Total RNA collected from CMV and C23 cells were used as a template in the reverse transcription reactions (see *2.2.3.* for detailed methodology). Mac Vector 6.5.3 software was used to design primer combinations that specifically amplify 500-900bp sequences from the mRNA of target genes (identified in the microarray experiment) in PCR reactions. A blast search of the National Center for Biotechnology Information (NCBI) database was performed to check that the RT-PCR reaction would amplify a sequence that was unique for mRNA transcribed from the target gene. Mac Vector 6.5.3 was also used for the identification of potential FKHR consensus DNA-binding sequence (5′-GTAAACAA-3′) in the promoters of genes downstream of PAX3-FKHR.

The 50µl probe labelling reaction consisted of approximately 50ng of DNA in 1× Polymerase buffer, 1× BSA, 2.5 mM dNTP-c (all from Promega), and 2ng/ml random hexanucleotide primer (Invitrogen). The mixture was heated to 95°C for 5 minutes, then immediately cooled to 4°C for 3 minutes. 1µl of Klenow DNA Polymerase (Promega) and 3µl of $^{\alpha 32}$P-dCTP were then added to the 50µl reaction volume, mixed and incubated at room temperature overnight. Unincorporated $^{\alpha 32}$P-dCTP was removed using NucTrap Probe Purification Columns (Stratagene). The radio-labelled probe was denatured at 95°C for 5 minutes, immediately cooled on ice for 3 minutes, and added to the prehybridisation mix.

2.2.3. RT-PCR:

First strand synthesis reactions were performed using 4µg of DNase treated total RNA in a 40µl reaction volume. The reverse transcription reaction contained 0.1µg/µl of random hexanucleotide primer, 1× Reverse Transcription buffer, 0.5mM dNTP mix, 1mM DTT, 1µl of RNasin, and 200 units of SuperScript II reverse transcriptase (Gibco). The samples were incubated at 37°C for 60 minutes.

2µl of cDNA from the first strand synthesis reaction was used as the template for the PCR reaction, in a 50µl reaction volume. The PCR reaction contained 1× PCR buffer, 1.5mM $MgCl_2$, 0.2mM dNTP mix, 0.2µM 5′ and 3′ amplification primers (called P3F4 and FKHR1, respectively), and 2 units of *Taq* DNA polymerise (Promega). The PCR reaction samples were initially denatured at 94°C for 2 minutes, followed by 30 cycles

of 94°C for 30 seconds, 55°C for 30 seconds, and 72°C for 1 minute, finishing with an extension at 72°C for 10 minutes. A 10µl aliquot of each sample was electrophoresed on a 0.6-2% agarose gel. In negative control samples, no cDNA was added to the PCR reaction. In RT-PCR reactions amplifying *PAX3-FKHR* RNA, additional controls were performed to confirm that the *PAX3-FKHR* was amplified from RNA and not remaining genomic DNA. In these controls, the first strand cDNA synthesis was performed without SuperScript II reverse transcriptase, and then used as a template for the *PAX3-FKHR* PCR reaction.

A 5′ primer specific for a PAX3 sequence (5′-TTCCAGCTATACAGACAGCT-3′) and a 3′ primer specific for a FKHR sequence (5′-GGCCAGACTGGAGAGATGCT-3′) were used to amplify the 350bp PAX3-FKHR product. Primers specific for β-actin (5′-GAGCGGGAAATCGTCCGTGACATT-3′ and 5′-TTTGAACTCCCCGTTGGTCC-3′) amplified a 130bp product and were used to check for equal loading and integrity of the total RNA. All the primers were purchased for Sigma Genosys (UK).

2.3. Microarray analysis:

Each cell line was grown in triplicate cultures, and the three cell cultures were treated as independent samples. The CMV, C23 and C24 cell lines were harvested during their exponential phase of growth, at approximately 50-75% confluency. Total RNA was extracted from the cell lysates using the RNeasy mini kit (Qiagen), following the manufacturer's protocol exactly.

Preparation of biotin-labelled cRNA, hybridisation, and scanning were performed according to Affymetrix guidelines (Affymetrix, USA). Briefly, 12µg of total RNA was used as template for the synthesis of double-stranded cDNA, using SuperScript II reverse transcriptase and T7-$(dT)_{24}$ oligo primer (Invitrogen) in the first strand synthesis reaction. Following the second strand synthesis, the cDNA was used to synthesize biotin-labelled cRNA in an *in vitro* transcription reaction. The biotin-labelled cRNA was fragmented and hybridised to murine Affymetrix MG-U74 microarrays, consisting of more than 12,000 expressed sequences. The microarrays were then washed and scanned. Genespring 4.2.1 and Data Mining Tool were used to analyse the data.

2.4. Cell lines, transfections, and reporter assays:

2.4.1. Cell lines:

The mouse methylcholanthrene induced RMS cell line called 76-9 was a gift from R. Evans (Jackson Laboratories, USA), and was maintained in RPMI media supplemented with 10% fetal calf serum (FCS), 2mM glutamine, 100IU/ml penicillin and 100µg/ml streptomycin (all from Gibco). The human RMS cell lines RH30 and RH18 were a gift from P. Houghton (Saint Jude's Children's Research Hospital, USA), and J. Shipley (Institute of Cancer Research, UK) donated the human RMS cell lines RMS, RD, and SCMC. All the human RMS cell lines were grown in Dulbecco's Modified Eagle's Medium (DMEM) containing 10% FCS and the other components as listed above. All cell lines were cultured at 37°C in 5% CO_2 under sterile conditions.

The cell lines were grown in tissue culture dishes (TPP, Switzerland) and spit when the cells reached 90% confluency. The cell lines were split following a standard protocol, in which the adherent cells were washed in PBS, then covered in 1× trypsin (Gibco) and incubated at 37°C until fully detached (2-5 minutes). Once the cells had detached from the plastic, the cells were suspended in media and centrifuged at 130g for 5 minutes. After removing the supernatent, the cells were resuspended in media and replated at the required density.

The cells were tested for *Mycoplasma* infection several times per year. Cell lines contaminated with *Mycoplasma* were treated with 10µg/ml Ciproxin (Bayer, Germany) for three weeks, then with 8µg/ml Tylosin (Sigma) for 1 week.

2.4.2. Stable transfection of cells:

76-9 cells were stably transfected with pBK-CMV empty vector or pBK-CMV-P3F DNA using FuGENE 6 Transfection Reagent (Roche). The 76-9 cells were trypsinised, the number of viable cells calculated using a haemacytometer, and 1.5×10^5 cells plated out in 35mm culture dishes in 3 ml media. The cells were incubated at 37°C overnight, allowing them to adhere and start to proliferate. The cells were then transfected with the optimised ratio of 6µl of Fugene:2µg of DNA in 100µl of serum free RPMI, following the manufacturer's protocol. Cell transfectants containing pBK-CMV or pBK-CMV-P3F were selected for resistance to 500µg/ml G418 (Gibco), isolated as individual colonies using cloning loops, and expanded into cell lines. Early passages of clones

stably expressing empty vector or PAX3-FKHR were frozen down in RPMI containing 10% FCS, supplemented with 10% dimethyl sulphoxide (DMSO) (Sigma), and stored in liquid nitrogen. To re-culture, the frozen down cells were thawed in a 37°C water bath, washed in media, and plated out in RPMI with 10% FCS.

Wild type RD cells were similarly transfected with empty vector or pBK-CMV-P3F DNA using FuGENE 6 Transfection Reagent by J. Anderson. He gave me access to the G418 resistant clones, which had been frozen down in 10% DMSO and stored in liquid nitrogen.

2.4.3. Transient transfection of cells:

In transient transfection experiments, 3×10^5 cells were plated in 60mm culture dishes and transfected the following day, at approximately 70% confluency. The 76-9-derived cell lines were transiently transfected using FuGENE 6 Transfection Reagent, as described above. The human RMS cell lines were transfected using Lipofectamine 2000 (Invitrogen) because optimisation assays revealed that the tranfection efficiency was higher in these cell lines with Lipofectamine 2000 than with FuGENE 6 Tranfection Reagent. For each Lipofectamine 2000 transfection sample, 4μg DNA was diluted into 250μl of serum free OptiMEM medium (Invitrogen) and incubated for 5 minutes at room temperature. A ratio of 8μg of reporter plasmid DNA: 1μg of transfection efficiency control plasmid DNA was typically used. Simultaneously, 20μl of Lipofectamine 2000 was diluted into 250μl of serum free OptiMEM medium. The diluted DNA and Lipofectamine 2000 solutions were then mixed and incubated at room temperature for 20 minute to allow DNA-Lipofectamine complexes to form. The DNA-Lipofectamine complex solution was added to the cells in 5ml DMEM plus 10% FCS. After 3 hours, the media was changed over the cells because the transfection reagent was toxic to the cells when left for longer periods.

After 48 hours, the cells were lysed using Reporter Lysis Buffer (Promega), following the manufacturer's protocol. Briefly, the cells in each 60mm dish were covered with 200μl of 1× Reporter Lysis Buffer and incubated for 15 minutes at room temperature. The cells were detached from the plate with a cell scraper, transferred to an eppendorf tube, and centrifuged at 15,800g for three minutes. The supernatant was then collected and assayed directly using the relevant reporter assay or stored at -70°C.

Transfection experiments were performed in triplicate wells where possible. Control wells of cells were treated with FuGENE 6 Transfection Reagent or Lipofectamine 2000 alone, without any DNA. These negative controls took into account the effect of the transfection reagent on the cells.

The reporter constructs used included PRS9-CAT, IGFBP-1-luciferase, *c-MET* promoter-luciferase, *MITF* promoter-luciferase, and two BIM-luciferase reporters. The two transfection efficiency control plasmids used were pGL3-Control luciferase and pSV-β-galactosidase. Normalised reporter gene expression values were plotted as arbitrary units, and calculated as the reporter value divided by the transfection efficiency control plasmid value.

2.4.4. Reporter assays:

2.4.4.1. CAT thin layer chromatography (TLC) and enzyme-linked immunosorbent assay (ELISA):

In early experiments, the CAT activity in cell lysates was measured using a standard enzymatic assay. Following the preparation of cell lysates using Reporter Lysis Buffer, the lysates to be used for CAT TLC were heated at 60°C for 10 minutes to inactivate endogenous deacetylases. 100µl of cell lysate was mixed with 3µl of [^{14}C]-labelled chloramphenicol (at 0.05mCi/ml), 5µl of n-Butyryl Coenzyme A (Promega) and made up to a reaction volume of 125µl using water. In positive controls, CAT was added to the reaction mix instead of cell lysate. In negative control samples, no cell lysate was added to the reaction mix. The reactions were incubated at 37°C overnight. The reactions were terminated by the addition of 500µl of ethyl acetate and centrifuged at 15,800g for 3 minutes. The top, aqueous phase containing the acetylated forms of chloramphenicol was collected, placed in a new eppendorf tube, and dried by centrifugation at 50°C. The reaction product was re-dissolved in 20µl of ethyl acetate and 10µl was dotted onto the Polygram TLC sheet (Macherey-Nagel, Germany). The TLC sheet was stood in a chromatography chamber containing 190ml of chloroform mixed with 10ml of methanol, so that the samples were slightly above the alcohol level. The TLC sheet was incubated at room temperature for 30 minutes to allow the solvent front to migrate up the sheet. The TLC sheet was then dried and exposed on a phosphoimager screen overnight. In each sample, the radioactive spot that has migrated the least distance up the TLC sheet consists of deacetylated chloramphenicol. The faster

migrating radioactive spot, located higher up on the TLC sheet, is acetylated chloramphencol. To quantitate CAT activity, the intensities of the acetylated chloramphenicol spots were measured on the phosphoimager using ImageQuant software.

In later experiments, CAT activity in the cell extracts was measured by ELISA using a commercially available CAT ELISA kit (Roche), following the recommended protocol. The concentration of CAT present in the cell extracts was extrapolated from a standard curve.

2.4.4.2. β-galactosidase enzyme assay:

β-galactosidase activity in lysates prepared from cells transfected with pSV-β-galactosidase control vector was assayed using the β-galactosidase enzyme assay system (Promega). 50μl of cell lysate in 1× Reporter Lysis Buffer was mixed with 50μl of 2× Assay Buffer in a 96-well plate (Nunc, Denmark), and incubated at 37°C for 30 minutes. The reaction was stopped by the addition of 150μl of 1M sodium carbonate. The absorbance of the samples was read at 420nm in a plate reader. Alongside the experimental wells, a range of standards (0-5mU of β-galactosidase activity) were assayed to generate a standard curve. In some instances, β-galactosidase activity was measured using the Galacto-Light (Tropix, USA) assay system, following the manufacturer's protocol exactly.

2.4.4.3. Luciferase assay:

The luciferase activity in cell lysates was measured using a commercially available luciferase assay system (Promega). 10μl of cell lysate was added to a luminometer tube containing 100μl of Luciferase Assay Reagent, mixed by briefly vortexing, and read using a manual luminometer machine (Jencons, UK).

2.5. Tissue culture experiments using the 76-9-derived cell lines:

2.5.1. In vitro proliferation assay:

The rate of proliferation of 76-9, CMV, C23, and C24 cells were compared in serum free RPMI and in RPMI supplemented with 2% FCS or 10% FCS, using a colourimetric method for determining the number of viable cells. Briefly, the cell lines were plated out in 96-well culture plates in 100μl of media at two densities, 0.5×10^4 and 1.0×10^4 cells

per well. Each cell line was tested in triplicate wells, and negative control wells contained 100µl of media alone. The number of viable cells in each dish were measured at various time points, ranging from 0 to 96 hours after plating, using a CellTiter Aqueous Non-Radioactive Cell Proliferation Assay (Promega). The 3-(4,5-dimethylthiazol-2-yl)-5-(3-carboxymethoxyphenyl)-2-(4-sulfophenyl)-2H-tetrazolium (abbreviated to MTS) and phenazine methosulfate (PMS) solutions were mixed, and 20µl of combined MTS/PMS solution added to each well of the 96-well assay plate. The cells were incubated with the MTS/PMS solution for 1-4 hours, then the colourmetric reaction was terminated by the addition of 25µl of 10% SDS to each well. Viable cells are able to bioreduce the MTS salt into formazan, whose absorbance can be measured directly. The absorbances were read at 490nm using a plate reader, and standards ranging from 1×10^3 to 1×10^6 cells were assayed to allow the generation of a standard curve.

2.5.2. Matrigel invasion assay:

2.5×10^5 cells were suspended in 2ml of serum free RPMI media and plated in rehydrated BioCoat matrigel invasion inserts (Becton Dickinson, USA). The inserts contain an 8 micron pore size membrane covered with a thin layer of matrigel basement membrane matrix, which only metastatic cells are able to invade through. 2.5ml of RPMI supplemented with 5% FCS was used as a chemoattractant in the bottom of the wells, and the inserts were gently lowered into the wells, ensuring that no air bubbles formed between the insert and the chemoattractant. Following an overnight incubation at 37°C, the number of invasive and non-invasive cells was counted and the percentage invasion calculated as (the number of invasive cells/total number of invasive + non-invasive cells)×100.

2.5.3. All-trans-retinoic acid (ATRA) sensitivity assay:

The sensitivity of PAX3-FKHR negative (76-9 and CMV) and PAX3-FKHR positive (C23 and C24) cell lines to ATRA induced differentiation was examined. The human RMS cell line RH30 is known to differentiate when cultured in ATRA (Crouch and Helman, 1991), and served as a positive control. 2×10^4 cells were plated in each well of a 96-well plate in serum free RPMI or RPMI with 10% FCS. The following day, ATRA (Sigma) was reconstituted in ethanol, and added at a range of concentrations from

1×10^{-6} to 1×10^{-4} M. Control cells were treated with an equal volume of diluted ethanol, and assayed to show the normal rate of proliferation of the cell lines (in the absence of ATRA). The cells were cultured at 37°C in the dark for up to 72 hours following the addition of ATRA or ethanol. The rate of proliferation was used to measure the differentiation of the cells, as differentiation of RMS cell lines involves a block in proliferation (Crouch and Helman, 1991). The number of viable cells in each well was calculated using a CellTiter Aqueous Non-Radioactive Cell Proliferation Assay (as described in *2.5.1.*). The number of CMV and C23 cells cultured in the presence of 0.1% ethanol (10^{-4} M ATRA vehicle solution) was set as 100% cell growth.

2.6. Tissue culture experiments using the RD-derived cell lines:

2.6.1. Treatment with IFN-γ:

1×10^{5} cells were plated per 35mm culture dish. 24 hours later, recombinant human IFN-γ (PeproTech, UK) was reconstituted in PBS and added to the cells at 2ng/ml, 20ng/ml, and 200ng/ml. To control wells, an equal volume of PBS was added. After 24 and 48 hours incubation with IFN-γ, the cells were harvested and either stained for MHC class I expression or lysed for Western blot analysis.

2.6.2. Sensitivity to 12-O-tetradecanoyl phorbol-13-acetate (TPA) induced differentiation:

We examined whether PAX3-FKHR positive RD cell lines were less sensitive than PAX3-FKHR negative RD cell lines to TPA induced differentiation. TPA has been previously shown to cause the differentiation of RD cells *in vitro* (Aguanno *et al*, 1990). 1×10^{5} cells were plated per 35mm culture dish, and the following day TPA (Sigma) was dissolved in DMSO and added to the cells at 0.05μM, 0.1μM, and 0.2μM. In control dishes, the cells were treated with an equal volume of diluted DMSO (vehicle solution). The cells were cultured for up to 72 hours at 37°C in the dark. To investigate TPA induced differentiation, we compared the proliferation rate of each cell line cultured in TPA relative to control cells cultured with diluted DMSO, using a CellTiter Aqueous Non-Radioactive Cell Proliferation Assay (as described in *2.5.1.*).

2.6.3. Treatment with AG490:

1×10^{5} cells were seeded in 35mm culture dishes and left overnight to adhere. The janus tyrosine kinase (JAK) inhibitor AG490 (Calbiochem, UK) was reconstituted in DMSO and added to the cells at 5μM and 50μM. The concentrations of AG490 used in our

experiments were similar to those used in published AG490 experiments (Hovey *et al*, 2002; Rendon-Mitchell *et al*, 2003; Ruchatz *et al*, 2003). To control wells, an equal volume of diluted DMSO was added to the cells. After 48 hours incubation with AG490, the cells were harvested and either stained for MHC class I expression or lysed for Western blot analysis. Examining cell viability with trypan blue staining revealed that AG490 was not toxic to the cells.

2.7. Western blot analysis:

2.7.1. Lysis of adherent cells:

Cells were washed in PBS, then lysed in 100µl of RIPA buffer (containing 150mM NaCl, 1% NP40, 0.1% SDS, 50mM Tris, 1mM sodium orthovanadate, and the protease inhibitors spermine at 2µg/ml and PMSF at 20µg/ml) per 35mm culture dish, at 4°C for 30 minutes. Cells were detached from the plate with a cell scraper, transferred to eppendorf tubes, and centrifuged for 10 minutes at 15,800g at 4°C. The supernatants were collected and stored at -70°C. 2-5µl of lysate was used to quantify the protein concentration present in each sample, using a commercially available colourimetric assay (Bio-Rad, UK). A standard curve, of standards ranging from 0-2 µg/µl BSA, diluted in RIPA buffer, was used to calculate protein concentrations.

2.7.2. Western blot:

Whole cell lysates were mixed with 2× sample buffer (125mM Tris-HCl (pH 6.8), 20% glycerol, 4% SDS, 0.1% bromophenol blue, 20mM EDTA, 1mM PMSF, 5% β-mercaptoethanol) and denatured at 95°C for 5 minutes. An equal amount of denatured protein was loaded in each well of the SDS-polyacrylamide gel, and made up to an equal volume with 1× sample buffer. The denatured cell lysates were resolved on 8%-10% SDS-polyacrylamide gels alongside a protein size marker (Kaleidoscope prestained standards, Bio-Rad), and transferred to nitrocellulose Hybond C-extra membranes (Amersham Biosciences) by wet transfer at 100 volts for 60 minutes.

Ponceau (Sigma) staining was performed to check the successful transfer of protein to the membrane. Subsequently, the membranes were blocked in 5% powdered milk in PBS-0.1% Tween (abbreviated to PBS-Tween) (Tween 20 from BDH laboratories) overnight at 4°C. The membranes were rinsed with PBS-Tween, then probed with the relevant primary antibody in 2% powdered milk in PBS-Tween, for 1 hour at room

temperature. Following three separate washes in PBS-Tween for 10 minutes, the corresponding secondary antibody was added to the membrane in 2% powdered milk in PBS-Tween, and incubated at room temperature for 1 hour. The unbound antibody was then washed off in 6 separate washes in PBS-Tween for 5 minutes. Membranes were incubated for 1 minute in ECL reagent (Amersham Biosciences) and exposed to Hyperfilm ECL autoradiography film (Amersham Biosciences). The intensity of the bands was measured by densitometry (GS-800 densitometer; Bio-Rad). Membranes were stored moist at 4°C, and only reprobed with antibodies that detected proteins of significantly different size from the original antibody combination.

2.7.3. Antibody combinations:

The mouse anti-human PAI-1 (C-9) monoclonal antibody (Santa Cruz Biotechnology, USA) was used at 1 in 2,000 dilution, and detected using a goat anti-mouse IgG-horse radish peroxidase (HRP) secondary antibody at 1 in 2,000 dilution. Rat anti-α-tubulin (Serotec, UK) monoclonal antibody was used at 1 in 5,000 dilution in combination with a goat anti-rat IgG-HRP secondary antibody used at 1 in 5,000 dilution. Phospho-Akt protein was detected using a polyclonal rabbit anti-phospho-Akt (Ser473) antibody (Cell Signalling Technology, USA) at 1 in 1,000 dilution with goat anti-rabbit IgG-HRP at 1 in 2,000 dilution. The anti-BIM polyclonal antibody (Chemicon, USA) was used in combination with goat anti-rabbit IgG-HRP, with both antibodies diluted 1 in 2,000. The rabbit anti-BIM polyclonal antibody (Chemicon) was bound by the goat anti-rabbit IgG-HRP antibody. All the secondary antibodies used were obtained from Santa Cruz Biotechnology.

The primary antibodies we used to try to detect PAX3-FKHR protein included: rabbit anti-PAX3 polyclonal antibody (Active Motif, USA); rat anti-HA monoclonal antibody (clone 3F10) (Roche); sheep anti-FKHR polyclonal antibody (Upstate, USA).

2.8. Fluorescence activated cell sorter (FACS) staining and analysis:

2.8.1. Staining of cell surface antigens:

Approximately 5×10^5 cells were suspended in 50µl of PBS and stained with the optimised concentration of primary antibody, in the dark at 4°C for 30 minutes. To wash off unbound antibody, the samples were centrifuged at 180g for 4 minutes at 4°C, the supernatant was discarded, and the cells were resuspended in PBS. The cell samples were washed in this way a total of three times. Where necessary, the secondary antibody

was added to the cells suspended in 50µl of PBS, and incubated in the dark at 4°C for 30 minutes. The secondary antibody was washed off with three changes of PBS as described above, and the cells fixed in 300µl of PBS containing 1% paraformaldehyde. Each cell line was also stained with an isotype control antibody (an antibody derived from the same species and with the same fluorescent conjugate as the test antibody, but not specific for the test antigen being examined) as a control for the analysis. Cells were stored in the dark at 4°C before being analysed using a Beckman Coulter Epics FACS machine and Expo 32 software (Beckman Coulter, USA). Cells stained with the isotype control were analysed first, and set with 1% of the cells gated as positive for the test antigen. This allowed sensitive detection of any positively stained cells in the test samples.

The following test antibodies and isotype control antibodies were used: anti-mouse H2-K^b-Phycoerythrin (PE) and anti-mouse H2-D^b-PE (both from Caltag, USA) were used at 2µg/ml, with 2µg/ml of mouse IgG_2-PE serving as the isotype control (Becton Dickinson); purified anti-human MHC class I (Abcam, UK) was used at 2 µg/ml as a primary antibody, followed by staining with goat polyclonal anti-mouse IgG-PE (Abcam) secondary antibody at 5µg/ml, and the secondary antibody alone was used as a negative control equivalent to an isotype control; 10µl of monoclonal anti-human CXCR-4-PE (clone 12G5) (R&D Systems, USA) or mouse IgG_2-PE isotype control.

To determine the optimum concentration for use, each antibody was tested at a range of concentrations on a positive control cell line. The results were plotted on a graph with antibody concentration on the x-axis and mean fluorescence intensity (MFI) on the y-axis. The optimal concentration was near the top end of the linear phase of the curve of best fit, before it plateaus out.

2.8.2. Staining with propidium iodide (PI) to determine DNA content:
5×10^5 cells were washed and resuspended in a small volume of PBS. The cell solution was then added to 2ml of 70% ethanol (precooled to -20°C) and incubated at 4°C for 60 minutes. The cells were centrifuged at 200g for 5 minutes at 4°C, resuspended in a solution of PI and RNase A, and incubated at room temperature for 10 minutes. The samples were then analysed by flow cytometry. This staining allowed the determination

of DNA content of the cells tested, and the detection of any aneuploid cells when compared to normal C57BL/6 mouse cells.

2.9. Tumour allograft experiment:

Syngeneic C57BL/6 mice were injected sub-cutaneously with 1×10^6 cells. Three weeks after injection, the mice were culled by a schedule 1 method, and the tumours were excised and weighed. The bone marrow was extracted from the femur of the mice, and cultured in RPMI containing 10% FCS for several weeks in the presence of 500μg/ml of G418.

3. Results

3.1. Stable transfection of the murine RMS cell line 76-9 with PAX3-FKHR:

A *PAX3-FKHR* mixed murine/human cDNA sequence was amplified by PCR and cloned into the pBK-CMV vector by J. Anderson (construct called pBK-CMV-P3F; Figure 2), allowing high level *PAX3-FKHR* expression under the control of the CMV promoter (Anderson *et al*, 2001a). The alternative construct pBK-MyoD-P3F, contains the 7 Kb MyoD enhancer inserted upstream of *PAX3-FKHR* (Anderson *et al*, 2001a). There is more than 90% homology between the DNA sequences of mixed murine/human PAX3-FKHR, human PAX3-FKHR and the N-terminus of mouse PAX3, and the amino acid sequences are identical. Hence, the mixed murine/human PAX3-FKHR protein should have no functional differences from human PAX3-FKHR.

The mouse methylcholanthrene induced RMS cell line called 76-9 (Evans, 1983) was stably transfected with pBK-CMV empty vector (stably transfected cells termed CMV), pBK-CMV-P3F (clones called C1 up to C48), and pBK-MyoD-P3F (clones termed M1-M24). Expression of *PAX3-FKHR* mRNA in various CMV-P3F and MyoD-P3F clones was shown by RT-PCR, using PCR primers that specifically amplify *PAX3-FKHR* fusion transcripts (Figure 3). In controls to confirm that *PAX3-FKHR* was amplified from RNA and not from remaining genomic DNA, the first strand cDNA synthesis was performed without SuperScript II reverse transcriptase and then used as a template for the *PAX3-FKHR* PCR reaction. No bands were detected in the control lanes, confirming that *PAX3-FKHR* RNA is expressed in clones M1, M7, M12, C10, C20, C23, and C24. SCMC is a human RMS cell line that expresses endogenous *PAX3-FKHR* (see Figure 13), and served as a positive control. PCR amplification of actin mRNA confirmed that the RNA was intact and equally loaded in all the samples (data not shown).

Both the pBK-CMV-P3F and pBK-MyoD-P3F constructs contain a six amino acid HA epitope tag at their N-terminus. However, we were unable to detect the expression of PAX3-FKHR protein in 76-9 cells by Western blot analysis using an antibody specific for the HA epitope (data not shown). The HA epitope contains a caspase cleavage site (caspase consensus recognition sequence is DXXD; Clohessy *et al*, 2004), and it is possible that the HA epitope is cleaved in the 76-9 cells. Unfortunately, there are no commercially available antibodies that bind to the N-terminus of PAX3 or the C-

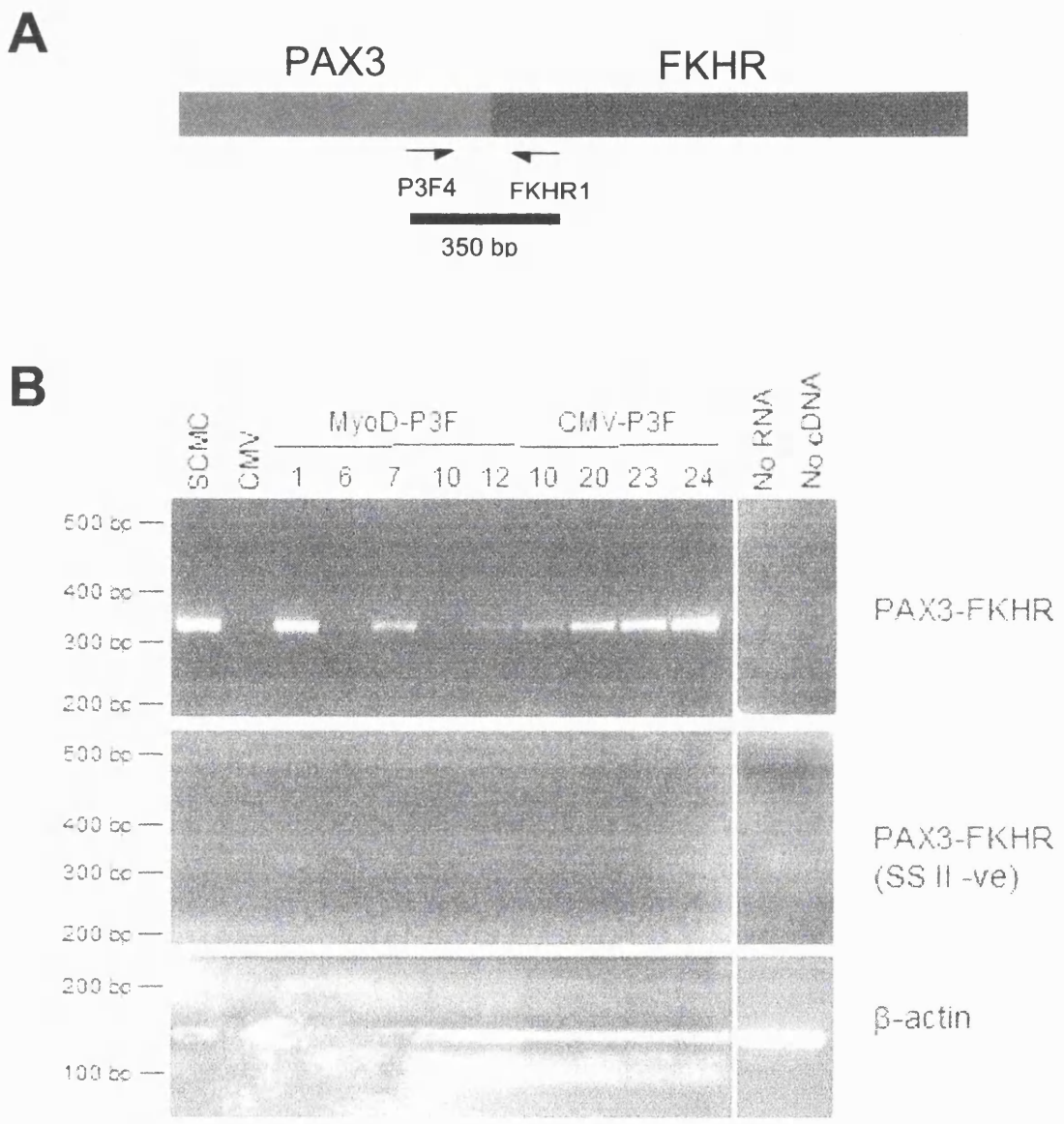

Figure 3. RT-PCR analysis of *PAX3-FKHR* mRNA expression in MyoD-P3F and CMV-P3F 76-9 clones. A The design of primers to specifically amplify *PAX3-FKHR* mRNA. The combination of a 5′ primer specific for *PAX3* and a 3′ primer specific for *FKHR* resulted in the PCR amplification of a 350 bp product from *PAX3-FKHR* RNA template. **B** *PAX3-FKHR* mRNA expression in CMV, MyoD-P3F, and CMV-P3F 76-9 clones. RT-PCR was performed on DNase-treated total cellular RNA. The photo of the β-actin RT-PCR was heavily smudged, nonetheless it is possible to observe that the levels of β-actin were roughly equal in all samples tested. SCMC, the human ARMS cell line, is known to express endogenous PAX3-FKHR and acted as a positive control. In control wells no RNA was added to the 1st strand synthesis reaction (labelled No RNA), and no cDNA was added to the PCR reaction (labelled No cDNA). To confirm that *PAX3-FKHR* was amplified from total RNA and not remaining genomic DNA, the 1st strand synthesis reaction was performed without the SS II reverse transcriptase (SS II –ve), and subsequently used as a template for the PCR reaction.

terminus of FKHR with high affinity, and thus suitable for detecting the presence of PAX3-FKHR.

The activity of the ectopically expressed PAX3-FKHR protein in both CMV-P3F and MyoD-P3F clones was tested in transient transfection experiments using the PRS9-CAT reporter construct. The PRS9-CAT plasmid contains 6 direct repeats of the PAX3 PB and HD consensus recognition sequences, upstream of a CAT reporter gene. Both wild type PAX3 and the chimeric PAX3-FKHR transcription factors can specifically bind to these sites, resulting in the transcriptional activation of the CAT reporter gene (Bennicelli *et al*, 1996). We detected the CAT reporter protein using both TLC enzymatic assay and ELISA. An initial experiment showed that the CMV-P3F clone C23 expresses significant amounts of functional PAX3-FKHR, detected as acetylated chloramphenicol (Figure 4A). However, when normalised for transfection efficiency, we found that C23 ectopically expresses less functional PAX3-FKHR than found endogenously in the human RMS cell line, SCMC (Figure 4B). In contrast wild type 76-9 cells and 76-9 cells stably transfected with pBK-CMV empty vector (CMV) express undetectable levels of PAX3 and PAX3-FKHR (supported by Northern blot analysis, Figure 12). The MyoD-P3F clone M8 was shown to express *PAX3-FKHR* RNA by RT-PCR (data not shown), but has dramatically less functional PAX3-FKHR protein than the CMV-P3F clone C23. This suggests that the MyoD promoter is not as active as the CMV promoter in 76-9 cells, and the pBK-MyoD-P3F construct is not suitable for stably expressing PAX3-FKHR at high levels in 76-9 cells.

In subsequent transient transfection experiments, the CAT reporter protein was detected by ELISA. Figure 4C shows that both C23 and C24 clones express high levels of PAX3-FKHR protein, whereas 76-9 and CMV cells express undetectable amounts of PAX3 or PAX3-FKHR. C23 expresses slightly more PAX3-FKHR than C24, though the difference is not significant (student *t*-test; p=0.20).

An *in vitro* transcription-translation (IVT) experiment was performed to check that the pBK-CMV-P3F construct was cloned successfully, and hence codes for a protein that is the size expected for PAX3-FKHR (for methodology see Chapter 3, *2.5.4.*). The mixed murine/human PAX3-FKHR protein is approximately 130 KDa, and a protein of the expected size was detected in the lane corresponding to IVT of *pBK-CMV-P3F* (Figure 5). Smaller sized bands are also detected, and probably represent degradation products

A. PRS9-CAT thin layer chromatography

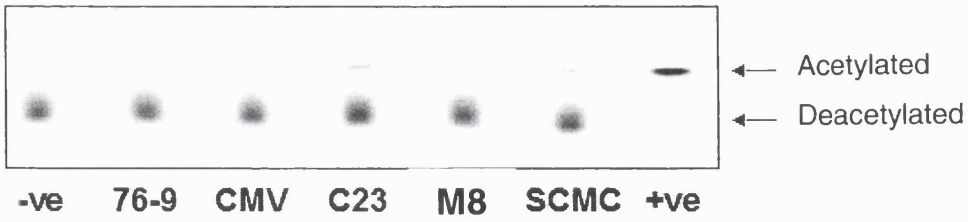

B. Normalised acetylated CAT activity

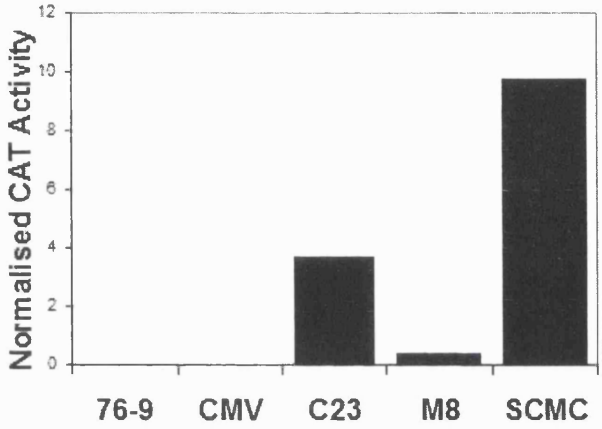

C. PRS9-CAT ELISA

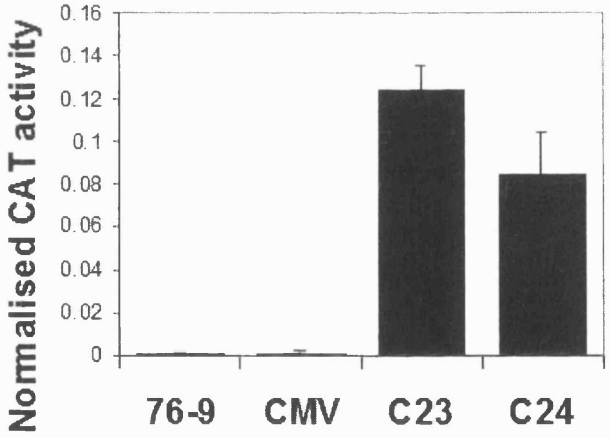

Figure 4. PAX3-FKHR protein function in 76-9 cells stably transfected with pBK-CMV-P3F and pBK-MyoD-P3F. **A** PRS9-CAT Thin layer chromatogram comparing PAX3-FKHR protein function in 76-9 cells ectopically expressing PAX3-FKHR (C23 and M8) with the human RMS cell line SCMC expressing endogenous PAX3-FKHR. CAT expression is detected as an acetylated (shifted) chloramphenicol band. **B** Normalised acetylated chloramphenicol levels from chromatogram depicted in A. Band intensities were quantified on a phosphoimager. **C** CAT ELISA demonstrating PAX3-FKHR protein function in the CMV-P3F clones C23 and C24. Normalised CAT activity is plotted in arbitrary units, and error bars are standard error of the mean (S.E.M.) of triplicate samples. In all these experiments, PAX3-FKHR function was measured in transient transfection experiments using the PRS-9 CAT reporter construct, containing 6 direct repeats of the PAX3 PB and HD consensus binding sequences. Co-transfection with the pGL3-Control luciferase vector enabled normalisation of transfection efficiency.

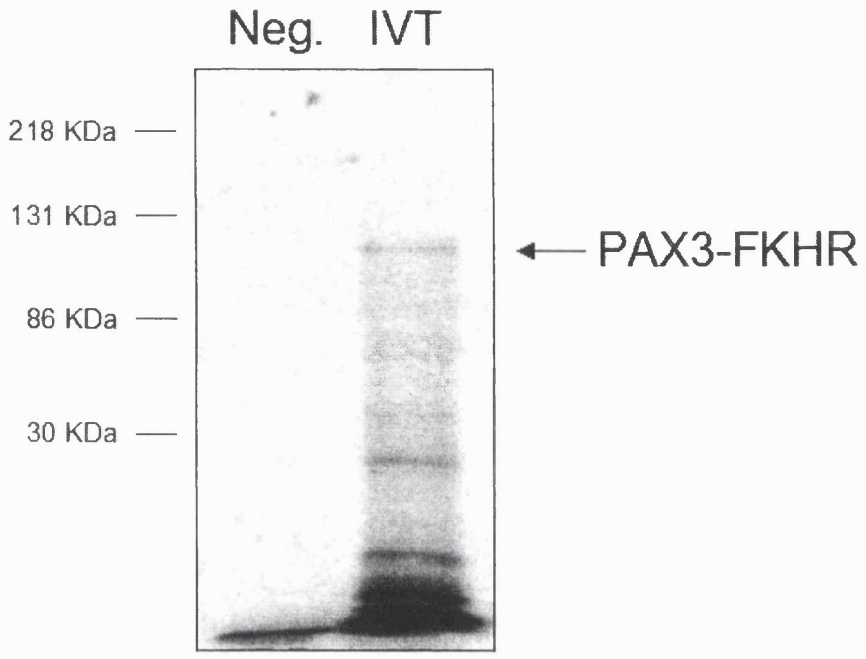

Figure 5. *In vitro* transcription-translation of PAX3-FKHR protein from the pBK-CMV-P3F plasmid. The *in vitro* transcription reaction was performed using the T3 RNA polymerase (Promega) and the *in vitro* translation reaction was performed using the TNT coupled reticulocyte lysate kit (Promega). Full length PAX3-FKHR protein is approximately 130 KDa. In the negative control lane (Neg.), no linearised plasmid DNA was added to the TNT coupled reticulocyte lysate reaction mix. The RNA B positive control is not known.

of full length PAX3-FKHR protein (cleaved by proteinases present in the *in vitro* translation reaction). In the negative control, no linearised plasmid DNA was added to the TNT coupled reticulocyte lysate reaction. Overall, this result suggests that the pBK-V-P3F plasmid is functional and codes for the full length PAX3-FKHR protein.

3.2. Effects of PAX3-FKHR expression on 76-9 cell phenotype:

3.2.1. In vitro proliferation assays:

We first examined the effects of PAX3-FKHR expression on the proliferation rate of 76-9 cells. *In vitro* growth assays revealed that PAX3-FKHR does not provide 76-9 cells with a growth advantage in serum free conditions. After 24 hours in serum-starved conditions, there was a dramatic decrease in the number of viable 76-9, CMV, and PAX3-FKHR-expressing C23 and C24 cells (Figure 6A). Staining with trypan blue revealed that virtually all the cells were dead after 48 hours incubation in serum free media. The cells were left for up to 96 hours in serum free media to observe whether PAX3-FKHR expression results in the production of growth factors that allow cell survival and proliferation in the absence of serum. However, after 96 hours we were unable to detect any viable cells in any well.

Comparative *in vitro* proliferation assays demonstrated that there are similar numbers of viable CMV and C23 cells throughout a 48 hour time course, when cultured in media supplemented with 10% serum (Figure 6B). There was also no noticeable difference in the number of viable CMV and C23 cells over extended periods of time (counting the number of cells when splitting cell lines once a week for up to 3 weeks; data not shown). Additionally, PAX3-FKHR expression did not result in an increased rate of growth once the cells reached confluency.

3.2.2. In vitro matrigel invasion assays:

Matrigel invasion assays were performed to examine the effect of PAX3-FKHR on the invasive ability of 76-9 cells *in vitro*. In a preliminary experiment, we found that CMV cells were weakly invasive, with more than 10,000 cells invading through a layer of matrigel basement membrane matrix to reach the 5% FCS chemoattractant. However, 76-9 cells transfected with PAX3-FKHR (C23 and C24) were significantly more invasive than CMV cells (Figure 7A). *In vitro* proliferation assays demonstrated that CMV, C23 and C24 cells are equally viable over a similar time course. Counting the number of invasive cells is therefore a satisfactory means of comparing the invasive

A. Serum free

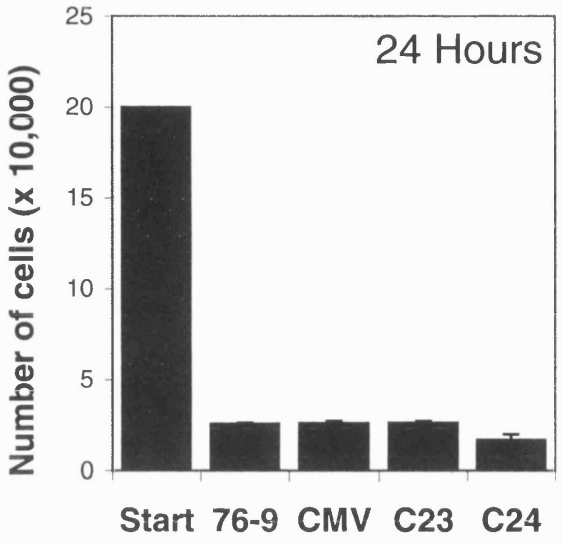

B. 10% serum

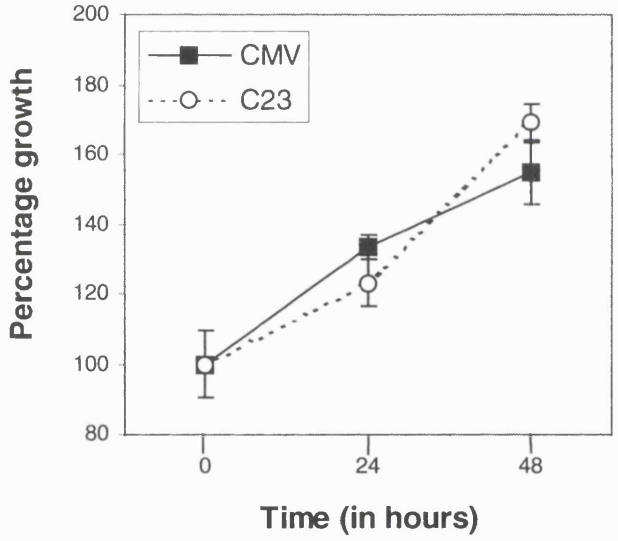

Figure 6. The effect of PAX3-FKHR on the growth rate of 76-9 cells in serum free conditions and in 10% serum. **A** Comparing the proliferation rate of CMV and C23 cells grown in serum free conditions for 24 hours. 200,000 cells of each clone were plated out in 6-well plates and incubated for 24 hours in 2ml serum free RPMI. The number of viable cells was determined using an MTS assay and trypan blue staining. Error bars are standard deviation (S.D.) of duplicate cultures. This experiment is representative of three separate experiments. **B** Comparing the growth rate of CMV and C23 cells in 10% serum. 20,000 cells were plated out in 96-well plates in 100µl RPMI supplemented with 10% FCS. Percentage growth is plotted (instead of total number of cells) to normalise for the slight variation in number of cells plated out at time point 0. Error bars are S.D. of quadruplicate cultures, combining the results of two separate experiments. In all comparative proliferation assays, the number of viable cells was measured using an MTS assay.

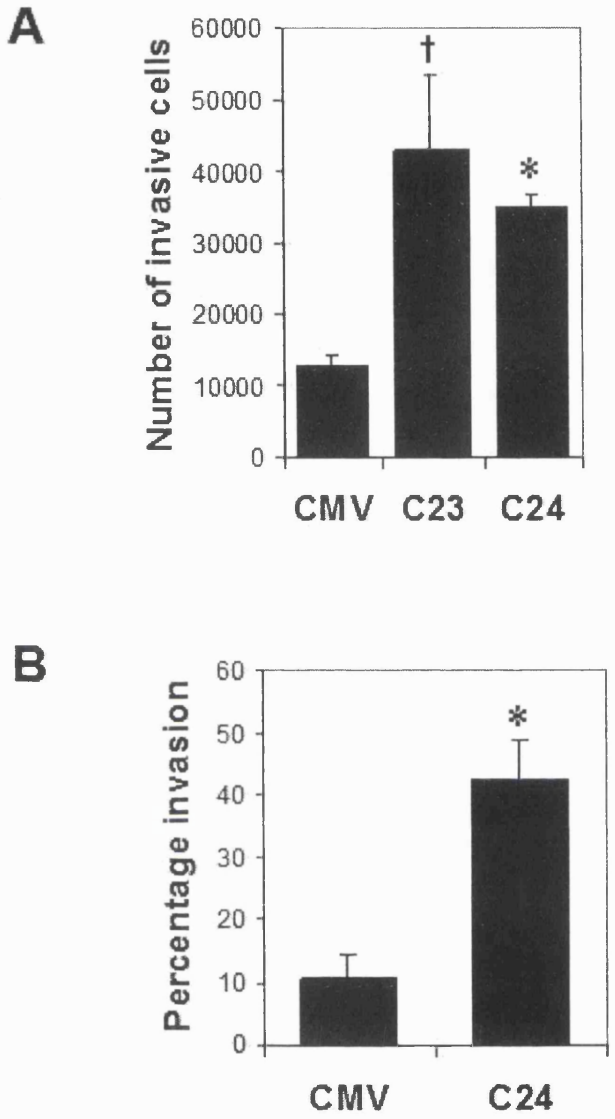

Figure 7. PAX3-FKHR increases the invasive ability of 76-9 cells *in vitro*. A Matrigel invasion assay using 76-9 cells stably transfected with empty vector (CMV) or PAX3-FKHR (C23 and C24). Invasion was measured as the number of invasive cells after 24 hours incubation. The mean values are plotted, and the error bars shown are S.E.M. of triplicate samples. A student *t*-test revealed that both C23 and C24 cells were significantly more invasive than CMV ($p<0.05$ (†), and $p<0.01$ (*), respectively). **B** Matrigel invasion assay comparing the invasive ability of CMV and C24 cells. The percentage invasion is plotted, and was calculated as (the number of invasive cells/total number of cells)×100. Mean values are plotted and the error bars shown are S.E.M. of quadruplicate samples. PAX3-FKHR-expressing C24 cells were significantly more invasive than empty vector transfected CMV cells (student t-test; $p<0.01$).

ability of these cell lines. In subsequent assays, we measured the number of invasive cells and the number of non-invasive cells, allowing us to calculate the percentage invasion of each cell line. This measure of invasive ability further demonstrated that PAX3-FKHR increases the invasive ability of 76-9 cells (Figure 7B).

3.2.3. Tumour allograft experiments:

To determine the effect of PAX3-FKHR on 76-9 cell growth and metastasis *in vivo*, syngeneic C57BL/6 mice were injected sub-cutaneously with 1×10^6 76-9-derived cells. Tumours formed in mice injected with both PAX3-FKHR negative (76-9 and CMV) and PAX3-FKHR positive (C23 and C24) 76-9 cells, however there was a large amount of intra-group variation in the tumour weights (Figure 8). Tumours that formed in mice injected with PAX3-FKHR-expressing 76-9 cells (C23 and C24) were not significantly larger than tumours derived from PAX3-FKHR negative 76-9 and CMV cells (student *t*-test; p=0.46).

To examine the *in vivo* metastatic properties of the 76-9, CMV, C23, and C24 cells, total RNA was isolated from the tumours, the lungs, and the bone marrow of representative mice after 3 weeks of tumour growth. We chose to look for metastatic 76-9 cells in the lungs and bone marrow because these are the sites where ARMS commonly metastasises to in patients (Barr, 2001; Anderson *et al*, 1999a). RT-PCR analysis demonstrated that *PAX3-FKHR* RNA was expressed in the tumours of mice injected with C23 or C24 cells, but not in the 76-9 or CMV-derived tumours, as expected (all the data not shown) (Figure 9). *PAX3-FKHR* RNA was not amplified from any lung or bone marrow sample isolated from mice injected with C23 or C24 cells. Additionally, bone marrow samples were extracted and grown in culture for several weeks to determine whether any PAX3-FKHR negative (76-9 and CMV) or PAX3-FKHR positive (C23 and C24) cells had metastasised to the bone marrow. Metastatic 76-9-derived cells that expanded from these bone marrow cultures were detected by their aneuploidy (DNA index = 1.2) and G418 resistance. Metastatic 76-9 cells were expanded from the bone marrow of 1 out of the 3 mice injected with CMV and 1 out of the 4 mice injected with C24 (data not shown). Overall, this data does not provide any evidence that PAX3-FKHR increases the metastatic ability of 76-9 cells *in vivo*.

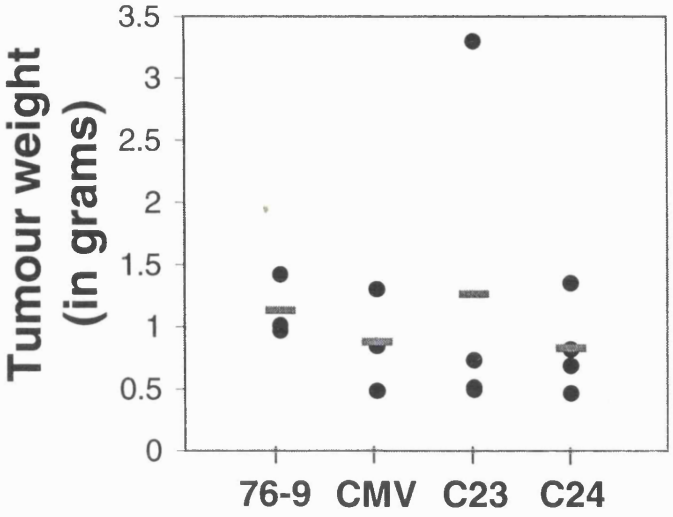

Figure 8. The effect of PAX3-FKHR expression on 76-9 RMS growth *in vivo*. 1×10^6 wild type 76-9 cells, 76-9 cells stably transfected with pBK-CMV (CMV), and 76-9 cells stably transfected with pBK-CMV-P3F (C23 and C24) were injected sub-cutaneously into syngeneic C57BL/6 mice. Three weeks post injection the mice were culled, and the tumours were excised and weighed. There were 3 mice in the 76-9 and CMV groups and 4 mice in the C23 and C24 groups. The black dots represent the weight of each individual tumour, and the grey lines represent the mean tumour weight in each group. Tumours that formed in mice injected with PAX3-FKHR-expressing 76-9 cells (C23 and C24) were not significantly larger than tumours derived from PAX3-FKHR negative wild type 76-9 and CMV cells (student *t*-test; p=0.46).

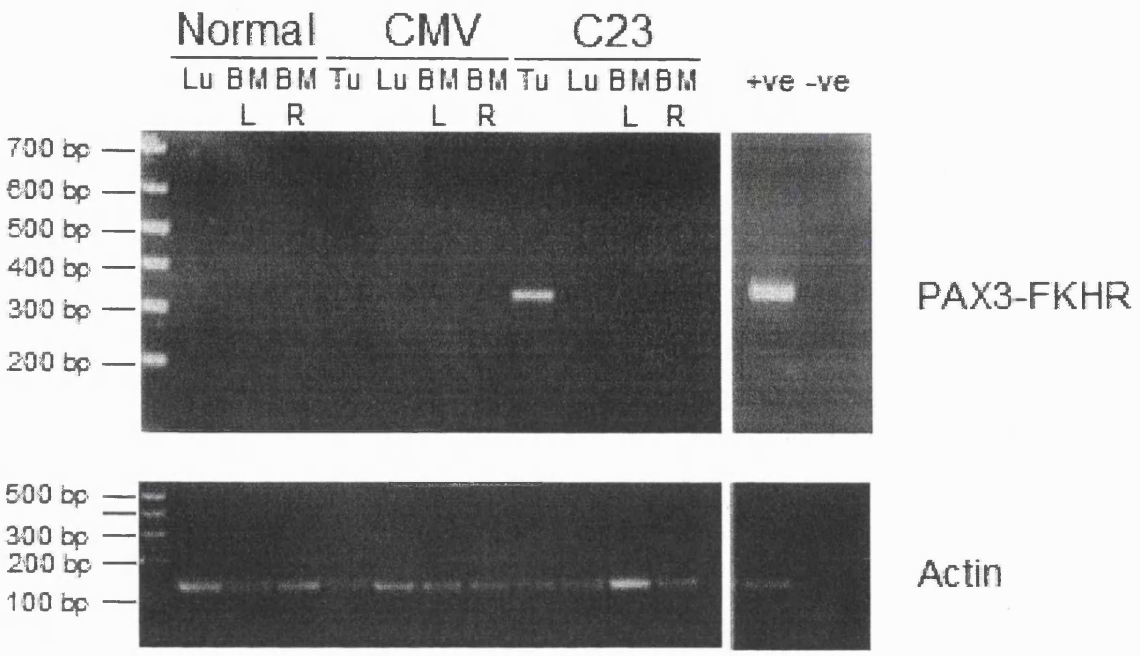

Figure 9. *PAX3-FKHR* RNA expression in various organs of C7BL/6 mice, isolated 3 weeks post sub-cutaneously injection of 1×10^6 76-9-derived cells. After 3 weeks tumour growth, the mice were culled, total RNA was isolated from various organs using Trizol reagent, and RT-PCR was performed using primers specific for *PAX3-FKHR* and actin. Total RNA extracted from the C23 cell line acted as a positive control, and no RNA was added to the RT-PCR reactions as a negative control. Abbreviations: Normal, non-injected C57BL/6 control mouse; CMV, mouse injected with 76-9 cells stably transfected with pBK-CMV; C23, mouse injected with 76-9 cells stably transfected with pBK-CMV-P3F; Tu, tumour; Lu, lung; BM L, bone marrow extracted from left femur; BM R, bone marrow extracted from right femur.

3.3. 76-9 cells express a myogenic transcription program:

76-9 cells are a methylcholanthrene-induced RMS cell line (Evans, 1983). We investigated whether 76-9 cells express myogenic-related transcription factors, in the absence and presence of ectopically expressed PAX3-FKHR.

We first examined the ability of PAX3-FKHR to activate transcription of *c-MET* in 76-9 cells, using a *c-MET* promoter-luciferase reporter gene in transient transfection experiments. *c-MET* is characteristically expressed in epithelial cells (Wang *et al*, 1994). Nonetheless, Epstein *et al* (1996) noted that c-*MET* is also expressed in muscle progenitor cells, and demonstrated that *c-MET* is a downstream target of PAX3. Figure 10A shows that the *c-MET* promoter-luciferase reporter gene is activated by transcription factors present in wild type 76-9 cells, consistent with a myogenic transcriptional program already being active in this mouse RMS cell line. The C23 cells have elevated luciferase activity relative to 76-9, CMV, and C24, suggesting that PAX3-FKHR is able to further transactivate the *c-MET* promoter when expressed at very high levels. Testing these cell lines by Northern blot analysis using a *c-MET*-specific probe, and by Western blot analysis using a c-MET-specific antibody, is required to confirm this preliminary finding.

We next measured the ability of PAX3-FKHR to transactivate *MITF* in 76-9 cells, using a *MITF* promoter-luciferase reporter construct. *MITF* is involved in several developmental processes, plays a vital role in the survival of melanocytes, and is transactivated by PAX3 *in vivo* (Epstein *et al*, 1991; Watanabe *et al*, 1998). Consistent with published findings, we see extremely high luciferase levels in human SCMC cells, which endogenously express *PAX3* and *PAX3-FKHR* (Figure 10B). The *MITF* promoter-luciferase reporter gene is moderately activated in wild type 76-9 cells, which we have shown to lack *PAX3* and *PAX3-FKHR* expression (see Figure 12). The luciferase activity in PAX3-FKHR-expressing C23 and C24 cells is equivalent to that found in 76-9 and CMV cells, suggesting that PAX3-FKHR does not transactivate the *MITF* promoter in this cell type.

3.4. Microarray analysis to identify PAX3-FKHR target genes in 76-9 cells:

PAX3-FKHR driven expression changes in the murine RMS 76-9 cell line were examined by comparing the mRNA patterns of two independent PAX3-FKHR-expressing 76-9 clones (C23 and C24) with empty vector transfected 76-9 cells (CMV),

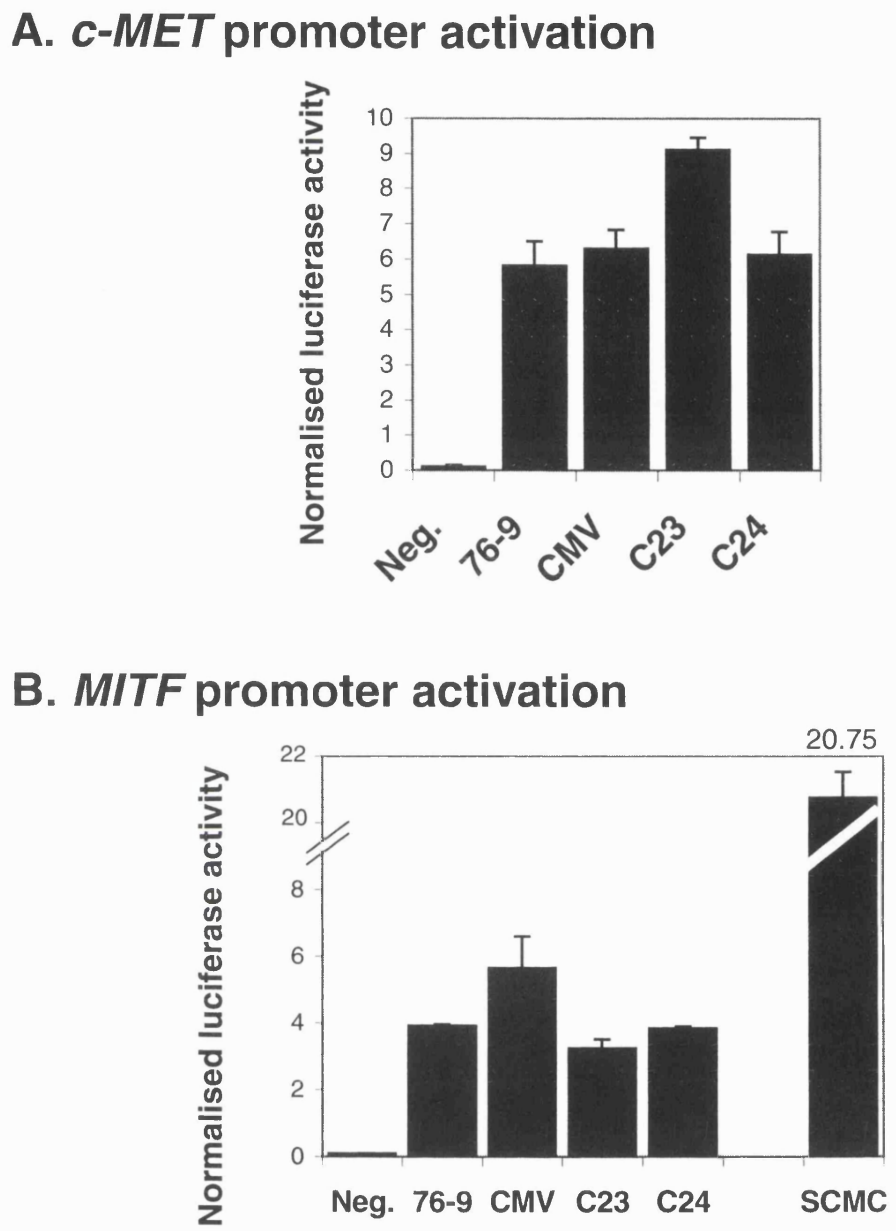

Figure 10. Transcriptional activation of the *c-MET* and *MITF* promoters in 76-9, CMV, and the PAX3-FKHR-expressing C23 and C24 cell lines. **A** Transcativation of the myogenic-specific *c-MET* promoter in the 76-9-derived cell lines. Neg., non-transfected 76-9 cells. Error bars represent S.E.M of triplicate cultures. SCMC cells were also tested but were negative for *c-MET* promoter activity. **B** Transactivation of the *MITF* promoter in 76-9-derived cell lines. Neg., non-transfected 76-9 cells. Error bars represent S.E.M of triplicate cultures. In all experiments, the *c-MET* and *MITF* reporter constructs were co-transfected with a pSV-β-galactosidase control vector and the cells were lysed after 48 hours incubation. Luciferase and β-galactosidase activity were measured and the normalised luciferase activity calculated.

using cDNA microarray gene expression analysis. Each cell line was analysed in triplicate, using MG-U74 affymetrix microarrays containing more than 12,000 expressed sequences. Using Genespring 4.2.1 software, the data for each target gene was normalised relative to the gene's mean intensity in CMV cells (CMV set as 1). A global error model was applied, based on the 3 replicates. A filter was used to identify genes that showed more than 2 fold difference in intensity in clones C23 and C24 relative to the mean intensity of CMV. Testing the significance of the difference in target sequence intensity in C23 and C24 compared to CMV by *t*-test identified 35 sequences that were significantly up-regulated by PAX3-FKHR and 69 sequences that were significantly down-regulated by PAX3-FKHR ($p<0.05$). Table 3 and Table 4 summarise the microarray analysis results (Appendix Tables 1 and 2 contain the complete list of sequences). Target sequences derived from the 5′ sequence of *PAX3* and the 3′ sequence of *FKHR* were not present on the microarray. The total RNA collected from CMV, C23, and C24 cells for the microarray experiments was also used in an RT-PCR reaction to confirm *PAX3-FKHR* mRNA expression in C23 and C24 cells (Figure 11).

The 35 sequences found to be up-regulated by more than 2 fold in C23 and C24 relative to CMV, are derived from 31 genes. The genes *PLA2*, *COL1A1*, *TRAM1*, and *GSTT1* were all identified as being up-regulated from 2 independent target sequences. Reassuringly the fold induction of these genes was similar in both target sequences. For example, *PLA2* was found to be induced 3.74 and 3.7 fold, in C23 relative to CMV, using the target sequences with the affymetrix identity codes 94665_at and 101328_at, respectively. 7 of the up-regulated sequences are expressed sequence tags (ESTs) and their function is currently unknown. Of the 69 sequences found to be significantly down-regulated in C23 and C24 cells relative to CMV cells, 27 are ESTs.

Remarkably, 21 of the 69 sequences down-regulated by PAX3-FKHR are known IFN-γ stimulated genes (Boehm *et al*, 1997). Only 44 of the sequences repressed by PAX3-FKHR have a known function (see Appendix Table 2), hence 48% (21 out of 44) of the sequences with known function are stimulated by IFN-γ. These include *H2-K*, *H2-D1*, and *TAP1*, all of which are key genes involved in the expression of MHC class I-peptide complexes on the cell surface. The only IFN-γ stimulated gene found to be up-regulated in C23 and C24 cells relative to CMV cells is *COL1A2*. Microarray analysis revealed that *LCK* and *COL1A1* are both up-regulated by PAX3-FKHR in 76-9 cells, and these

Gene	GenBank accession number	Identity code	Description	CMV fold change	C23 fold change	C24 fold change	t-test p-value
IGF2	X71922	98623_g_at	Insulin like growth factor 2	1	5.02	6.03	<0.001
PLA2	AA408341	94665_at	Phospholipase A2 group 5	1	3.74	4.44	<0.001
PLA2	U66873	101328_at	Phospholipase A2 group 5	1	3.70	3.05	0.002
TGOLN2	D50032	93882_f_at	Trans-golgi network protein 2	1	2.33	2.22	<0.001
XMR	X72697	102818_at	Xlr-related, meiosis regulated gene	1	6.88	7.19	<0.001
CSTF2T	AI854864	104126_at	Cleavage stimulation factor, 3' pre-RNA subunit	1	2.06	2.36	0.002
TRAM1	AA763937	160936_at	Translocating chain-associating membrane protein 1	1	2.65	2.89	<0.001
AKR1C13	AB027125	95015_at	Aldo-keto reductase family 1, member C13	1	2.13	3.08	<0.001
COL3A1	X52046	98331_at	collagen alpha I, type 3 subunit	1	3.31	4.06	<0.001

Table 3. Genes significantly up-regulated more than 2 fold by PAX3-FKHR. Data are presented as fold increase in expression relative to the parental cell line (CMV). The expression level of each target gene is set as 1 in the CMV cells. The values for each cell line are the mean of 3 probe arrays. The GenBank accession number from which the oligonucleotide sequence was drawn is shown as well as the Affymetrix identity code.

Gene	GenBank accession Number	Identity code	Description	CMV fold change	C23 fold change	C24 fold change	*t*-test p-value
Interferon regulated genes:							
G1P2	X56602	98822_at	Interferon, alpha inducible protein	1	0.25	0.20	<0.001
IFI204	M31419	98465_f_at	Interferon activated gene 204	1	0.15	0.11	<0.001
ISGF3G	U51992	103634_at	interferon stimulated gene factor 3 gamma	1	0.23	0.17	<0.001
H2-K	V00746	93120_f_at	MHC class I, Histocompatibility 2, K region	1	0.49	0.49	0.002
H2-D1	X52490	101886_f_at	Histocompatibility 2, D region locus 1 and beta(2) microglobulin	1	0.59	0.5	0.003
TAP1	U60020	103035_at	Transporter associated with antigen processing (TAP) 1	1	0.42	0.46	0.003
CXC10	M33266	93858_at	Chemokine (C-X-C motif) ligand 10 (Interferon inducible protein 10)	1	0.36	0.25	0.001
STAT1	U06924	101465_at	Signal transducer and activator of transcription 1	1	0.31	0.41	0.004
Additional genes:							
CRABP1	X15789	98108_at	Cellular retinoic acid binding protein 1	1	0.52	0.41	0.002
PAI-1	M33960	94147_at	Plasminogen activator inhibitor-1	1	0.26	0.34	0.001

Table 4. Genes significantly down-regulated more than 2 fold by PAX3-FKHR. Data are presented as expression level relative to the parental cell line (CMV). The expression level of each target gene is set as 1 in the CMV cells. For example, a C23 fold change value of 0.25 corresponds to a 4 fold reduction in target gene expression. The values for each cell line are the mean of 3 probe arrays. The GenBank accession number from which the oligonucleotide sequence was drawn is shown as well as the Affymetrix identity code.

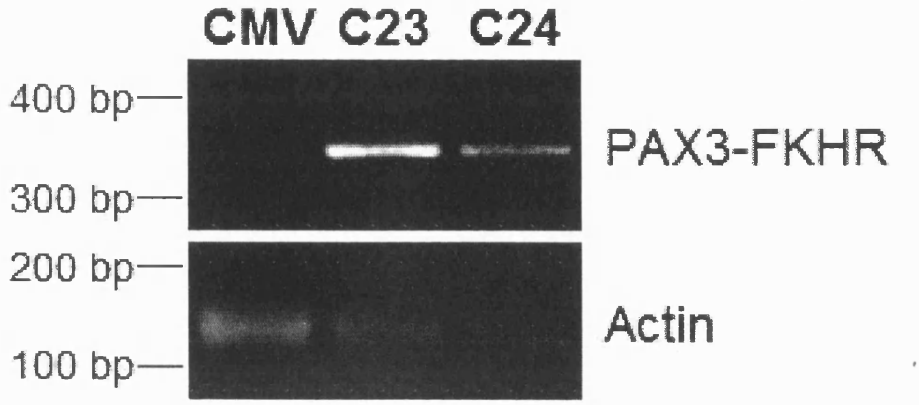

Figure 11. RT-PCR showing the expression of *PAX3-FKHR* mRNA in 76-9 cells stably transfected with pBK-CMV-P3F. In a negative control well, no cDNA was added to the PCR reaction mix (not shown). In other controls reactions, no SuperScript II reverse transcriptase was added to the 1st strand synthesis reaction and no bands were detected in these lanes (not shown). Amplification of actin acts as a loading control.

genes are known to be repressed by IFN-γ (Boehm *et al*, 1997). However, *PLA2* is up-regulated by PAX3-FKHR and is also up-regulated by IFN-γ. Overall, these findings suggest that PAX3-FKHR interferes with IFN-γ target gene expression.

IGF2 is a well documented downstream target of PAX3 and PAX3-FKHR, and is frequently over-expressed in RMS (Yun, 1992; Khan *et al*, 1999). Reassuringly, we found that *IGF2* is induced 5-6 fold by PAX3-FKHR in 76-9 cells, confirming that PAX3-FKHR is transcriptionally active in our cells. *XMR* is the target gene most dramatically up-regulated by PAX3-FKHR in 76-9 cells (approximately 7 fold induction).

Genes we found to be repressed by PAX3-FKHR but which are not known IFN-γ regulated genes include *CRABP1* and *PAI-1*. *CRABP1* is repressed approximately 2 fold in PAX3-FKHR-expressing 76-9 cells. *CRABP1* is involved in the transport of ATRA, an important regulator of cell growth and differentiation (Chen and Radominska-Pandya, 2000). *PAI-1* is repressed 3-4 fold by PAX3-FKHR in 76-9 cells. PAI-1 is the key inhibitor of urokinase-type plasminogen activator (uPA), a protease involved in tumour invasion through the disruption of extra cellular matrix (ECM; Duffy, 2002).

We then widened the search for genes that showed more than 1.5 fold difference in intensity in PAX3-FKHR-expressing C23 and C24 cells compared to empty vector transfected control cells (CMV). In this analysis, 750 genes were identified as being significantly changed by PAX3-FKHR. To narrow down the list of genes, we applied the Benjamini and Hochberg multiple testing correction during the *t*-tests. This resulted in the identification of 8 genes that are significantly induced and 27 genes that are significantly repressed by PAX3-FKHR. The genes identified in this analysis are indicated by an asterisk in the complete list of genes (Appendix Tables 1 and 2).

3.5. Northern blot analysis to examine PAX3-FKHR driven expression changes in RMS cells:

3.5.1. Confirmation of PAX3-FKHR-mediated expression changes in 76-9 cells:
To verify the microarray results, we examined the RNA levels of three representative target genes by Northern blot analysis of CMV and C23 cells (using newly extracted RNA samples, not the RNA used for the microarray experiments) (Figure 12). The levels of *PAI-1* RNA are diminished in C23 cells relative to CMV cells, and the fold

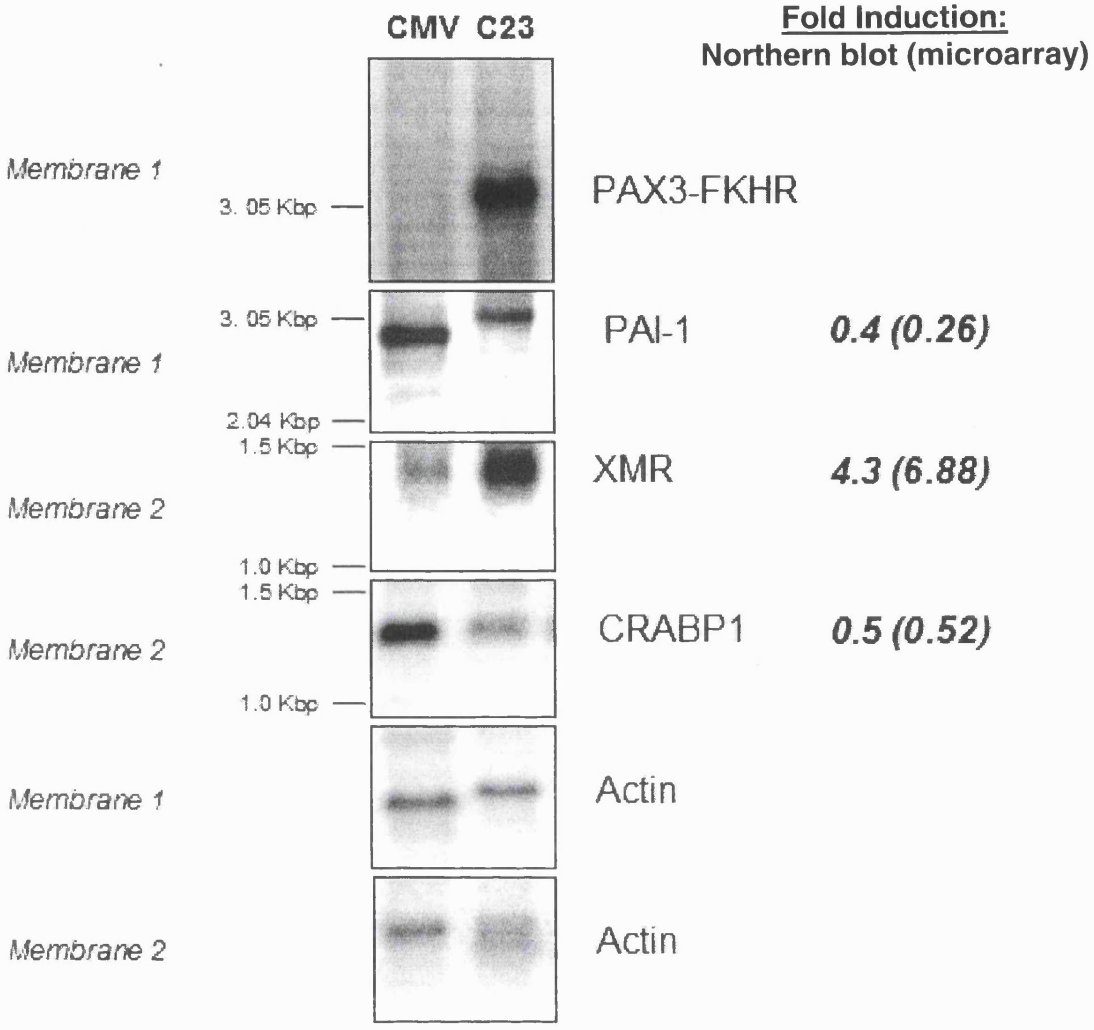

Figure 12. Northern blot analysis to verify the microarray results. The fold changes in target mRNA expression in C23 cells relative to CMV are shown for the Northern blots (and the microarrays) to the right of the images. The band intensities from the Northern blots were quantified on a phosphoimager and normalised relative to actin levels. Two identical Northern blots were performed and the membrane probed is indicated on the left of each image. The PAI-1 detected in C23 cells is slightly larger than the PAI-1 in the CMV cells. The actin bands show a similar difference in size, suggesting that this is a result of the RNA in these lanes not running at an equal speed during electrophoresis.

difference is similar to that found by microarray analysis (0.4 and 0.26, respectively). Similarly, Northern blot analysis demonstrated that *CRABP1* RNA is clearly repressed by PAX3-FKHR. *XMR* mRNA is barely detectable in the CMV cells, but highly expressed in PAX3-FKHR-expressing C23 cells. The 4.3 fold increase in *XMR* RNA levels in C23 cells measured by Northern blot analysis is similar to the fold induction calculated by microarray analysis (6.88 fold). Overall, the relative levels of target mRNA in CMV and C23 cells determined by Northern blot analysis were equivalent to that seen in the microarray results, confirming that the microarrays accurately reflected changes in mRNA expression. Unfortunately, during passage C24 lost expression of PAX3-FKHR, as shown by RT-PCR and PRS9-CAT reporter assays, and could not be tested in the Northern blots.

3.5.2. Target gene expression in various human RMS cell lines:

After genotyping several human RMS cell lines for expression of endogenous *PAX3* and *PAX3-FKHR* RNA, we examined the levels of *CRABP1* and *PAI-1* RNA in these cell lines (Figure 13). In the human RMS cell lines examined, only RH18 cells (*PAX3*$^-$, *PAX3-FKHR*$^-$) expressed *CRABP1* RNA. This is concordant with the hypothesis that PAX3-FKHR represses *CRABP1* expression in human ARMS. Unfortunately, we did not have an antibody to examine CRABP1 protein levels in the RMS cell lines.

Northern blot analysis revealed that *PAI-1* RNA was expressed at high levels in the ERMS RD cell line (*PAX3*$^+$, *PAX3-FKHR*$^-$), but was also expressed at detectable levels in the ARMS RH30 cell line (*PAX3*$^+$, *PAX3-FKHR*$^+$). The *PAI-1* RNA appeared as a double band, this may be because the probe binds other *PAI* family members which are a slightly different size, or that there are two *PAI-1* isoforms in these cells. Western blot analysis showed that PAI-1 protein is only detected in human RMS cell lines that lack *PAX3-FKHR* expression, and PAI-1 is expressed at the most elevated levels in the RD cell line (see Figure 18A). Interestingly, there were undetectable levels of PAI-1 protein in the RH30 cell line. The Western blot analysis result suggests that PAX3-FKHR might repress PAI-1 expression in human ARMS.

Northern blot analysis demonstrated the high level expression of *XMR* RNA in mouse 76-9 cells ectopically expressing PAX3-FKHR (Figure 12). However, this murine *XMR* probe was unable to detect a human *XMR* ortholog in any of the human RMS cell lines tested by Northern blot (data not shown). A NCBI blast search revealed that there is no

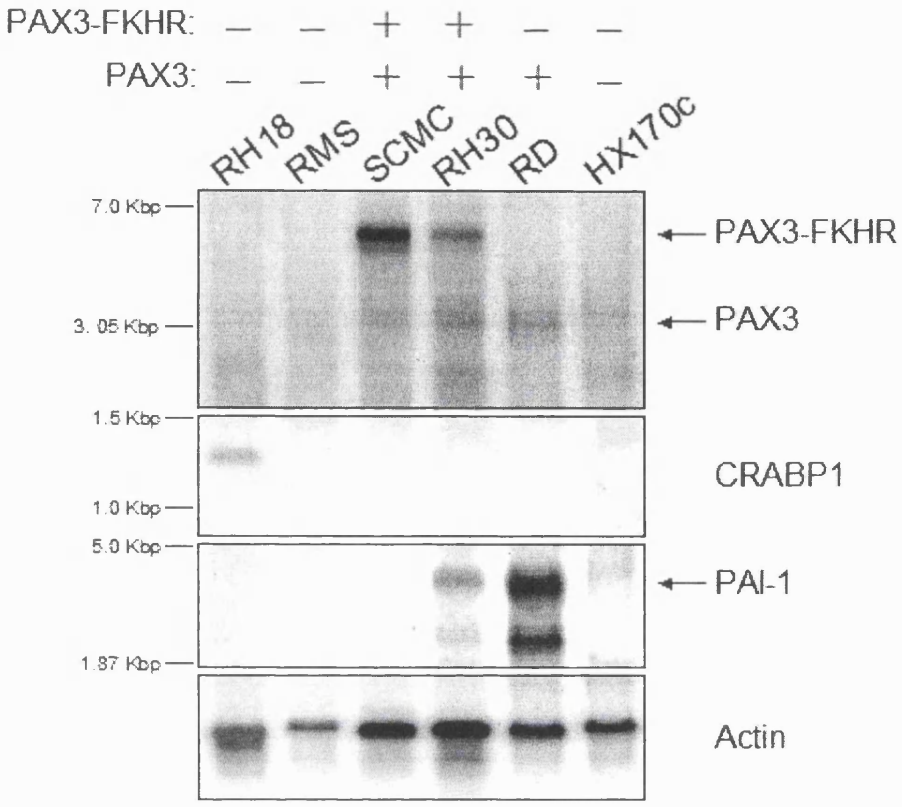

Figure 13. Northern blot analysis to examine the expression of *PAX3*, *PAX3-FKHR*, and two PAX3-FKHR target genes in several human RMS cell lines. *PAX3-FKHR* RNA is approximately 6 Kbp in size, whereas wild type *PAX3* RNA is 3 Kbp in size. The expression of endogenous *PAX3* and *PAX3-FKHR* is indicated at the top of the figure.

known human gene with homology to the mouse *XMR* target sequence on the MG-U74 microarray.

3.6. Effect of PAX3-FKHR-mediated repression of *CRABP1* on 76-9 cell phenotype:

Published findings indicate that ATRA inhibits the growth of human RMS cell lines in a dose dependent manner (Crouch and Helman, 1991), and diminished expression of CRABP2 reduces MCF-7 carcinoma cell sensitivity to ATRA-induced cell death (Budhu and Noy, 2002). We tested the hypothesis that diminished *CRABP1* expression in PAX3-FKHR-expressing 76-9 cells results in an insensitivity to ATRA-induced cell death. Comparative proliferation assays demonstrated that the number of viable CMV and C23 cells was dramatically reduced by treatment with 1×10^{-4} M ATRA for 24 hours (83.6% and 89.9% reduction in number of viable cells, respectively). After 72 hours in the presence of ATRA, no viable CMV or C23 cells were detected by MTS assay (Figure 14A). In contrast, treatment with 1×10^{-5} M ATRA for up to 72 hours had minimal inhibitory effects on the viability of CMV and C23 cells. RH30 cells were used as a control cell line, and we observed an 80% reduction in the number of viable RH30 cells after 24 hours treatment with 1×10^{-5} M ATRA, in agreement with published data (Crouch and Helman, 1991). In subsequent experiments, CMV and C23 cells were cultured in the presence of a range of ATRA concentrations ($1\text{-}8\times10^{-5}$ M ATRA) for 24 hours. We found that CMV and C23 cells were equally sensitive to ATRA-induced cell death, at all ATRA concentrations used (Figure 14B). Similarly, the numbers of viable CMV and C23 were reduced equal amounts when cultured in serum free media and treated with a range of ATRA concentrations (data not shown). These findings suggest that the repression of *CRABP1* by PAX3-FKHR does not render the 76-9 cells resistant to ATRA induced cell death.

3.7. PAX3-FKHR-directed down-regulation of MHC class I expression in RMS:

3.7.1. Effect of PAX3-FKHR on MHC class I expression in mouse 76-9 cells:

Expression of MHC class I *H2-K* and *H2-D1* mRNA was found to be significantly repressed by PAX3-FKHR in our microarray experiment. 76-9 cells are derived from C57BL/6 mice, a mouse strain that expresses H2-K^b and H2-D^b antigens on its cell surfaces. FACS analysis was performed to determine whether these MHC class I proteins are down-regulated on the cell surface of 76-9 cells expressing PAX3-FKHR. Wild type 76-9 cells and 76-9 cells stably transfected with pBK-CMV empty vector

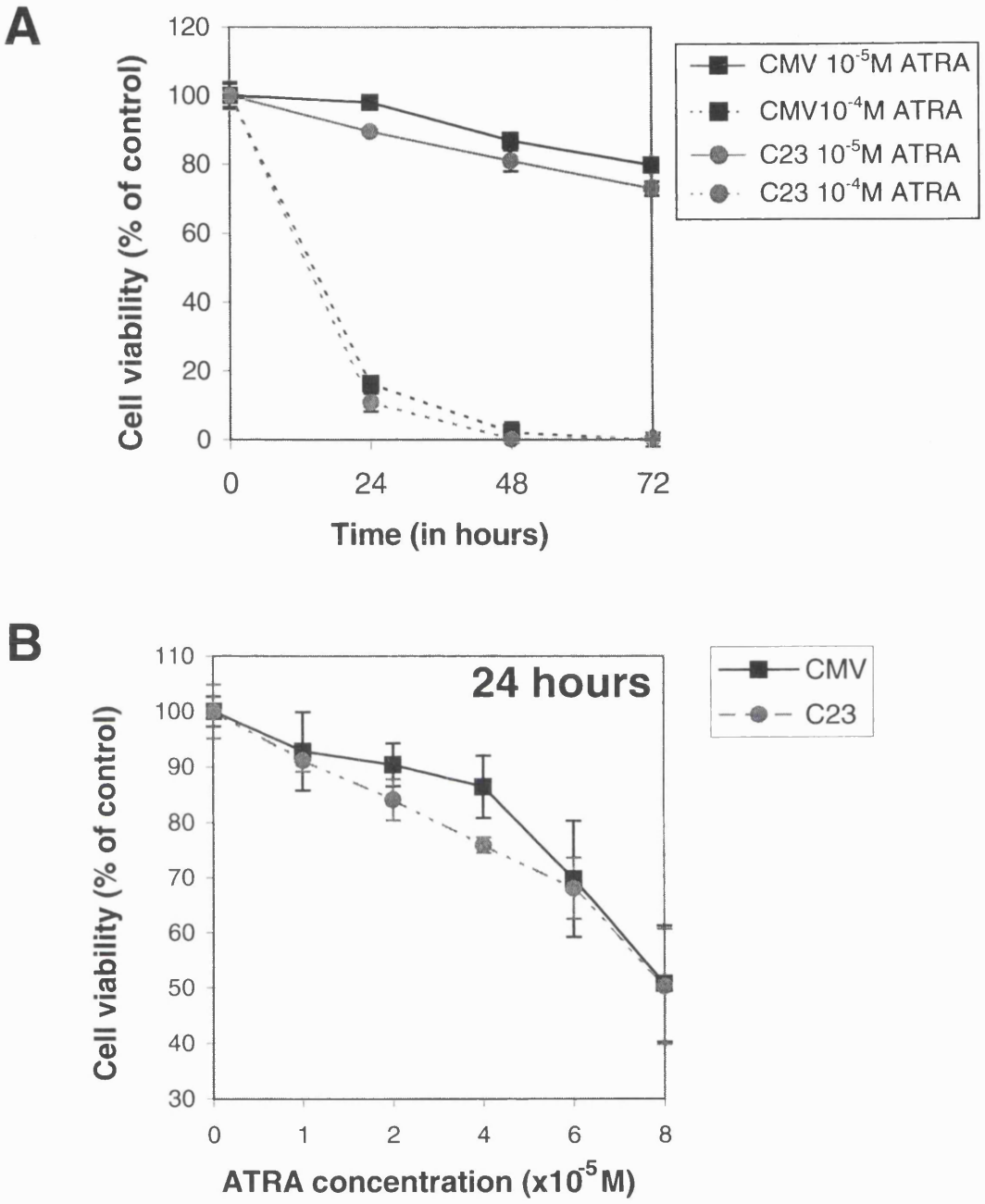

Figure 14. Sensitivity of 76-9 cells expressing empty vector (CMV) and PAX3-FKHR (C23) to ATRA-induced cell death. **A** Viability of CMV and C23 cells cultured in the presence of 1×10^{-5}M and 1×10^{-4}M ATRA for up to 72 hours. The number of CMV and C23 cells cultured in the presence of 0.1% ethanol (10^{-4}M ATRA vehicle solution) was calculated at each time point and set as 100% cell growth. The number of CMV and C23 cells cultured in the presence of ATRA was plotted as percentage cell growth relative to vehicle treated control cells. **B** Viability of CMV and C23 cells cultured for 24 hours in the presence of $1\text{-}8\times10^{-5}$M ATRA. The number of CMV and C23 cells cultured in the presence of 0.1% ethanol (10^{-4}M ATRA vehicle solution) for 24 hours was set as 100% cell growth. In all proliferation assays, the number of viable cells was calculated using an MTS assay. Mean values are plotted and the error bars are S.E.M. of triplicate cultures.

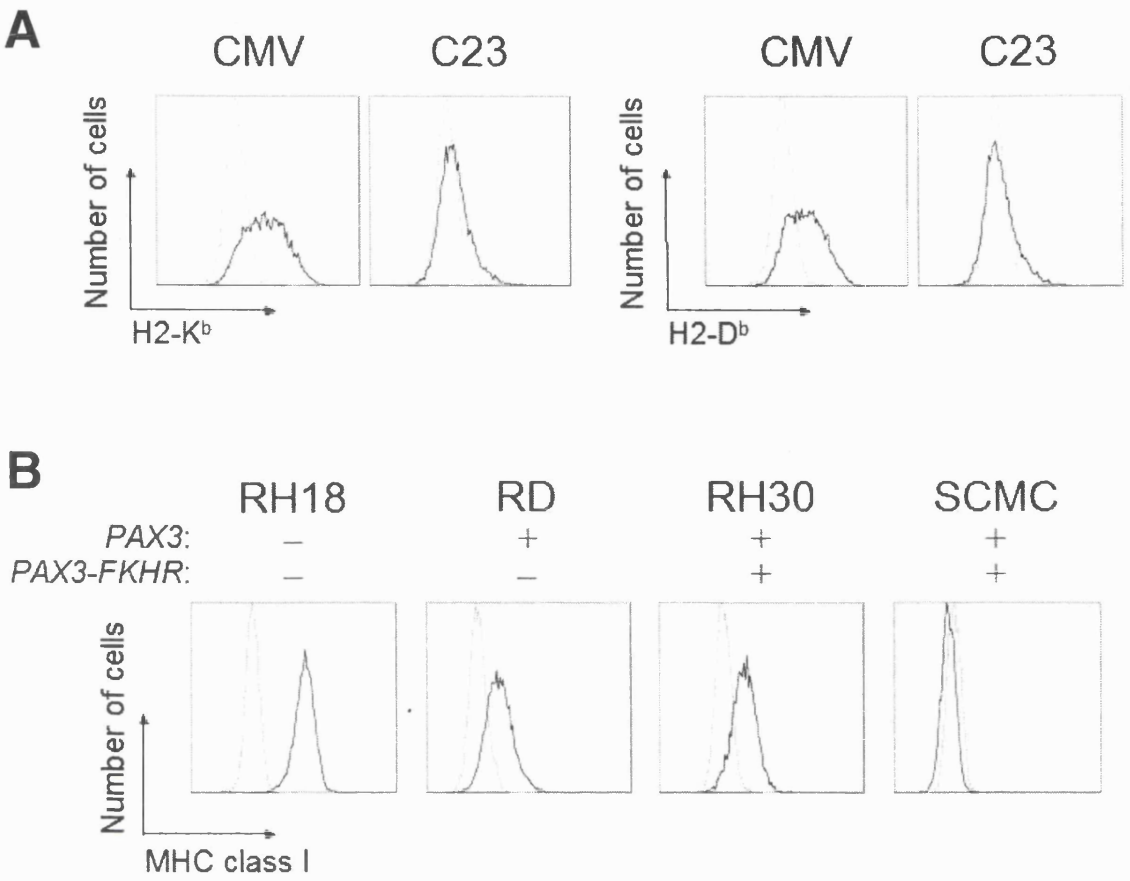

Figure 15. A PAX3-FKHR down-regulates H2-D^b and H2-K^b expression on the surface of the mouse RMS 76-9 cell line. The dotted grey line represents staining with an isotype control IgG_2-PE antibody; the black solid line represents staining with either PE-conjugated H2-D^b or H2-K^b PE antibody. This FACS staining is representative of 4 separate experiments. Log fluorescence of either H2-D^b or H2-K^b intensity is plotted on the x-axis and the number of cells on the y-axis. **B** MHC class I expression in several human RMS cell lines. The endogenous expression of *PAX3* and *PAX3-FKHR* (determined by Northern blot analysis, Figure 13) in each cell line is shown. The grey dotted line represents staining with PE-conjugated secondary antibody alone; the black solid line represents staining with purified MHC class I primary antibody and PE-conjugated secondary antibody. Log fluorescence of MHC class I intensity is plotted on the x-axis and the number of cells on the y-axis.

express intermediate levels of both H2-K^b and H2-D^b antigens on their cell surface (staining of CMV cells is shown in Figure 15A). Expression of H2-K^b and H2-D^b antigens is virtually abolished in PAX3-FKHR-expressing C23 and C24 cells (staining of C23 cells is shown in Figure 15A).

3.7.2. MHC class I expression in various human RMS cell lines:

Consistent with the hypothesis that PAX3-FKHR represses MHC class I expression in ARMS, none of the PAX3-FKHR-expressing human RMS cell lines tested have high levels of MHC class I antigen on their surface (Figure 15B). In contrast, RH18 ($PAX3^-$, $PAX3\text{-}FKHR^-$) expresses relatively high levels of MHC class I antigen. The human cell line called RMS has previously been shown to express *PAX3-FKHR* (Anderson, unpublished data), but in our experiments it appears to be negative for both *PAX3* and *PAX3-FKHR* (see Figure 13). We found that RMS does not express any detectable MHC class I on the cell surface (data not shown).

3.7.3. Effect of ectopically expressed PAX3-FKHR on MHC class I levels in human RMS cell lines:

To determine whether PAX3-FKHR-mediated down-regulation of MHC class I expression is a phenomenon specific to mouse 76-9 cells, we examined the human leukocyte antigen (HLA) class I levels on the surface of human RD cells ectopically expressing PAX3-FKHR. J. Anderson had previously stably transfected RD cells with pBK-CMV empty vector (cells called RD Empty) and pBK-CMV-P3F (clones called RDP3F#1 up to RDP3F#20). Wild type RD cells express low levels of endogenous *PAX3* RNA (see Figure 13), and small amounts of functional PAX3 protein that is able to bind to the PB and HD consensus recognition sequences in the PRS9-CAT reporter construct (Figure 16). Four independent RDP3F clones were identified that express functional PAX3-FKHR protein, capable of driving CAT expression from the PRS9-CAT reporter gene in transient-transfection experiments (Figure 16). The results suggest that the ectopically expressed PAX3-FKHR in these 4 clones is capable of transactivating the PRS9-CAT construct significantly more than the wild type PAX3 present in the RD cells.

We measured the expression of MHC class I antigen on the surface of RD cells stably transfected with empty vector (RD Empty) and PAX3-FKHR (RDP3F clones). Wild

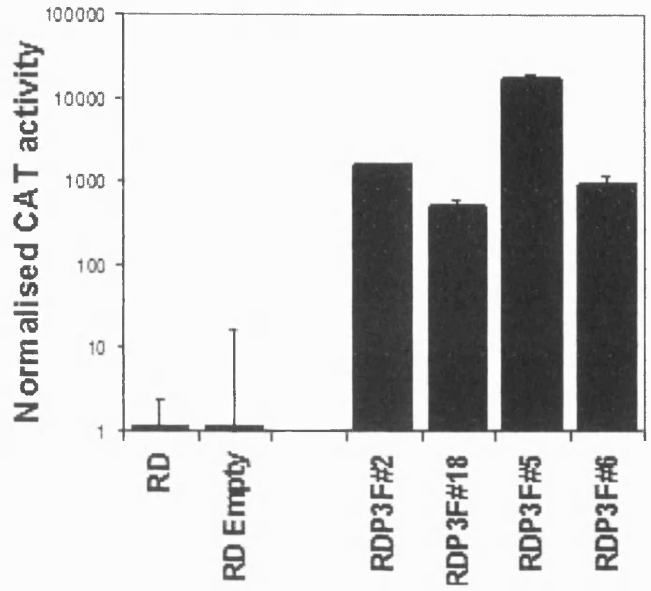

Figure 16. PAX3-FKHR protein function in RD-derived cell lines. The RD cell lines stably expressing empty vector (RD Empty) and PAX3-FKHR (RDP3F clones) were transiently transfected with PRS9-CAT and pGL3-Control luciferase DNA using Lipofectamine 2000. 48 hours post transfection, the cells were lysed and the levels of CAT and luciferase measured. CAT activity was normalised for transfection efficiency and is plotted on a log scale. Mean CAT values are shown and the error bars are S.E.M. of duplicate cultures.

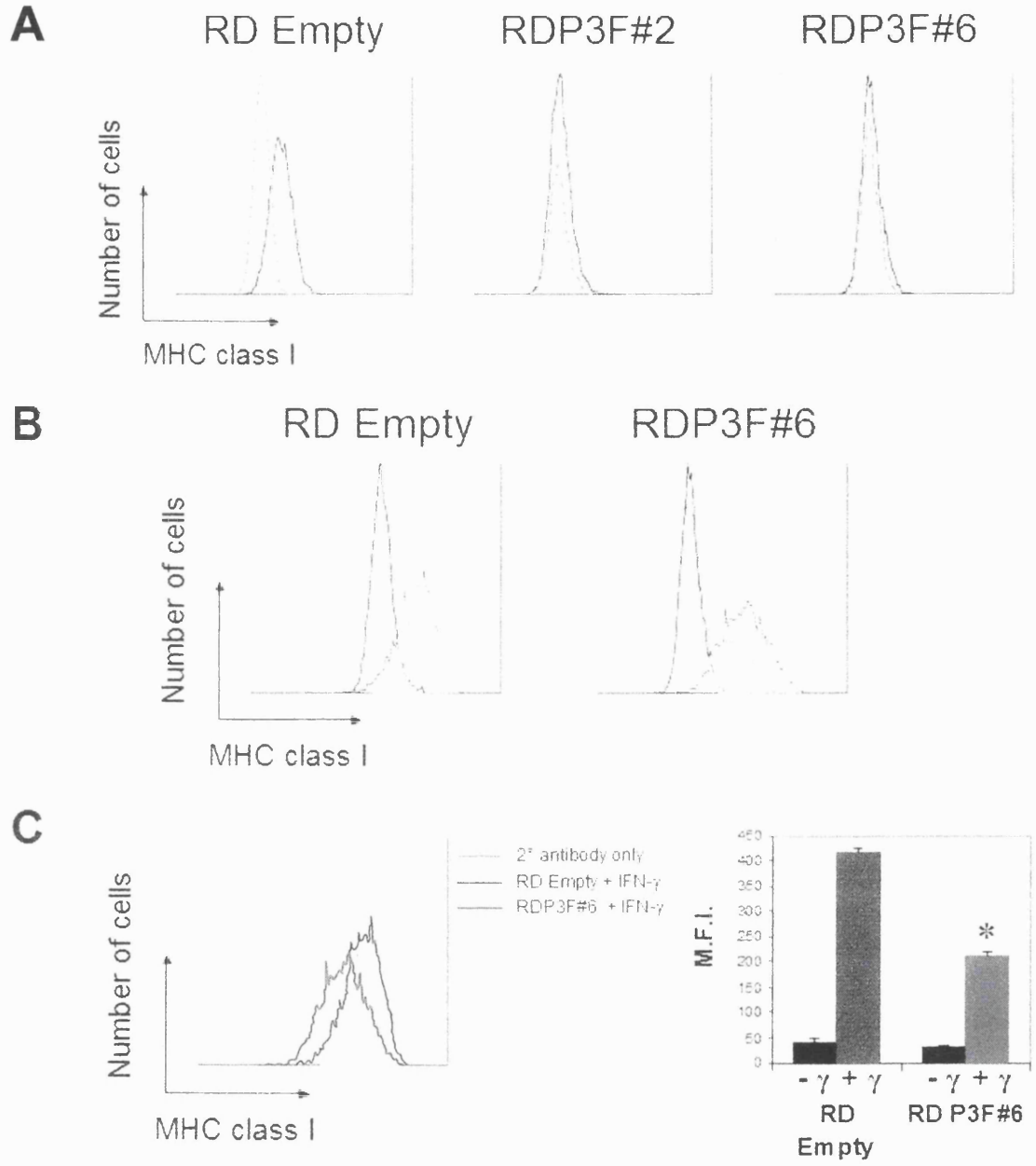

Figure 17. MHC class I expression on the surface of RD-derived cell lines. A PAX3-FKHR down-regulates MHC class I expression in the human ERMS cell line RD. The grey dotted line represents staining with PE-conjugated secondary antibody alone; the black solid line represents staining with purified MHC class I primary antibody and PE-conjugated secondary antibody. This FACS staining is representative of 4 separate experiments. **B** PAX3-FKHR causes a partial block in IFN-γ induced up-regulation of MHC class I. The grey line represents staining with the PE-conjugated secondary antibody alone; the black line represents MHC class I expression in the absence of IFN-γ; the filled in histogram represents MHC class I levels in the presence of 20ng/ml IFN-γ. This FACS staining is representative of 3 separate experiments. **C** Comparison of MHC class I expression on RD empty cells and RDP3F#6 cells when both cell lines are cultured in the presence of 20ng/ml IFN-γ for 48 hours. In the FACS plot, RD empty cells are represented by a blue line; the RDP3F#6 cells are represented by a red line; the grey line represents RD cells stained with the secondary antibody alone. The MFIs from each cell line are depicted in a bar graph. Error bars are S.E.M. from duplicate samples. A Kolmogorov-Smirnov statistical test revealed that the MHC class I levels in RDP3F#6 are significantly less than in RD Empty cells (K-S <0.001).

type RD and RD Empty cells weakly express MHC class I antigen on their cell surface (RD Empty is shown in Figure 17). In contrast, all four RD clones expressing PAX3-FKHR have undetectable levels of MHC class I on their cell surface (RDP3F#2 and RDP3F#6 are shown in Figure 17A).

In subsequent experiments, we examined the effect of transient PAX3-FKHR expression on MHC class I levels on the surface of RH18 cells. RH18 cells were co-transfected with pCMS-EGFP along with pBK-CMV or pBK-CMV-P3F. The pCMS-EGFP vector expresses GFP under the control of the SV40 promoter, and is routinely co-transfected into cells with the reporter vector, allowing GFP expression to be used as a marker of transfection. 72 hours post-transfection, the RH18 cells were stained with MHC class I antibody and analysed by flow cytometry. MHC class I expression was examined in GFP positive RH18 cells, with GFP expression being used as an indicator of successful pBK-CMV/pBK-CMV-P3F transfection. The GFP positive RH18 cells co-transfected with PAX3-FKHR had equivalent MHC class I levels to RH18 cells co-transfected with empty vector (data not shown). However, as a positive control, RD cells were transiently co-transfected with pCMS-EGFP and either pBK-CMV or pBK-CMV-P3F. The GFP positive RD cells expressing PAX3-FKHR had similarly high MHC class I levels as RD cells co-transfected with empty vector (data not shown). This is in contrast to the findings with RD cells stably transfected with PAX3-FKHR, where PAX3-FKHR caused a dramatic down-regulation of MHC class I expression (Figure 17A). This suggests that PAX3-FKHR only exerts its effect on MHC class I expression when stably expressed in cells.

3.7.4. Effect of PAX3-FKHR on IFN-γinduced up-regulation of MHC class I:

MHC class I is a well documented IFN-γ target gene (Boehm *et al*, 1997). A preliminary experiment revealed that culturing wild type RD cells with 2ng/ml IFN-γ had no effect on MHC class I levels, whereas both 20ng/ml and 200ng/ml IFN-γ caused a similarly dramatic increase in MHC class I levels. Therefore, in subsequent experiments, the cell lines were treated with IFN-γ at 20ng/ml.

As expected, culturing RD Empty cells with 20ng/ml IFN-γ for 48 hours resulted in a dramatic up-regulation of MHC class I expression (Figure 17B). While incubation of RDP3F#6 cells with 20ng/ml IFN-γ for 48 hours resulted in the induction of MHC class I expression, their MHC class I expression was significantly less than that observed in

RD Empty cells. This is shown in Figure 17C, where the MHC class I FACS plots for RD Empty cells cultured with 20ng/ml IFN-γ and RDP3F#6 cells cultured with 20ng/ml IFN-γ are overlaid. It is important to note that in all the FACS plots, the MHC class I levels are plotted on a log axis. In Figure 17C, the MHC class I mean fluorescence intensities (MFIs) are plotted on a linear scale in a bar graph. The bar graph emphasises the partial block in IFN-γ induced up-regulation of MHC class I in RD cells expressing PAX3-FKHR. A Kolmogorov-Smirnov statistical test showed that this PAX3-FKHR driven partial block in IFN-γ induced up-regulation of MHC class I was significant (K-S value <0.001).

3.8. PAX3-FKHR-directed repression of PAI-1 in RMS cell lines:

3.8.1. Effect of PAX3-FKHR on PAI-1 expression in mouse and human RMS cell lines:

Northern blot analysis was used to verify the microarray results, and confirmed that PAX3-FKHR represses *PAI-1* expression in 76-9 cells. We examined the expression of PAI-1 mRNA and protein levels in various human RMS cell lines by Northern blot and Western blot analysis (Figure 13 and 18A, respectively). PAI-1 protein is expressed at high level in RD cells ($PAX3^+$, $PAX3\text{-}FKHR^-$), but is not detected in any PAX3-FKHR-expressing human RMS cell line (Figure 18A).

We were interested in PAI-1 as a down-regulated target of PAX3-FKHR because of its known role in the inhibition of tissue invasion (Binder *et al*, 2002; Praus *et al*, 2002). To test the hypothesis that PAX3-FKHR represses PAI-1 expression in ARMS, we examined PAI-1 levels in RD cells stably transfected with empty vector (RD Empty) and PAX3-FKHR (RDP3F) (Figure 18B). RD Empty cells express high levels of PAI-1 protein. The introduction of PAX3-FKHR into RD cells results in a dramatic reduction in the levels of PAI-1. Upon longer exposure a faint PAI-1 band was detected in all 4 RDP3F clones, suggesting that PAI-1 expression is not completely abolished in PAX3-FKHR-expressing RD cells.

3.8.2. Effect of PAX3-FKHR on IFN-γ induced up-regulation of PAI-1:

Because a large number of down-regulated target genes identified from the microarray data are known IFN-γ stimulated genes, we investigated whether PAI-1 might also be an IFN-γ target. Culturing RD Empty cells for 48 hours in the presence of 20ng/ml of IFN-

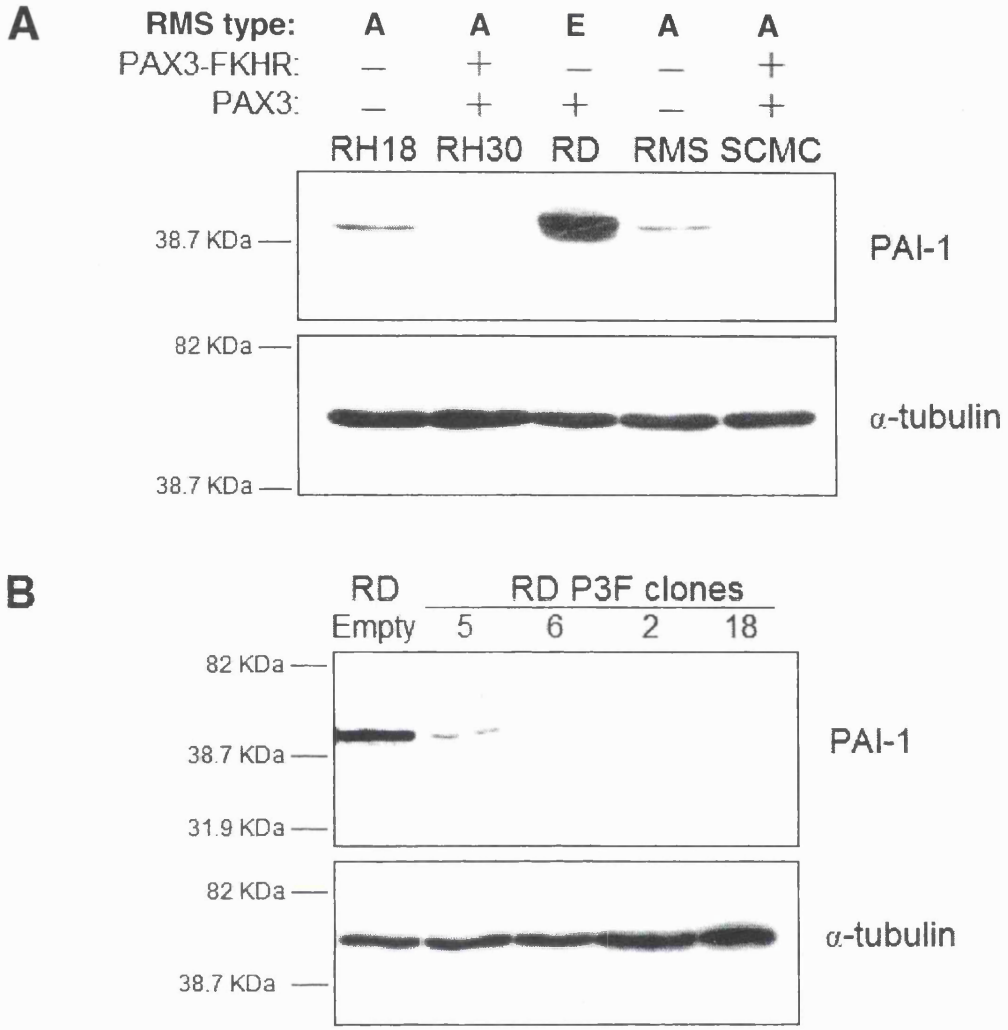

Figure 18. Expression of PAI-1 in human RMS cell lines. A Western blot analysis examining PAI-1 protein expression in several human RMS cell lines. The RMS type (A = ARMS; E = ERMS) and the expression of endogenous *PAX3* and *PAX3-FKHR* RNA (determined by Northern blot, Figure 13) for each cell line is indicated above the picture. **B** Western blot analysis examining PAI-1 protein expression in RD cells stably transfected with pBK-CMV empty vector (RD Empty) and pBK-CMV-P3F (termed RDP3F). In a longer exposure, very faint bands can be detected in the RDP3F#6, RDP3F#2, and RDP3F#18 lanes. In the Western blots, human PAI-1 was detected at a molecular weight of approximately 47 KDa, and α-tubulin expression was used as a loading control.

γ resulted in a large increase in PAI-1 protein levels (Figure 19). This novel finding suggests that PAI-1 is an IFN-γ stimulated gene in RD cells. In contrast, there was only a modest increase in PAI-1 levels in RDP3F#5 cells and no noticeable increase in PAI-1 levels in RDP3F#6 cells following 48 hours incubation with 20ng/ml IFN-γ. This result supports the MHC class I findings (Figure 17), suggesting that PAX3-FKHR down-regulates IFN-γ stimulated genes, and renders RD cells partially resistant to the effects of IFN-γ.

3.8.3. Effect of PAX3-FKHR-directed repression of PAI-1 on the phenotype of RMS cells:

Aguanno *et al* (1990) reported that TPA induces the differentiation of the RD human ERMS cell line. TPA mediates this effect through the up-regulation of PAI-1, which results in TGF-β remaining in an inactive form (Figure 20A) (Mayer *et al*, 1988; Aguanno *et al*, 1990). We were interested in whether the PAX3-FKHR-directed down-regulation of PAI-1 in RD cells (shown in Figure 18B) results in a degree of resistance to TPA-induced differentiation. We investigated TPA-induced differentiation by measuring the reduction in cell proliferation using a MTS assay. In a preliminary optimisation experiment, we found that 0.1μM TPA is optimal to induce maximum growth inhibition of wild type RD cells. Figure 20B shows that treatment of wild type RD, RD Empty, and RDP3F#5 cells with 0.1μM TPA for 72 hours causes a 30-35% reduction in the number of viable cells, relative to non-treated control cultures. TPA has slightly less effect on the proliferation rate of RDP3F#6 cells, which show only a 15.1% reduction in viable cell number after 72 hours. This preliminary experiment demonstrates that expression of PAX3-FKHR does not render RD cells significantly more resistant to the growth inhibiting effect of 0.1μM TPA.

One major problem of this assay was that an unequal number of cells were plated out for each cell line, despite careful counting using a haemocytometer. This may influence the proliferation rate of the cell lines, and distort the TPA treatment results. In an attempt to circumvent this uneven counting problem, J. Anderson tried to generate an RD cell line that expresses PAX3-FKHR in an inducible fashion. Unfortunately, the expression of PAX3-FKHR was not tightly controlled, and the cell line was unsuitable for examining the effects of PAX3-FKHR in a regulatable manner.

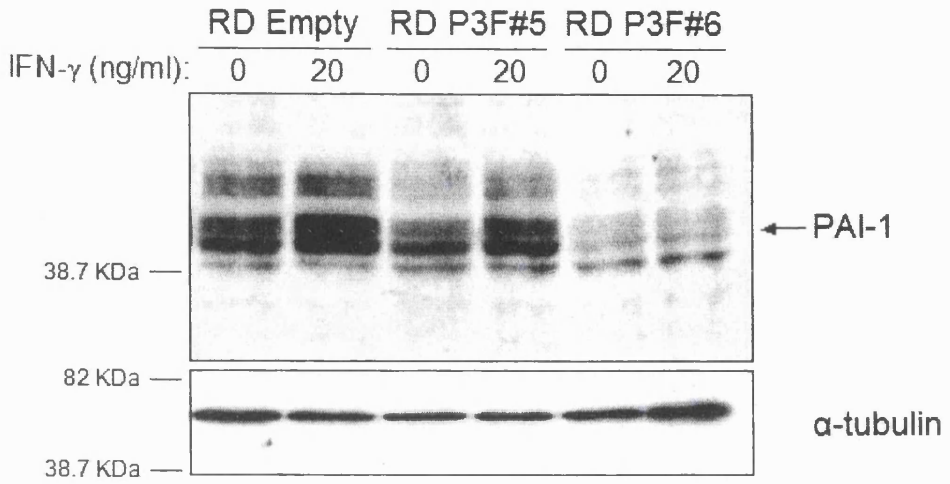

Figure 19. Western blot analysis revealing that PAX3-FKHR renders RD cells partially unresponsive to IFN-γ induced up-regulation of PAI-1. The membrane was exposed for a long time (15 minutes) in order to detect the PAI-1 present in the RDP3F#6 cells. This long exposure also resulted in picking up non-specific bands. The 47 KDa PAI-1 band appears as a doublet in this experiment. This is probably due to slight deterioration of the antibody, rather than phosphorylation of PAI-1, because when we reprobed several membranes with a new aliquot of antibody we detected a single PAI-1 band in each lane. The levels of α-tubulin were used as a loading control. This Western blot is representative of two independent experiments.

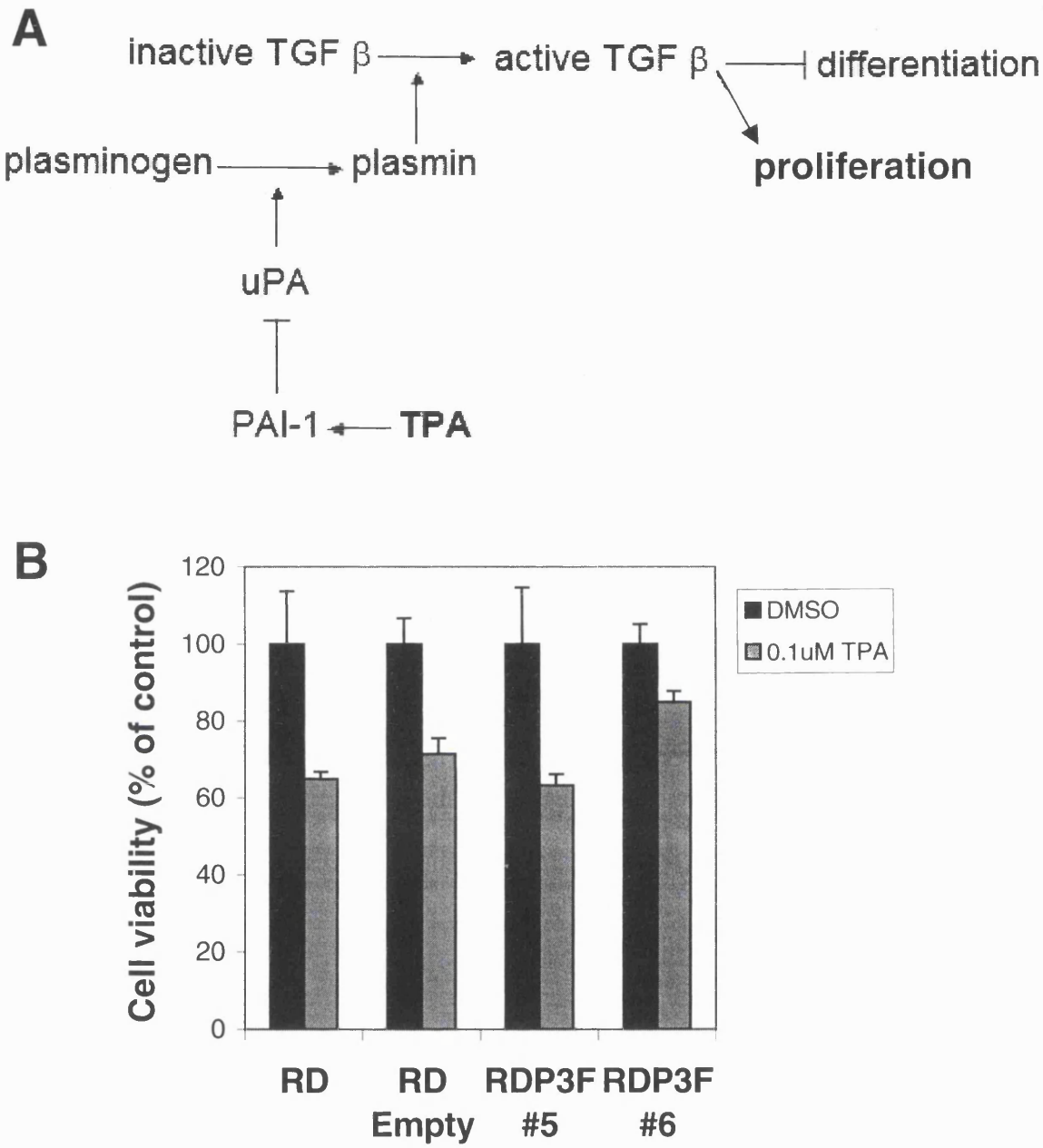

Figure 20. Effect of TPA on the viability of RD-derived cell lines. **A** Schematic summarising the putative effect of TPA on RD cells (Mayer *et al*, 1988; Aguanno *et al*, 1990; Mauro *et al*, 2002). **B** Comparative *in vitro* proliferation assay, examining TPA-induced growth arrest in RD cells. The RD-derived cell lines were treated with 0.1μM TPA or an equal volume of DMSO (delivery vehicle for TPA) for 72 hours, and then the number of viable cells was measured using a MTS assay. The number of viable cells present in wells treated with diluted DMSO was set as 100% cell growth, and the number of viable cells in the wells treated with 0.1μM TPA was calculated as a percentage relative to DMSO treated controls. The mean values are plotted and the error bars are S.D. of duplicate cultures.

3.9. Effect of PAX3-FKHR on CXCR4 expression:

We were also interested in investigating the effect of PAX-FKHR on the expression of genes known to be down-regulated by IFN-γ. We chose to look at *CXCR4* because it is documented as being repressed by IFN-γ (Gupta *et al*, 1998). Libura and colleagues (2002) recently found that CXCR4 expression was induced by the introduction of PAX3-FKHR into RD cells.

We found that the human ARMS cell line RH30 expresses high levels of *PAX3-FKHR* (see Figure 13) and has elevated levels of CXCR4 protein on its cell surface (Figure 21). Wild type RD cells and RD cells stably transfected with empty vector (RD Empty) express minimal amounts of CXCR4 (3.5% and 8.7%, respectively). Transfection of RD cells with PAX3-FKHR results in the induction of CXCR4 expression (18.2% RDP3F#6 cells were positive for CXCR4) (Figure 21). This result is concordant with our proposal that PAX3-FKHR interferes with IFN-γ target gene expression, including up-regulation of genes that are normally inhibited by IFN-γ.

3.10. Investigation into the molecular mechanisms of PAX3-FKHR-mediated interference of IFN-γ target gene expression:

3.10.1. Effect of PAX3-FKHR expression on IFN-γ signalling:

We have demonstrated using microarrays, Northern blots, Western blots and FACS analysis that PAX3-FKHR represses numerous IFN-γ stimulated genes and induces expression of several genes known to be down-regulated by IFN-γ. Next, we investigated the potential pathways involved in PAX3-FKHR-mediated interference of IFN-γ target gene expression.

IFN-γ mediates some of its effects through JAK-signal transducers and activators of transcription (STAT) signalling within cells. AG490 is a JAK family tyrosine kinase inhibitor that selectively inhibits JAK2, inhibits the constitutive activation of STAT3, and inhibits the autokinase activity of JAK3. We investigated the role of JAK-STAT signalling in PAI-1 and MHC class I expression in RD-derived cell lines. Figure 22 shows that the treatment of RD Empty and RDP3F#6 cells with 5μM and 50μM AG490 for 48 hours has no effect on PAI-1 levels. Additionally, treatment of RD Empty and RDPF#6 cells with AG490 for 48 hours did not have any effect on the levels of MHC class I (data not shown). Unfortunately, there was no suitable positive control cell line

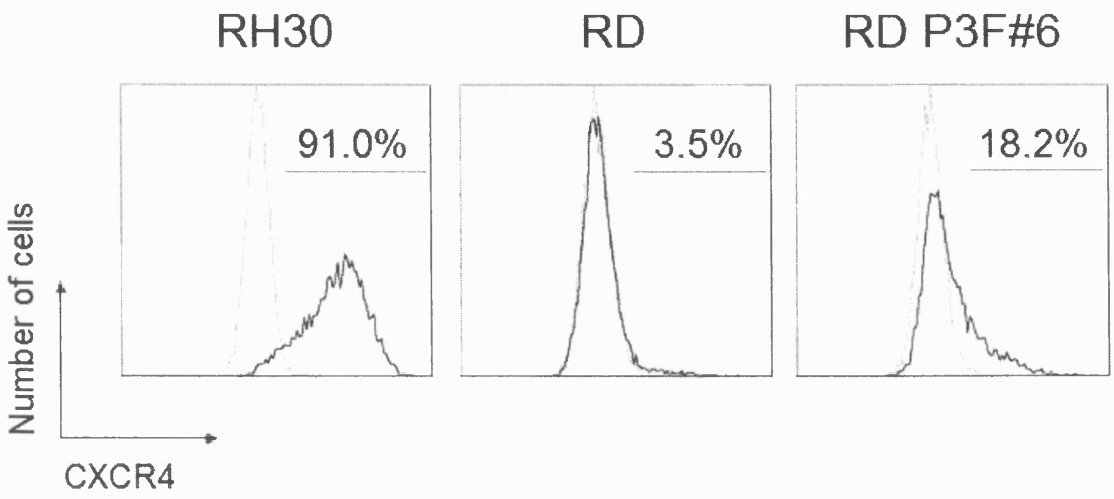

Figure 21. PAX3-FKHR up-regulates CXCR4 expression in human RMS cell lines. FACS histograms showing CXCR4 expression levels in the following 3 human RMS cell lines: RH30 cells expressing endogenous PAX3-FKHR; wild type RD cells that do not express endogenous PAX3-FKHR; RDP3F#6 cells ectopically expressing PAX3-FKHR. The grey line represents staining with a PE-conjugated isotype control antibody; the black line represents staining with a PE-conjugated anti-CXCR4 antibody. Log fluorescence of CXCR4 intensity is plotted on the x-axis and the number of cells on the y-axis. The percentage of cells that tested positive for CXCR4 expression is indicated on each plot.

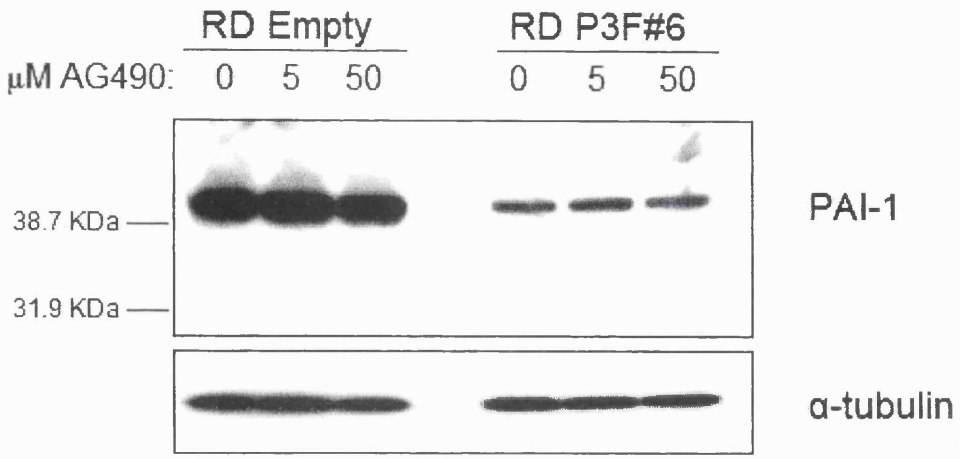

Figure 22. Western blot analysis examining the effect of AG490 treatment on PAI-1 levels in RD-derived cell lines. Treatment with 5μM and 50μM AG490 for 48 hours did not have any effect on the levels of PAI-1 expressed in RD Empty and RDPF#6 cells. The membrane was exposed for a long period (10 minutes) to detect the very low levels of PAI-1 expression in the RDP3F#6 cells. Human PAI-1 protein was detected as a 47 KDa band, and α-tubulin acted as a loading control. RDP3F#6 is representative of all 4 RDP3F clones treated with AG490.

to demonstrate that the AG490 was functional and able to block JAK-STAT signalling. Nonetheless, this result suggests that PAX3-FKHR may mediate its effect on PAI-1 and MHC class I expression via a JAK-STAT independent mechanism.

3.10.2. PAX3-FKHR does not interfere with FKHR target genes:

3.10.2.1. Identification of potential FKHR DNA-binding sites in the promoters of several genes downstream of PAX3-FKHR:

We identified the FKHR consensus DNA-binding sequence (5′-GTAAACAA-3′) in the promoter region of the genes *PAI-1* and *CXC10*, both of which were found to be down-regulated by PAX3-FKHR in 76-9 cells. Vulin and Stanley (2002) showed that FKHR directly activates PAI-1 by binding to the FKHR DNA-binding site in the promoter of *PAI-1*. Overall, this data raises the possibility that PAX3-FKHR disrupts normal FKHR signalling in RMS cells.

3.10.2.2. Effect of PAX3-FKHR expression on BIM protein levels in RD cells:

FKHR family members can directly activate *BIM*, a pro-apoptotic *BCL-2* family member, via two FKHR binding sites in the *BIM* promoter (Gilley *et al*, 2003). *BIM* is not expressed on the MG-U74 microarray, so Western blot analysis was performed to determine whether PAX3-FKHR can affect BIM protein levels in human RMS cells. Figure 23 shows that BIM is not down-regulated in RDP3F cells relative to RD Empty cells, in the absence of IFN-γ. Plotting the normalised BIM protein levels in a bar graph reveals that BIM levels are in fact elevated in the presence of PAX3-FKHR. This finding suggests that PAX3-FKHR does not block FKHR signalling in RMS cells. Culturing RD Empty and RDP3F cells in the presence of 20ng/ml IFN-γ for 48 hours resulted in a reduction in BIM expression, suggesting that BIM may be repressed by IFN-γ in these cells. We attempted to determine the levels of FKHR protein in the RD-derived cell lines by Western blot analysis. However, the antibody (purchased from Upstate Cell Signalling, USA) was not specific for human FKHR, and no meaningful result could be interpreted from the Western blot (data not shown).

Two BIM-luciferase reporter constructs were kindly donated by J. Gilley. The BIM-luciferase reporter contains the 5.2 Kb region 5′ to the *BIM* initiation codon, placed upstream of a luciferase reporter gene. The mutant BIM-luciferase reporter contains mutations in both the FKHR binding sites of the BIM reporter, which completely abrogates FKHR binding to the mutant *BIM* promoter (Gilley *et al*, 2003). Transient

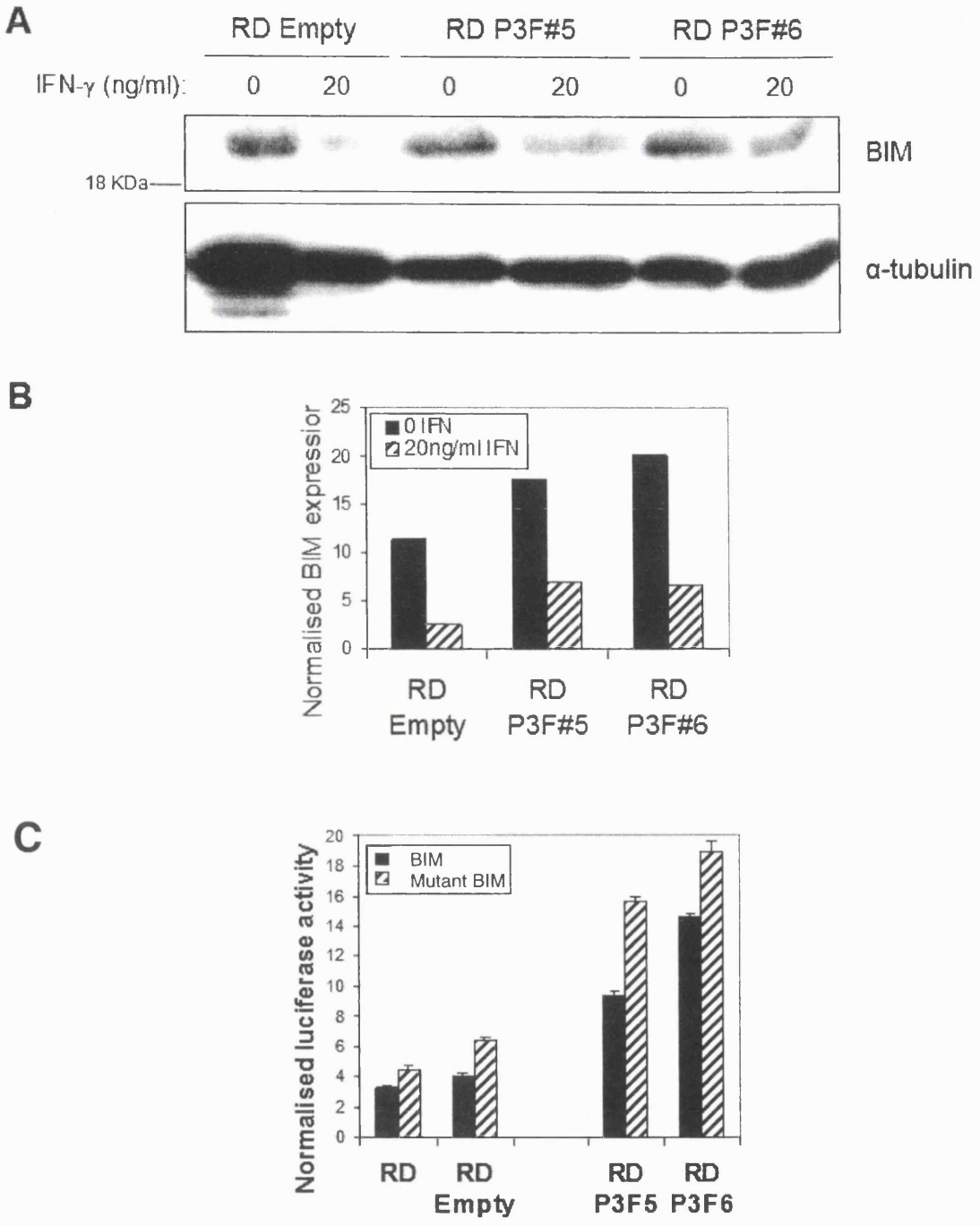

Figure 23. PAX3-FKHR does not down-regulate BIM expression in RD cells. A Western blot analysis showing BIM protein levels in RD Empty and RDP3F cells, following treatment with 20ng/ml IFN-γ and diluted PBS (delivery vehicle for IFN-γ) for 48 hours. BIM protein was detected at 23 KDa. The levels of α-tubulin were used as a loading control. **B** Bar graph showing the normalised levels of BIM protein in the Western blot depicted in A. Band intensities were measured by densitometry. **C** Luciferase assay measuring the activation of BIM-luciferase and mutant BIM-luciferase reporter genes in transiently transfected RD-derived cell lines. The mean luciferase activity values are plotted, and the error bars represent S.E.M. of duplicate cultures. Non-transfected RD cells contain undetectable luciferase activity (data not shown). This experiment is representative of two independent experiments.

transfection experiments using the BIM-luciferase reporter demonstrated that there is some activation of the *BIM* promoter in wild type RD cells. The ectopic expression of PAX3-FKHR in RD cells results in an up-regulation of *BIM* promoter activation, as determined by luciferase levels (Figure 23C). Transient transfection experiments suggest that there is enhanced activation of the mutant BIM-luciferase reporter, relative to the BIM-luciferase reporter, in all the RD-derived cell lines. This result suggests that PAX3-FKHR driven activation of the *BIM* promoter in RD cells is not mediated through binding to the FKHR consensus DNA-binding sequences in the *BIM* promoter. There are no PAX PB and HD binding sites in the *BIM* promoter.

3.10.2.3. Effect of PAX3-FKHR on IGFBP-1 expression in RD cells:

FKHR has been shown to bind the insulin-responsive sequence in the *IGFBP-1* promoter (Guo *et al*, 1999). We tested the ability of PAX3-FKHR to influence the activation of normal FKHR targets in transient transfection experiments using the IGFBP-1-luciferase reporter construct, consisting of the *IGFBP-1* promoter upstream of a luciferase reporter gene (Figure 24). The luciferase activity was very similar in the wild type RD, RD Empty, and both the RDP3F clones tested. This result suggests that PAX3-FKHR does not down-regulate *IGFBP-1* expression in RD cells. *IGFBP-1* was present on the MG-U74 microarray, and its level of expression was not significantly different in C23 and C24 cells compared to CMV cells.

3.10.2.4. PAX3-FKHR does not repress PAI-1 through phosphatidylinositol 3′-kinase (PI3K)-Akt signalling:

We found that PAX3-FKHR up-regulates *IGF2* mRNA expression in mouse RMS 76-9 cells, in agreement with published data (Khan *et al*, 1999). Another member of the insulin like growth factor family, IGF1, has been previously shown to signal via IGF receptor-1 to activate the PI3K-Akt signalling pathway (Thimmaiah *et al*, 2003). The PI3K-Akt pathway has been implicated in controlling many biological functions including cell proliferation, survival, and insulin responses (Coffer *et al*, 1998; Lawlor and Alessi, 2001). Del Peso and colleagues (1999) demonstrated that activated Akt represses the transcriptional ability of FKHR. In contrast, Akt can not inhibit the transcriptional activity of PAX3-FKHR (Del Peso *et al*, 1999). The PAI-1 promoter contains a potential FKHR DNA-binding site and PAI-1 has been shown to be up-regulated by active FKHR (Vulin and Stanley, 2002). Compilation of this published data results in a potential pathway for how PAX3-FKHR down-regulates PAI-1 in

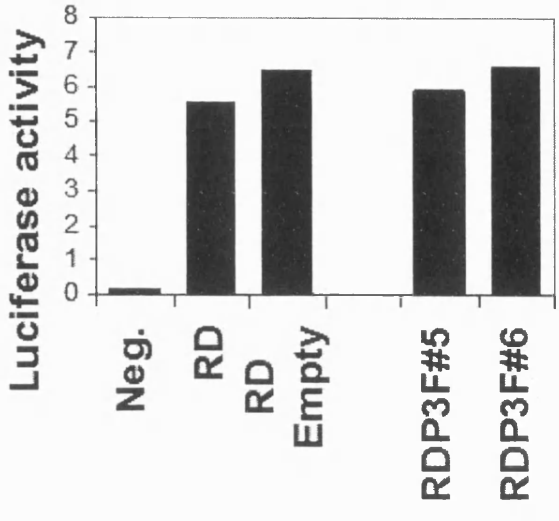

Figure 24. Luciferase assay demonstrating that PAX3-FKHR does not effect the level of *IGFBP-1* promoter activation in RD cells. RD-derived cells lines were transiently transfected with the IGFBP-1-luciferase reporter construct and the pSV-β-galactosidase control vector. 48 hours post transfection, the cells were lysed and the luciferase and -β-galactosidase levels measured. Luciferase activity (normalised for transfection efficiency) is plotted on the y-axis. Neg. represents non-transfected RD cells. There are no error bars as only single cultures were tested for each cell line.

ARMS cells (depicted in Figure 25A). To investigate whether PAX3-FKHR-mediated up-regulation of IGF2 is sufficient to repress FKHR through the PI3K-Akt pathway, we examined phospho-Akt levels in the RD-derived cell lines. If this pathway is active in PAX3-FKHR-expressing RD cells, we would expect to see elevated levels of phospho-Akt in RDP3F cells relative to RD Empty cells. Western blot analysis revealed that the levels of phospho-Akt are unaffected by the presence of PAX3-FKHR, suggesting that this pathway is not responsible for the repression of PAI-1 in RDP3F cells (Figure 25B).

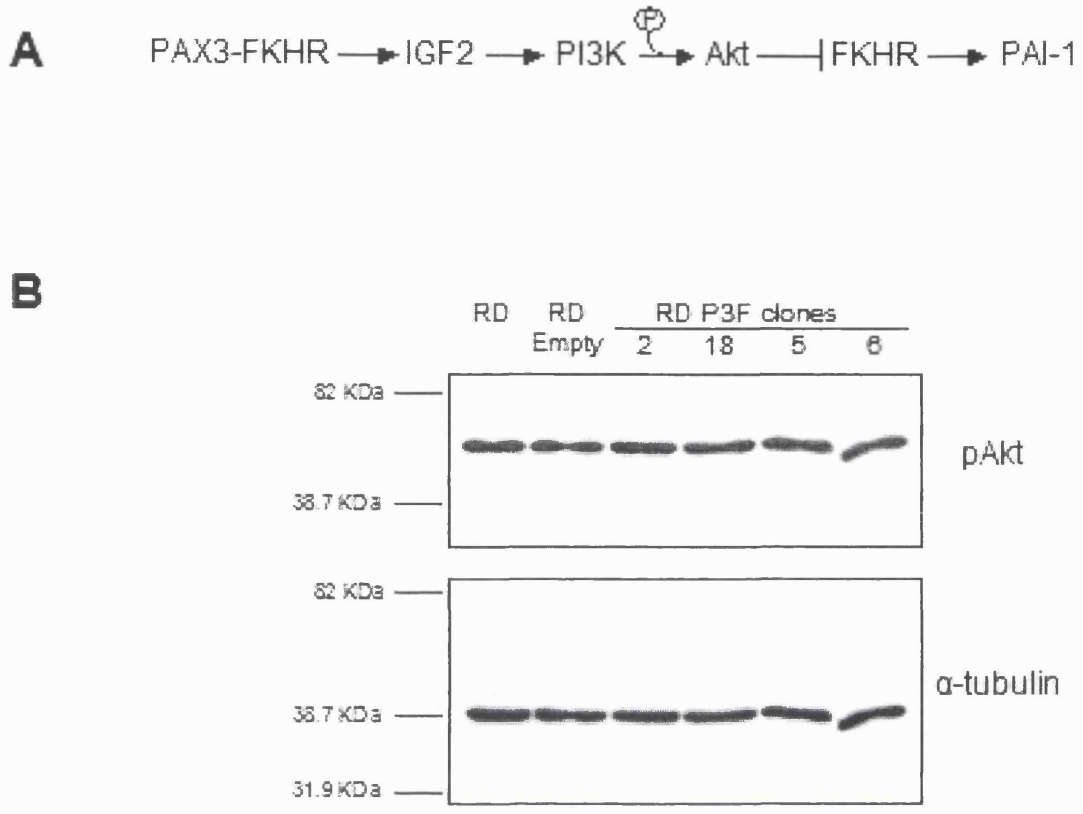

Figure 25. Levels of phospho-Akt in RD-derived cell lines. **A** A potential pathway for PAX3-FKHR-mediated down-regulation of PAI-1. **B** Western blot analysis of phospho-Akt expression in wild type RD, RD transfected with empty vector, and 4 clones of RD transfected with PAX3-FKHR.

4. Discussion

Chimeric transcription factors generated by chromosomal translocations are found in a wide range of leukaemias and paediatric sarcomas (Barr, 1998). The translocation t(2;13)(q35;q14) is a cytogenetic hallmark of ARMS, generating a PAX3-FKHR fusion protein that plays an important role in tumourigenesis (Bernasconi *et al*, 1996; Scheidler *et al*, 1996; Epstein *et al*, 1998).

4.1. Effect of the PAX3-FKHR fusion protein on RMS cell phenotype:

The 76-9 cells were stably transfected with a pBK-CMV-P3F plasmid containing the mixed murine/human PAX3-FKHR and neomycin resistance genes (clones used termed C23 and C24). After transfection with FuGENE 6 transfection reagent, 76-9 cells with stable plasmid DNA integration were selected by culturing with 500μg/ml of G418, isolated as individual clones and expanded into cell lines. It is important to note that the PAX3-FKHR transgene might not be expressed in 100% of the cells within each clone. In the absence of an antibody that specifically binds PAX3-FKHR, it is incredibly hard to prove that the fusion protein is expressed in all of the transfectants.

We found that PAX3-FKHR did not increase the *in vitro* proliferation rate of mouse RMS 76-9 cells. This is in contrast to published reports, in which ectopic PAX3-FKHR expression increased the growth rate of both the human RD RMS cell line and fibroblasts, in low serum conditions (Anderson *et al*, 2001a; Zhang and Wang, 2003). Zhang and Wang (2003) infer that PAX3-FKHR increases the rate of proliferation in fibroblasts by accelerating the G_0/G_1 to S cell cycle transition by degrading $p27^{Kip1}$ protein, an important cell cycle inhibitor. Our findings with 76-9 cells might represent a cell type-specific phenomenon.

Nonetheless, we found that ectopic expression of PAX3-FKHR did cause a more aggressive RMS cell phenotype, with elevated invasive ability *in vitro* (Figure 7). Whilst analysing this data, it is important to note that the matrigel assay might be measuring invasion, chemotaxis or both. Sub-cutaneous injection of 76-9-derived cells into syngeneic mice revealed that both wild type 76-9 cells and 76-9 cells stably expressing PAX3-FKHR are weakly metastatic. Following sub-cutaneous injection, only highly metastatic cells are able to migrate into the sub-cutaneous micro-vasculature, survive in the blood or lymphatic circulation, invade distant tissues, and

establish metastatic nodules within a 3 week period. To further investigate the effect of PAX3-FKHR on 76-9 cell metastasis *in vivo*, the cells should be injected intravenously, increasing the likelihood of finding 76-9 cells in the bone marrow and the lungs. Additionally, factors such as angiogenesis and immune evasion influence metastasis *in vivo*, but matrigel invasion assays do not address these.

4.2. Justification for our microarray experiment:

We chose to investigate the target genes of PAX3-FKHR in the murine RMS 76-9 cell line for several reasons. Firstly, ectopic expression of PAX3-FKHR has a physiologically meaningful phenotypic effect in these cells, characteristic of the aggressive ARMS subtype. Secondly, we wanted to identify the genes targeted by PAX3-FKHR in cells that already express a myogenic transcription program (expressing genes such as *MyoD*), mimicking the situation found in ARMS cells as closely as possible. Khan and colleagues (1999) expressed PAX3-FKHR in fibroblasts and found that 10 of the 11 genes activated by PAX3-FKHR in these cells were muscle related. Since many of these genes are already switched on in 76-9 cells, we hoped to detect novel targets of PAX3-FKHR.

4.3. Identification of secondary, tertiary and later transcriptional targets of PAX3-FKHR:

Interestingly, we found that PAX3-FKHR significantly down-regulated 69 genes and only significantly up-regulated 31 genes in 76-9 cells. The best understood function of PAX3-FKHR is as a potent transcriptional activator (Fredericks *et al*, 1995; Bennicelli *et al*, 1996) suggesting that many of these genes are not direct targets.

Several studies have demonstrated that PAX3-FKHR transcriptional activation utilizes solely the PAX3-derived PB and HD DNA-binding domains to recognize target sequences (Fredericks *et al*, 1995; Sublett *et al*, 1995; Bennicelli *et al*, 1996). However, none of the genes downstream of PAX3-FKHR in 76-9 cells, that we have examined, contain a PAX3 PB or HD consensus recognition sequence in their promoter. Barber *et al* (2002) used a cyclic amplification and selection of targets (CASTing) strategy to identify primary target genes directly bound by PAX3 and PAX3-FKHR proteins. None of the putative primary target genes that they identified were significantly changed by PAX3-FKHR in our microarray experiment. An explanation for these findings is that most of the global genetic change induced by PAX3-FKHR in 76-9 cells are not

primary transcriptional phenomena but might be secondary, tertiary or later transcriptional targets of PAX3-FKHR. This is further supported by our finding that PAX3-FKHR represses MHC class I expression in the human ERMS RD cell line when stably transfected into the cells, but not within 72 hours after transiently transfection into the cells. The identification of tertiary and later targets of PAX3-FKHR is still important, because these events are physiologically relevant and affect the phenotype of ARMS cells. An alternative explanation is that the transcriptional effect of the fusion protein requires more elements than the *PAX3*-derived PB and HD domains. Barber and colleagues (2002) found that DNA associates with PAX3-FKHR in an artificial environment, but provided no evidence that these genes are switched on by PAX3-FKHR in cells.

To determine the primary targets of PAX3-FKHR in mouse RMS 76-9 cells, the fusion protein needs to be expressed in an inducible manner. This could be accomplished by attaching the hormone-binding domain of the oestrogen receptor to the PAX3-FKHR cDNA. The fusion protein will only be expressed when the cells are cultured in the presence of the ligand tamoxifen. Microarray analysis could then to be performed on RNA isolated from cells in which PAX3-FKHR has been induced and subsequent translation blocked using cyclahexamide.

4.4. Genes significantly up-regulated by PAX3-FKHR in 76-9 cells:

Microarray analysis revealed that PAX3-FKHR induces expression of a limited number of genes in 76-9 cells. However, these genes influence a diverse range of cell behaviours, including survival, proliferation, angiogenesis, and metastagenesis. Due to time constraints we have only been able to investigate a few of these genes in more detail.

4.4.1. The imprinted genes IGF2 and H19:

We found that *IGF2* is significantly induced by PAX3-FKHR in mouse RMS 76-9 cells, consistent with published data showing over-expression of *IGF2* in human ARMS (Yun, 1992; Wang *et al*, 1998). This result also confirms that ectopically expressed PAX3-FKHR is able to stimulate transcription of genes from chromatin within 76-9 cells.

The IGF2 growth factor plays an important role in the survival and proliferation of normal cells (DeChiara *et al*, 1991). However, when aberrantly expressed IGF2 has the ability to transform mouse embryonic fibroblasts (Hernandez *et al*, 2003), and *IGF2* is one of the most frequently up-regulated genes in human tumour progression (Ogawa *et al*, 1993; Zhang *et al*, 1997). Zhang and colleagues (1999) reported that IGF2 over-expression in a mouse myoblast cell line shortens cell cycle time and diminishes the G_1 checkpoint after DNA damage. The authors speculate that the effects of IGF2 on the cell cycle might contribute to the fast growth rate and the accumulation of genetic alterations observed in ARMS.

H19 was induced approximately 2.5 fold in PAX3-FKHR-expressing 76-9 cells relative to empty vector transfected controls (Appendix Table 1). High level expression of the *H19* gene is associated with a more malignant phenotype in human bladder carcinomas (Ariel *et al*, 1995). It would be interesting to determine whether elevated levels of *H19* are an indicator of aggressive ARMS cases.

Interestingly, *IGF2* and *H19* are both imprinted genes located in the same region on mouse chromosome 7 (human 11p15). Loss of imprinting (LOI) is one of the most common epigenetic changes observed in cancer development (Ogawa *et al*, 1993). LOI of *IGF2* and *H19* involves activation of silent imprinted genes, and LOI of these two genes has been reported in a high proportion of rhabdomyosarcoma cases. (Anderson *et al*, 1999b).

4.4.2. Some PAX3-FKHR target genes are cell type-specific:

It is interesting to note that Khan and colleagues (1999) also identified *IGF2* and *H19* as genes induced by PAX3-FKHR in NIH 3T3 fibroblasts. However, there are no further similarities in the microarray results. Khan *et al* (1999) found that PAX3-FKHR activates a myogenic transcription program when introduced into fibroblasts. However, we found that several of the muscle-related genes they identified as up-regulated by PAX3-FKHR, such as *SIX1*, *SLUG*, and troponin T (*TNNT2*), were already expressed at relatively high levels in empty vector expressing 76-9 cells, and PAX3-FKHR was unable to increase the level of expression of these genes (analysed using Data Mining Tool software). Other downstream targets of PAX3-FKHR in NIH 3T3 cells were not expressed in either CMV or C23 cells, such as Myogenin (*MYOG*) and Complement

factor H (*HF1*). Overall, this indicates that some genes regulated by PAX3-FKHR are cell type dependent.

4.4.3. PLA2:

Two different sequences derived from phospholipase A2 (*PLA2*) were found to be up-regulated 3-4 fold by PAX3-FKHR in 76-9 cells. PLA2 enzymes metabolise the release of arachidonic acid, a key regulator of cellular proliferation, from cellular phospholipids in various tissues (Balsinde *et al*, 1999). Elevated *PLA2* levels have been detected in neoplastic prostatic tissue (Jiang *et al*, 2002) and non-small cell lung cancer (Blaine *et al*, 2001). PLA2 has been reported to be involved in cell cycle progression in neuroblastoma cells (van Rossum *et al*, 2002), and may play a similar role in ARMS.

4.4.4. Genes encoding for collagen proteins:

We identified 2 collagen genes that are induced by PAX3-FKHR in 76-9 cells, namely *COL3A1* and *COL1A1*. The expression of collagen has been correlated with an increase in the invasive ability and metastasis of melanomas (Maniotis *et al*, 1999; Clark *et al*, 2000) and adenocarcinomas (Ramaswamy *et al*, 2003). Clark *et al* (2000) used an *in vivo* selection procedure to isolate highly metastatic melanoma cells from a population of tumour cells with low metastatic potential. They identified *COL3A1* and *COL1A2* as genes expressed at elevated levels in highly metastasis melanoma cells compared to the poorly metastatic tumour cell starting population. Clark and colleagues (2000) speculate that high level expression of ECM proteins, such as collagen, may promote tumour angiogenesis. Maniotis and colleagues (1999) demonstrated that increased production of collagen allows ocular melanoma cells to lay down their own pro-migratory matrix, forming microvascular channels. It would be interesting to infer from our results that expression of these two collagen genes also promotes metastasis of RMS cells. However, we found that *COL1A2* is repressed by PAX3-FKHR in 76-9 cells. It will be important to determine whether the overall levels of collagen protein are increased in PAX3-FKHR-expressing 76-9 cells and whether they contribute to increased microvascuar channel formation and metastasis of RMS cell lines.

The role of the above mentioned genes in tumour progression is relatively well studied. Hence, we decided to examine the genes repressed by PAX3-FKHR in 76-9 cells, and how diminished expression of these genes might aid tumour progression.

4.4.5. PAX3-FKHR does not up-regulate expression of the myogenic-related c-MET and MyoD genes in 76-9 cells:

The ability of PAX3-FKHR to activate *c-MET* expression is contentious. Several studies have found that both PAX3 and PAX3-FKHR can induce expression of *c-MET* (Epstein *et al*, 1996; Ginsberg *et al*, 1998; Relaix *et al*, 2003). However, Khan and colleagues (1999) found that *c-MET* expression was not up-regulated by PAX3-FKHR in fibroblasts. Similarly, we found using microarray analysis that *c-MET* was expressed in 76-9 cells stably transfected with empty vector, and was expressed at a similar level in 76-9 cells transfected with PAX3-FKHR. In contrast, our transient transfection experiments, using a *c-MET* promoter-luciferase reporter construct, suggest that high levels of PAX3-FKHR do cause a slight increase in *c-MET* expression in 76-9 cells (Figure 10A). Northern blot and Western blot analyses are required to further investigate the levels of *c-MET* expression in these cells.

PAX3 and PAX3-FKHR-mediated up-regulation of *MyoD* is well documented (Tajbakhsh *et al*, 1997; Khan *et al*, 1999; Ridgway *et al*, 2001). However, in our microarray experiment, we found that PAX3-FKHR down-regulated *MyoD1* expression in 76-9 cells. This result needs to be verified, but does appear to contradict published findings.

4.4.6. Induction of genes that code for potential tumour-specific antigens:

4.4.6.1. XMR:

XMR was the gene most dramatically induced by PAX3-FKHR in 76-9 cells, showing approximately 7 fold up-regulation in both PAX3-FKHR-expressing clones (C23 and C24). Escalier and Garchon (2000) found that XMR protein is expressed in mouse primary spermatocytes and propose a role for XMR in chromatin condensation during meiosis. XMR has a restricted expression in adult tissue, detected solely in the testes (Escalier and Garchon, 2000), making XMR a potential tumour-specific antigen. However, XMR does not have a human ortholog that could be targeted by directed immunotherapy in the treatment of patients with ARMS.

4.4.6.2. OTT:

Similarly, the ovary testis transcribed (*OTT*) gene codes for a potential tumour-specific antigen and is up-regulated approximately 2 fold in PAX3-FKHR-expressing 76-9 cells

compared to empty vector transfected controls. However *OTT* also has no human ortholog that could be targeted by immunotherapy.

4.4.6.3. LBX1:

The homeobox gene *LBX1* has been shown to be activated by PAX3 during myogenesis (Mennerich *et al*, 1998; Brohmann *et al*, 2000), and plays a role in the proliferation and migration of muscle precursors (Brohmann *et al*, 2000; Mennerich and Braun, 2001). Unfortunately, *LBX1* was not represented on the MG-U74 microarray, so we do not know the effect of PAX3-FKHR expression on *LBX1* levels in mouse 76-9 cells. It would be interesting to examine *LBX1* mRNA levels in mouse and human RMS cells by Northern blot analysis. *LBX1* is expressed specifically during embryogenesis (Jagla *et al*, 1995) and is another potential tumour-specific antigen.

4.5. PAX3-FKHR functions are more complex than acting solely as a transcriptional activator:

Several investigators have demonstrated that the chimeric PAX3-FKHR transcription factor functions as a more potent transcriptional activator of PAX3 target genes than wild type PAX3 (Fredericks *et al*, 1995; Bennicelli *et al*, 1996). Previous transcriptional profiling studies examining PAX3-FKHR target genes have supported this model by identifying transcriptional up-regulation of myogenic factors thought to be developmentally downstream from PAX3 (Khan *et al*, 1999). However, Khan and colleagues (1999) also identified a number of target genes down-regulated by PAX3-FKHR in fibroblasts.

Surprisingly we found that PAX3-FKHR represses more genes than it induces. Of the 31 genes up-regulated in PAX3-FKHR-expressing 76-9 cells relative to empty vector transfected controls, only *IGF2* is currently recognized as being activated downstream of PAX3 in myogenic development and ARMS (Khan *et al*, 1999; Mayanil *et al*, 2001). Therefore, our data does not support a model of PAX3-FKHR as solely a potent transcriptional activator.

4.6. Genes significantly repressed by PAX3-FKHR in 76-9 cells:

The most striking finding of the microarray experiment was that a large proportion of the genes down-regulated by PAX3-FKHR in 76-9 cells are known IFN-γ stimulated genes (21 out of 44 genes with know function), including the MHC class I genes *H2-K*

and *H2-D1* (Appendix Table 2). Another gene found to be repressed by PAX3-FKHR in our microarray experiment is *PAI-1*, which we discovered is also stimulated by IFN-γ in human RD cells (Figure 19). Previously only *PAI-2* was known as an IFN-γ stimulated gene (Boehm *et al*, 1997). Chimeric transcription factors, generated by chromosomal translocations, have not been previously shown to interfere with IFN-γ regulated gene expression.

4.6.1. Multiple genes involved in the MHC class I antigen processing and presentation pathway are down-regulated by PAX3-FKHR in RMS cell lines:
Microarray analysis revealed that PAX3-FKHR down-regulates numerous genes critical for the expression of peptide-MHC class I complexes on the cell surface. For instance, the PAX3-FKHR-mediated down-regulation of *TAP1* may prevent the transport of peptides into the endoplasmic reticulum (ER) for loading into the peptide binding groove of newly synthesized MHC class I molecules (Dovhey *et al*, 2000). In this way, putative tumour-specific peptides derived from the fusion region of the PAX3-FKHR protein might not be presented to T lymphocytes.

In subsequent experiments, we demonstrated that MHC class I protein expression is abrogated by PAX3-FKHR in both mouse and human RMS cell lines (Figures 15 and 17). The down-regulation of MHC class I antigens might prevent recognition by T lymphocytes (Ferrone and Marincola, 1995), hence circumventing detection and rejection by the host immune system. Down-regulation of MHC class I expression on the cell surface has been detected in numerous murine and human tumour cell lines (Cordon-Cardo *et al*, 1991; Delp *et al*, 2000; Seliger *et al*, 2000), however the molecular mechanisms underlying these changes are not fully understood. It is interesting that the diminished expression of MHC class I in RMS can be specifically attributable to PAX3-FKHR expression, and that PAX3-FKHR may be exerting its effect through interfering with IFN-γ signalling within the RMS cells.

To investigate whether PAX3-FKHR actively down-regulates MHC class I expression in RMS, we could block endogenous PAX3-FKHR expression in the RH30 and SCMC cell lines using anti-sense oligonucleotides or interference RNA. We could then examine whether repressing PAX3-FKHR expression in these cells causes MHC class I levels to rise. However, Bernasconi and colleagues (1996) reported that specific down-regulation of the PAX3-FKHR fusion protein in RH30 cells using anti-sense

oligonucleotides results in apoptosis of the cells. We would be unable to investigate MHC class I levels in these dying cell lines reliably.

RD cells transiently transfected with *PAX3-FKHR* do not show any reduction in the level of MHC class I antigen on their surface. PAX3-FKHR appears to exert its effect on MHC class I expression only when stably transfected into RD cells. In normal circumstances, MHC class I synthesis and expression on the cell surface takes less than 48 hours (Cullell-Young *et al*, 2001), and the half life of MHC class I-peptide complexes on the cell surface is less than 5 hours (Hallermalm *et al*, 2001). However, in PAX3-FKHR-expressing RMS cells, the MHC class I genes (and *TAP* genes) could potentially be a long way downstream of PAX3-FKHR. Hence, it is possible that it might take longer than 72 hours after transient transfection with PAX3-FKHR to observe repression of MHC class I antigen on the surface of RD cells. An alternative explanation of our result is that PAX3-FKHR is expressed at higher levels in stably transfected RD cells than transiently transfected RD cells, and the PAX3-FKHR-mediated repression of MHC class I is dose dependent.

4.6.2. PAI-1 is down-regulated by PAX3-FKHR in mouse and human RMS cell lines: Northern blot analysis confirmed the microarray result, demonstrating that *PAI-1* is repressed by PAX3-FKHR in the mouse RMS 76-9 cell line (Figure 12). Western blot analysis showed that no human RMS cell line endogenously expressing PAX3-FKHR has detectable levels of PAI-1 protein. In contrast, the human ERMS RD cell line ($PAX3^+$, $PAX3\text{-}FKHR^-$) expresses high levels of PAI-1 (Figure 18A). Ectopic expression of PAX3-FKHR in RD cells results in the down-regulation of PAI-1 protein levels (Figure 18B). These combined results suggest that PAI-1 is repressed by PAX3-FKHR in ARMS.

4.6.2.1. Potential roles of diminished PAI-1 expression in tumourigenesis: PAI-1 has been implicated in three pathways involved in tumourigenesis. PAI-1 is the primary endogenous inhibitor of uPA, a serine protease involved in cancer progression (Duffy, 2002). When PAI-1 levels are repressed, uPA can catalyse the conversion of plasminogen into active plasmin, a protein that mediates degradation of ECM components, resulting in increased invasive ability (Figure 26) (Binder *et al*, 2002).

Consistent with this hypothesis, Praus and colleagues (2002) found that over-expression of PAI-1 reduces HT1080 fibrosarcoma metastatic ability *in vitro* and *in vivo*. Similarly, high levels of uPA are associated with poor prognosis in breast cancer patients (Duffy, 2002).

However, elevated levels of PAI-1 are a marker of poor outcome in several cancers, including breast cancer (Binder *et al*, 2002; Harbeck *et al*, 2002). This is counterintuitive considering the role of PAI-1 as the primary physiological inhibitor of uPA, which itself is regarded as a marker of poor prognosis. One explanation of the correlation between PAI-1 levels and malignancy of the tumour cells is that it reflects the other functions of the PAI-1 protein. PAI-1 has been shown to be pro-angiogenic (Bajou *et al*, 1998; Devy *et al*, 2002) and inhibit apoptosis (Kwaan *et al*, 2000). We postulate that the repression of PAI-1 by PAX3-FKHR is important in increasing the metastatic ability of ARMS cells, whereas the other PAI-1 functions (inhibiting apoptosis and promoting angiogenesis) may be compensated for in ARMS by other genes targeted by PAX3-FKHR, such as *IGF2*. We chose not to examine whether the re-introduction of PAI-1 reduces the invasive ability of PAX3-FKHR-expressing 76-9 cells. This is because only one component of the ECM that is normally degraded by plasmin (laminin) is not present in the matrigel basement membrane matrix used in our *in vitro* matrigel invasion assays.

Cancer cells are involved in a matrix remodelling process that includes both degradation of existing ECM to promote invasiveness, and also the induction of new matrix formation to promote angiogenesis and metastasis. PAX3-FKHR may therefore repress PAI-1 to promote uPA-directed ECM degradation, and also up-regulate overall collagen levels in RMS cells to promote angiogenesis. The disruption of tissue architecture associated with invasion and metastasis leads to the release of proinflammatory cytokines, which activate the innate and adaptive immune system (Pardoll, 2003). Tumours therefore need a mechanism to elude immune surveillance. In ARMS cells, this might occur through PAX3-FKHR driven repression of IFN-γ stimulated genes involved in the MHC class I antigen processing and presentation pathways.

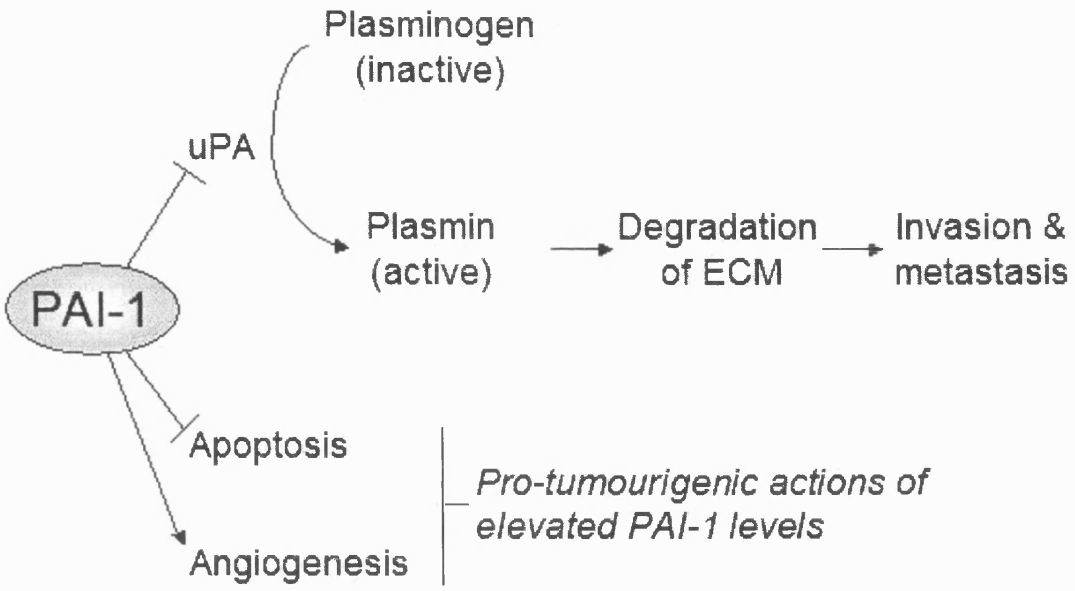

Figure 26. The anti-tumourigenic and pro-tumourigenic effects of PAI-1. Information for this figure is derived from reviews of PAI-1 and uPA function (Binder *et al*, 2002; Duffy, 2002).

4.6.2.2. Reduced levels of PAI-1 do not affect the sensitivity of human RD cells to TPA-induced growth arrest:

TPA has been shown to induce differentiation and growth arrest of the human ERMS RD cell line (Aguanno *et al*, 1990; Mauro *et al*, 2002). RD cellular differentiation is at least in part a result of TPA induction of PAI-1, which blocks the catalytic actions of uPA, hence TGF-β remains in an inactive form, unable to prevent cell differentiation (Mayer *et al*, 1988; Aguanno *et al*, 1990). In contrast, active TGF-β promotes cell proliferation and elevated levels of active TGF-β are associated with increased tumourigenicity (Wu *et al*, 2001). We examined whether the PAX3-FKHR-directed down-regulation of PAI-1 in RD cells results in increased levels of activated TGF-β, which are able to block TPA-induced differentiation. The results from our preliminary comparative proliferation assay indicate that PAX3-FKHR-mediated repression of PAI-1 in RD cells does not result in resistance to TPA-induced growth arrest (Figure 20). TPA is not present naturally in cells, and resistance to TPA *per se* is not important to tumour cells. However, the results suggest that RDP3F cells do not secrete higher levels of autocrine growth factors, such as IGF2 and TGF-β, that can overcome the differentiation signals stimulated by TPA (including activation of PKC and PAI-1). In future experiments the levels of biologically active TGF-β in RD cells expressing PAX3-FKHR could be measured directly by ELISA (Promega).

4.6.3. Future experiments to analyse the role of PAX3-FKHR as a transcription factor:

Additional experiments are required to determine whether PAX3-FKHR-directed down-regulation of PAI-1 and MHC class I levels in RMS cells is the result of PAX3-FKHR functioning as a transcription factor, binding to target genes via the PAX3-derived PB and HD DNA-binding domains. The consensus DNA-binding sequences of the PB and HD have been characterised (Chalepakis and Gruss, 1995) and mutations that abolish the DNA-binding capacity of these domains have been reported (Lam *et al*, 1999). A PAX3-FKHR expression construct containing mutations that abolish PB and HD DNA-binding needs to be cloned and stably expressed in human RMS cell lines. The levels of MHC class I and PAI-1 in 76-9 and RD cell lines expressing mutant PAX3-FKHR could be compared to the existing C23 and RDP3F cell lines.

4.6.4. PAX3-FKHR renders human RD cells partially unresponsive to IFN-γ.

RD cells expressing PAX3-FKHR are partially unresponsive to IFN-γ induced up-regulation of MHC class I and PAI-1, most noticeably in the RDP3F#6 clone (Figures 17 and 19). Together these results suggest that PAX3-FKHR interferes with IFN-γ signalling in ARMS. Dovhey and colleagues (2000) found that the renal cell carcinoma cell line Caki-2 is defective in the IFN-γ signalling pathway, unable to up-regulate TAP1 levels following IFN-γ treatment.

PAX3-FKHR also inhibits expression of IFN-γ stimulated genes in mouse C23 cells. However, we were unable to identify the source of IFN-γ in normal 76-9 cell cultures. Mouse 76-9-derived CMV and C23 cells do not secrete IFN-γ (tested by enzyme linked immunospot assay; data not shown). One possible explanation of our findings is that IFN-γ signalling in the 76-9 cells is initiated by exogenous IFN-γ present in the culture media or serum. To investigate the effect of PAX3-FKHR on MHC class I and PAI-1 expression in the absence of exogenous IFN-γ, the 76-9-derived cell lines would have to be grown in serum free media. However, these cells die within 48 hours when grown in serum free media. An alternative explanation of our findings is that PAX3-FKHR expression results in the inhibition of STAT-mediated signalling downstream of interleukin-6. Such cross talk between cytokine signalling pathways could result in the down-regulation of certain IFN-γ stimulated genes in PAX3-FKHR-expressing 76-9 cells, yet have nothing to do with IFN-γ in physiological conditions.

IFN-γ is a pleiotropic cytokine. The roles of IFN-γ include regulation of several aspects of the immune response, including stimulation of antigen presentation through MHC class I and class II molecules, as well as effects on cell proliferation and apoptosis (Boehm *et al*, 1997). Blanck (2002) claimed that the IFN-γ signalling pathway is anti-tumourigenic in tumour cells, through increasing the expression of immune function proteins that aid immune detection, and initiating an apoptosic pathway.

We postulate that PAX3-FKHR interferes with IFN-γ signalling in ARMS cells, resulting in a co-ordinated repression of multiple genes of the MHC class I antigen processing and presentation pathway, and this allows ARMS cells to evade immunosurveillance. It would be interesting to examine the levels of MHC class I

expression in numerous patient RMS samples (using tissue arrays), and correlate MHC class I levels with PAX3-FKHR expression.

IFN-γ treatment might be useful to augment the immunogenicity of ARMS tumour cells. IFN-γ has been widely tested in clinical trials of patients with renal cell carcinoma, and response rates of 15% have been reported (Bukowski, 1999). Sub-cutaneous injection of IFN-γ has more recently been used in conjunction with chemotherapy as the first-line therapy of ovarian cancer in randomised phase III trials (Windbichler *et al*, 2000). The investigators found that treatment with IFN-γ increased the progression-free survival at 3 years from 38% (in placebo treated controls) to 51%. However, administration of IFN-γ is associated with toxicity, some patients experience fevers and flu-like syndromes, which may limit treatment (Dranoff, 2004).

4.6.5. CRABP1 is down-regulated by PAX3-FKHR in mouse 76-9 cells:
Microarray analysis identified *CRABP1* as a gene that is repressed by PAX3-FKHR in 76-9 cells. *CRABP1* does not appear to be an IFN-γ stimulated gene. Northern blot analysis verified the microarray result, demonstrating that *CRABP1* is down-regulated by PAX3-FKHR in 76-9 cells. Western blot analysis using a CRABP1-specific antibody (Alexis Biochemicals, UK) is required to confirm that CRABP1 is down-regulated by PAX3-FKHR at the protein level, in both mouse and human RMS cell lines.

CRABP1 and CRABP2 proteins are directly involved in the transport of ATRA, an important regulator of cell proliferation and differentiation (Chen and Radominska-Pandya, 2000). Crouch and Helman (1991) reported that ATRA inhibits the growth of the human RMS cell lines RD and RH30. Budhu and Noy (2002) found that diminished expression of CRABP2 in MCF-7 carcinoma cells reduces cell sensitivity to ATRA induced cell death. However, we found that the repression of *CRABP1* by PAX3-FKHR did not render the 76-9 cells resistant to ATRA induced growth inhibition (Figure 14). Two possible explanations for this finding are: (i) PAX3-FKHR does not down-regulate CRABP1 levels sufficiently to prevent CRABP1 function, so the cells remain sensitive to the inhibitory effects of ATRA; (ii) CRABP1 levels do not affect the ATRA sensitivity of 76-9 cells. The later explanation is supported by the recent finding that the levels of CRABP1 and CRABP2 do not affect the sensitivity of acute myeloid leukaemia cells to ATRA induced growth inhibition (Lehmann *et al*, 2002).

4.7. PAX3-FKHR induces the expression of genes that are down-regulated by IFN-γ:

We have demonstrated using microarrays, Northern blots, Western blots and FACS analysis that PAX3-FKHR represses numerous IFN-γ stimulated genes, including the MHC class I genes *H2-K* and *H2-D1*, and *PAI-1*. We were also interested in whether PAX3-FKHR up-regulates any genes known to be repressed by IFN-γ.

4.7.1. In 76-9 cells, PAX3-FKHR up-regulates two genes that are known to be repressed by IFN-γ signalling:

Detailed analysis of the complete list of genes induced by PAX3-FKHR in 76-9 cells (Appendix Table 1) identified two genes, *LCK* and *COL1A1*, that are documented as being down-regulated by IFN-γ (Boehm *et al*, 1997). Unfortunately, time constraints prevented us from investigating the expression of these genes in more detail. However, microarray analysis also identified one IFN-γ stimulated gene (*PLA2*) that appears to be up-regulated by PAX3-FKHR. This finding needs confirmation, but conflicts with our proposal that PAX3-FKHR up-regulates genes that are repressed by IFN-γ signalling.

4.7.2. PAX3-FKHR induces CXCR4 expression in human RD cells:

CXCR4 is reported as being repressed by IFN-γ in a concentration-dependent and time-dependent manner (Gupta *et al*, 1998). Microarray analysis revealed that *CXCR4* is slightly up-regulated by PAX3-FKHR in 76-9 cells, but the induction is not significant (*t*-test; $p>0.05$). However, we found that ectopic expression of PAX3-FKHR in human RD cells induces expression of CXCR4 on the cell surface (Figure 21), in agreement with published findings (Libura *et al*, 2002). The CXCR4 induction we saw in PAX3-FKHR-expressing RD cells was less marked than that reported by Libura *et al* (2002). A possible explanation is that PAX3-FKHR was expressed at higher levels in RD cells generated by Libura *et al* (2002) and the higher PAX3-FKHR levels resulted in a more significant up-regulation of CXCR4 expression. It is possible that the 'tail' of CXCR4 positive cells we observed in RDP3F#6 cells (Figure 21) are the RD cells ectopically expressing the highest levels of PAX3-FKHR. Unfortunately, we were unable to test this theory because we do not have an antibody that specifically binds to PAX3-FKHR.

4.7.3. Role of CXCR4 expression in the metastasis of RMS cells:

CXCR4 is expressed on the surface of $CD34^+$ early haematopoietic cells and plays a role in the migration of these progenitors to haematopoietic niches in the bone marrow

via CXCR4-α-chemokine stromal-derived factor-1 (SDF-1) signalling (Aiuti *et al*, 1997). Libura and colleagues (2002) postulate that PAX3-FKHR-expressing RMS cells are able to metastasise to the bone marrow utilizing the CXCR4-SDF-1 axis.

This result is in accordance with our proposal that PAX3-FKHR interferes with IFN-γ target gene expression, by up-regulating genes normally repressed by IFN-γ and down-regulating genes normally induced by IFN-γ.

4.8. Effect of PAX3-FKHR on normal FKHR signalling:

4.8.1. Reasons to investigate the effects of PAX3-FKHR on normal FKHR target gene expression:

We decided to investigate whether PAX3-FKHR interferes with normal FKHR function for several reasons. Firstly, all reported cases of *PAX* gene rearrangements in ARMS involve fusion of *PAX* genes (*PAX3* or *PAX7*) to either *FKHR* (Turc-Carel *et al*, 1986; Douglass *et al*, 1991) or the FKHR family member *AFX* (Barr *et al*, 2002). In contrast, other oncogenic transcription factors, such as MLL fusions, are more promiscuous in their choice of fusion partner (Rowley, 1994). Secondly, these gene rearrangements cause FKHR haploinsufficiency. However, the function of the intact FKHR in ARMS has not been investigated. Thirdly, FKHR family members are involved in pro-apoptotic signalling pathways (Dijkers *et al*, 2000; Schmidt *et al*, 2002; Gilley *et al*, 2003), and it is possible that the PAX-FKHR/AFX fusion proteins are oncogenic because they abrogate FKHR-mediated apoptosis signals in RMS cells. Finally, we identified two genes (*PAI-1* and *CXC10*) that are downstream of PAX3-FKHR in 76-9 cells, and contain conserved FKHR DNA-binding sites in their promoters.

4.8.2. Effect of PAX3-FKHR on levels of BIM and IGFBP-1 in RD cells:

Gilley and colleagues (2003) demonstrated that FKHR transcriptionaly activates *BIM* directly to promote apoptosis in sympathetic neurons. Figure 23 suggests that BIM is not repressed by PAX3-FKHR in RD cells. PAX3-FKHR also appears unable to interfere with FKHR-mediated activation of the *IGFBP-1* promoter (Figure 24). These results suggest that PAX3-FKHR does not exert its survival effects in ARMS by abrogating the apoptotic signalling pathways initiated by FKHR. It is worth noting that in our PAX3-FKHR-expressing cell lines both chromosomal copies of FKHR are undisturbed, and the effect of FKHR haploinsufficiency in ARMS can not be examined.

In our experiments we looked at the effects of PAX3-FKHR on FKHR signalling, when FKHR is expressed at basal levels. There is no commercially available antibody that binds to human FKHR with high affinity, so we were unable to look at the levels of FKHR expression in our RD cells. It would be interesting to specifically activate FKHR expression in our RD cells, and then examine the effect of PAX3-FKHR on FKHR signalling. Unfortunately, there is no specific way to activate FKHR in RMS cells. Low-level irradiation would be expected to activate FKHR, but would also activate many other apoptotic molecules. An alternative approach could be to stably transfect our RD-derived cell lines with a FKHR transgene so that the cells over-express FKHR.

4.8.2.1. BIM appears to be an IFN-γ repressed gene in RD cells:

Culturing RD Empty and RDP3F cells in the presence of 20ng/ml IFN-γ for 48 hours resulted in a reduction in BIM protein expression, suggesting that BIM might be an IFN-γ repressed gene in these cells. It is interesting to note that BIM protein levels are slightly elevated in PAX3-FKHR-expressing RD cells compared to empty vector transfected controls (Figure 23). This suggests that *BIM* is another gene, along with *CXCR4*, that is repressed by IFN-γ, but activated by PAX3-FKHR in RD cells.

4.8.3. PAX3-FKHR does not repress PAI-1 through PI3K-Akt signalling:

We reasoned that PAI-1 might be inhibited as a result of PAX3-FKHR-mediated up-regulation of IGF2, which could potentially activate the PI3K-Akt pathway, resulting in down-regulation of FKHR target genes, including *PAI-1* (Figure 25A). However, there was no increase in Akt phosphorylation in PAX3-FKHR-expressing RD cells (Figure 25B), suggesting that this pathway is not activated by PAX3-FKHR. To investigate further the role of PI3K-Akt signalling in RD cells expressing PAX3-FKHR, we could treat the RD-derived cell lines with LY 294002, a specific inhibitor of PI3K and then examine phospho-Akt and PAI-1 protein levels.

4.8.4. No evidence for the direct interaction of PAX3-FKHR and FKHR:

We have not excluded the possibility that PAX3-FKHR directly interacts with FKHR. However, there is no data from yeast 2 hybrid studies to support this interaction (Lam *et al*, 1999), and there is no known dimerisation motif in the C-terminal portion of FKHR that is retained in the fusion protein.

4.9. The molecular mechanism of PAX3-FKHR-mediated interference of IFN-γ regulated gene expression:

4.9.1. IFN-γ signalling via the JAK-STAT pathway is not affected:

IFN-γ mediates its effects through JAK-STAT-dependent and -independent signalling pathways (Boehm *et al*, 1997; Ramana *et al*, 2002). Microarray analysis revealed that *STAT1* is down-regulated by PAX3-FKHR in 76-9 cells. However, the major draw back of microarray analysis is that it cannot identify post-transcriptional changes in protein expression or activity. JAK-STAT signalling is primarily regulated by post transcriptional changes, such as phosphorylation (Kerr *et al*, 2003). Hence additional studies were required to investigate JAK-STAT signalling in RMS cells.

We investigated whether PAX3-FKHR interferes with the JAK-STAT signalling pathway in the human ERMS RD cell line, using a JAK family tyrosine kinase inhibitor called AG490. Figure 22 demonstrates that treatment of RD Empty and RDP3F#6 cells with 5μM and 50μM AG490 for 48 hours has no effect on PAI-1 expression. This result suggests that PAX3-FKHR down-regulates PAI-1 (and MHC class I) via a JAK2, STAT3 and JAK3 independent mechanism. However, there was no positive control in our experiments to confirm that AG490 was functional and able to inhibit JAK-STAT signalling at the concentrations used. Nonetheless, the AG490 was used at the recommended concentrations. These preliminary findings need to be repeated with a suitable positive control.

4.9.1.1. Potential interaction of PAX3-FKHR and STAT3:

STAT3, an important transcription factor downstream of IFN-γ, is constitutively activated in a wide range of human tumours (Burdelya *et al*, 2002; Kerr *et al*, 2003). Wang and colleagues (2004) suggest that STAT3 can function as a dominant oncogene. FKHR has been shown to activate STAT3 directly, and the interaction requires the C-terminus of FKHR (Kortylewski *et al*, 2003), which is retained in the PAX3-FKHR fusion protein. FKHR activation of STAT3 is inhibited by Akt, which phosphorylates FKHR on Thr^{24}, Ser^{256}, and Ser^{319} (Del Peso *et al*, 1999; Guo *et al*, 1999). However, the Thr^{24} phosphoylation site is absent from the PAX3-FKHR fusion protein and this might render the chimeric transcription factor insensitive to Akt-mediated negative regulation. This raises the possibility that PAX3-FKHR interacts with STAT3, resulting in aberrant IFN-γ target gene expression. It is therefore important to repeat the AG490 experiments in PAX3-FKHR-expressing RD cells to examine the role of STAT3 in these cells.

4.9.2. Methylation-induced silencing of IFN regulated genes:

Kulaeva *et al* (2003) recently reported that spontaneous immortalisation of Li-Fraumeni fibroblasts involves methylation-induced silencing of multiple genes, with a high percentage (46%) being IFN regulated genes. The repression of numerous IFN-γ stimulated genes in C23 and C24 cells could be explained by PAX3-FKHR driven methylation. This hypothesis can be tested in future experiments, treating CMV and PAX3-FKHR-expressing C23 cells with the demethylating agent 5-Aza-2'-deoxycytidine (5-Aza dC; Sigma). If PAX3-FKHR methylates IFN-γ regulated gene promoters, then treatment with 5-Aza dC should cause an increase in PAI-1 and MHC class I levels in C23 cells back to the basal levels observed in CMV cells. However, 5-Aza dC is a non-selective agent and might alter the transcription of other genes, which have effects on IFN-γ targets. Kulaeva *et al* (2003) postulate that promoter methylation is an epigenetic silencing mechanism important during tumourigenesis to overcome cell senescence, and that cell senescence is induced at least in part by the IFN growth suppressive pathway. There is now revived interest in using 5-Aza dC as a therapeutic agent for the treatment of cancers where epigenetic silencing of tumour suppressor genes has occurred (Christman, 2002).

4.10. Conclusions:

Our studies indicate that in 76-9 and RD RMS cells, the expression of PAX3-FKHR results in aberrant IFN-γ regulated gene expression. IFN-γ signalling in tumour cells is regarded as anti-tumourigenic (Blanck, 2002), and PAX3-FKHR-mediated inhibition of transcription downstream from IFN-γ signalling is likely to have pleiotropic effects on tumour cell behaviour. Abolished MHC class I expression might aid immune escape and tumour progression. Repression of PAI-1 could increase the invasive ability of ARMS cells, while induction of CXCR4 might allow metastasis to the bone marrow utilising the CXCR4-SDF-1 axis signalling (Libura *et al*, 2002). IFN-γ treatment might be clinically beneficial for the partial correction of these PAX3-FKHR-mediated effects in ARMS patients.

Publications:

- Nabarro, S., Papanastasiou, A., Gilmour, K., Hubank, M., Thrasher, A., and Anderson, J. (2004) Expression profiling suggests a role for PAX3-FKHR fusion oncoprotein in the inhibition of interferon-γ signalling in rhabdomyosarcoma cells. In preparation for submission.

Appendix Table 1. The complete list of 35 sequences (derived from 31 different genes) significantly up-regulated by more than 2 fold in C23 and C24 cells relative to CMV. The asterisks in the left-hand column identify the genes that were also found to be significantly up-regulated by more than 1.5 fold in C23 and C24 cells relative to CMV cells in a higher stringency analysis.

Gene	GenBank	Affymetrix ID	Description	CMV	C23	C24	p-value
PTK7	AI326889	92325_at	Protein tyrosine kinase 7	1	2.33	1.86	0.038
LRG21	U19118	104155_f_at	Transcription factor LRG-21	1	1.64	2.41	0.032
	AW124049	104116_at	EST	1	2.18	2.2	0.031
CSNK	M10114	99065_at	Casein kappa precursor	1	2.86	3.69	0.03
	AV314618	161738_f_at	EST, adult male thymus mRNA	1	2.09	1.4	0.03
	AA770736	161067_at	EST	1	1.41	2.03	0.03
MATN2	U69262	98475_at	Matrilin-2 precursor	1	1.99	2.4	0.028
PLTP	U28960	100927_at	Plasma phospholipid transfer protein	1	2.33	2.27	0.024
NQO1	U12961	94351_r_at	NAD(P)H dehydrogenase, quinone 1	1	2.62	2.59	0.02
LCK	M12056	102809_s_at	Lymphocyte protein tyrosine kinase	1	2.09	1.91	0.017
GSTT1	L06047	96085_at	Glutathione S-transferase	1	2.44	4.16	0.016

	Gene	GenBank	Affymetrix ID	Description	CMV	C23	C24	p-value
		AW048977	102383_at	EST	1	1.48	2.06	0.014
		AI841270	102094_f_at	EST	1	1.86	2.12	0.013
	H19	X58196	93028_at	H19	1	2.55	2.3	0.01
	GFRA2	AF002701	92449_at	Glial cell line derived neurotrophic factor family receptor alpha 2	1	2.4	1.69	0.009
		Y15001	99034_at	Iroquois homeobox protein 3	1	2	3.03	0.008
	GKLF	U20344	99622_at	Zinc finger protein, gut-enriched Kruppel-like factor GKLF	1	1.8	2.27	0.006
		AA413015	97154_f_at	EST	1	2.27	2.12	0.005
	KDELR3	AI642389	104464_s_at	KDEL endoplasmic reticulum protein retention receptor 3	1	1.96	2.53	0.002
*	*CSF*	AI854864	104126_at	Cleavage stimulation factor, 3' pre-RNA subunit	1	2.06	2.36	0.002
*	*PLA2*	U66873	101328_at	Phospholipase A2 group 5	1	3.7	3.05	0.002
	COL1A1	U03419	94305_at	Procollagen type I, alpha 1	1	1.63	2.95	<0.001
	TCN2	AF090686	93736_at	Transcobalmin II	1	1.77	2.07	<0.001
*	*TGN*	D50032	93882_f_at	Trans-Golgi network, TGN38B	1	2.33	2.22	<0.001

	Gene	GenBank	Affymetrix ID	Description	CMV	C23	C24	p-value
		AI006228	96771_at	EST	1	2.43	2.19	<0.001
*	*XMR*	X72697	102818_at	Xlr related, meiosis regulated	1	6.88	7.19	<0.001
	COL1A1	AA763466	103709_at	Procollagen, type I, alpha 1	1	1.54	2.03	<0.001
*	*TRAM1*	AA763937	160936_at	Translocating chain-associating membrane protein 1	1	2.65	2.89	<0.001
	OTT	X96603	92306_at	Ovary testis transcribed	1	1.87	2.1	<0.001
	GSTT1	X98055	95019_at	Glutathione S-transferase	1	1.99	2.48	<0.001
	TRAM1	AI844979	98956_at	Translocating chain-associating membrane protein 1	1	1.8	3.82	<0.001
*	*AKR1C13*	AB027125	95015_at	Aldo-keto reductase AKR1C13	1	2.13	3.08	<0.001
*	*PLA2*	AA408341	94665_at	Phospholipase A2 group 5	1	3.74	4.44	<0.001
	COL3A1	X52046	98331_at	collagen type 3, alpha I	1	3.31	4.06	<0.001
*	*IGF2*	X71922	98623_g_at	Insulin like growth factor 2	1	5.02	6.03	<0.001

Appendix Table 2. The complete list of 69 sequences significantly down-regulated by more than 2 fold in C23 and C24 cells relative to CMV. The asterisks in the left-hand column identify the genes that were also found to be significantly down-regulated by more than 1.5 fold in C23 and C24 cells relative to CMV cells in a higher stringency analysis.

Gene	GenBank	Affymetrix ID	Description	CMV	C23	C24	p-value
		100410_at	EST	1	0.45	0.67	0.047
		98423_at	Gap junction membrane channel protein beta 2	1	0.38	0.55	0.033
		98016_at	EST, Stratagene mouse macrophage (#937306)	1	0.35	0.75	0.029
BMP-4	L47480	93456_r_at	Bone morphogenetic protein 4	1	0.42	0.63	0.025
		100511_at	EST, Soares mammary gland NbMMG	1	0.46	0.72	0.025
PEM		101368_at	Placenta and embryonic expression early gene, oncogene	1	0.45	0.7	0.024
HSR	M55219	101845_s_at	HSR	1	0.3	0.54	0.017
DCN	X53929	93534_at	Decorin	1	0.35	0.59	0.013
		161562_f_at	EST, Adult male testis (DH10B)	1	0.55	0.42	0.012
		93411_at	EST, Soares NMPu	1	0.48	0.5	0.01
BLNK	AF068182	100771_at	B cell linker protein	1	0.28	0.39	0.006
		103066_at	EST similar to thymidylate kinases	1	0.42	0.48	0.005
		100013_at	EST	1	0.48	0.5	0.004

Gene	GenBank	Affymetrix ID	Description	CMV	C23	C24	p-value
	X52574	103025_at	Moloney leukemia virus 10	1	0.48	0.53	0.003
		102848_f_at	EST	1	0.49	0.54	0.003
		97540_f_at	EST	1	0.49	0.52	0.003
TSA-1	U47737	101487_f_at	Thymic shared antigen-1	1	0.42	0.53	0.003
		100030_at	Uridine phosphorylase	1	0.49	0.4	0.003
		104538_at	Prostacyclin synthase	1	0.53	0.42	0.002
CCL5	AF065947	98406_at	Chemokine (C-C motif) ligand 5	1	0.41	0.26	0.002
PPICAP	X67809	97507_at	Peptidylprolyl isomerase C-associated protein	1	0.45	0.44	0.002
		98005_at	EST	1	0.48	0.39	0.002
		94537_at	EST	1	0.42	0.42	0.002
		98518_f_at	EST	1	0.55	0.38	0.002
CRABP1	X15789	98108_at	Cellular retinoic acid binding protein 1	1	0.52	0.41	0.002
		101424_at	EST	1	0.42	0.22	0.002

	Gene	GenBank	Affymetrix ID	Description	CMV	C23	C24	p-value
*	*PAI-1*	M33960	94147_at	Plasminogen activator inhibitor	1	0.26	0.34	0.001
*			92718_at	EST	1	0.19	0.24	0.001
			161046_at	EST	1	0.33	0.35	0.001
			104177_at	EST	1	0.27	0.36	0.001
	RGSr		161609_at	RIKEN cDNA similar to retinally abundant regulator of G-protein signaling	1	0.43	0.37	0.001
*			95052_at	EST	1	0.29	0.31	0.001
*	*MyoD1*	M18779	102986_at	Myogenic differentiation 1	1	0.34	0.35	<0.001
*			100880_at	EST	1	0.29	0.28	<0.001
	FGFBP-1		103995_at	Heparin and fibroblast growth factor binding	1	0.59	0.32	<0.001
*	*BLNK*		100772_g_at	B cell linker protein	1	0.28	0.23	<0.001
*	*COL1A2*	X58251	101130_at	Collagen, type I, alpha II	1	0.29	0.31	<0.001
*	*IIGP*		96764_at	IIGP	1	0.12	0.14	<0.001
*	*RGS-r*		94378_at	Retinally abundant regulator of G-protein signaling	1	0.39	0.29	<0.001

	Gene	GenBank	Affymetrix ID	Description	CMV	C23	C24	p-value
*			93775_at	EST	1	0.3	0.26	<0.001
	FISP-12		93294_at	FISP-12	1	0.36	0.2	<0.001
*			94224_s_at	EST	1	0.24	0.21	<0.001
*			103446_at	EST	1	0.31	0.12	<0.001
*			102906_at	EST, T-cell specific mRNA	1	0.18	0.15	<0.001
*			96643_at	EST	1	0.22	0.17	<0.001
*			161511_f_at	EST, hippocampus C57BL/6J mRNA sequence	1	0.16	0.16	<0.001
*	*TPD52L1*	AF004428	101446_at	Tumor protein D52-like 1	1	0.35	0.1	<0.001
*			103202_at	EST	1	0.17	0.08	<0.001
*	*USP18*		95024_at	Ubiquitin specific protease 18	1	0.03	0.01	<0.001
	Interferon stimulated genes:							
*	*LFI-47*	M63630	104750_at	Interferon inducible protein, IFI-47	1	0.23	0.32	0.003
	UBC4	U62483	93069_at	Ubiquitin conjugating enzyme	1	0.47	0.6	0.03

Gene	GenBank	Affymetrix ID	Description	CMV	C23	C24	p-value
Interferon stimulated genes:							
IFI204	AA960657	92251_f_at	EST, similar to Interferon activated gene 204	1	0.46	0.33	0.009
H-2	X00246	97541_f_at	H-2 histocompatibility antigen fragment	1	0.45	0.49	0.004
STAT1	U06924	101465_at	Signal transducer and activator of transcription 1	1	0.31	0.41	0.004
H-2K	AI117211	93714_f_at	Soares thymus 2NbMT similar to Mouse MHC class I H-2K gene	1	0.46	0.54	0.003
TAP1	U60020	103035_at	Transporter associated with antigen processing (TAP) 1	1	0.42	0.46	0.003
H2-D1	X52490	101886_f_at	Histocompatability 2, D region locus 1 and beta(2) microglobulin.	1	0.58	0.5	0.003
H2-K	V00746	93120_f_at	MHC class I antigen Histocompatability 2, K region	1	0.49	0.49	0.002
LMP7	U22033	102791_at	20S proteasome subunit Lmp7 (Lmp7k, s, f allele)	1	0.47	0.45	0.002
CXC10	M33266	93858_at	Chemokine (C-X-C motif) ligand 10, (interferon inducible protein 10)	1	0.36	0.25	0.001
B2M	M18837	99378_f_at	Mouse MHC class I beta-2-microglobulin	1	0.54	0.4	0.001
* *IGTP*	AJ007972	98410_at	Interferon-gamma induced GTPase	1	0.32	0.37	0.001

Gene	GenBank	Affymetrix ID	Description	CMV	C23	C24	p-value
Interferon stimulated genes:							
* *ISGF3*	U51992	103634_at	Interferon stimulated gene factor 3 gamma	1	0.23	0.17	<0.001
* *IFI204*	M31419	98465_f_at	Interferon activated gene 204	1	0.15	0.11	<0.001
* *G1P2*	X56602	98822_at	Interferon alpha inducible protein	1	0.25	0.2	<0.001
* *LRG47*	U19119	97409_at	G-protein-like LRG-47	1	0.3	0.27	<0.001
* *IGTP*	U53219	160933_at	Interferon gamma induced GTPase	1	0.29	0.2	<0.001
* *IFIT3*	U43086	93956_at	Interferon-induced protein with tetratricopeptide repeats 3	1	0.25	0.11	<0.001
* *IFIT1*	U43084	100981_at	Interferon-induced protein with tetratricopeptide repeats 1	1	0.15	0.07	<0.001

Chapter 3:

The Use of Pulsed Dendritic Cell Vaccine Strategies to Target PAX3-FKHR-Expressing Alveolar Rhabdomyosarcoma Cells

Abstract

Dendritic cells (DCs) are professional antigen presenting cells, and have been used as immune adjuvants for the treatment of cancer. 70% of alveolar rhabdomyosarcoma (ARMS) cases are characterised by the translocation t(2;13)(q35;q14) that generates the PAX3-FKHR fusion protein. We have explored the use of DCs pulsed with PAX3-FKHR antigen as a vaccine for the treatment of ARMS. We examined three different strategies for the delivery of PAX3-FKHR antigen to DCs. First, we evaluated the ability of tumour lysate-pulsed DC immunisations to protect C57BL/6 mice from a subsequent tumour challenge, using a PAX3-FKHR-expressing syngeneic rhabdomyosarcoma cell line called C23. We found that both C23 lysate-pulsed DCs and non-pulsed DCs induced anti-tumour immune responses, which did not appear to be PAX3-FKHR-specific. The small tumours that did form in DC-immunised mice were shown to contain large numbers of tumour infiltrating lymphocytes, consisting of approximately equal numbers of $CD8^+$ T cells and $CD4^+$ T cells. Results from experiments performed using beige C57BL/6 mice, that lack natural killer (NK) cell function, suggest that the DC-initiated non-specific protective effect was not primarily NK cell- mediated. For the development of peptide-pulsed DC vaccines, T cell epitopes derived from the tumour-rejection antigen need to be identified. The N-terminal PAX3 region of PAX3-FKHR is a potential tumour-associated antigen, and could be a target for antigen-specific cell-mediated immunotherapy. We utilized our mouse model of ARMS, in which C23 cells express mixed murine/human PAX3-FKHR, to examine the peptide-pulsed DC approach. We selected and chemically synthesised 3 peptides, derived from the PAX3 amino acid sequence retained in mixed murine/human PAX3-FKHR, which are potential cytotoxic T lymphocyte (CTL) epitopes. Two of the synthetic peptides enhanced the surface expression of $H2\text{-}D^b$ molecules on antigen processing defective RMA-S cells, suggesting that the peptides were able to bind this mouse major histocompatibility complex (MHC) class I molecule. In future experiments, we shall examine the ability of DCs loaded with these PAX3-derived peptides to stimulate PAX3-FKHR-specific T cell responses, *in vivo* and *in vitro*. Additionally, we attempted to identify CTL epitopes specific for the PAX3 domain of human PAX3-FKHR that might be useful for developing peptide-pulsed DC vaccines against ARMS. One theoretical HLA-A*0201-restricted CTL epitope, KLTEARVQV, was identified, and shown to bind to the HLA allele with intermediate affinity in T2 peptide binding assays. It has been shown that DCs transfected with tumour-derived

RNA are capable of inducing anti-tumour immunity. However, we were unable to investigate the ability of mouse DCs transfected with *in vitro* transcribed *PAX3-FKHR* mRNA to induce antigen-specific T cell responses *in vivo*, because we could not efficiently transfect mouse DCs with mRNA.

1. Introduction

1.1. Clinical features of ARMS:

ARMS is characterised in 70% of cases by the translocation t(2;13)(q35;q14) that juxtaposes a truncated *PAX3* gene on chromosome 2 with the 3´ sequences of the forkhead (*FKHR*) gene on chromosome 13. The hybrid gene codes for a PAX3-FKHR fusion protein (Turc-Carel *et al*, 1986; Galili *et al*, 1993; Shapiro *et al*, 1993) (see Chapter 2, Figure 1). The recent advances made in multimodal therapy (chemotherapy, radiotherapy, and surgery) have increased the long-term survival rate in ARMS to approximately 70% (Pappo *et al*, 1995). However, the survival of patients presenting with metastatic ARMS remains dismal, despite aggressive treatment (Anderson *et al*, 1999a). The development of novel therapeutic approaches is urgently required for the treatment of patients with metastatic ARMS.

1.2. Suitability of ARMS for targeted immunotherapy:

The generation of CTLs that can specifically kill tumour cells represents a potentially powerful immunotherapeutic approach to treating malignancy (Finn, 2003). We propose targeting the PAX3-FKHR fusion protein using a DC-based immunotherapeutic strategy to treat ARMS patients.

1.2.1. The break point region of PAX3-FKHR is potentially tumour-specific:

The junction-spanning peptide sequence of the oncogenic PAX3-FKHR fusion protein is a potential neoantigen that is uniquely expressed by tumour cells, and a suitable target for antigen-specific cell-mediated immunotherapy

To induce an ARMS-specific CTL response, the fusion protein must be processed, with the tumour-specific peptide epitope(s) bound by MHC class I molecules and displayed on the cell surface. Furthermore, the resulting MHC-peptide complex must be sufficiently immunogeneic to provoke an effective but specific immune response, and T cells with the capacity to respond must be in the immune repertoire (Banchereau and Steinman, 1998).

Other malignancies associated with hallmark chromosome translocations include chronic myeloid leukaemia (CML; generation of the BCR-ABL fusion protein) and B-lineage childhood acute lymphoblastic leukaemia (ALL; generation of the TEL-AML1

fusion protein) (Heisterkamp *et al*, 1985; Romana *et al*, 1994). Several groups have successfully demonstrated the induction of MHC class I-restricted BCR-ABL fusion peptide-specific CTLs in mice and humans, and these CTLs appeared to kill CML cells in an antigen-specific manner (Osman *et al*, 1999; He *et al*, 2001).

1.2.2. PAX3 is over-expressed in ARMS, Ewing's sarcoma, and melanoma:
PAX3 is normally expressed during early embryogenesis, within the neural crest and muscle precursors (Goulding *et al*, 1991; Bober *et al*, 1994). PAX3 has a very limited expression pattern in adult human tissues. Reverse transcriptase-polymerase chain reaction (RT-PCR) analysis revealed that *PAX3* gene transcripts are very weakly expressed in the adult cerebellum and skeletal muscle, but not in any other tissues examined (Stoykova and Gruss, 1994; Tsukamoto *et al*, 1994).

In contrast, PAX3 is detected at elevated levels in approximately 50% of all RMS samples (Schafer *et al*, 1994; Frascella *et al*, 1998; Tiffin *et al*, 2003), and is also highly expressed in most Ewing's sarcoma family of tumours (Schulte *et al*, 1997). Additionally, PAX3 expression has been detected in the majority of human melanoma primary cultures tested, and may contribute to melanoma cell survival (Scholl *et al*, 2001). Hence, PAX3 can be described as a potential tumour-associated antigen.

An *in vivo* immune response targeting the N-terminus of PAX3, which is retained in PAX3-FKHR, should kill PAX3-FKHR^{+ve} ARMS cells, in addition to PAX3^{+ve} ARMS, embryonal RMS (ERMS), Ewing's sarcoma, or melanoma cells. The risk of autoimmunity caused should be minimal, especially since the brain is an immune privileged site. A concern is that CTLs that react specifically against the PAX3 antigen might have been deleted in the thymus or rendered non-responsive (anergised) in the periphery (Ho *et al*, 2003). It might be possible to overcome immune tolerance by stimulating CTLs *ex vivo* with antigen-loaded DCs expressing optimal co-stimulatory signals (Small *et al*, 2000). Novel strategies to overcome tolerance include the adoptive transfer of allogeneic CTLs, and retroviral transfer of genes encoding high avidity tumour antigen-specific T cell receptors (Morris *et al*, 2003). In contrast to PAX3, wild type FKHR is widely expressed in adult mice and humans (Furuyama *et al*, 2000), and an immune response targeting the C-terminus of FKHR, which is retained in PAX3-FKHR, might cause autoimmunity.

1.2.3. PAX3-FKHR is a model tumour antigen:

Overall, there are several reasons why PAX3-FKHR is an ideal target for immunotherapy. Firstly, the potentially tumour-specific fusion protein is expressed in approximately 70% of ARMS patients (Turc-Carel *et al*, 1986; Galili *et al*, 1993). Hence, immunotherapy targeting PAX3-FKHR would be suitable for the majority of ARMS patients. Secondly, PAX3-FKHR and PAX3 are expressed in malignant but not normal cell types. Thirdly, the chimeric fusion protein appears to be vital for the growth and survival of the tumour (Bernasconi *et al*, 1996; Scheidler *et al*, 1996; Ayyanathan *et al*, 2000). This minimises the risk of the malignant cells mutating or loosing expression of PAX3-FKHR to avoid immune detection. Finally, immunotherapy would be appropriate for relapsed or resistant patients, and PAX3-FKHR expression is associated with an increased risk of relapse (Anderson *et al*, 1999a).

1.2.4. Identification of novel ARMS-associated antigens:

The chimeric PAX3-FKHR acts as an oncogenic transcription factor through the deregulation of normal PAX3 target genes (Fredericks *et al*, 1995; Bennicelli *et al*, 1996), and transcriptionally activating novel target genes (Epstein *et al*, 1998). Some of genes downstream of PAX3-FKHR may also serve as good targets for immunotherapy. Candidate genes that are over-expressed in ARMS relative to normal myogenic cells could be identified using microarray expression analysis (see Chapter 2), and then screened for immunogenicity.

1.3. Use of DCs as vehicles to deliver tumour-rejection antigens to the patient immune system:

The induction of a strong tumour-specific cellular immune response requires the presentation of tumour-rejection antigens by antigen presenting cells (APCs) to T cells, leading to the activation and clonal expansion of tumour-reactive T cell clones (Gunzer *et al*, 2001). DCs are a system of potent APCs, uniquely capable of initiating primary immune responses from naïve T lymphocytes (Banchereau and Steinman, 1998). This DC function is attributable to their high level expression of MHC class I and class II, coupled with the additional signals required for activating naïve T cells, namely co-stimulation and cytokine production (Steinman, 1991).

There is huge interest in exploiting the antigen presenting capacity of DCs for the induction of specific anti-tumour therapies. Recent developments have allowed the *in*

vitro generation of DCs in sufficiently large numbers and purity for clinical investigation. Human DCs can be differentiated *in vitro* from peripheral blood monocytes and $CD34^+$ progenitors in the presence of granulocyte macrophage-colony stimulating factor (GM-CSF) and interleukin (IL)-4 (Romani *et al*, 1994; Sallusto and Lanzavecchia, 1994; Kiertscher and Roth, 1996). *In vitro* cultured monocyte-derived DCs (MoDCs) show functional and phenotypic characteristics of immature DCs. MoDCs can be matured by the addition of bacterial lipopolysaccharide (LPS), inflammatory cytokines, Fms-like tyrosine kinase 3 ligand, or CD40 ligand (Sallusto and Lanzavecchia, 1994; Verhasselt *et al*, 1997; Panoskaltsis *et al*, 2002). Additionally, DCs can be isolated directly from the peripheral blood of patients. In current clinical trials, investigators are attempting to induce cancer immunity, both by the activation of DCs *in vivo* as well as by the *ex vivo* manipulation and reinfusion of DCs.

1.4. *Ex vivo* loading of DCs with tumour antigens:

Several *ex vivo* approaches have been used to load DCs with tumour antigens (Figure 1). The optimal strategy for the delivery of antigens to DCs has not been established, and might vary for different cancer types.

1.4.1. DCs pulsed with whole tumour lysate:

This approach involves the isolation and lysis of autologous tumour cells to generate whole tumour lysate. Pulsing DCs with tumour cell extracts enables the DCs to process and present the tumour antigens most relevant to raising an effective anti-tumour response *in vivo*. This antigen loading method is similar to the physiological process in which APCs endocytose necrotic and apoptotic tumour cells *in vivo*.

Murine models have demonstrated that DCs pulsed with whole tumour lysate are capable of initiating potent and specific anti-tumour immune responses, *in vitro* and *in vivo* (Nair *et al*, 1997; Fields *et al*, 1998). In one of the earliest phase I clinical trials utilizing pulsed DC vaccines, Nestle *et al* (1998) generated MoDCs from the peripheral blood of 4 melanoma patients and pulsed the MoDCs with autologous tumour lysate *ex vivo*. Vaccination with the tumour lysate-pulsed DCs induced delayed-type hypersensitivity (DTH) towards a melanoma-associated antigen in 2 of the patients, and those same 2 patients also showed a beneficial clinical response. Since then, DCs pulsed

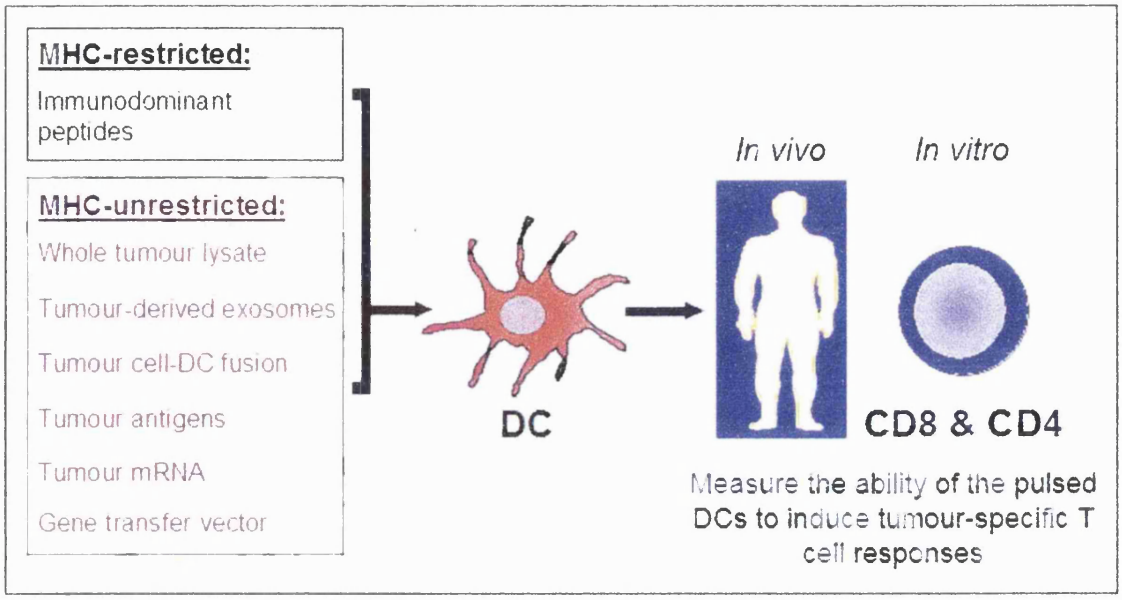

Figure 1. Use of pulsed DC vaccines for the induction of anti-tumour immunity. DCs can be isolated from peripheral blood, but are more commonly differentiated *ex vivo* from either $CD14^+$ blood monocytes or $CD34^+$ progenitors. Depicted are the main ways used to load DCs *ex vivo* with tumour antigen(s). The DC pulsing strategies are divided into MHC-restricted and MHC-unrestricted categories. The site of DC injection is important, and the administration routes used in clinical trials include intravenous, intradermal, and intralymphatic. The ability of pulsed DC vaccines to induce tumour-specific host T cell responses is typically measured *in vitro* using patient PBMCs in DTH, ELISpot and/or cytotoxicity assays. *In vivo* efficacy is determined by monitoring the clinical response to the DC vaccine, such as stalling the progression of the disease, or regression of tumour metastases.

with tumour cell lysate have been used in numerous clinical trials to treat various cancers, including metastatic renal cell carcinoma and B chronic lymphocytic leukaemia. The tumour lysate-pulsed DC immunisations have been shown to induce tumour-specific CTL responses in more than three quarters of the patients, leading to a beneficial clinical response in a small proportion of patients (Holtl *et al*, 2002; Kokhaei *et al*, 2003).

There are several advantages of using whole tumour lysate as a source of tumour antigen for pulsing DCs. Firstly, tumour lysate-pulsed DC vaccines represent an attractive approach when the tumour-specific antigens, immunodominant peptides, and/or human leukocyte antigen (HLA) restricting alleles are unknown. Secondly, tumour cell protein extracts potentially represent a source of multiple tumour-associated antigens. This minimises the risk that the tumour will develop escape variants that have lost expression of the tumour antigens being targeted by the pulsed DC vaccine. It is important to note that exogenous antigens captured by DCs are not solely processed and presented by MHC class II molecules. APCs are able to process exogenous antigen using a non-conventional MHC class I pathway, and present antigenic peptide-MHC class I complexes (Albert *et al*, 1998). This enables the tumour lysate-pulsed DCs to elicit both $CD8^+$ CTL responses and $CD4^+$ helper T (Th) cell responses, which is vital for inducing optimal systemic anti-tumour immunity (Pardoll and Topalian, 1998; Banchereau *et al*, 2001b).

A concern is that DCs pulsed with tumour cell extracts might elicit T cell responses against self antigens present in the lysate, causing autoimmunity when administered to the patient. However, several investigators noted that there were no signs of autoimmunity detected in any of the patients following tumour lysate-pulsed DC immunisation (Nestle *et al*, 1998; Holtl *et al*, 1999).

1.4.1.1. Similar approaches for loading DCs with tumour antigen:

When cultured *in vitro*, tumour cell lines have been shown to release exosomes into the supernatant, which are rich in peptide-MHC complexes and heat shock proteins (Wolfers *et al*, 2001). In pre-clinical models, DCs pulsed with tumour exosomes have been shown to induce T cells responses specific for tumour-associated antigens, *in vitro* and *in vivo* (Wolfers *et al*, 2001; Andre *et al*, 2002).

As an alternative approach to loading DCs with whole tumour lysate, Jenne and colleagues (2000) cultured human MoDCs with apoptotic melanoma cells. To induce apoptosis, the investigators irradiated the melanoma cells with ultraviolet light. The DCs phagocytosed the apoptotic bodies, and were able to prime $CD8^+$ CTL responses specific for the melanoma-associated antigens Melan A and MAGE3, *in vitro*.

A novel approach to combine the expression of tumour antigens with the co-stimulatory capabilities of APCs is to fuse tumour cells with DCs (Gong *et al*, 1997). One main limitation of this strategy is the efficiency with which tumour cells and DCs can be fused in the absence of selection (Pardoll, 2002). Trefzer and colleagues (2004) vaccinated 17 melanoma stage III and IV patients with fusions of autologous melanoma cells and allogeneic DCs. The investigators reported that of 17 patients, 1 treated with the hybrid vaccine experienced a complete response, 1 a partial response, and 6 achieved disease stabilisation. Kugler *et al* (2000) performed a hybrid cell vaccination study on a small number of metastatic renal cell carcinoma patients, and reported a beneficial clinical response in 7 of the 17 patients. However, the scientific quality of the paper has been criticised, and the authors have recently retracted the paper. In two recent phase I/II clinical trials using hybrid cell vaccination, the authors were unable to demonstrate a statistically significant treatment-associated response rate (Kikuchi *et al*, 2001; Haenssle *et al*, 2004) Overall, there is no evidence that immunotherapy with tumour-DC hybrids can initiate beneficial clinical responses in a large proportion of cancer patients.

1.4.2. DCs pulsed with defined tumour-specific antigens:

1.4.2.1. DCs loaded with unique tumour proteins:

A rapidly growing number of tumour-specific and tumour-associated antigens have been discovered that are suitable candidates for vaccination therapy, especially for melanomas (Rosenberg, 1997). In such cases, it is possible to load the DCs with the defined tumour-associated antigen instead of whole tumour cell lysate.

B cell malignancies are attractive immunotherapy targets because the monoclonal tumour cells express a unique idiotypic immunoglobulin receptor that is truly tumour-specific. Hsu and colleagues (1996) isolated DCs from the peripheral blood of patients with follicular B cell lymphoma, pulsed them with the tumour-specific idiotypic protein *ex vivo*, then infused the DCs back into the patients as a vaccine. All the patients

developed anti-idiotype cellular immune responses, and clinical responses were detected in three quarters of the patients.

In phase I and II clinical trials, Small *et al* (2000) pulsed autologous DCs with recombinant fusion protein *ex vivo*, and used the antigen-loaded DCs as a vaccine to treated hormone-refractory prostate cancer patients. All the patients developed antigen-specific immune responses leading, in some cases, to a delay in disease progression. Interestingly, the antigen-loaded DC vaccine was able to break immune tolerance to the prostate-specific antigen.

The attractive features of loading DCs with defined tumour antigens (either recombinant proteins or synthetic peptides) is that the amount of antigen administered can be controlled, and it is relatively easy to monitor the emerging immune response (Gunzer *et al*, 2001). The use of recombinant proteins circumvents the need to consider HLA restriction, and a broad spectrum of peptide epitopes, recognizable by $CD8^+$ and $CD4^+$ T lymphocytes, can originate from each protein. However, manufacturing recombinant proteins is difficult and expensive. Furthermore, the use of DCs loaded with defined tumour antigens is restricted to the few cancers in which tumour-associated and tumour-specific antigens have been identified. Current consensus is that stimulating cellular responses against a single tumour-rejection antigen might be insufficient to eliminate many cancers. This is because most tumours consist of polyclonal cells, with a range of antigens expressed and lost (Melero *et al*, 2000). Immune responses comprised of multiple T cell clones against multiple tumour antigens might be more desirable.

1.4.2.2. DCs loaded with synthetic peptides:

Numerous tumour-specific peptide epitopes recognized by tumour-reactive CTLs and Th cells have been identified. This has led to the development of peptide-pulsed DC vaccines.

Peptide epitopes that bind to HLA molecules and stimulate anti-tumour T cell responses have been identified by various methods. One approach involves eluting the peptides expressed in the peptide binding groove of MHC molecules on the surface of tumour cells (Slingluff *et al*, 1994). However, a predictive approach is more widely used. A rapidly growing number of tumour-specific and tumour-associated antigens have been discovered, and the predictive approach identifies peptide sequences within the tumour

protein that can bind to MHC class I and class II molecules. Sophisticated computer-based algorithms have been developed that identify potential HLA binding peptide sequences. They utilize our detailed knowledge about the typical number of amino acids in HLA binding peptides, and the need for key MHC anchor residues at certain positions (Rammensee *et al*, 1993). Two excellent computer-based predictive programs are SYFPEITHI and BIMAS, and these programs give every possible peptide sequence within the protein a MHC binding affinity score (Rammensee *et al*, 1999). The peptide sequences with the highest scores can then be synthesised and tested for their ability to stimulate antigen-specific T cell responses *in vitro*. For example, a 9mer peptide derived from the junction-spanning region of the ALL-specific fusion protein ETV6-AML1 has been identified that contains the appropriate anchorage motifs for binding to HLA-A2 molecules (Yotnda *et al*, 1998). The ETV6-AML1 breakpoint peptide was shown to stimulate an antigen-specific CTL response in normal HLA-$A2^+$ individuals. Investigating the immunogenicity of the CML-associated BCR-ABL fusion protein, several groups have shown that normal DCs pulsed with BCR-ABL breakpoint peptides can elicit potent CML-specific T cell responses *in vitro* (Nieda *et al*, 1998; Osman *et al*, 1999).

To minimise the chances of immune escape, DCs are typically loaded with multiple peptides, derived from several tumour antigens. In a phase I clinical trial, Nestle *et al* (1998) pulsed autologous MoDCs *ex vivo* with a cocktail of peptides derived from multiple melanoma-associated antigens. Adoptive transfer of the peptide-pulsed DCs to melanoma patients stimulated antigen-specific immunity, and objective responses were observed in 3 of the 11 patients. More recently, Lau and colleagues (2001) treated HLA-$A2^+$ melanoma patients with autologous MoDCs pulsed with HLA-A2-restricted peptides derived from the melanoma-associated antigens tyrosinase and gp100. A third of the patients exhibited melanoma-specific immune responses. In a similar study, Banchereau and colleagues (2001a) immunised 18 HLA-$A2^+$ melanoma patients with autologous $CD34^+$ progenitor-derived DCs pulsed with HLA-restricted peptides derived from melan A, tyrosinase, MAGE-3 and gp100. They found that following DC vaccination, immune response against the melanoma-associated antigens correlated with clinical outcome.

The results from these pilot studies illustrate the peptide-pulsed DC vaccines are far from optimal, and require refining to induce beneficial clinical responses in a higher

proportion of patients. Recently, investigators have immunised patients with peptide-pulsed DCs, in which the peptides are modified (by 1 amino acid) to increase HLA binding affinity (Parkhurst *et al*, 1996; Dyall *et al*, 1998; Yun *et al*, 1999). Initial studies suggest that the use of modified peptides improves the ability of the pulsed DCs to activate T cells that are specific for the original wild type peptide, resulting in enhanced systemic anti-tumour immunity (Slansky *et al*, 2000).

A major concern about peptide-loaded DC vaccination is that the cancer cells might loose expression of the tumour-associated antigens targeted by the vaccine, thus avoiding immune detection. One approach to minimise the risk of immune escape might be to pulse MoDCs with synthetic peptides in combination with autologous tumour lysate (Andersen *et al*, 2001). A major limitation of peptide-based vaccines is that they are restricted to a given HLA haplotype, and tumour peptides have not been identified for every HLA haplotype. Therefore, peptide-pulsed DC vaccines are only suitable for the limited subset of the population that express the HLA haplotype required to bind the tumour-specific peptide epitopes used. Hence, clinical trials have focused on HLA-$A2^+$ patients, as this is the most common HLA allele found in the Caucasian population.

Nonetheless, peptide-pulsed DC strategies have several advantages and further clinical trials are definitely warranted. Firstly, this subunit vaccine strategy might have superior safety and efficacy compared with tumour cell lysate-pulsed DC vaccine approaches. The clinical studies to date suggest that peptide-pulsed DC vaccinations are well tolerated without significant adverse effects (Banchereau *et al*, 2001a; Lau *et al*, 2001; Sadanaga *et al*, 2001). However, there are no reports of significant toxicity from tumour lysate-pulsed DCs either. Secondly, large amounts of clinical grade peptides can by easily synthesised.

1.4.2.3. Induction of $CD4^+$ Th responses:

A lot of work has focused on the development of $CD8^+$ CTL responses capable of lysing tumour cells. Recently, investigators have demonstrated the ability of DCs pulsed with MHC class II-restricted peptides to stimulate $CD4^+$ Th1 responses (Schuler-Thurner *et al*, 2002; Cathcart *et al*, 2004). Banchereau *et al* (2001b) suggest that the induction of Th1 responses is crucial for effective and long lasting anti-tumour immunity. The ability of cancer vaccines to induce multiple components of the immune system is paramount.

1.4.3. DCs transfected with tumour RNA or DNA:

An alternative strategy is to transfect DCs with RNA encoding tumour-associated antigens. This allows the DCs to process and present endogenously translated tumour antigens. mRNA can be synthesised *in vitro* from cDNA templates or isolated directly from tumour cells.

The polypeptide component of telomerase (TERT) is a proposed tumour rejection antigen, silent in the majority of normal cells but expressed at elevated levels in up to 85% of cancers (Kim *et al*, 1994). Nair and colleagues (2000) transfected mouse DCs with *in vitro* transcribed *TERT* RNA, and vaccination with these DCs resulted in potent TERT-specific CTL responses *in vivo*. The investigators also found that human DCs transfected with *in vitro* transcribed *TERT* RNA were able to induce CTL responses specific for cancer cells expressing telomerase *in vitro*. More recently, Nair and colleagues (2003) have pulsed DCs with mRNA encoding vascular endothelial growth factor (VEGF) and its receptor VEGF-R, proteins that are preferentially expressed during neoangiogenesis. Immunisation of mice with *VEGF* and *VEGF-R* mRNA-pulsed DCs caused the regression of pre-existing tumours.

Boczkowski and colleagues (2000) isolated total mRNA from mouse melanoma cells and transfected the mRNA into *ex vivo* cultured DCs. Immunisation of mice with the tumour mRNA-transfected DCs resulted in the induction of tumour-specific CTL responses and the regression of lung metastases. Similarly, human MoDCs transfected with total RNA from myeloma cell lines stimulated myeloma-specific CTLs in culture (Milazzo *et al*, 2003). Nair *et al* (2000) reported that immunisation with total tumour RNA-transfected DCs was superior to immunisation with *TERT* RNA-transfected DCs at inducing anti-tumour immunity. An advantage of transfecting DCs with tumour-derived mRNA, rather than mRNA encoding specific antigens, is that the transfected DCs can process and present peptides to induce immune responses against multiple immunogenic tumour antigens (Milazzo *et al*, 2003). Furthermore, the characterisation of the relevant tumour rejection antigens is not required.

The encouraging findings from these pre-clinical studies have led to a phase I clinical trial, in which autologous DCs transfected with prostate-specific antigen (*PSA*) RNA were used as a vaccine to treat patients with metastatic prostate cancer (Heiser *et al*, 2002). The vaccinations were not associated with any adverse effects and PSA-specific

T cell responses were generated in all the patients. Future clinical trials are warranted to determine the clinical benefit of RNA-transfected DC vaccines.

A major advantage of using tumour antigens in the form of RNA is that biologically active mRNA can be amplified from small amounts of tumour sample by RT-PCR, proving sufficient amounts of antigen from practically every patient (Boczkowski *et al*, 2000). Additionally, antigens encoded by RNA present multiple peptide epitopes for different MHC haplotypes, expanding the scope of vaccination to virtually every cancer patient.

A similar approach, transducing DCs with genes encoding tumour-associated antigens, has had encouraging results in pre-clinical studies. In mouse experiments, DCs retrovirally transduced with the cDNA encoding a model antigen (beta-galactosidase; β-gal) were able to elicit strong antigen-specific CTL responses, capable of rejecting pre-established tumours that express β-gal (Song *et al*, 1997; Specht *et al*, 1997). Human MoDCs transfected with *TERT* plasmid DNA were able to generate CTL responses that kill telomerase positive but not telomerase negative tumour cell lines *in vitro* (Frolkis *et al*, 2003). Tuting and colleagues (1998) transfected human MoDC with plasmid DNA encoding 5 different melanoma-associated antigens. The genetically modified DCs were able to elicit melanoma antigen-specific CTLs from peripheral blood mononuclear cells (PBMCs) *in vitro*.

1.4.4. Current clinical trials utilizing ex vivo antigen-loaded DCs:

There is great promise in the application of DCs as immune adjuvants for treating cancer, and multiple tumour antigen-pulsed DC vaccine strategies are currently being tested in clinical trials. However, the most effective method of antigen loading DCs *ex vivo* has yet to be elucidated. Additionally, investigators are yet to agree on the optimal maturation state of the *ex vivo* manipulated DCs and the most suitable route of administration for initiating anti-tumour immune responses (Nestle *et al*, 2001; Pardoll, 2002).

1.5. Manipulation of DCs *in vivo*:

A limitation of *ex vivo* manipulated DC vaccines is that they are a form of personalised therapy, tailored to the individual patient. Hence, they are expensive and not feasible for

large-scale immunisation. This has led some scientists to study the stimulation of DCs *in vivo*.

The melanoma vaccine Melacine (Corixa, USA) has recently progressed through late stage clinical trials, and is now available for sale in Canada. Melacine consists of lysate from two human melanoma cell lines mixed with a novel adjuvant suitable for human use (http://www.corixa.com). The vaccine is injected intradermally, where residing Langerhans cells (an epidermal DC subset) capture the melanoma antigens *in situ*, migrate to draining lymph nodes, and initiate tumour-specific immune responses. In clinical trials, Melacine induced response rates equivalent to that of aggressive chemotherapy, with the advantage of Melacine being that it did not generate any toxic side effects, in contrast to chemotherapy (Mitchell, 1998). The ability of DCs, pulsed with the extracts of HLA-mismatched tumour cell lines, to stimulate T cell responses against the autologous tumour is the result of cross-priming (Berard *et al*, 2000).

A major problem of antigen delivery systems is the paucity of adjuvants suitable for human treatment that can induce cellular immunity. To overcome this, McKenzie and colleagues (2003) designed a 'DC tag' to target defined tumour antigens to DCs *in vivo*, ensuring effective presentation of the tumour antigen to the immune system. The investigators covalently conjugated a tumour antigen (MUC1) to an inert carrier protein. Following injection, the conjugated MUC1 was captured by DCs, processed and presented by MHC molecules, which induced potent T cell responses. More detailed pre-clinical studies should reveal the potential of using this DC tag system to treat cancer patients.

1.6. Previous studies investigating potential immunotherapeutic strategies for the treatment of ARMS:

It has proved difficult to demonstrate that T cell responses can be generated that recognize and kill tumour cells expressing the PAX3-FKHR fusion protein. There are no examples in the literature of PAX3-FKHR-specific T cells in ARMS patients. In mouse experiments, there is preliminary evidence that CTL lines can be generated and are able to lyse murine tumour cells expressing PAX3-FKHR (Mackall *et al*, 2000). Unfortunately, there were no figures depicting their data, and the specificity of the splenic $CD8^+$ T cells for PAX3-FKHR was not demonstrated.

Dagher and colleagues (2002) attempted to target the tumour-specific breakpoint region of PAX3-FKHR using a peptide-pulsed DC vaccine strategy to treat ARMS patients. However, they were unable to detect a beneficial clinical response in any of the 4 patients. The study was severely flawed for several reasons. Firstly, the peptide sequences used to pulse autologous DCs were selected purely on their theoretical HLA binding affinities. *In vitro* binding assays are clearly required to examine the actual HLA binding affinities of the peptides, which often do not correlate with the predictions. Additionally, the ability of peptide-pulsed DCs to stimulate CTLs specific for PAX3-FKHR-expressing cells should be examined *in vitro*, to confirm that the selected peptides are immunogenic, and naturally processed and presented by ARMS cells. Most importantly, the patients were not HLA typed. Hence, it is uncertain that the peptides used could be presented by HLA molecules expressed on the patient-derived DCs.

1.7. Aims of the current study:

Additional pre-clinical studies are clearly required to investigate the ability of tumour antigen-pulsed DCs to induce ARMS-specific immune responses, *in vivo* and *in vitro*. We have established and utilized a mouse model of ARMS to examine the ability of tumour lysate-pulsed DC immunisations to protect from a subsequent tumour challenge. Tumour lysate-pulsed DCs as well as non-pulsed DCs provided non-specific protection against a subsequent tumour challenge, which appeared to be T cell-mediated. We also identified two H2-D^b binding peptide motifs derived from the N-terminus of PAX3-FKHR. The ability of DCs pulsed with these peptides to elicit tumour-specific immunity *in vivo* will be examined in the future using the mouse ARMS model. Additionally, we identified an HLA-A*0201 binding motif in the PAX3 amino acid sequence retained in human PAX3-FKHR. Future studies are required to determine whether MoDCs pulsed with this peptide are able to stimulate PAX3-FKHR-specific CTL responses in HLA-$A*0201^+$ ARMS patients.

2. Methods and Materials

2.1. *In vivo* tumour growth experiments:

2.1.1. Animals:

Wild type and beige C57BL/6 mice (6-8 week old males) were purchased from Harlan Laboratories (UK). Mice were housed in a pathogen-free environment and treated in accordance with the University College London guidelines.

2.1.2. Generation of bone marrow-derived DCs:

Bone marrow was flushed out of the tibias and femurs of C57BL/6 mice with a 25-gauge needle and syringe, using serum free Roswell Park Memorial Institute (RPMI) media (Gibco, UK). The extracted bone marrow was pipetted up and down until in a single cell suspension, then passed through a cell strainer to remove debris. The bone marrow cells were pelleted by centrifugation at 130g for 5 minutes. The supernatant was discarded and the cells resuspended in complete media, consisting of RPMI media supplemented with 10% heat-inactivated fetal calf serum (FCS), 2mM glutamine, 100IU/ml penicillin, 100μg/ml streptomycin, 25mM HEPES (all from Gibco), and 50μM β-mercaptoethanol (Sigma, UK). The bone marrow cells collected from one mouse were typically resuspended in 60ml of complete media, and plated into two 150mm tissue culture dishes (TPP, Switzerland). Recombinant mouse (rm) GM-CSF (PeproTech, UK) was immediately added to the DC cultures at 25ng/ml, and the cells cultured for 7 days at 37°C in 5% CO_2 under sterile conditions. On day 3 of culture, the media (containing contaminating non-adherent granulocytes) was discarded and replaced with fresh complete media with 25ng/ml rmGM-CSF and 10ng/ml rmIL-4 (PeproTech). By day 6 of culture, the DCs were in the non-adherent fraction, and the majority of adherent cells were macrophages. As a DC enrichment step, the non-adherent cells were collected and re-plated in new culture dishes. On day 7 of culture, the non-adherent cells, containing immature DCs, were harvested and centrifuged at 130g for 5 minutes. The media was discarded, the cells resuspended in fresh complete media, and plated in a new dish. The immature DCs were used for fluorescence activated cell sorting (FACS) analysis, DC maturation cultures, or tumour antigen pulsing.

To mature the DCs, the day 7 non-adherent cell fraction was cultured in complete media supplemented with 50μg/ml keyhole limpet haemocyanin (KLH; Calbiochem, UK),

25ng/ml rmGM-CSF, and 10ng/ml rmIL-4 for 24 hours. The loosely adherent cells were dislodged by pipetting media over the cells, added to the non-adherent cell fraction, and used for immunophenotyping by FACS analysis or as a source of activated DCs in subsequent experiments.

LPS contamination was minimised to avoid unwanted activation of immature DC cultures. All culture media and tissue culture solutions were endotoxin-free, and glassware was baked at 180°C for 4 hours to remove LPS.

2.1.3. Antigen pulsing of DCs:

The generation of the CMV (PAX3-FKHR^{-ve}) and C23 (PAX3-FKHR^{+ve}) 76-9-derived cell lines has been described earlier (see Chapter 2, *2.4.2.*). The cell lines were maintained in R10 RPMI media (RPMI media supplemented with 10% FCS, 2mM glutamine, 100IU/ml penicillin and 100µg/ml streptomycin), and cultured at 37°C in 5% CO_2 under sterile conditions.

To generate cell lysate, the C23 cells were trypsinised, washed in phosphate buffered saline (PBS; Gibco), and resuspended in a small volume of R10 RPMI media. The cells were counted using a haemocytometer, and 3×10^6 cells aliquoted per cryovial. The C23 cells were then lysed by three freeze-thaw cycles (liquid nitrogen to 37°C water bath), with lysis confirmed using trypan blue staining. The lysates were vortexed briefly, and large particles removed by passing the lysate through a 0.45µM filter. The lysate aliquots were stored in liquid nitrogen until use.

On day 7 of culture, immature DCs were harvested and used for tumour antigen pulsing. 1×10^6 immature DCs were incubated with lysate generated from 3×10^6 C23 cells for 24 hours, in 2ml of complete media containing 50µg/ml KLH, 25ng/ml rmGM-CSF, and 10ng/ml rmIL-4. For immunisation with non-pulsed DCs, 1×10^6 immature DCs were cultured in 2ml of complete media containing 50µg/ml KLH, 25ng/ml rmGM-CSF, and 10ng/ml rmIL-4. The C23 lysate-pulsed DCs and non-pulsed DCs were harvested, washed twice in PBS, and resuspended in 150µl of PBS for injection.

2.1.4. DC immunisations and tumour challenges:

C57BL/6 mice were immunised sub-cutaneously in the right flank with 1×10^6 C23 lysate-pulsed DCs or non-pulsed DCs, twice at 7 day intervals. Mice were challenged 7 days after the last DC immunisation with 1×10^6 viable C23 or CMV cells (resuspended in 150µl of PBS) by sub-cutaneous injection into the left flank. The diameter of the tumours was measured on a regular basis using callipers. To convert the tumour diameter into tumour volume, the following formula was used:
Volume = $4/3\pi$ (diameter/2)^3. The mice were individually identified by the unique stripe markings on their tails. The mice had to be sacrificed if the tumours grew to 10% of the size of the animal, or if the tumour ulcerated the skin.

2.2. *In vitro* assays utilizing the tumours and spleens of DC-immunised mice:

2.2.1. Disaggregation of tumours by enzymatic digestion:

The sub-cutaneous tumours were excised and any non-malignant tissue removed. The tumours were cut into small pieces and transferred to 6-well plates (TPP). The tumour pieces were incubated in 2ml of Hank's balanced salt solution (HBSS) supplemented with 4mg/ml collagenase (Sigma), at 37°C for 1 hour. The tumour cell suspensions were then passed through a cell strainer, and used for FACS analysis to immunophenotype any tumour infiltrating lymphocytes.

2.2.2. Interferon (IFN)-γenzyme linked immunospot (ELISpot) assays:

Splenocytes were harvested from mice on day 2 post C23 tumour challenge or at the end of the *in vivo* tumour growth experiment (19-24 days after C23 tumour challenge). Spleens were pressed through a cell strainer into complete media, and a single cell suspension generated by pipetting. The splenocytes were pelleted by centrifugation at 130g for 5 minutes. The media was discarded and the splenocytes resuspended in red blood cell lysis buffer (equivalent of 1ml/spleen; Sigma). Following a 1 minute lysis incubation period, complete media was added to dilute the lysis buffer. The splenocytes were centrifuged, the media decanted, and the cells resuspended in complete media at approximately 4×10^6 cells/ml. Splenocytes were then cultured in tissue culture dishes for 3 hours. The non-adherent cells were harvested and cryopreserved in complete media plus 10% dimethyl sulphoxide (DMSO; Sigma). Cryopreserved splenocytes were thawed and washed once in complete media before use in ELISpot experiments as a source of effector cells.

ELISpot 96-well plates (Millipore, USA) were pre-wet with 100µl/well of sterile 70% ethanol for 1 minute, then all traces of ethanol were aspirated. The ELISpot plates were coated with 100µl/well of anti-mouse IFN-γ monoclonal antibody (XMG1.2; eBiosciences, USA) at 5µg/ml in PBS, and incubated at 4°C overnight. The plates were then washed five times with 200µl/well of wash buffer (PBS plus 0.05% Tween 20; Tween 20 from BDH Laboratories, UK) and blocked with 200µl/well of complete media for 1 hour at room temperature. The blocking solution was removed, and the effector cells, along with stimulator cells or KLH, were then seeded into the wells of the ELISpot 96-well plate in 100µl of complete media (see below). The cells were cultured in the ELISpot plate for 48 hours at 37°C in 5% CO_2.

At the end of the 48 hour incubation period, the cells were removed, and the plates were washed 5 times with wash buffer. 100µl of biotin-conjugated anti-mouse IFN-γ detection antibody (R4-6A2, eBiosciences) was added to the wells at 1µg/ml in assay diluent buffer (PBS with 10% FCS). The plates were incubated with the detection antibody at room temperature for 2 hours. Following another 5 washes in wash buffer, 50µl of 1×Extravadin Alkaline Phosphatase Conjugate (Sigma) was added per well and the plates incubated at 37°C for 1 hour. After washing, 100µl of Alkaline Phosphatase Substrate (Bio-Rad, UK) was added to the wells and incubated at room temperature until spots developed. The colour reaction was terminated by washing the wells twice with distilled water. Once the plates had air dried, the number of spots was counted on an ELISpot plate reader (BioReader 3000; BioSys, Germany) using BioSys analysis software. Assays were performed in at least triplicate wells.

2.2.2.1. Stimulation of splenocytes with CMV or C23 stimulator cells:
Non-adherent splenocytes were used as effector cells and seeded at 1×10^5 cells/well in complete media. CMV (PAX3-FKHR^{-ve}) or C23 (PAX3-FKHR^{+ve}) cells were used as stimulator cells, and added at 1×10^4 cells /well in complete media, with the total volume adjusted to 100µl/well. An effector to stimulator cell ratio of 10:1 was used in all experiments. In negative control wells, effector cells and stimulator cells were cultured alone, and the number of spots in these controls was subtracted from the corresponding test values.

2.2.2.2. Stimulation of splenocytes with exogenous KLH:

1×10^6 non-adherent splenocytes were seeded per well of a coated ELISpot 96-well plate, in 100µl of complete media with or without 8µg of KLH. In positive control wells, 2µl of hamster anti-mouse CD3 purified monolclonal antibody (Becton Dickinson, USA) was added to the splenocytes. The number of spots that were observed in negative control wells containing no splenocytes was subtracted from all the test well values.

2.3. Flow cytometric analysis:

2.3.1. Staining procedure:

Immature and mature DC cultures, as well as disaggregated tumour samples, were immunophenotyped using FACS analysis. Approximately 5×10^5 cells were suspended in 30µl of PBS and incubated with the optimised concentration of primary antibodies (unconjugated or fluorochrome-conjugated monoclonal antibodies), in the dark at 4°C for 30 minutes. To wash off unbound antibody, the samples were centrifuged at 180g for 4 minutes at 4°C, the supernatant was decanted, and the cells were resuspended in PBS. This washing step was performed three times in total. Where necessary, the cells were resuspended in 30µl of PBS and incubated with a secondary antibody in the dark at 4°C for 30 minutes. The secondary antibody was washed off with three changes of PBS as described above, and the cells fixed in 300µl of PBS containing 1% paraformaldehyde (PFA). Cells were stored in the dark at 4°C until being analysed using a Beckman Coulter Epics FACS machine and Expo 32 software (Beckman Coulter, USA).

2.3.2. Panels of antibodies used:

The mouse bone marrow-derived DC cultures were immunophenotyped using the following antibodies against: CD86 (fluoroscein isothiocyanate (FITC)-conjugated), CD11c (Phycoerythrin (PE)-conjugated), I-A/I-E (PE-conjugated), CD80 (unconjugated; all from Becton Dickinson), and DEC205 (unconjugated; Serotec, UK). The cells incubated with CD80 or DEC205 primary antibodies were subsequently incubated with a FITC-conjugated mouse anti-rat IgG secondary antibody (Jackson ImmunoResearch Laboratories, USA). The isotype control antibodies required were rat IgG_{2a} (FITC-conjugated), rat IgG_{2b} (PE-conjugated), hamster Ig group 1,λ (PE-conjugated; all from Becton Dickinson). Cells were stained with FITC-conjugated

mouse anti-rat IgG antibody alone as a control for the secondary antibody staining. The optimal concentration of each primary and secondary antibody was determined by titration in a preliminary experiment.

The following antibodies were used to immunophenotype tumour infiltrating lymphocytes in disaggregated tumour samples: anti-mouse CD3 (PE-conjugated), anti-mouse CD4 (tri-colour (TC)-conjugated), anti-mouse CD8 (TC-conjugated), anti-mouse CD69 (PE-conjugated), anti-mouse CD19 (PE-conjugated; all from Becton Dickinson), and anti-mouse NK1.1 (unconjugated; eBiosciences). PE-conjugated anti-mouse IgG secondary antibody (Becton Dickinson) was used for cells stained with unconjugated anti-mouse NK1.1 primary antibody. Species and isotype-matched monoclonal antibodies were used as controls, along with staining using the secondary antibody alone.

2.3.3. FACS analysis using Expo 32 software:

For DC analysis, large granular cells were selected using forwards scatter (FSC) versus side scatter (SSC) gating. In experiments analysing tumour infiltrating lymphocytes, splenocytes were used as a positive control for antibody staining efficiency. The FSC versus SSC gate used to select splenic lymphocytes was retained for the analysis of disaggregated tumour samples, in an attempt to isolate tumour infiltrating lymphocytes from the other tumour cell types. During analysis, 1% of the cells stained with the relevant isotype control antibody were set as positive for the test antigen. This allowed the calculation of the percentage of positively stained cells in test samples.

2.4. Peptide binding assays:

2.4.1. Predictive computer programs:

We used the SYFPEITHI (http://syfpeithi.bmi-heidelberg.com/scripts/MHCServer.dll) and BIMAS (http://bimas.dcrt.nih.gov/cgi-bin/molbio/ken_parker_comboform) computer algorithms to identify potential MHC class I binding peptide motifs. The computer programs were used to predict H2-K^b or H2-D^b binding peptides motifs in the mixed murine/human PAX3-FKHR amino acid sequence (NCBI identity: AF178854). We also attempted to identify HLA-A*0201 binding motifs in the human PAX3-FKHR amino acid sequence (NCBI identity: U02368). The scoring systems of the 2 computer algorithms are explained in detail on their respective websites.

2.4.2. Peptide synthesis:

The mixed murine/human PAX3-FKHR-derived peptides QLMAFNHL, GVFINGRPL, and GGVFINGRPL, and the human PAX3-FKHR-derived peptide KLTEARVQV were synthesised by Zinsser Analytic (UK). The peptides were found to be more than 95% pure by high performance liquid chromatography, and the expected molecular weights were observed using matrix-assisted laser desorption mass spectrometry. The peptides were reconstituted in PBS to a concentration of 1mM and stored at –20°C. O. Williams (Institute of Child Health, UK) donated the H2-D^b binding NP68 peptide, which is derived from influenza virus nucleoprotein. The HLA-A*0201 binding flu matrix peptide (FMP) was a gift from A. Thrasher (Institute of Child Health, UK).

2.4.3. Mouse RMA-S peptide binding assay:

The RMA-S and RMA cell lines were kindly provided by H. Stauss (Imperial College, UK). RMA-S is an $H2^b$ antigen processing defective cell line, whilst its parental cell line RMA has normal antigen processing ability. RMA-S and RMA cells were cultured in complete media at 37°C in 5% CO_2, and maintained at 3×10^5-1×10^6 cells/ml. The cell lines were split 24 hours before use in peptide binding assays.

For peptide binding assays, the RMA-S cells were washed in serum free RPMI media, and resuspended in RPMI supplemented with 5% boiled FCS (to prevent protease activity). RMA-S cells were seeded at 2×10^5 cells/well in 96-well plates, and incubated for 3 hours with a range of concentrations of each synthetic peptide (0.001μM-100μM). In negative control wells, RMA-S cells were incubated with no exogenous peptide. Subsequently, the cells were washed twice in PBS, and stained with 2μg/ml PE-conjugated anti-H2-K^b antibody or 4μg/ml PE-conjugated anti-H2-D^b antibody (both from Caltag, USA), in the dark at 4°C for 30 minutes. As an isotype control, RMA-S cells were incubated with 4μg/ml of PE-conjugated mouse IgG_2 (Becton Dickinson). The cells were washed twice with PBS, then fixed in 300μl of PBS containing 1% PFA. The cells were analysed using a Beckman Coulter Epics FACS machine and Expo 32 software. Viable cells were selected by FSC versus SSC gating, and surface H2-K^b or H2-D^b expression measured. The mean fluorescence intensity (MFI) was determined for each sample. RMA cells were used as a positive control for antibody staining efficiency.

2.4.4. Human T2 peptide binding assay:

T2 is an HLA-A*0201$^+$ antigen processing defective cell line, and was a gift from H. Stauss. T2 cells were cultured at 3×10^5-1×10^6 cells/ml in R10 RPMI media at 37°C in 5% CO_2. The T2 cells were split 24 hours before use in peptide binding assays.

T2 cells were washed in serum free RPMI media, and resuspended in RPMI supplemented with 5% boiled FCS. In 96-well plates, 3×10^5 T2 cells/well were incubated overnight with serial dilutions of peptides (0.01μM-100μM), in the presence of 2μg/ml β_2-microglobulin (Sigma). Wells containing T2 cells without exogenous peptide or with known HLA-A*0201 binding FMP were used as negative and positive controls, respectively. The T2 cells were then washed in PBS, and stained with FITC-conjugated monoclonal antibody specific for HLA-A*0201 (2μg/ml; Becton Dickinson) in the dark at 4°C for 30 minutes. In control wells, T2 cells were stained with 2μg/ml isotype control FITC-conjugated mouse IgG_{2b} antibody (Becton Dickinson). After 2 wash steps with PBS, FACS analysis of HLA-A*0201 surface expression was performed, and the MFIs compared.

*2.4.5. Screening for HLA-A*0201$^+$ normal donors and RMS cell lines*:

We screened PBMCs from 5 healthy donors and multiple human RMS cell lines (including RD, RH18, RH30, SCMC, RMS and HX170c) for surface HLA-A*0201 expression. 5×10^5 cells were incubated with 2μg/ml FITC-conjugated anti-HLA-A*0201 monoclonal antibody or FITC-conjugated mouse IgG_{2b} antibody in the dark at 4°C for 30 minutes. The MFIs were determined by FACS analysis, and compared to positive control HLA-A*0201$^+$ PBMCs.

2.5. Transfection of cells with RNA:

2.5.1. Generation of green fluorescent protein (GFP) mRNA by in vitro transcription:

The pGEM4Z/GFP/A64 plasmid was a gift from E. Gilboa (Duke University Medical Center, USA), and contains a 741 bp *Bam*HI-*Not*I *GFP* DNA fragment (isolated from pEGFP-N1; Clontech, USA) and a 64 A-T bp oligonucleotide (Nair *et al*, 1999). The plasmid was linearised using the restriction enzyme *Spe*I (Promega, USA), purified using a gel extraction kit (Qiagen, UK), and used as a template for *in vitro* transcription. The *in vitro* transcription reaction was performed using T7 RNA polymerase (Promega)

and 5′ m^7G capping analogue (Promega), according to the protocol provided by the manufacturer. The *in vitro* transcripts were treated with DNase I (Roche, USA) to remove template DNA, and the RNA was recovered by phenol:chloroform and chloroform extraction, followed by isopropanol precipitation. The *GFP* mRNA was washed in 70% ethanol, and resuspended in RNase free water (see Chapter 2, *2.2.1.* for detailed methodology). The *in vitro* transcripts were examined for size and integrity by agarose-formaldehyde gel electrophoresis, and stored at –80°C.

2.5.2. Transfection of RD cells with GFP mRNA:

The human RD cell line was a gift from J. Shipley (Institute of Cancer Research, UK) and grown in Dulbecco's Modified Eagle's Medium (DMEM) containing 10% heat inactivated FCS, 2mM glutamine, 100IU/ml penicillin, and 100µg/ml streptomycin. 4×10^5 cells were seeded into 6-well plates, and cultured overnight to adhere. The cells were transfected with *in vitro* transcribed *GFP* mRNA using TransMessenger Reagent (Qiagen), following the manufacturer's instructions. Briefly, 4µl of Enhancer R and 2µg of *GFP* mRNA were mixed in buffer EC-R, and incubated at room temperature for 5 minutes. 8µl of TransMessenger Reagent was added to the RNA-enhancer solution, and incubated at room temperature for a further 10 minutes. The transfection cocktail was then diluted in 900µl of serum free DMEM and added to the cells (media above the cells was aspirated immediately before addition of the diluted transfection cocktail). After 3 hours incubation with the transfection cocktail, the cells were washed and cultured overnight in DMEM plus 10% FCS (also containing 2mM glutamine, 100IU/ml penicillin, and 100µg/ml streptomycin). In negative control wells, the RD cells were mock transfected with Enhancer R and TransMessenger Reagent without mRNA. As a positive control, RD cells were transfected with *GFP* DNA (pCMS-EGFP plasmid; Clontech) using FuGENE 6 Transfection Reagent (Roche; see Chapter 2, *2.4.2.* for methodology). Approximately 30 hours post transfection, the RD cells were harvested and checked for GFP expression by FACS analysis. Viable cells were selected by FSC versus SSC gating, and the number of GFP-expressing cells quantified.

2.5.3. Transfection of mouse DCs with GFP mRNA:

Both day 7 immature DCs and day 8 mature (KLH activated) DCs were used for the transfection experiments. The DCs were harvested, washed in serum free RPMI, and seeded at 8×10^5 cells/well of a 6-well plate. The DCs were incubated with the *GFP*

mRNA transfection cocktail (formed exactly as described in *2.5.2.*) in 1ml of serum free RPMI. After 3 hours, the DCs were washed, and cultured overnight in RPMI complete media with 25ng/ml rmGM-CSF and 10ng/ml rmIL-4. The DCs were then harvested, stained with PE-conjugated anti-human I-A/I-E monoclonal antibody or isotype control PE-conjugated mouse IgG_{2b} antibody, and analysed by FACS. DCs were identified by their large size (FSC), high granularity (SSC), and surface expression of the MHC class II molecules I-A/I-E. The gated DCs were then evaluated for GFP protein expression.

2.5.4. In vitro transcription and translation (IVT) of PAX3-FKHR and GFP proteins: IVT reactions were performed to confirm that mixed murine/human PAX3-FKHR protein and GFP protein can be synthesised from the PBK-CMV-P3F plasmid and the pGEM4Z/GFP/A64 plasmid, respectively.

The pBK-CMV-P3F vector was linearised using the restriction enzyme *Mlu*I (Promega). The IVT reactions were performed using the TNT Coupled Reticulocyte Lysate System (Promega), following the manufacturer's protocol. In the TNT lysate reaction, 1µg of linearised pBK-CMV-P3F vector DNA was mixed with 12.5µl of TNT rabbit reticulocyte lysate, 20 units of T3 RNA polymerase, 1µl of [^{35}S]methionine (Amersham Biosciences, UK), 0.5µl of amino acid mixture (minus methionine), 20 units of RNasin ribonuclease inhibitor, and 1µl of TNT reaction buffer in a final volume of 25µl. Linearised pGEM4Z/GFP/A64 vector (linearised using *Spe*I) and *in vitro* transcribed *GFP* mRNA (see *2.5.1.*) were used in TNT coupled reticulocyte lysate reactions. T7 RNA polymerase was used in the reactions using linearised pGEM4Z/GFP/A64 vector as a DNA template, while no RNA polymerase was added to the reactions using *in vitro* transcribed *GFP* mRNA. In the negative control samples, no linearised plasmid or *in vitro* transcribed RNA was added to the TNT lysate reaction. Luciferase DNA was used in the TNT lysate reaction as a positive control. The reactions were incubated at 30°C for 90 minutes.

12.5µl of IVT reaction were mixed with 2× SDS sample buffer (125mM Tris-HCl (pH 6.8), 20% glycerol, 4% SDS, 0.1% bromophenol blue, 20mM EDTA, 1mM PMSF, 5% β-mercaptoethanol) and denatured at 95°C for 5 minutes. The denatured IVT samples were then electrophoresed on an 8-10% SDS-polyacrylamide gel. Next, the polyacrylamide gel was submerged in fixing solution (50% methanol, 10% glacial acetic acid, 40% water) for 30 minutes at room temperature. The gel was rinsed for 5

minutes in solution consisting of 7% acetic acid, 7% methanol, and 1% glycerol. Finally, the gel was air dried under vacuum, wrapped in cling film, and exposed on a phosphoimager screen overnight. The incorporated [^{35}S]methionine was measured on the phosphoimager (Molecular Dynamics, UK), using ImageQuant software (Molecular Dynamics). The expected sizes of the PAX3-FKHR, luciferase, and GFP proteins are 130 KDa, 60 KDa, and 30 KDa, respectively.

3. Results

3.1. Whole cell lysate-pulsed DC vaccine strategy:

3.1.1. Generation of a mouse model of ARMS:

The mouse RMS cell line 76-9 was stably transfected with a pBK-CMV vector containing *PAX3-FKHR* mixed murine/human cDNA under the control of a CMV immediate early gene promoter (the clones used in experiments were called C23 and C24). As a control cell line, 76-9 cells were stably transfected with empty pBK-CMV vector (termed CMV). Expression of *PAX3-FKHR* mRNA in the C23 and C24 clones was shown by RT-PCR. The activity of the ectopically expressed PAX3-FKHR protein in both clones was confirmed using the PRS9-CAT reporter construct, in transient transfection assays (see Chapter 2, **3.1.**).

Next, we injected 1×10^6 76-9-derived cells sub-cutaneously into syngeneic C57BL/6 mice. PAX3-FKHR negative (76-9 and CMV) and PAX3-FKHR positive (C23 and C24) 76-9 cells formed sub-cutaneous tumours of similar size (student *t*-test; p=0.46; see Chapter 2, Figure 8). RT-PCR analysis demonstrated that *PAX3-FKHR* RNA was expressed in the tumours of mice injected with C23 and C24 cells, but was not amplified from any lung or bone marrow sample (see Chapter 2, Figure 9).

3.1.2. Ex vivo loading of murine bone marrow-derived DCs with C23 lysate:

We chose to use the PAX3-FKHR-expressing C23 cell line as a source of tumour lysate, rather than tumour cells isolated from syngeneic C57BL/6 mice following injection with viable C23 cells. Lysates were generated from C23 cells by freeze-thawing, as described in Materials and Methods (*2.1.3.*).

DCs were differentiated from C57BL/6 bone marrow progenitors using rmGM-CSF and rmIL-4 (as described in Materials and Methods *2.1.2.*). During the culture period, the cells changed morphology from a rounded shape to cells with short cytoplasmic projections, characteristic of DC morphology (Banchereau and Steinman, 1998). After 7 days of culture with rmGM-CSF and rmIL-4, the dendritic-like cells expressed high levels of the DC marker CD11c and the MHC class II molecules I-A/I-E, and intermediate levels of the co-stimulatory molecules CD80 (B7-1) and CD86 (B7-2) (Figure 2). The immature DCs were subsequently pulsed with C23 lysate, in the presence of 50μg/ml KLH. The non-pulsed DCs used for immunisations were activated

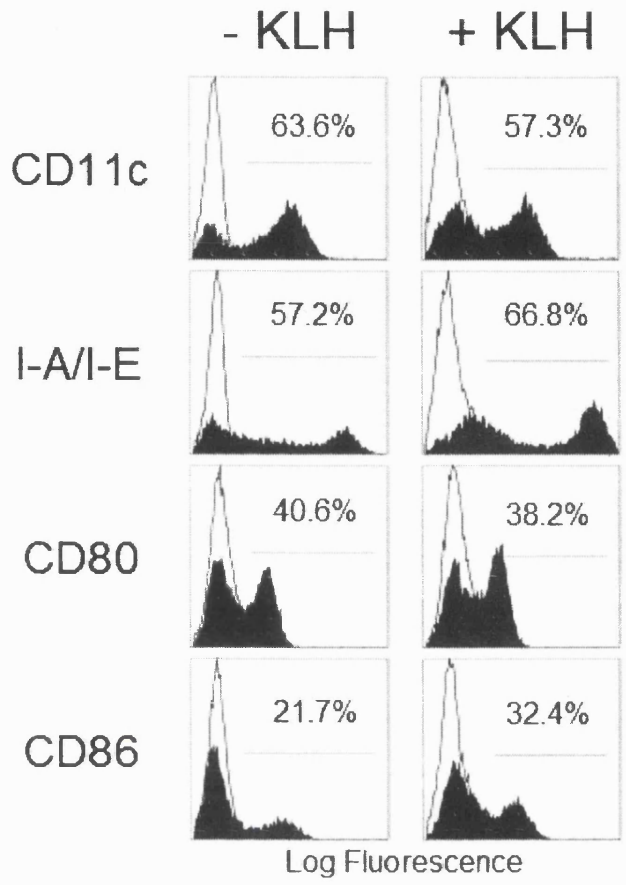

Figure 2. Immunophenotype of a representative DC culture. DCs were differentiated *in vitro* from C57BL/6 mouse bone marrow progenitors. Bone marrow leukocytes were cultured with rmGM-CSF for 7 days. On day 3, non-adherent granulocytes were removed and rmIL-4 added to the culture media. Immature DCs were pulsed with C23 lysate in the presence of KLH, for 24 hours. DCs were harvested on day 7 (immature DCs) or on day 8 following incubation with C23 lysate and KLH (mature DCs), stained with a panel of immunofluorescent antibodies and analysed by flow cytometry. Cells were gated on large, granular cells, and gated cells are shown in the histogram plots. The black filled areas in histograms represent staining with the indicated monoclonal antibody, the unfilled white histograms indicate staining with an appropriate isotype control antibody. The percentage cells positive for the indicated monoclonal antibody is indicated in each histogram.

with KLH alone. The addition of KLH to the immature DC cultures resulted in some degree of activation of the DCs, as indicated by an increase in the expression of two or more of the following surface antigens: I-A/I-E, CD80 and CD86 (Figure 2). DEC205 (CD205) was not expressed by any of the bone marrow-derived DCs.

3.1.3. Initial C23 tumour lysate-pulsed DC vaccine experiment:

3.1.3.1. In vivo tumour growth assay:

First, we investigated the ability of C23 lysate-pulsed DCs to protect mice from a subsequent challenge with viable syngeneic C23 RMS cells (Figure 3A). As expected, large tumours formed in control mice that received the C23 tumour challenge alone. Immunisation with C23 lysate-pulsed DCs resulted in strong protection against a subsequent C23 tumour challenge (Figure 3B). However, immunisation with non-pulsed DCs generated similarly effective protection against a subsequent C23 tumour challenge. The mean tumour sizes in the two groups of mice receiving DC immunisations were significantly smaller than in the mice that received no DC immunisations, from day 14 post challenge onwards.

100% of the mice that received the C23 tumour challenge alone developed large sub-cutaneous tumours. In contrast, immunisation with C23 lysate-pulsed DCs or non-pulsed DCs resulted in a high percentage of the mice remaining disease free up to 24 days after the C23 tumour challenge (30% and 50%, respectively). The tumours that did form in the DC-immunised mice (C23 lysate-pulsed DCs or non-pulsed DCs) had a slower growth rate than the tumours that developed in challenge only mice. Mice were sacrificed when the tumours grew to 10% of the size of the animal or when the tumour ulcerated the skin. Figure 3C shows that immunisation with C23 lysate-pulsed DCs or non-pulsed DCs prolonged the survival of mice following a subsequent C23 tumour challenge. The raw data from this *in vivo* tumour growth experiment is shown in Appendix 1.

3.1.3.2. IFN-γsecretion by splenic T lymphocytes in vitro:

When the mice were sacrificed, we isolated the splenocytes and used them as a source of T lymphocytes for *in vitro* assays. Flow cytometric analysis of splenocytes isolated from naïve C57BL/6 mice demonstrated that approximately 15-20% of the viable leukocytes collected were $CD3^+CD8^+$ CTLs, 15-20% were $CD3^+CD4^+$ Th cells, and there were very few $CD3^-CD8^+$ NK cells.

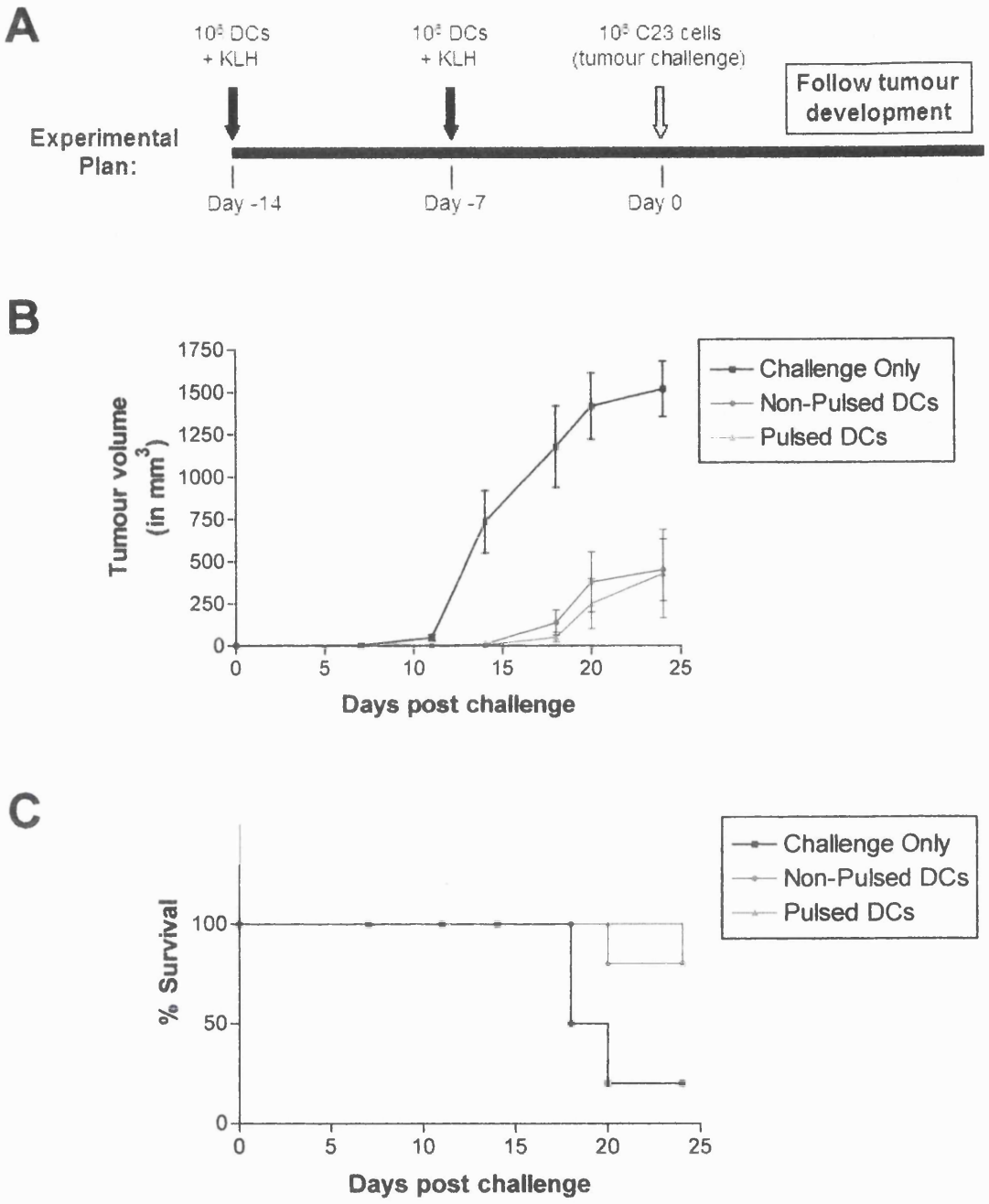

Figure 3. Immunisation with C23 lysate-pulsed DCs or non-pulsed DCs protects C57BL/6 mice from a subsequent C23 tumour challenge. **A** Schematic of the experimental plan. Mice were immunised sub-cutaneously in the right flank with 1×10^6 C23 lysate-pulsed DCs (labeled Pulsed DCs) or non-pulsed DC immunisations (labeled Non-pulsed DCs), twice at 7 day intervals. Mice were challenged 7 days after the last DC immunisation with 1×10^6 C23 cells, by sub-cutaneous injection into the left flank. **B** Tumour volumes following C23 tumour challenge. Following culling, the size of the tumours at the last measurement were used in subsequent time points. Data represent the mean tumour volume (in mm^3) of 10 mice per group. The error bars are standard error of the mean (S.E.M.). **C** Survival curve analysis of data from B.

KLH was used to activate the DCs *ex vivo*, and served as an immunological marker following vaccination. To confirm that the C23 lysate-pulsed DCs and non-pulsed DCs (both activated *ex vivo* with KLH) were successfully injected into the recipient mice, we examined the anti-KLH responses of splenic T cells using an *in vitro* IFN-γ ELISpot assay. Figure 4 summarises the data which shows that only a very limited number of splenocytes isolated from naïve mice (never been exposed to KLH) secreted IFN-γ when cultured *in vitro* in the absence of exogenous KLH. Addition of 8μg of KLH to the naïve splenocyte cultures caused a more than 4-fold increase in the number of IFN-γ secreting activated T cells. Similarly, only a small number of splenocytes isolated from mice that received the C23 challenge alone were activated and secreted IFN-γ when cultured *in vitro* in the absence of exogenous KLH. However, the addition of KLH to the tumour challenge only mouse splenocytes resulted in a more than 2-fold increase in the number of activated T cells secreting IFN-γ. In contrast, a large number of splenic T cells collected from mice that were immunised with KLH-activated DCs (C23 lysate-pulsed DCs or non-pulsed DCs) were activated and secreted IFN-γ, even in the absence of exogenous KLH (more than 175 IFN-γ spots/well). In the DC-immunised mouse splenocyte cultures, there was no observable increase in the number of IFN-γ secreting cells following incubation with KLH, and this was because of the high background level.

Next, we investigated IFN-γ secretion of the splenocytes when cultured *in vitro* with CMV (PAX3-FKHR^{-ve}) or C23 (PAX3-FKHR^{+ve}) target cells. Both the CMV and C23 RMS cell lines moderately activated the splenic T cell population derived from naïve mice (Figure 5). A similarly small number of splenocytes isolated from C23 tumour challenge only mice were activated by CMV and C23 cells, as indicated by IFN-γ secretion. The splenocytes collected from mice that received DC immunisations (C23 lysate-pulsed DCs or non-pulsed DCs) showed an elevated IFN-γ response against both CMV and C23 targets, relative to naïve and challenge only mouse spleneocytes. C23 lysate-pulsed DC immunisations and non-pulsed DC immunisations were equally effective at priming splenic T cells that are activated by CMV or C23 targets.

The number of splenic T cells activated by CMV targets was not significantly different from the number of splenic T cells activated by C23 targets, in any of the mouse spleens

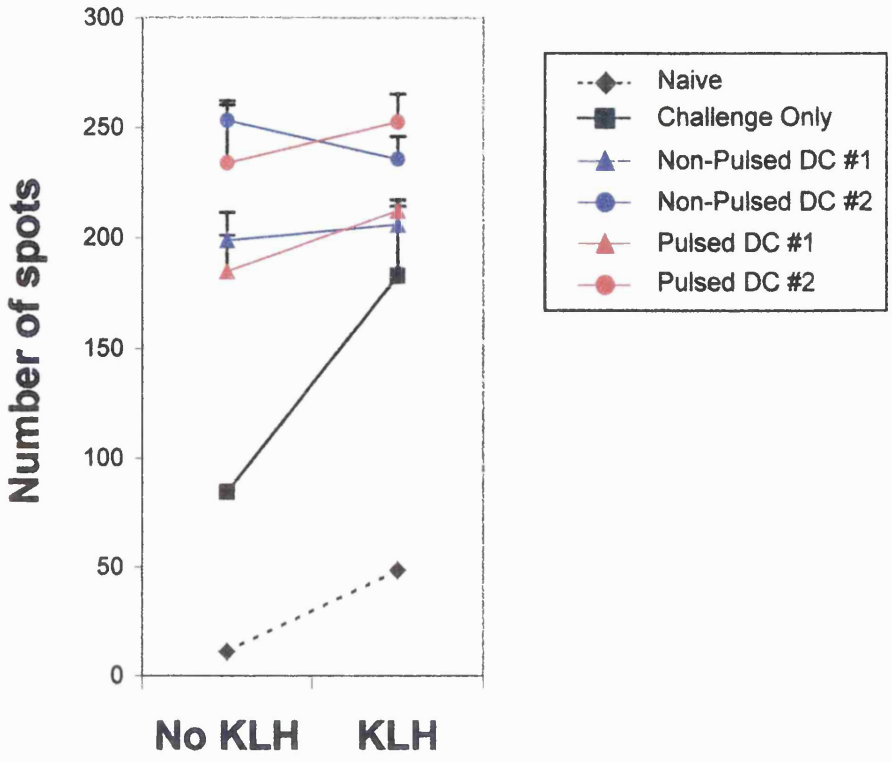

Figure 4. ELISpot assay measuring IFN-γ secretion by splenic T lymphocytes cultured *in vitro* in the presence or absence of KLH. Splenocytes were isolated from the mice at the end of the *in vivo* tumour growth assay. The treatment groups shown in this figure are: naïve mice (naïve); mice that received the C23 tumour challenge alone (Challenge Only); mice that were immunised with non-pulsed DCs prior to a C23 tumour challenge (Non-pulsed DC); and, mice that were immunised with C23 lysate-pulsed DCs prior to a C23 tumour challenge (Pulsed DC). In this ELISpot assay, we plated out 1×10^6 splenocytes/well of a 96-well plate, and measured the number of splenic T cells secreting IFN-γ when cultured with or without 8μg of KLH at 37°C for 48 hours. Depicted is a representative assay. Values are mean ± S.E.M. of quadruplicate cultures per animal.

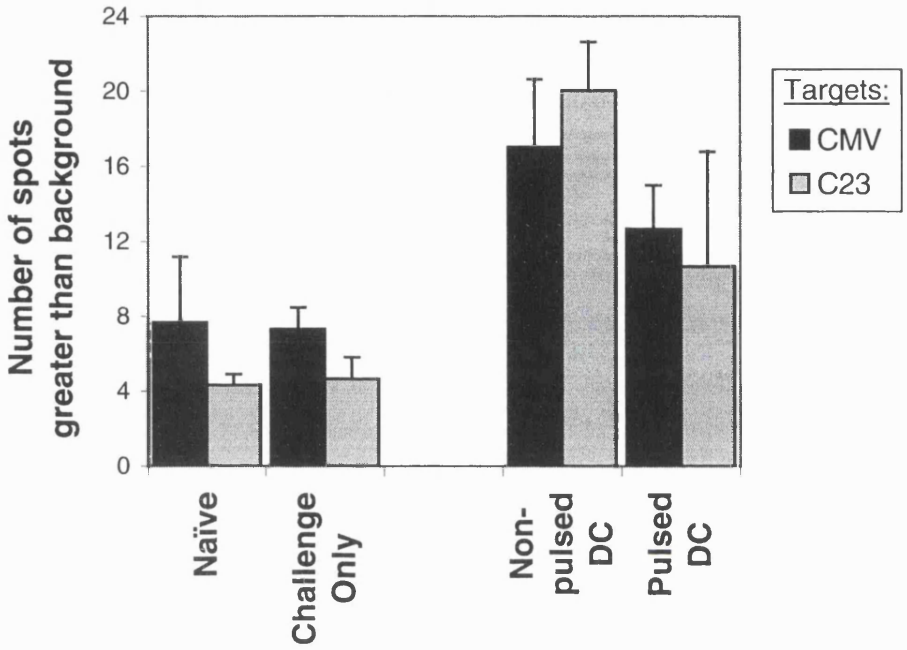

Figure 5. IFN-γ secretion by splenic T lymphocytes cultured *in vitro* with CMV (PAX3-FKHR^{-ve}) or C23 (PAX3-FKHR^{+ve}) RMS target cells. Splenocytes were isolated from the mice from all treatment groups at the end of the *in vivo* tumour growth assay. In this ELISpot assay, 1×10^5 splenocytes were plated out with 1×10^4 target cells/well of a 96-well plate (effector to target ratio of 1:10), and incubated at 37°C for 48 hours. We measured splenocyte IFN-γ secretion in triplicate wells, and analysed splenocytes from two mice per group. The values plotted are mean ± S.E.M. of each group. In control wells, splenocytes were cultured alone and the number of IFN-γ secreting cells was subtracted from the values of the test wells. In negative control wells, CMV and C23 cells were cultured alone and secreted undetectable levels of IFN-γ.

tested (student *t*-tests; for each treatment group $p>0.16$). Each splenocyte sample was tested in two separate experiments, and differences in the number of splenocytes activated by CMV cells versus C23 cells could be explained by counting inaccuracies, where more of 1 target cell type was plated out than the other.

A control performed in all the ELISpot experiments consisted of culturing the splenocytes from each mouse with no target cells. To determine the number of splenic T cells activated by CMV or C23 targets, the number of IFN-γ secreting cells in the spleen only wells was subtracted from the values of the test wells (see Appendix 2).

3.1.4. Repeat of the C23 tumour lysate-pulsed DC vaccine experiment:

3.1.4.1. In vivo tumour growth assay:

We repeated the C23 lysate-pulsed DC vaccination experiment to confirm our preliminary findings. To investigate the specificity of the immune response elicited by the C23 lysate-pulsed DCs *in vivo*, we added an extra group of mice to the experiment. The additional group received two immunisations with C23 lysate-pulsed DCs, but were challenged with 1×10^6 viable syngeneic PAX3-FKHR^{-ve} CMV cells, in order to determine if the presence of PAX3-FKHR in the target cells contributed to the response. In the first experiment the splenocytes had been collected up to 24 days after the tumour challenge and might represent the memory T cell response. Therefore, in the current study, one mouse from each group was sacrificed 2 days after the tumour challenge, and splenocytes were isolated and used for *in vitro* cytotoxicity assays examining the primary immune response induced by the DC immunisations (Figure 6A).

The results from this *in vivo* tumour growth experiment confirmed our preliminary data, showing that DCs pulsed with C23 lysate, as well as non-pulsed DCs, are able to protect mice from a subsequent C23 tumour challenge (Figure 6B). In this experiment, $\geq 60\%$ of the mice that were immunised with C23 lysate-pulsed DCs or non-pulsed DCs remained disease free 19 days after C23 tumour challenge. In contrast, the majority of mice that did not receive any DC immunisations formed large tumours by day 14 after the C23 tumour challenge. Surprisingly, 2 of the mice that received the C23 challenge

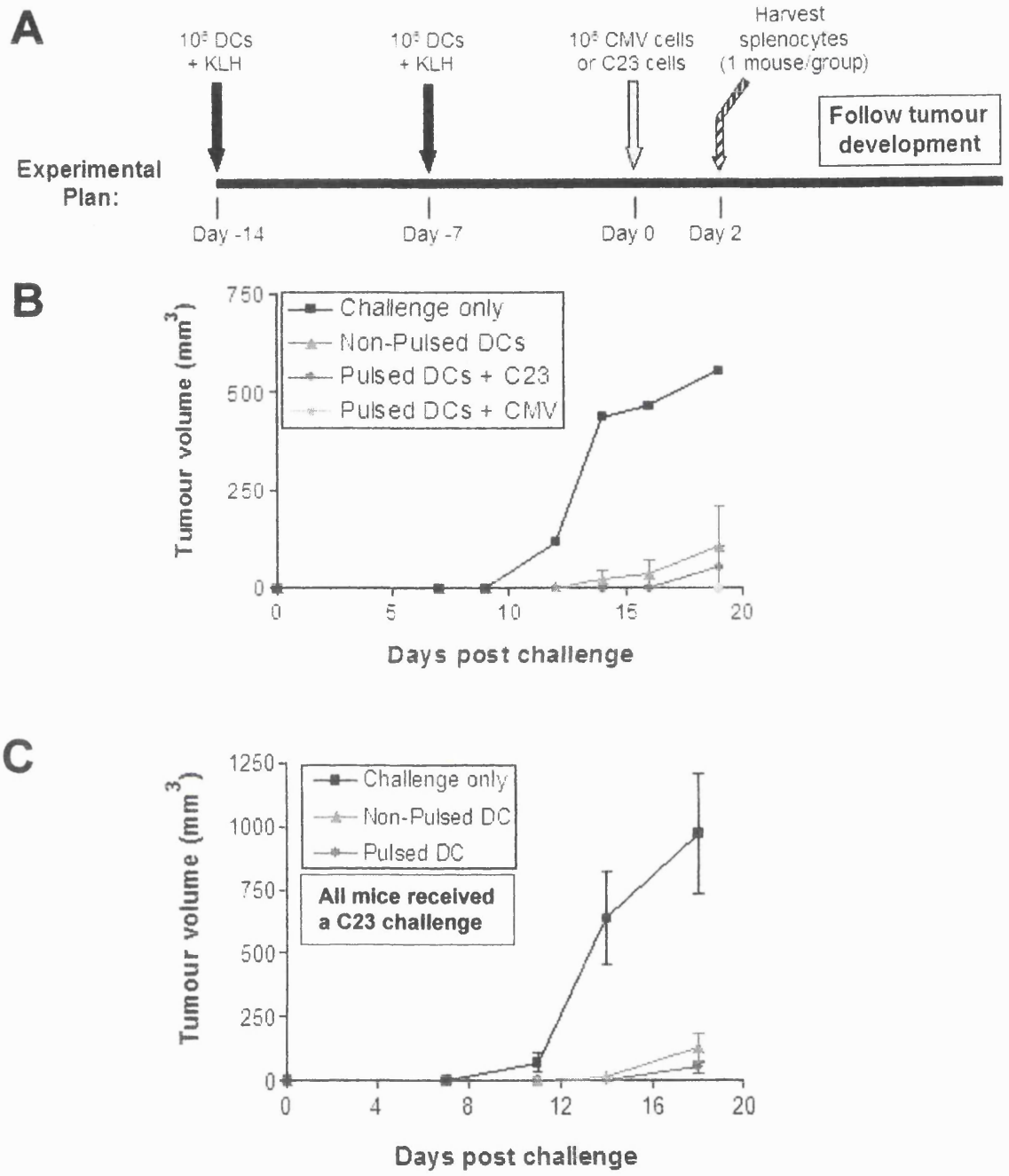

Figure 6. Immunisation with C23 lysate-pulsed DCs protects mice from a subsequent challenge with C23 or CMV RMS cells. **A** Schematic of the experimental plan. Mice were sub-cutaneously immunised with 1×10^6 C23 lysate-pulsed DCs or non-pulsed DCs, twice at 7 day intervals. 7 days after the last DC immunisation, mice were challenged with 1×10^6 C23 (PAX3-FKHR^{+ve}) or 1×10^6 CMV (PAX3-FKHR^{-ve}) cells, injected sub-cutaneously on the opposite flank. **B** Tumour volumes following C23 or CMV tumour challenge. Data represent the mean tumour volume (in mm^3) of 5-6 mice per group. Error bars indicating S.E.M. are shown for all groups except the challenge only mice. **C** Combined data from two DC vaccine experiments (marked *3.1.3.* and *3.1.4.*) performed using wild type C57BL/6 mice. All 3 groups of mice shown were challenged with C23 cells. The additional group challenged with CMV cells in the repeat experiment is not shown in this figure. To combine the data, tumour volumes were plotted where measurements were taken on the same day (± 1 day) in both experiments. Data represent the mean tumour volume (in mm^3) ± S.E.M. of 15-16 mice per group.

alone did not form tumours. This is probably the result of failed sub-cutaneous injection of the C23 tumour challenge. In every other tumour challenge in this series of experiments, injection of 1×10^6 C23 cells, in the absence of prior DC vaccinations, resulted in the formation of large tumours. Figure 6C shows the combined data from the two DC vaccine experiments (marked *3.1.3.* and *3.1.4.*) for these three mouse treatment groups.

The data from the additional group of mice shows that the C23 lysate-pulsed DC immunisations were able to protect mice from a subsequent CMV tumour challenge equally as efficiently as the protection they provided against a C23 tumour challenge (Figure 6B). Previous data has demonstrated that CMV cells form tumours just as quickly as C23 cells, when injected sub-cutaneously into syngeneic C57BL/6 mice (Chapter 2, Figure 8). Therefore, there is no evidence that PAX3-FKHR renders the tumour more immunogenic for lysate-pulsed DC vaccination. 80% of the mice immunised with C23 lysate-pulsed DCs remained disease free 19 days after a challenge with CMV cells. The raw data from this *in vivo* tumour growth experiment is shown in Appendix 3.

A percentage survival curve was not plotted for the results from these repeat tumour lysate-pulsed DC vaccine experiments because the mice were sacrificed at an earlier time point than in the initial experiments. However, by sacrificing the animals from the different treatment groups at the same time point, the splenocytes were directly comparable.

3.1.4.2. Tumour infiltrating lymphocytes:

We noticed that in the few mice that did develop tumours after vaccination with C23 lysate-pulsed DCs or non-pulsed DCs, the tumours were small, hard, and fibrous. In contrast, the mice that received the C23 challenge alone formed large, soft tumours. We hypothesised that the hard, fibrous tumours were the result of inflammation secondary to immune responses against the C23 tumour challenge cells.

Tumours cells were isolated and disaggregated with collagenase, then analysed by flow cytometry. Cells with the forward scatter (FSC) and side scatter (SSC) typical for lymphocytes were gated and immunophenotyped. Figure 7B shows the

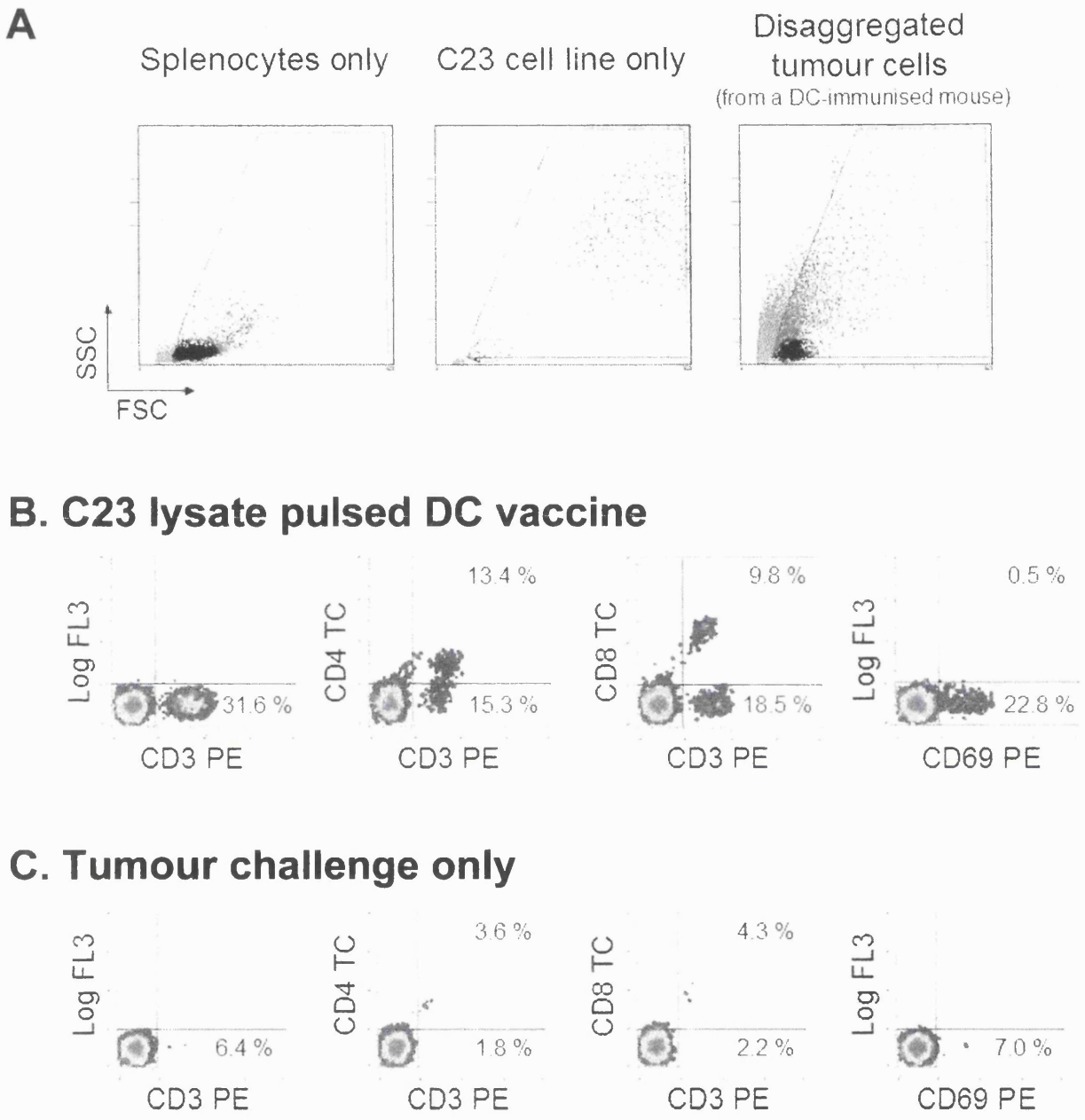

Figure 7. Flow cytometric analysis of tumour infiltrating lymphocytes (from the pulsed DC vaccine experiment marked *3.1.4.*). **A** Size and granulatiry of splenocytes, C23 cells and disaggregated tumour cells isolated from a DC-immunised mouse. Viable cells with the forward scatter (FSC) and side scatter (SSC) typical for lymphocytes were gated and are shown in black. These cells were subsequently immunophenotyped (see B and C). All other viable cells were gated and are shown in red. Cell debris is shown in grey. **B** The immunophenotype of lymphocytes isolated from a representative small, hard, fibrous tumour excised from C57BL/6 mice immunised with C23 lysate-pulsed DCs or non-pulsed DCs. **C** The immunophenotype of cells with a FSC and SSC typical of lymphocytes, isolated from a representative large, soft tumour excised from a C57BL/6 mouse that received the C23 challenge alone. Tumour cells were disaggregated with collagenase, stained with a panel of antibodies, and analysed by flow cytometry.

immunophenotype of lymphocytes isolated from a representative small, hard, fibrous tumour excised from C57BL/6 mice immunised with C23 lysate-pulsed DCs or non-pulsed DCs. There are $CD3^+$ T lymphocytes infiltrating into the tumour, and the tumour contains an approximately equal number of $CD3^+CD8^+$ CTLs and $CD3^+CD4^+$ Th cells. In contrast, Figure 7C shows that there are far fewer lymphocytes infiltrating into the tumours that formed in mice receiving the C23 challenge alone.

The flow cytometric data collected from immunophenotyping multiple disaggregated tumours are summarized in Figure 8. The data suggests that both the C23 lysate-pulsed DCs and non-pulsed DCs are inducing an immune response against the C23 tumour challenge that primarily consists of $CD3^+CD8^+$ CTLs and $CD3^+CD4^+$ Th cells. It is interesting to note that there are virtually no B lymphocytes ($CD19^+$ cells) infiltrating into the C23-derived tumours following immunisation with pulsed or non-pulsed DCs. There were undetectable levels of $CD3^-CD8^+$ NK cells infiltrating the tumours (Figure 7B). CD69 is an activation marker of T cells, but is also induced on other activated leukocytes (Ziegler *et al*, 1994). This finding suggests that the majority of leukocytes infiltrating the tumours, which mainly consists of T cells, are in an activated state.

3.1.4.3. IFN-γ secretion by splenic T lymphocytes from vaccinated mice:
Splenocytes were isolated from the mice 19 days after the tumour challenge, and used in IFN-γ ELISpot assays examining the ability of CMV and C23 cells to activate the splenic T cells *in vitro*. Figure 9 shows that both CMV and C23 cells activated a small number of splenic T cells isolated from naïve mice and C23 challenge only mice. Splenocytes isolated from mice that were immunised with DCs (C23 lysate-pulsed DCs or non-pulsed DCs), prior to a C23 tumour challenge, showed an elevated IFN-γ response against both CMV and C23 targets. This result supports the data from the initial C23 tumour lysate-pulsed DC vaccine experiment (see Figure 5), demonstrating that C23 lysate-pulsed DCs and non-pulsed DCs are equally effective at priming splenic T cell responses against CMV or C23 targets. In the splenocyte samples collected from DC-immunised mice, more splenic T cells were activated by C23 targets than by CMV targets. However, this difference was not significantly different in either treatment

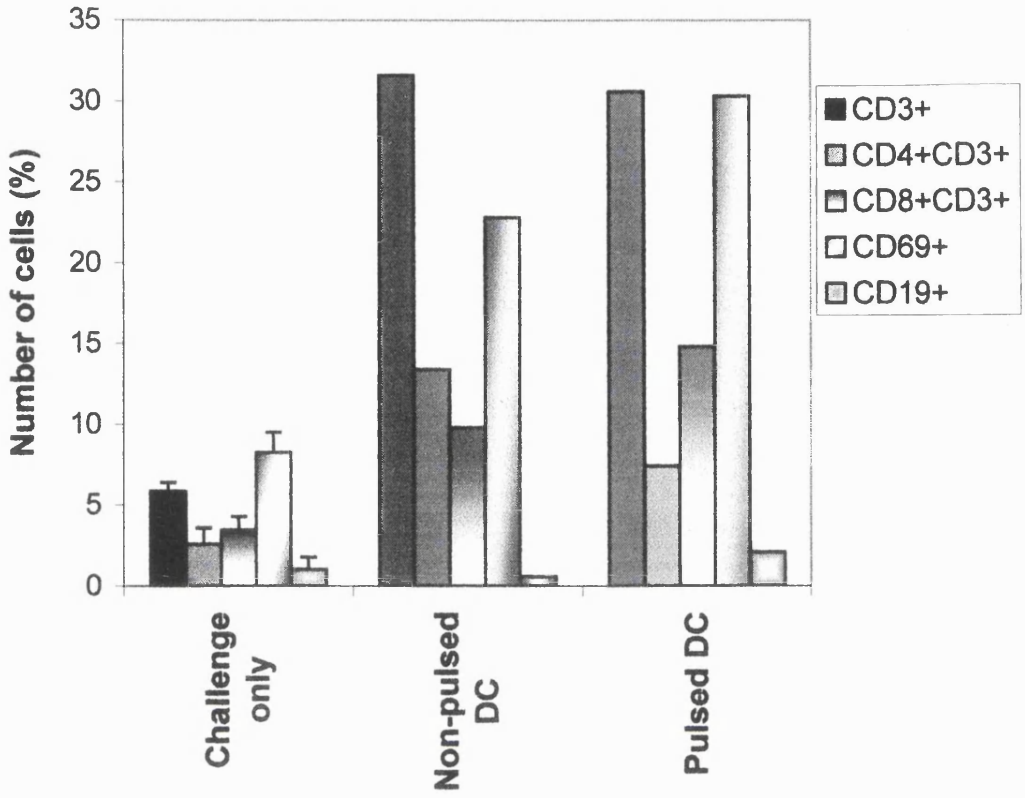

Figure 8. Flow cytometric analysis of tumour infiltrating lymphocytes (from the pulsed DC vaccine experiment marked *3.1.4.*). The samples are disaggregated tumour cells isolated from mice, from the different treatment groups, collected on day 19 post C23 tumour challenge. One or two tumours from each treatment group were analysed for tumour infiltrating lymphocytes, and mean ± S.E.M. values are plotted where possible. Tumour cells were disaggregated with collagenase, stained with a panel of antibodies, and analysed by flow cytometry. Cells with the FSC and SSC typical for lymphocytes were gated and analysed. Staining with the NK cell specific marker NK1.1 was associated with very high background levels, which masked any positively stained cells. The C23 cell line did not express any of the surface antigens shown in this figure (data not shown).

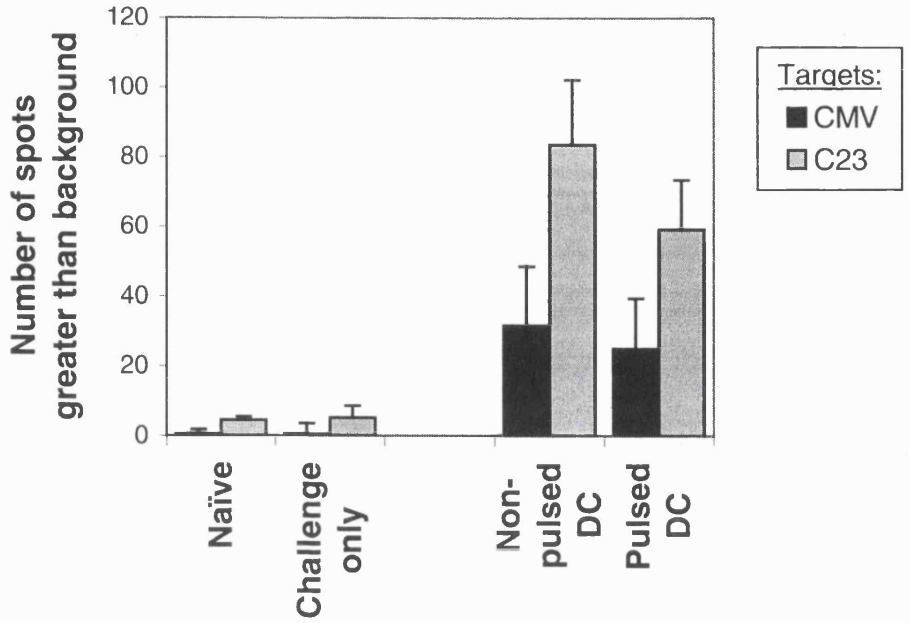

Figure 9. IFN-γ secretion by splenic T cells cultured *in vitro* with CMV (PAX3-FKHR^{-ve}) or C23 (PAX3-FKHR^{+ve}) RMS target cells. Splenocytes were isolated from the mice 19 days after the C23 or CMV tumour challenge. The treatment groups shown in this figure were all challenged with C23 cells (splenocytes collected from mice immunised with C23 lysate-pulsed DCs and challenged with CMV cells were not used in this assay). In this ELISpot assay, 1×10^5 splenocytes were plated out with 1×10^4 target cells/well of a 96-well plate (effector to target ratio of 1:10), and incubated at 37°C for 48 hours. We measured splenic T cell secretion of IFN-γ in triplicate wells. The values plotted are mean ± S.E.M. of each group. In negative control wells, splenocytes were cultured alone and the number of IFN-γ secreting cells was subtracted from the values of the test wells.

group (student *t*-tests; Non-pulsed DC mice p = 0.19; Pulsed DC mice p = 0.25), and might be the result of plating unequal numbers of targets.

Splenocytes isolated from mice 2 days after the tumour challenge were used in cytotoxicity assays to examine further the specificity of the immune response induced by the DC vaccinations. Unfortunately, the LDH release cytotoxicity assay was associated with high spontaneous LDH release by the effector and target cell populations, which masked any effector-mediated target cell killing in the test samples (data not shown).

3.1.5. C23 tumour lysate-pulsed DC vaccine experiment in beige C57BL/6 mice:

3.1.5.1. In vivo tumour growth assay:

To examine the role of NK cells in targeting the C23 challenge cells *in vivo*, we repeated the C23 lysate-pulsed DC vaccine experiment using beige C57BL/6 mice, which have a severe deficiency of NK cell cytotoxicity (Bannai *et al*, 2000).

All of the beige mice that were given the C23 tumour challenge alone developed large sub-cutaneous tumours. Figure 10B shows that C23 lysate-pulsed DCs and non-pulsed DCs were equally effective at protecting beige C57BL/6 mice from a subsequent challenge with viable syngeneic C23 RMS cells. 40% of the mice that were immunised with C23 lysate-pulsed DCs remained disease free 19 days after the challenge with C23 cells, while 20% of the mice immunised with non-pulsed DCs remained disease free 19 days after the C23 tumour challenge. The tumours that did form in the DC-immunised mice were significantly smaller than the tumours found in challenge only mice. Interestingly, in the absence of DC immunisations, syngeneic C23-derived tumours grew at a faster rate in beige C57BL/6 mice than in wild type C57BL/6 mice (Figure 10C). The raw data from this *in vivo* tumour growth experiment in beige mice is shown in Appendix 4.

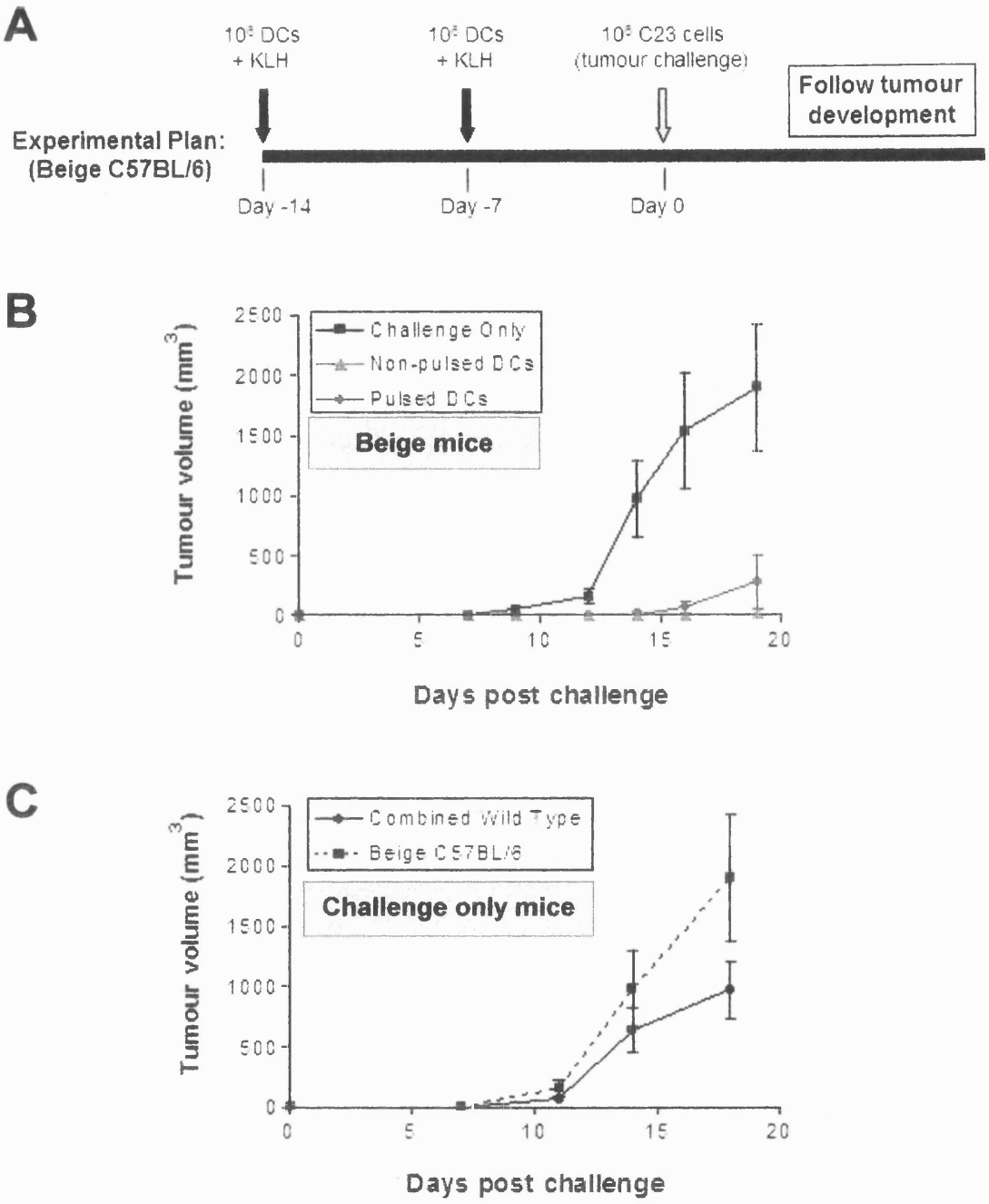

Figure 10. Immunisation with C23 lysate-pulsed DCs or non-pulsed DCs protects beige C57BL/6 mice from a subsequent C23 tumour challenge. **A** Schematic of the experimental plan. The only differences from the initial C23 lysate-pulsed DC vaccine experiment (Figure 3; marked *3.1.3.*) are that the C57BL/6 mice used are NK deficient (called beige C57BL/6), and there are only 5 mice per group. **B** C23 tumour lysate-pulsed DC vaccine experiment in beige C57BL/6 mice. Data represent the mean tumour volume (in mm^3) ± S.E.M.. **C** Comparing the tumour volumes in wild type C57BL/6 mice (—●—) and beige C57BL/6 mice (--■--) that received the C23 challenge alone. The C23 lysate-pulsed DC vaccines experiments in wild type mice (the repeat experiment; marked *3.1.4.*) and beige mice were performed simultaneously and are therefore directly comparable. The rate of tumour growth was very similar in the both C23 lysate-pulsed DC vaccines experiments in wild type mice, hence the combined data is shown in this figure. Data represent the mean tumour volume ± S.E.M..

3.1.5.2. Tumour infiltrating lymphocytes:

Flow cytometric analysis revealed that the small, hard, fibrous tumours that formed in the DC-immunised mice contained a large number of tumour infiltrating lymphocytes, relative to the large, soft tumours that formed in challenge only mice (Figure 11). The C23 lysate-pulsed DCs and non-pulsed DCs induced immune responses from the same effector cell types, with the tumour infiltrating lymphocytes from both mouse groups consisting of approximately equal numbers of $CD8^+$ CTL and $CD4^+$ Th cells.

3.1.5.3. IFN-γ secretion by splenic T lymphocytes in vitro:

Splenocytes were isolated from the beige mice 19 days after the C23 tumour challenge, and used in IFN-γ ELISpot assays to examine the ability of CMV and C23 cells to activate the splenic T cells *in vitro* (Figure 12). A large number of splenocytes from DC-immunised mice were activated by CMV or C23 targets (> 40 spots/1×10^5 splenocytes), relative to naïve and challenge only splenocytes (< 22 spots/1×10^5 splenocytes). Splenic T cells from mice immunised with C23 lysate-pulsed DCs or non-pulsed DCs were activated by the targets to an equal extent. CMV and C23 cells were equally immunogenic, activating a similar number of splenic T cells, in each treatment group.

3.2. Peptide-pulsed DC vaccine strategy:

3.2.1. Mouse RMA-S peptide binding assays:

We next investigated the potential of a peptide-pulsed DC vaccine approach to induce PAX3-FKHR-specific T cell responses, using our mouse model of ARMS. The C23 cell line, which would be used as a target in cytotoxicity assays, stably expresses mixed murine/human PAX3-FKHR cDNA. The amino acid sequence of the synthetic mixed murine/human PAX3-FKHR protein (NCBI identity: AF178854) is 100% homologous to the amino acid sequence of human PAX3-FKHR (NCBI identity: U02368) and the N-terminus of mouse PAX3 (NCBI identity: X59358). Because the C23 cell line, and syngeneic C57BL/6 mice, have a $H2^b$ haplotype, we used SYFPEITHI and BIMAS computer programs to identify potential peptide motifs in the mixed murine/human PAX3-FKHR fusion protein that bind to the mouse H2-K^b and H2-D^b MHC class I molecules (Table 1).

No peptide sequences in the tumour-specific breakpoint region of the fusion protein were identified that theoretically should bind to H2-K^b and H2-D^b molecules with

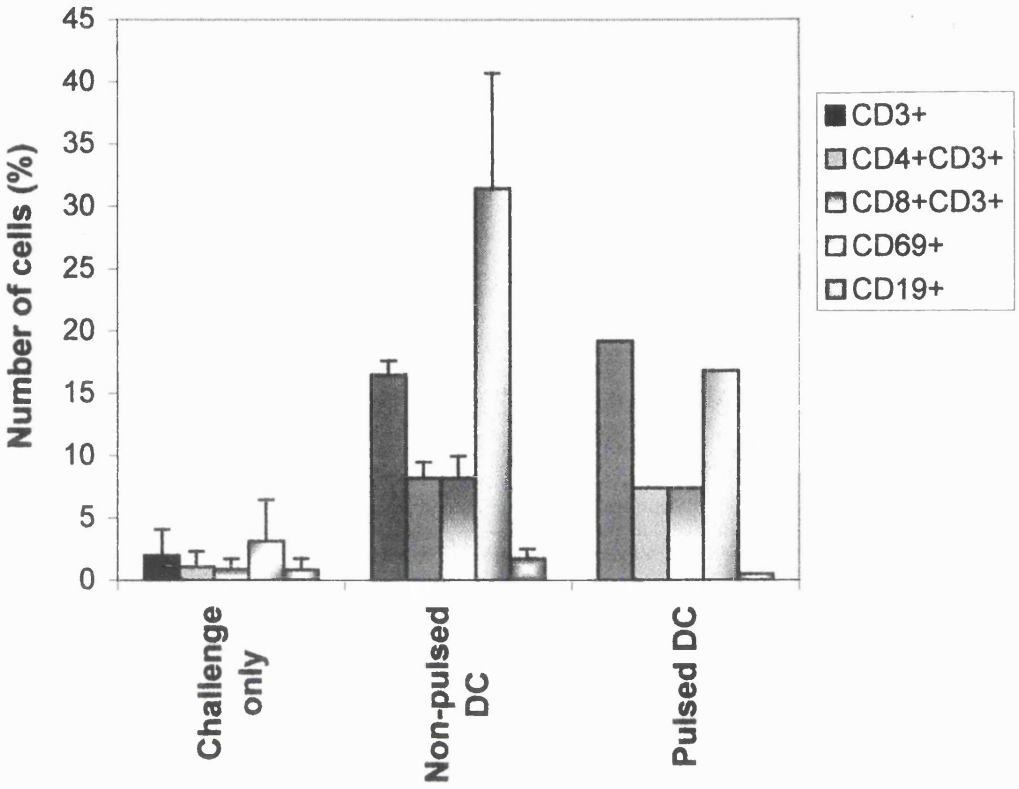

Figure 11. Flow cytometric analysis of tumour infiltrating lymphocytes from NK-deficient beige C57BL/6 mice (pulsed DC experiment marked *3.1.5.*). The samples are disaggregated tumour cells isolated from beige C57BL/6 mice, from the different treatment groups, collected on day 19 post C23 tumour challenge. One or two tumours from each treatment group were analysed for tumour infiltrating lymphocytes, and mean ± S.E.M. values are plotted where possible. Tumour cells were disaggregated with collagenase, stained with a panel of antibodies, and analysed by flow cytometry. Cells with the FSC and SSC typical for lymphocytes were gated and analysed.

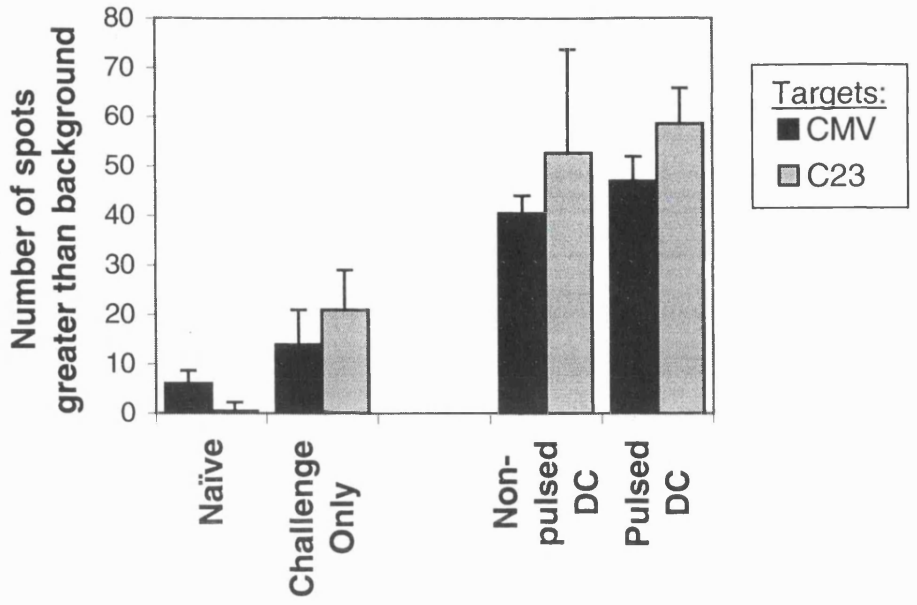

Figure 12. IFN-γ secretion of beige mouse splenocytes cultured *in vitro* with CMV (PAX3-FKHR^{-ve}) or C23 (PAX3-FKHR^{+ve}) RMS target cells. Splenocytes were isolated from the beige C57BL/6 mice 19 days after the C23 tumour challenge. In this assay, splenocytes isolated from a naïve wild type C57BL/6 mouse were used as control effector cells (naïve). 1×10^5 splenocytes were plated out with 1×10^4 target cells/well of a 96-well plate (effector to target ratio of 1:10), and incubated at 37°C for 48 hours. We measured IFN-γ secretion in triplicate wells, and analysed splenocytes from two mice per group. The values plotted are mean ± S.E.M. of each group. In control wells, splenocytes were cultured alone and the number of IFN-γ secreting cells was subtracted from the values of the test wells.

A. H2-K^b binding peptides

	Start position	Residues (single letter amino acid code)	SYFPEITHI score	BIMAS score
	Octamers:			
+	282	QLMAFNHL	20	10
	245	DIYTREEL	18	0
	239	ERTHYPDI	16	0
	Nonamers:			
	281	NQLMAFNHL	0	12
	Decamers:			
	280	ANQLMAFNHL	0	47.5

B. H2-D^b binding peptides

	Start position	Residues (single letter amino acid code)	SYFPEITHI score	BIMAS score
	Nonamers:			
+	43	GVFINGRPL	19	200
	277	QAGANQLMA	0	13
	388	LSPQNSIRH	17	9.36
	25	FPLEVSTPL	18	7.9
	Decamers:			
+	42	GGVFINGRPL	14	780
	276	KQAGANQLMA	0	10
	298	AMPTLPTYQL	18	8.6
	277	QAGANQLMAF	22	0
	Positive Control Peptide:			
	NP68	ASNENMDAM	28	343.2

Table 1. Screening the PAX3 amino acid sequence present in mixed murine/human PAX3-FKHR for the presence of potential H2-K^b and H2-D^b binding motifs. A Theoretical H2-K^b binding peptide sequences derived from the N-terminal PAX3 region of the synthetic mixed murine/human PAX3-FKHR protein (NCBI identity: AF178854). **B** Theoretical H2-D^b binding peptide sequences derived from the N-terminal PAX3 region of the synthetic mixed murine/human PAX3-FKHR protein. **+** denotes peptides synthesised and tested in RMA-S binding assays. The predicted binding affinities of the NP68 positive control peptide are shown for comparison. NP68 comprises residues 366-374 of the nucleoprotein of influenza virus strain A/NT/60/68. The SYFPEITHI and BIMAS programs can be found at: http://syfpeithi.bmi-heidelberg.com and http://bimas.dcrt.nih.gov/molbio/hla_bind/, respectively. Using the SYFPEITHI scoring system, every amino acid within a given peptide is evaluated and given an arbitrary value. For example, a value of 1 is given to amino acids that are only slightly preferred in the respective position, and optimal anchor residues are given the value of 15 (Rammensee *et al*, 1999). The BIMAS algorithm is based on similar binding principles, however the scoring system is on a different scale. Known MHC binding peptides have BIMAS scores in the hundreds.

intermediate or high affinity (data not shown). We therefore, looked for CTL epitopes in the N-terminal PAX3 region of the fusion protein, which is potentially a tumour-associated antigen. One PAX3-derived peptide motif was predicted to bind to H2-K^b with intermediate affinity, and two theoretical H2-D^b binding PAX3 peptide motifs were also identified (indicated by + in Table 1A and 1B). The three PAX3-derived peptides were synthesised, and their ability to bind to H2-K^b and H2-D^b class I molecules determined in an RMA-S peptide binding assay.

The mouse lymphoma cell line RMA-S is deficient in the genes encoding the transporter associated with antigen processing (TAP) proteins (Schumacher *et al*, 1990). This TAP deficiency prevents efficient loading of newly synthesised H2-K^b and H2-D^b class I molecules with endogenous peptides. The empty H2-K^b and H2-D^b molecules are unstable and only transiently expressed on the cell surface. The addition of exogenous H2-K^b or H2-D^b binding peptides stabilises the H2-K^b or H2-D^b class I molecules on the cell surface, which can be detected by immunoflourescence analysis. The parental RMA cell line does not have a TAP-deficiency, and expresses high levels of H2-K^b and H2-D^b molecules on the cell surface, bound to endogenously processed peptides.

In setting up the peptide binding assay, we determined the optimal peptide-RMA-S cell incubation time, and titrated the PE-conjugated antibodies to calculate the best concentration for staining (data not shown). Figure 13A shows that the level of H2-K^b expression is equally low in RMA-S cells cultured with the PAX3-derived QLM peptide (at 0.001-100μM), a non binding negative control GVFI peptide (at 0.001-100μM), and no exogenously added peptide. This suggests that the PAX3-derived QLM peptide does not bind to H2-K^b, even at high peptide concentrations. We did not have a positive control peptide, known to bind to H2-K^b. However, the high levels of H2-K^b detected on the surface of the parental RMA cell line acted as a positive control for the antibody staining efficiency.

The peptide NP68 is derived from influenza virus nucleoprotein and is known to bind to H2-D^b with high affinity (Williams *et al*, 1996). We detected a 4-fold increase in the H2-D^b levels in RMA-S cells cultured with 100μM NP68, relative to RMA-S cells cultured with 100μM QLM negative control peptide (Figure 13B). The NP68 peptide

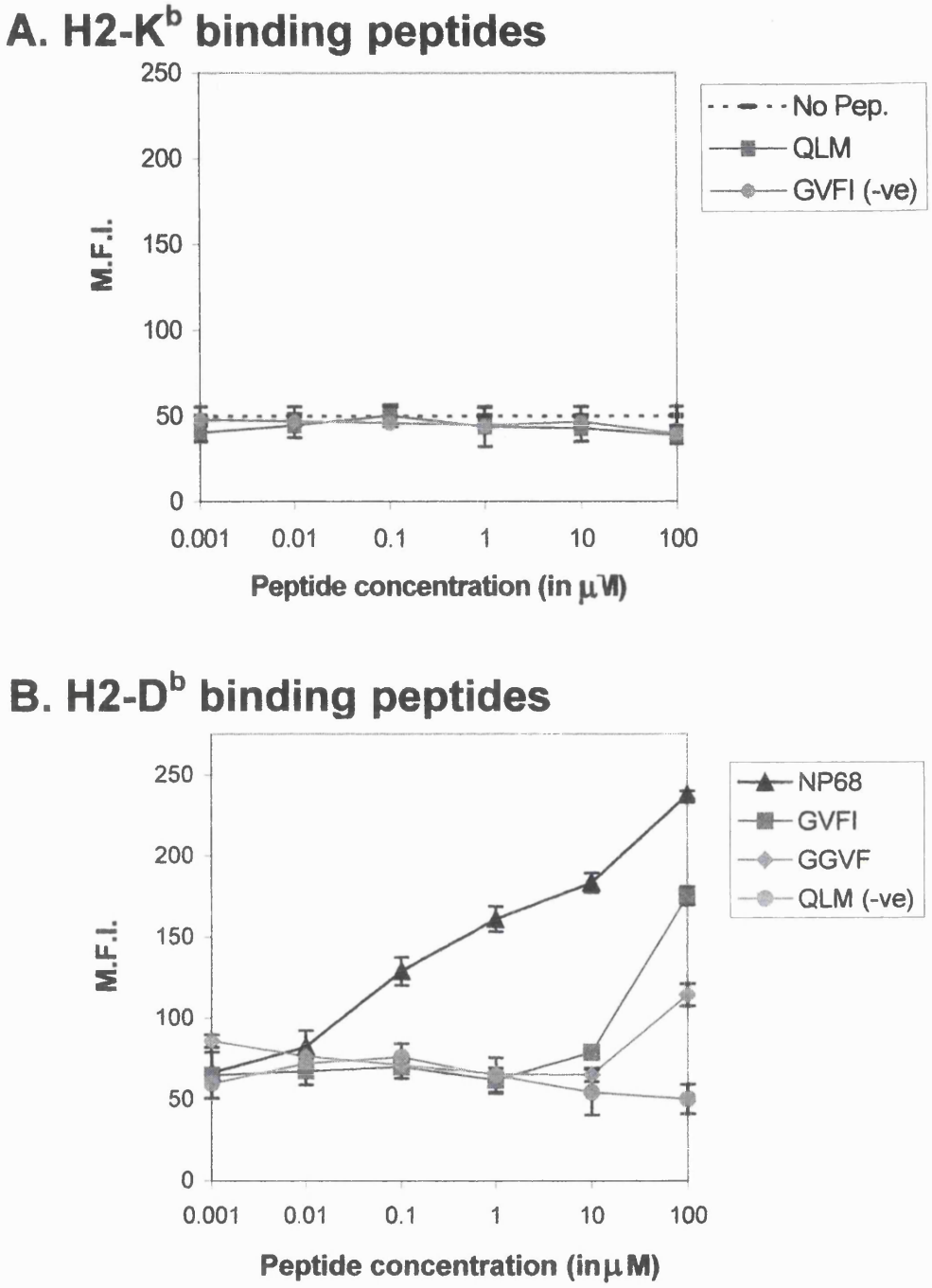

Figure 13. Mouse RMA-S peptide binding assays. A Binding of peptides derived from mixed murine/human PAX3-FKHR protein to mouse H2-K^b. Error bars are standard deviation (S.D.) of triplicate samples. However, the negative control GVFI peptide was only tested in single wells, and no error bars are shown for this peptide. Parental RMA cells were stained with the anti-H2- K^b antibody as a positive control (data not shown). **B** Binding of peptides derived from mixed murine/human PAX3-FKHR protein to mouse H2-D^b. NP68 is derived from the influenza virus nucleoprotein, and served as an H2-D^b binding positive control peptide. Error bars are S.D. of triplicate samples. In the figure keys, each peptide is identified by its first 3-4 amino acid residues (see Table 1 for complete peptide sequences), and 'No Pep.' indicates samples where no exogenous peptide was added. 2×10^5 RMA-S cells were incubated with various concentrations of peptide for 3 hours, and the level of MHC class I quantified by FACS analysis of cells stained with PE-counjugated antibodies. Mean fluorescence intensity (M.F.I) is plotted against peptide concentration (in μM).

showed significant binding to H2-D^b even at low concentrations (0.1μM NP68; student *t*-test, $p<0.001$). The PAX3-derived peptides GVFI and GGVF were unable to bind to H2-D^b at the lower peptide concentrations, but showed significant binding at the highest concentration tested (100μM; student *t*-tests, $p<0.001$). Incubation of RMA-S cells with 100μM GVFI or GGVF resulted in a more than 2-fold increase in the levels of H2-D^b on the cell surface, compared to RMA-S cells cultured with 100μM QLM negative control peptide (Figure 13B).

3.2.2. Human T2 peptide binding assays:

We also attempted to identify HLA-A*0201 binding peptide motifs derived from human PAX3-FKHR that can be used to pulse MoDCs in a vaccine strategy for the treatment of ARMS. Published data has shown that natural peptides with high affinity to HLA-A*0201 are typically nonamers or decamers, with conserved anchor residues at position P2, and P9 or P10 (Rammensee *et al*, 1999). Table 2A shows that the SYFPEITHI and BIMAS computer programs predicted that no peptide sequences spanning the breakpoint of human PAX3-FKHR can bind to HLA-A*0201 with intermediate or high affinity. However, several peptide motifs derived from the tumour-associated N-terminal PAX3 region of the fusion protein were predicted to bind strongly to HLA-A*0201 (Table 2B). We selected the peptide KLTEARVQV as it gained a high binding affinity score with both SYFPEITHI and BIMAS algorithms. The peptide was synthesised and tested for HLA-A*0201 binding.

Similar to the mouse RMA-S cell line, human T2 cells are TAP-deficient and express unstable HLA-A*0201 on their surface (Alexander *et al*, 1989; Cerundolo *et al*, 1990). The HLA-A*0201 binding ability of exogenously added peptides can be determined by measuring the increase in cell surface HLA-A*0201 expression, using immunoflourescence analysis.

Setting up the T2 peptide binding assay, multiple parameters were optimised to allow the detection of maximum peptide-specific up-regulation of HLA-A*0201. We found that overnight incubation of T2 cells with the exogenous peptides was superior to incubation periods of 3 hours or 6 hours. The addition of β_2-microglobulin to the culture media helped to stabilise HLA-peptide complexes on the cell surface. Incubating the T2 cells with peptides in media supplemented with 5% boiled FCS was better than

A. Peptides spanning the PAX3-FKHR breakpoint

Start position	Residues (single letter amino acid code)	SYFPEITHI scores	BIMAS scores
Nonamers:			
5	NGLSPQ/NSI	14	0.252
9	PQ/NSIRHNL	9	0.048
6	GLSPQ/NSIR	13	0.006

B. Peptides derived form the N-terminal PAX3 region

	Start position	Residues (single letter amino acid code)	SYFPEITHI score	BIMAS score
Nonamers:				
+	257	KLTEARVQV	24	998
	226	FTAEQLEEL	25	0
	2	TLAGAVPRM	23	11.4
	282	QLMAFNHLI	21	147
Positive Control Peptide:				
	FMP	GILGFVFTL	30	550.9

Table 2. Screening the human PAX3-FKHR amino acid sequence for the presence of potential HLA-A*0201 binding motifs. A The predicted HLA-A*0201 binding affinities of nonamers spanning the breakpoint region of human PAX3-FKHR (NCBI identity: U02368). The amino acids sequence derived from the breakpoint region that was analysed: PTIGNGLSPQ/NSIRHNLSLH (/ denotes the breakpoint). Shown are the strongest predicted HLA-A*0201 binders. **B** The theoretical HLA-A*0201 binding affinities of peptides derived from the PAX3 amino acid sequence present in human PAX3-FKHR. Shown are the strongest predicted HLA-A*0201 binders. + denotes peptides synthesised and tested in T2 peptide binding assays. The predicted HLA-A*0201 binding affinities of the flu-matrix peptide (FMP; positive control) are shown for comparison. The SYFPEITHI and BIMAS programs can be found at: http://syfpeithi.bmi-heidelberg.com and http://bimas.dcrt.nih.gov/molbio/hla_bind/, respectively.

experiments using serum free media. The FITC-conjugated anti-human HLA-A2 antibody detected stabilised HLA-A*0201 on the cell surface, and produced a higher MFI than HB54 or HB117 antibodies used with the corresponding FITC-conjugated secondary antibody (data not shown).

Depicted in Figure 14 are two representative T2 peptide binding experiments. Figure 14A shows that the negative control peptide (QLM) was unable to bind and stabilise HLA-A*0201 molecules at any peptide concentration tested. However, the positive control FMP showed significant binding to HLA-A*0201 when added at ≥ 10μM (student *t*-tests; $p<0.01$). The PAX3 KLT peptide was only able to show significant HLA-A*0201 binding at the highest peptide concentration tested (100μM; student *t*-test, $p=0.01$). The addition of 100μM FMP caused a 5.3 fold increase in HLA-A*0201 expression relative to 100μM negative control peptide (QLM), whereas 100μM PAX3 KLT peptide only induced MHC expression 1.9 fold. Overall, the result from this experiment suggests that the PAX3 KLT peptide binds to HLA-A*0201 with intermediate affinity. In the T2 assay depicted in Figure 14B, 100μM PAX3 KLT peptide binds strongly to HLA-A*0201 (3.8 fold induction, relative to 100μM QLM), with a binding efficiency nearly as high as the positive control FMP peptide (4.8 fold induction). This demonstrates the variation in the results between independent T2 assays, performed under identical conditions.

Next, we wanted to test the immunogenicity of the PAX3 KLT peptide. We screened PBMCs from five healthy donors and identified one HLA-A*0201$^+$ individual (data not shown). The HLA-A*0201$^+$ PBMCs were to be used as a source of MoDCs and responder CD8$^+$ T cells. We also screened multiple human RMS cell lines, to identify HLA-A*0201$^+$ cell lines that expressed PAX3 or PAX3-FKHR, to use as targets in a cytotoxicity assay. Unfortunately the two RMS cell lines that were HLA-A*0201$^+$ (RMS and HX170c) did not express elevated levels of *PAX3* or *PAX3-FKHR* mRNA (see Chapter 2, Figure 13). Time constraints prevented the *in vitro* stimulation of CD8$^+$ T cells (isolated from the PBMCs of a HLA-A*0201$^+$ healthy donor) with autologous PAX3 KLT peptide-pulsed MoDCs for CTL priming.

3.3. Transfection of DCs with *PAX3-FKHR* mRNA:

Investigating this alternative immunotherapeutic strategy, we attempted to transfect *in vitro* cultured mouse DCs with mRNA encoding PAX3-FKHR. To optimise the

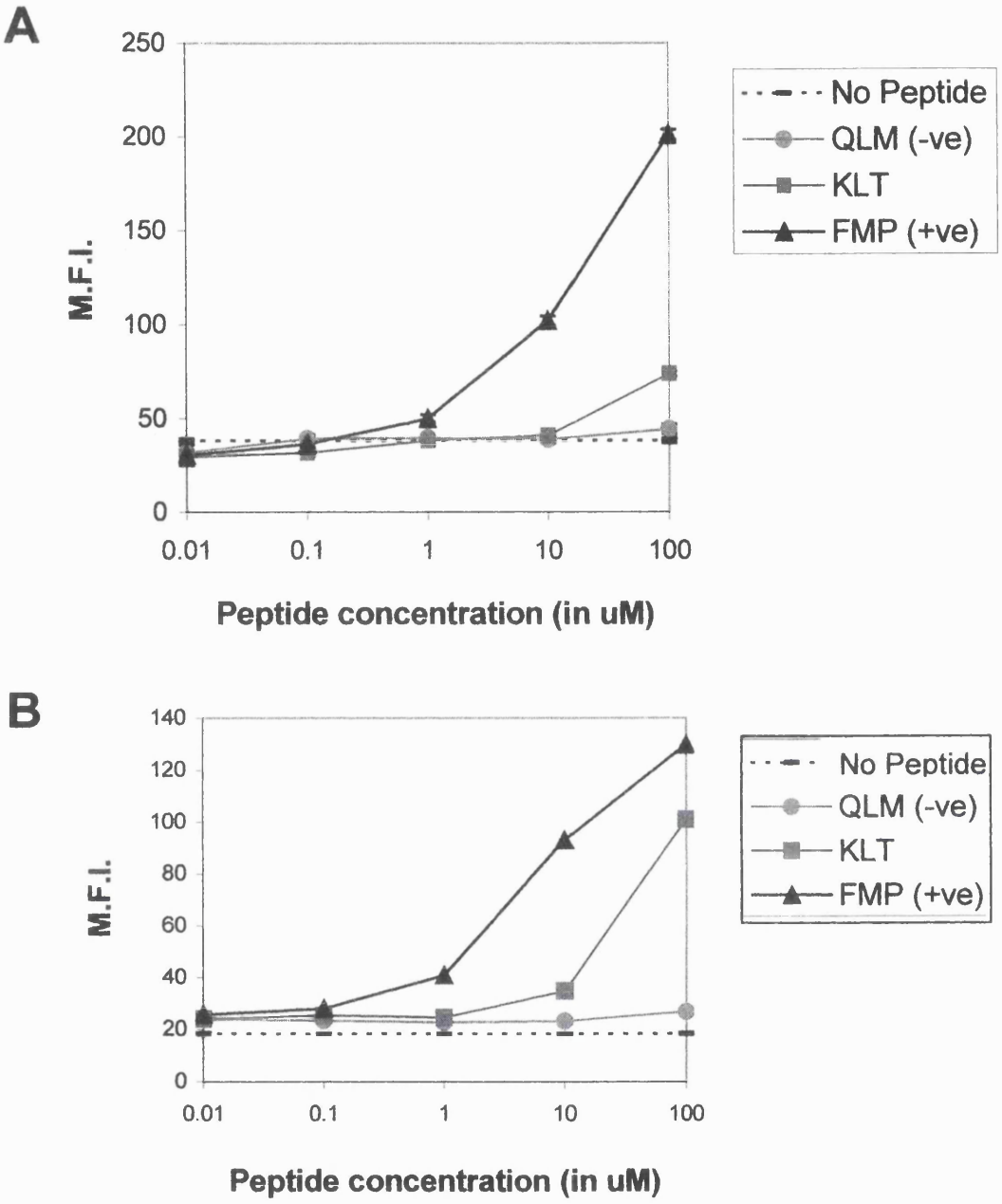

Figure 14. Up-regulation of HLA-A*0201 expression on T2 cells after incubation with the PAX3 peptide KLT. The KLT peptide epitope is derived from the N-terminal region of PAX3, which is retained in the PAX3-FKHR fusion protein. Flu matrix peptide (FMP) was used as a positive control, and the QLM peptide (see Table 1 for full amino acid sequence) was used as a negative control. **A** and **B** are two representative experiments, showing MFI at varying peptide concentrations (uM is used an abbreviation of micromolar). The two T2 peptide binding assays were performed under identical conditions. In **A**, the error bars are S.D. of triplicate samples. In **B**, each peptide concentration was tested in single cultures, and no error bars are shown. 3×10^5 T2 cells were incubated with various concentrations of peptide overnight in media supplemented with 5% boiled FCS. The cells were then stained with FITC-counjugated mouse anti-human HLA-A2 monoclonal antibody or a FITC-conjugated isotype control antibody, and the level of HLA-A*0201 quantified by flow cytometric analysis.

transfection procedure using TransMessenger Reagent, we initially attempted to transfect the human RD cell line with *GFP* mRNA. We synthesised the *GFP* mRNA from a cDNA template in the pGEM4Z/GFP/A64 plasmid, using an *in vitro* transcription reaction with T7 polymerase. Figure 15A shows that GFP protein can be synthesised from the pGEM4Z/GFP/A64 plasmid in an *in vitro* transcription translation (IVT) reaction.

Preliminary experiments demonstrated that without the addition of a 5′ cap to the *GFP* mRNA during the *in vitro* transcription reaction, the GFP protein could not be translated *in vivo*, following transfection. Approximately 29% of RD ERMS cells were successfully transfected with *in vitro* transcribed *GFP* mRNA (possessing a 5′ cap) and expressed GFP protein, as shown by flow cytometry (Figure 15B). However, the level of GFP protein expressed in the *GFP* mRNA-transfected RD cells was less than in RD cells successfully transfected with *GFP* DNA. We next attempted to transfect *in vitro* differentiated mouse DCs with *in vitro* transcribed *GFP* mRNA (with a 5′ cap). DCs were identified during FACS analysis by their large size, high granularity and expression of the MHC class II molecules I-A/I-E. Unfortunately, only 2% of the immature DCs (Figure 16A) and 1.7% of the mature DCs (data not shown) were successfully transfected and expressed GFP protein. The poor transfection efficiency was not the result of using degraded *GFP* mRNA, as the *in vitro* transcribed *GFP* mRNA appeared as a single band of the correct size (850 bp) when electrophoresed on a 1.2% agarose gel (not shown).

Unfortunately, this transfection efficiency was too low to examine the ability of *PAX3-FKHR* mRNA-pulsed mouse DCs to induce PAX3-FKHR-specific immune responses *in vitro* or to protect against a subsequent lethal dose of C23 challenge cells *in vivo*. Nonetheless, *PAX3-FKHR* mRNA can be transcribed *in vitro* from the pBK-CMV-P3F plasmid (Figure 16B), and is suitable to use for the transfection of DCs when a superior RNA transfection technique is established in the laboratory.

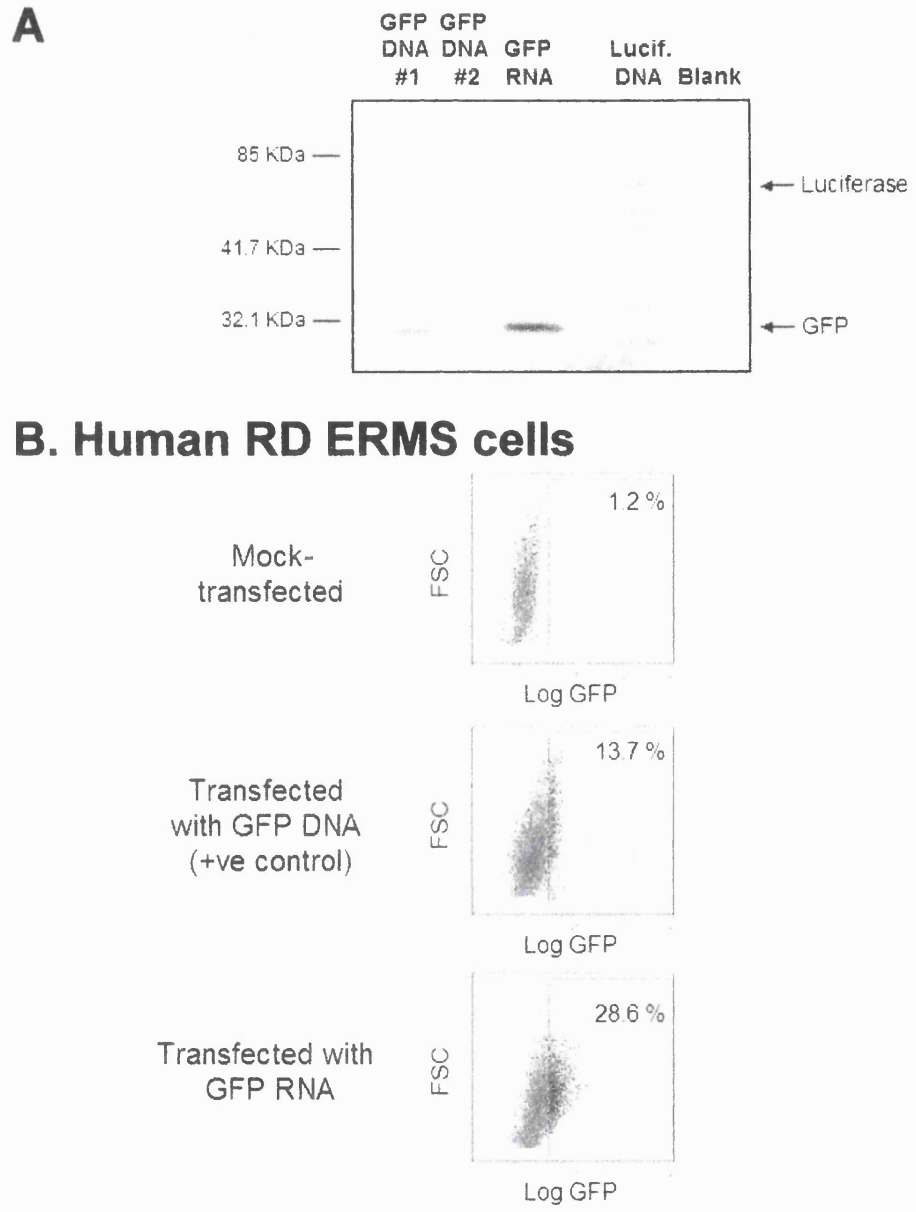

Figure 15. Transfection of the human RD cell line with *in vitro* transcribed *GFP* mRNA. A *In vitro* transcription and translation (IVT) of GFP protein from the pGEM4Z/GFP/A64 plasmid, using the TNT coupled reticulocyte lysate system. The starting genetic material used for the IVT reaction was linearised plasmid DNA or RNA transcribed *in vitro* from the plasmid using T7 polymerase. A luciferase DNA plasmid was used in an IVT reaction as a positive control. The sample labelled blank contains all the TNT reaction reagents, without any DNA or RNA added. The expected sizes of the luciferase and GFP proteins are 60 KDa and 30 KDa, respectively. The incorporated [^{35}S]methionine was detected by exposing the membrane on a phosphoimager screen. **B** GFP protein expression in human RD cells after transfection with *GFP* mRNA (+ 5′ cap) using TransMessenger Reagent. *GFP* mRNA was *in vitro* transcribed from the pGEM4Z/GFP/A64 plasmid using T7 polymerase, in the presence of m^{7}G capping analogue. Mock-transfected cells were cultured with the TransMessenger Reagent alone. As a positive control, one well of RD cells were transfected with *GFP* DNA (pCMS-EGFP plasmid) using FuGENE 6 Transfection Reagent. 30 hours post transfection, the cells were harvested and analysed by FACS. Viable cells were gated and analysed for GFP expression. The number of GFP-positive cells was set as 1.2% in the mock-transfected cell samples, and the GFP-positive cells are shown in blue.

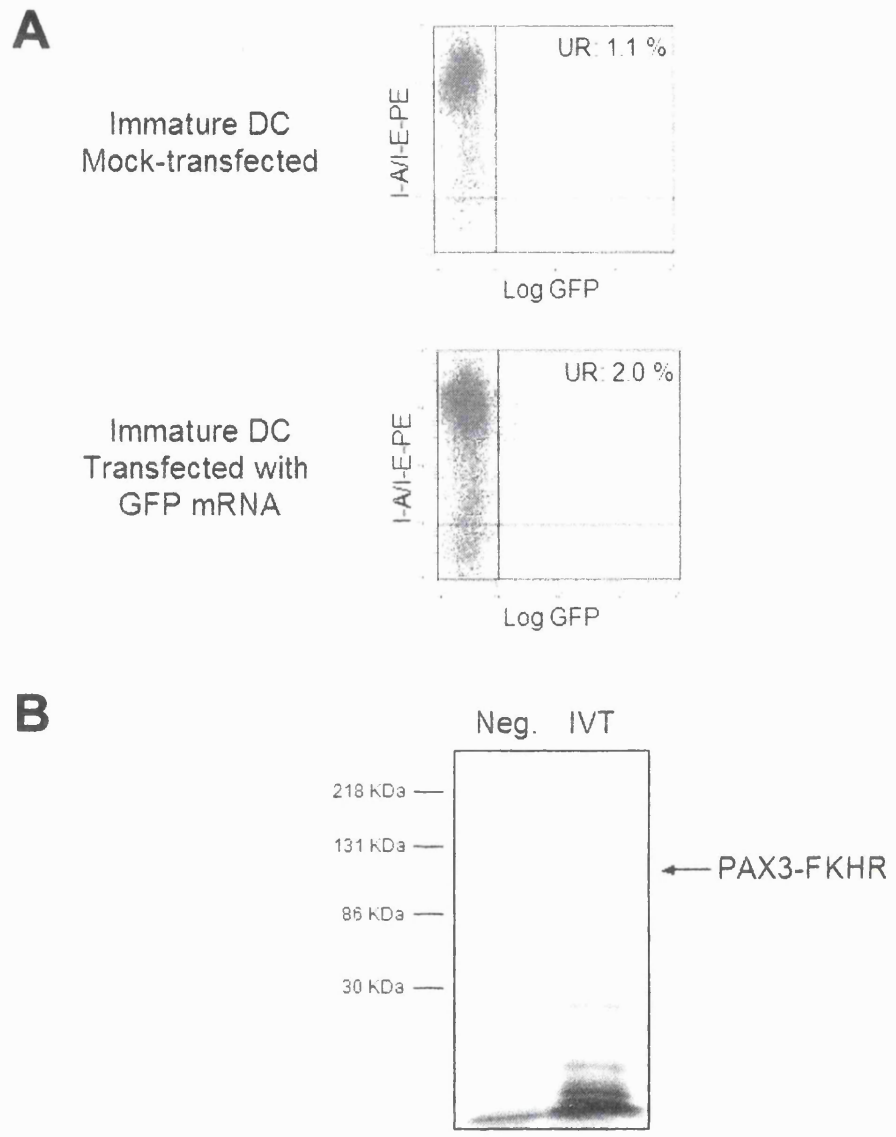

Figure 16. **A** GFP protein expression in immature mouse DCs after transfection with *in vitro* transcribed *GFP* RNA (+ 5′ cap), using TransMessenger Reagent. Immature DCs were cultured *in vitro* from $CD34^+$ bone marrow progenitors in rmGM-CSF and rmIL-4 for 7 days. *GFP* mRNA was *in vitro* transcribed from linearised pGEM4Z/GFP/A64 plasmid using T7 polymerase and 5′ m^7G capping analogue. Mock-transfected cells were cultured with the TransMessenger Reagent alone. 30 hours post transfection, the cells were harvested, stained with flourochrome-conjugated antibodies, and analysed by FACS. Large, granular cells were gated and analysed for I-A/I-E and GFP expression. DCs were identified by their high level expression of I-A/I-E, and *GFP*-transfected DCs appear in the upper right (UR) quadrant ($I\text{-}A/I\text{-}E^+$, GFP^+). The number of GFP-positive DCs was set as 1.1% in the mock-transfected cell sample. **B** *In vitro* transcription and translation of mixed murine/human PAX3-FKHR protein from the pBK-CMV-P3F plasmid, using the TNT Coupled Reticulocyte Lysate System. The mixed murine/human PAX3-FKHR protein is approximately 130 KDa, and a band of the expected size was detected in the lane corresponding to the IVT of pBK-CMV-P3F (labelled IVT). In the negative control lane (Neg.), no linearised pBK-CMV-P3F DNA was added to the TNT lysate reaction. The incorporated [^{35}S]methionine was detected by exposing the membrane on a phosphoimager screen.

4. Discussion

Although multimodal therapy has been shown to improve the survival rate of ARMS patients, relapse is common and patients diagnosed with metastatic disease generally have low survival rates (Pappo *et al*, 1995; Anderson *et al*, 1999a). Hence, there is a need for alternative treatments, such as immunotherapy. In the present study, we have examined several pulsed DC vaccine strategies that could be used to target PAX3-FKHR-expressing ARMS cells.

4.1. Use of DCs loaded with tumour lysate to induce tumour-specific immunity:
We investigated the ability of tumour lysate-pulsed DC immunisations to induce PAX3-FKHR-specific immune responses *in vivo*, using a mouse model of ARMS. Mouse 76-9 RMS cells stably expressing mixed murine/human PAX3-FKHR were generated (clone used was called C23). Sub-cutaneous injection of 1×10^6 viable C23 cells into syngeneic C57BL/6 mice led to the formation of large sub-cutaneous tumours that were shown to express *PAX3-FKHR* mRNA.

4.1.1. Preparation and administration of tumour-lysate pulsed DCs:
Immunophenotypic analysis demonstrated that we successfully cultured DCs *in vitro* from C57BL/6 bone marrow progenitors using rmGM-CSF and rmIL-4 (Figure 2). The DCs were pulsed with C23 tumour cell lysate in the presence of KLH, which has been shown to improve the efficacy of pulsed DC immunisations *in vivo* (Shimizu *et al*, 2001). Interestingly, the DCs cultured with KLH alone underwent maturation, as indicated by an increase in the expression of at least two of the following surface antigens: the MHC class II molecules I-A/I-E, and the co-stimulatory molecules CD80 and CD86. While CD40 ligand and LPS are known DC maturation stimuli (Labeur *et al*, 1999), KLH has not previously been shown to promote DC activation *in vitro*. In negative control DC maturation cultures, the *in vitro* generated immature DCs were harvested on day 7 and re-plated in fresh media without exogenous KLH for 24 hours. The finding that these DCs underwent maturation (data not shown) suggests either that the process of re-plating the immature DCs (cell handling included centrifugation and pipetting) was sufficient to activate the cells, or that one of the tissue culture solutions used was contaminated with endotoxin. The tissue culture media solutions, including the vial of KLH, should be tested for endotoxin contamination before future use.

The *in vitro* differentiated, bone marrow-derived DCs did not express detectable levels of the mouse DC marker DEC205. However, this can be explained by the fact that DEC205 expression is known to be absent in bone marrow cells (Inaba *et al*, 1995).

We used the PAX3-FKHR-expressing C23 cell line as a source of tumour cell lysate to maximise the chances of generating immune responses specific for PAX3-FKHR. Utilising lysate from tumours, isolated from syngeneic mice following injection with viable C23 cells, might result in the induction of immune responses against tumour antigens present in other cell types, such as the endothelial cells recruited to the tumour site.

The route of vaccine injection is an important factor to consider. Previous investigators have administered tumour lysate-pulsed DCs via several different routes (Fong *et al*, 2001; Lambert *et al*, 2001). However, there is no consensus on which administration route is optimal for DC induction of anti-tumour immunity. We chose sub-cutaneous injection, which is widely used in murine models of pulsed DC immunisations.

4.1.2. Immune responses against KLH:

In accordance with published murine antigen-pulsed DC vaccine studies, the DCs were loaded with tumour lysate and KLH. Shimizu and colleagues (2001) demonstrated that pulsing DCs with tumour lysate in the presence of KLH augments the efficacy of tumour lysate-pulsed DC immunisations *in vivo*. In addition to its role as a helper antigen, KLH serves as an immunological tracer molecule, and immune responses against this control immunogen can be measured following successful immunisation. Figure 4 shows that splenic T cells isolated from DC-immunised mice (C23 lysate-pulsed DCs or non-pulsed DCs) were in an activated state, with large numbers of cells secreting IFN-γ when cultured *in vitro* with no exogenous stimulus. In contrast, virtually all the splenic T cells of naïve mice were inactive when cultured *in vitro* with no stimulus. The data suggest that the mice were successfully immunised with C23 lysate-pulsed DCs or non-pulsed DCs, and the immunisations activated a large number of splenic T cells. Interestingly, splenocytes collected from challenge only mice, and cultured in the absence of exogenous KLH, contained a slightly elevated number of IFN-γ secreting cells relative to naïve mice. This suggests that the C23 tumour challenge was itself moderately immunogenic, activating some host T lymphocytes *in vivo*.

When naïve or challenge only mouse splenocytes were cultured *in vitro* with KLH for 48 hours we observed a large increase in the number of activated splenic T cells. However, there was no significant difference in the number of IFN-γ secreting splenic T cells when splenocytes of DC-immunised mice were cultured with or without KLH for 48 hours. One reason why splenic T cells from DC-immunised mice showed no IFN-γ response against KLH *in vitro* might be because the KLH-specific T cells were already in an activated state as a result of the DC immunisations. A better assay to quantify *in vitro* cellular responses against KLH might be to measure the proliferation ([^{3}H]-thymidine incorporation) of splenic T cells cultured *in vitro* with KLH for 5 days (see Holtl *et al*, 1999).

4.1.3. Non-pulsed DCs induce anti-tumour immune responses:

4.1.3.1. Vaccination with C23 lysate-pulsed DCs versus non-pulsed DCs:

Two separate *in vivo* tumour growth experiments performed using wild type C57BL/6 mice demonstrated that non-pulsed activated DC vaccinations were able to protect mice from a subsequent C23 tumour challenge as effectively as C23 lysate-pulsed DC vaccinations (Figures 3 and 6). The unexpected protection provided by non-pulsed DC vaccinations in control mice made it extremely difficult to evaluate the *in vivo* protective effect of immunisation with DCs pulsed with lysate containing PAX3-FKHR antigen.

The small tumours that did form in DC-immunised mice were shown to contain greatly increased numbers of tumour infiltrating lymphocytes relative to mice receiving the C23 tumour challenge alone. Immunophenotypic analysis revealed that C23 lysate-pulsed DCs and non-pulsed DCs activated similar immune effector cell types, with equal numbers of $CD8^+$ and $CD4^+$ T cells infiltrating the tumours in both treatment groups (Figure 8).

To investigate whether C23 lysate-pulsed DCs or non-pulsed DCs primed T cells that specifically target PAX3-FKHR-expressing C23 cells, we analysed the splenic T cells *in vitro*. Activated T cells secrete IFN-γ, however it is important to note that any natural killer T (NKT) cells or NK cells present in the splenocyte samples also secrete IFN-γ upon activation. Figures 5 and 9 show that neither C23 lysate-pulsed DCs nor unpulsed DCs induced an immune response with increased activity against C23 targets compared to CMV targets. This finding suggests that the DC vaccinations were unable to prime

naïve T cells towards PAX3-FKHR-specific T cells *in vivo*. Additionally, C23 lysate-pulsed DC immunisations protected mice from a subsequent CMV challenge as effectively as against a C23 challenge (Figure 6B). This further suggests that the C23 lysate-pulsed DCs did not prime PAX3-FKHR-specific T cells (or NK cells that target MHC class I negative cells).

In future *in vivo* tumour growth experiments, an additional treatment group should be investigated. Immunising mice with KLH alone prior to a C23 tumour challenge would allow us to discriminate between the non-specific protection provided by the KLH adjuvant, and the amount of protection provided by activated non-pulsed DCs.

4.1.3.2. Evidence in the literature for the protective effects of non-pulsed DCs:
Miller and colleagues (2002) demonstrated that DCs infected with an empty adenoviral vector lacking a therapeutic transgene (termed AdDCs) were activated and immunostimulatory. AdDC immunisations were able to protect mice from a subsequent tumour challenge. The investigators postulated that the activated AdDCs secreted IL-12, which induced T cell and NK cell responses *in vivo*, resulting in systemic anti-tumour immunity.

It is important to note that the AdDC immunisations were not as efficient as tumour antigen-pulsed DC immunisations at protecting mice from a subsequent tumour challenge (Miller *et al*, 2002). Hence, their findings cannot fully explain our results, in which non-pulsed DCs conferred an equal amount of tumour protection as C23 lysate-pulsed DCs. In future experiments, one group of mice could be immunised with immature non-pulsed DCs, followed by a C23 tumour challenge. This would address the question of whether immature non-pulsed DCs, that do not secrete IL-12, are able to protect mice from a subsequent C23 tumour challenge. However, immunising mice with DCs in an immature state is hard to achieve in practice.

4.1.3.3. Possible expression of endogenous retroviruses (ERVs) in the 76-9-derived cell lines:
The finding that there were consistently a few tumour infiltrating lymphocytes in the mice that received the C23 tumour challenge alone, along with the *in vitro* ELISpot results showing that C23 cells activated a small number of splenic T cells isolated from naïve and challenge only mice, suggests that the C23 cells are at least moderately

immunogenic. One possible explanation is that the extensively passaged 76-9-derived cell lines (CMV and C23) are immunogenic because they express ERV protein(s) that are not present in the C57BL/6 mouse and therefore act as tumour-associated T cell antigen(s).

Proviral remnants of ancestral retroviral infections are integrated in the genomes of all vertebrates, and are known as ERVs (Lower *et al*, 1996). ERV gene products can be processed, generating antigenic peptides for presentation. Members of the human and mouse ERV families are preferentially expressed in fresh tumours and cell lines rather than normal tissues (Wang *et al*, 1995; Huang *et al*, 1996; Schiavetti *et al*, 2002). Hence, ERVs serve as potential TAAs, which can be exploited in cancer immunotherapeutic strategies. Yang and Perry-Lalley (2000) reported that the envelope protein of a mouse ERV of the AKV family, which is found in the germline of C57BL/6 mice, serves as a TAA in two different syngeneic tumours. The investigators found that the envelope protein component p15E is naturally presented in the context of H2-K^b and is recognised by tumour infiltrating lymphocytes. Utilising the TS/A mouse mammary adenocarcinoma cell line in preclinical studies of cancer immunotherapy, Rosato and colleagues (2003) identified the gp70 envelope protein of a murine ERV as the target antigen for TS/A-specific CTLs. Immunisation of BALB/c mice with the carcinogen-induced colorectal tumour CT26, engineered to secrete GM-CSF, results in the expansion of CT26-specific CTLs. Huang *et al* (1996) showed that virtually all of these CT26-specific CTLs specifically recognised an immunodominant peptide derived from the gp70 envelope protein of murine leukaemia virus. Furthermore, adoptive transfer experiments showed that the CT26-specific CTLs were effective in eradicating established CT26 tumours *in vivo*.

It is possible that during heavy passaging, the 76-9 cell line has been infected with a retrovirus, which is absent from the parental C57BL/6 mouse, resulting in the emergence of new antigenic determinants. Following tumour challenge with the 76-9-derived C23 cells, the ERV gene products could be perceived as 'foreign' by the host immune system and targeted by a CTL response. We could test the 76-9-derived cell lines and C57BL/6 mouse strain for the presence of known murine ERVs by RT-PCR analysis.

The ability of human ERV gene products to serve as TAAs in human cancers has also been investigated. Muster *et al* (2003) reported that human ERV-K is expressed in human melanomas and metastases but not in normal melanocytes. Schiavetti and colleagues (2002) identified a human ERV gene product (called HERV-K-MEL) that acts as a melanoma-associated antigen, and demonstrated that melanoma patient CTLs can target cells expressing HERV-K-MEL peptide-HLA-A2 complexes, *in vitro*. The results of several preclinical studies using mouse models suggest that CTLs specific for ERV tumour antigens might be therapeutically useful for the treatment of some human cancers (Kershaw *et al*, 2001; Rosato *et al*, 2003).

4.1.4. Effector cell types targeting the C23 tumour challenge cells in vivo:

4.1.4.1. Role of T cells:

Immunophenotypic analysis revealed that the lymphocytes infiltrating the tumours of DC-immunised wild type C57BL/6 mice were primarily $CD8^+$ CTLs and $CD4^+$ Th cells (Figure 8). Furthermore, the splenic T cells of DC-immunised mice were activated and secreted IFN-γ when cultured with CMV or C23 target cells *in vitro* (Figures 5 and 9). The presence of $CD3^-CD4^-CD8^-$ γδ T cells infiltrating the tumours was not determined, and should be investigated in future experiments.

To examine further the mechanism of anti-tumour immunity in the DC-immunised mice, splenocytes collected 2 days following C23 tumour challenge were used for *in vitro* cytotoxicity assays. However, high spontaneous LDH release by the effector and target cell populations masked any effector-mediated target cell killing. We intended to determine whether C23 target cell killing was abrogated in DC-immunised mouse splenocyte cultures depleted of functional $CD8^+$CTLs, $CD4^+$ Th cells, or $NK1.1^+$ cells, using blocking antibodies.

To determine whether immunological memory was generated, we hoped to re-challenge the mice that did not develop tumours by day 70 following C23 tumour challenge. However, this experimental procedure was not permitted under our current animal project licence. In future experiments, the tumour infiltrating lymphocytes could be stained with CD3 and $CD45R_o/R_a$ antibody combinations, in order to determine whether the lymphocytes located at the tumour site are naïve or memory T cells.

4.1.4.2. Role of NK cells:

The finding that PAX3-FKHR virtually abolishes MHC class I expression in the mouse 76-9 cell line (Chapter 2, Figure 15A) suggests that C23 cells might be susceptible to NK cell attack. We hypothesized that the DC immunisations (C23 lysate-pulsed DCs and non-pulsed DCs) might trigger innate NK cell-mediated anti-tumour immunity *in vivo*. Activated mouse DCs secrete IL-12, which is known to play an essential role in activating NK cells (Trinchieri, 2003). Furthermore, Fernandez and colleagues (1999) reported that adoptively transferred DCs are able to promote NK cell responses against mouse MHC class I negative tumours.

Treatment of wild type C57BL/6 mice with monoclonal antibody against NK1.1 is the most commonly used method to block NK cell activity *in vivo*. However, money constraints prevented us from adopting this approach. Instead we performed the *in vivo* tumour growth experiment using beige C57BL/6 mice, which are deficient in NK cell function (Roder, 1979). Beige mouse cells are unable to secrete perforin and granzymes, and as a result NK cells are functionally defective because they rely solely on the perforin system to kill targets. In contrast, CTLs and NKT cells utilize both the perforin system and the Fas ligand-Fas system to lyse targets, and their cytotoxicity is only moderately compromised in beige mice (Bannai *et al*, 2000).

Figure 10B shows that both C23 lysate-pulsed DC immunisations and non-pulsed DC immunisations were capable of protecting beige C57BL/6 mice against a subsequent C23 tumour challenge, as observed in wild type C57BL/6 mice. This result suggests that NK cells are not the sole effector cell type responsible for anti-tumour immunity *in vivo*. More accurately, we can conclude that the perforin system of cell lysis is not crucial for killing C23 cells *in vivo*.

In the C23 challenge only groups, the syngeneic tumours grew at a faster rate in beige mice than in wild type mice (Figure 10C). This result suggests that in the absence of DC vaccination, the release of perforin by effector cells (NK cells, NKT cells and T cells) plays a role in slowing the growth of the tumour, but is insufficient to prevent tumour growth. Furthermore, effector cell killing via perforin release appears to be an important process for lysing the C23 tumour challenge cells, and cannot be entirely compensated for by other killing mechanisms.

It is worth noting that activated NK cells release IFN-γ (Chan *et al*, 1992). Hence, the wild type C57BL/6 splenocytes that secreted IFN-γ when cultured *in vitro* with CMV or C23 targets might have included activated NK cells. NK cells can be phenotypically identified as $CD3^-CD4^-CD8^-NK1.1^+$ or $CD3^-$ $CD4^-CD8^+$ $NK1.1^+$ cells. The immunophenotypic data collected from the tumour infiltrating lymphocytes (Figures 7 and 8) suggests that $CD3^-CD8^+$ NK cells do not play a major role in targeting C23 challenge cells *in vivo*. Unfortunately, the NK1.1-specific antibody displayed a lot of non-specific binding and meaningful results could not be obtained. Hence, we were unable to determine the numbers of $CD3^-CD8^-NK1.1^+$ NK cells infiltrating the tumours.

4.1.4.3. Role of NKT cells:

NKT cells have recently been discovered and are conventionally identified as $CD3^{+/low}CD4^+CD8^-$ or $CD3^{+/low}CD4^-CD8^-$ T cells, which also express several NK cell antigens, including NK1.1 (MacDonald, 1995). NKT cells do not express a normal T cell receptor repertoire, instead they possess an invariant T cell receptor that specifically binds to the non-classical MHC class I-like molecule CD1d presenting glycolipid antigens (Bendelac *et al*, 1995). NKT cells have been shown to interact with DCs via a CD40 ligand, and activated NKT cells secrete cytokines such as IFN-γ (Brutkiewicz and Sriram, 2002). Cui and colleagues (1997) reported that NKT cells are important in IL-12-mediated anti-tumour immunity.

It is feasible that in our mouse ARMS model, IL-12 secreted by the activated DCs administered to the mice (C23 lysate-pulsed DCs or non-pulsed DCs) is able to activate an NKT cell-mediated anti-tumour response. Theoretically, the IFN-γ secreting splenocytes stimulated by the CMV and C23 cells *in vitro* (Figures 5 and 9) might be activated NKT cells. The panel of antibodies used to immunophenotype the tumour infiltrating lymphocytes does not eliminate the possibility that some NKT cells are infiltrating the tumours. However, the majority of $CD3^+$ T cells present in the tumours appear to be either $CD3^+CD8^+$ CTLs or $CD3^+CD4^+$ Th cells.

4.1.5. Conclusions and future direction of the tumour lysate-pulsed DC project:

In this study we have shown that both C23 lysate-pulsed DC immunisations and non-pulsed DC immunisations protect mice against a subsequent C23 tumour challenge, and the tumour protection does not appear to be PAX3-FKHR-specific. The activated DCs administered to the mice, and the cytokines they secrete, are unlikely to persist until the

tumour challenge. Miller and colleagues (2002) postulated that activated non-pulsed DC immunisations might protect mice from a subsequent tumour challenge by inducing autoimmunity through the capture and presentation of self antigens. Alternatively, IL-12 secreted by the activated DCs might activate NKT cells that are important in innate anti-tumour immunosurveillance (Cui *et al*, 1997).

A crucial future experiment is to determine whether C23 tumour lysate can serve as an effective immunogen, when processed and presented by mouse DCs, to stimulate PAX3-FKHR-specific T cell responses *in vitro*. DCs loaded *ex vivo* with PAX3-FKHR peptides or *PAX3-FKHR* mRNA might be more effective at initiating antigen-specific immune responses.

4.2. Use of peptide-pulsed DCs to stimulate PAX3-FKHR-specific CTL responses: The SYFPEITHI and BIMAS computer programs were used to identify potential CTL peptide epitopes specific for the PAX3-FKHR protein that might be useful for developing peptide-pulsed DC vaccines to treat ARMS patients.

4.2.1. Targeting the tumour-specific PAX3-FKHR breakpoint region:
Unfortunately, no peptide sequences spanning the breakpoint of the human PAX3-FKHR fusion protein were predicted to bind strongly to HLA-A*0201 (Table 2A). We attempted to identify HLA-A*0201 binding peptide motifs as this is the most common HLA allele found in the human Caucasian population. Dagher and colleagues (2002) used the BIMAS computer program to identify peptide sequences in the breakpoint region of human PAX3-FKHR that might bind to other human HLA molecules. PAX3-FKHR breakpoint peptides were predicted to bind to HLA-A33, -A68, and -B7 with BIMAS binding affinity scores of 3.0, 7.5, and 120, respectively. These scores are far lower than that of the PAX3-derived KLT peptide (binding to HLA-A*0201) used in the current study, and the breakpoint peptides are unlikely to bind to the HLA molecules with intermediate to high affinity. These combined findings suggest that the tumour-specific breakpoint region of PAX3-FKHR is unlikely to be presented to the immune system of ARMS patients.

However, there are examples in the literature of natural HLA-A*0201 binding peptide epitopes that do not contain the HLA-A*0201 cononical binding motif at position 2, where a leucine residue is normally found (Yotnda *et al*, 1998). Such peptide motifs

gain a low HLA-A*0201 binding affinity score using SYFPEITHI and BIMAS algorithms. Therefore, there might be atypical HLA-A*0201 binding peptide motifs spanning the breakpoint of the human PAX3-FKHR protein, and only by testing all possible 9mer and 10mer breakpoint peptides in T2 peptide binding studies can we rule out the possibility of a tumour-specific presentable peptide.

4.2.2. PAX3-derived peptide motifs that bind to mouse H2-K^b or H2-D^b:

The N-terminal PAX3 region of PAX3-FKHR is potentially a tumour-associated antigen and suitable for targeted immunotherapy to treat ARMS (see *1.2.2.*). Investigating this immunotherapeutic approach in our mouse model of ARMS, we selected 3 peptides from the PAX3 amino acid sequence retained in mixed murine/human PAX3-FKHR that theoretically should bind to mouse H2-K^b or H2-D^b MHC class I molecules. The actual binding affinity of the peptides was determined using RMA-S cells. The PAX3 peptide QLM, which was predicted to be an H2-K^b motif, was unable to bind H2-K^b on the cell surface of RMA-S cells, at any peptide concentration tested (Figure 13A). In contrast, the PAX3 peptides GVFI and GGVF, which were predicted to bind to H2-D^b, were able to bind and stabilise H2-D^b molecules on the surface of RMA-S cells. As a result, incubation of RMA-S cells with 100μM of GVFI or GGVF peptide led to a more than two fold increase in H2-D^b levels (Figure 13B). These two PAX3 peptide motifs have an intermediate binding affinity, unable to bind to H2-D^b as strongly as the positive control NP68 peptide.

In future experiments, we shall examine the immunogenicity of the two H2-D^b binding PAX3 peptides. *In vitro* generated C57BL/6 mouse DCs will be loaded with GVFI and GGVF peptides and tested for their ability to initiate PAX3-specific immune responses, *in vitro* and *in vivo*. In future tumour growth assays, the ability of the peptide-pulsed DC vaccinations to protect mice from a subsequent PAX3-FKHR^{+ve} C23 tumour challenge or PAX3-FKHR^{-ve} CMV tumour challenge will be investigated. Mice could be challenged with 2×10^6 viable syngeneic C23 or CMV cells, instead of the current 1×10^6 cells, in order to elucidate any differences between the immunity induced by peptide-pulsed DCs and the non-specific immunity induced by non-pulsed DCs.

The amino acid sequence of the FKHR portion of mixed murine/human PAX3-FKHR is only 85% homologous to the C-terminus of mouse FKHR. Hence, the FKHR section of the mixed murine/human fusion protein is a neoantigen to the mouse immune system,

and it is possible that the C23 cells might be killed *in vivo* as a result of a T cell response specific for peptide epitopes derived from the FKHR portion of mixed murine/human PAX3-FKHR. An important control will be to challenge the DC-immunised mice with 76-9 cells stably expressing a truncated mixed murine/human PAX3-FKHR protein that lacks the C-terminal FKHR section (a pBK-CMV plasmid containing truncated mixed murine/human PAX3-FKHR cDNA has been generated in the laboratory).

*4.2.3. PAX3 peptides that bind to HLA-A*0201*:

Only one peptide derived from the PAX3 amino acid sequence present in human PAX3-FKHR contained the theoretical HLA-A*0201 binding motif (Table 2B). In an initial T2 peptide binding assay, the PAX3 peptide KLT showed significant binding to HLA-A*0201, but only with intermediate affinity (Figure 14A). We found that variables, such as the length of time in culture and splitting/feeding frequency of the T2 cells prior to the binding assay, affected the experimental results. In Figure 14B, PAX3 KLT bound to HLA-A*0201 with higher affinity, with 100μM KLT increasing HLA-A*0201 levels 3.8 fold relative to 100μM negative control peptide (QLM). The T2 peptide binding assay was performed 7 times in total, and in every experiment the PAX3 KLT peptide had an intermediate to high HLA-A*0201 binding affinity.

In future experiments to assess the immunogenicity of the PAX3 KLT peptide, $CD8^+$ T cells isolated from the PBMCs of an identified HLA-A*0201^+ healthy donor will be stimulated *in vitro* with autologous KLT peptide-pulsed MoDCs. MoDCs will have to be incubated with very high concentration of the KLT peptide, as peptide presentation requires the exogenous low-intermediate affinity peptides to be captured by DCs and loaded onto newly synthesized MHC class I molecules within the cell (Luft *et al*, 2001). The ability of the DC-stimulated CTLs to kill PAX3-expressing HLA-A*0201^+ target cells can then be determined using *in vitro* cytotoxicity assays. The targets would include T2 cells pulsed with KLT peptide and T2 cells pulsed with an irrelevant peptide (such as QLM). Furthermore, it is important to determine whether the KLT epitope can be processed and presented from endogenously expressed PAX3-FKHR protein in tumour cells. Hence, additional targets would include the HLA-A*0201^+ cell lines RMS and HX170c stably transfected with PAX3-FKHR or empty pBK-CMV vector.

If the KLT peptide-pulsed DCs are able to stimulate $CD8^+$ T cell responses that are capable of recognizing endogenously processed PAX3-FKHR protein, then the KLT peptide represents an attractive candidate for use in immunotherapy for HLA-A*0201^+ ARMS patients. The PAX3-FKHR fusion protein has been shown to be vital for the ARMS malignant phenotype (Bernasconi *et al*, 1996; Scheidler *et al*, 1996; Ayyanathan *et al*, 2000), therefore the tumour cells can not down-regulate this antigen to avoid immune detection without loosing its malignant behaviour.

If the PAX3 KLT peptide is found to be immunogenic, then attempts could be made to improve its HLA-A*0201 binding affinity, by making single amino acid substitutions at the key anchor positions (positions 2 and 9). A higher affinity binding KLT peptide might augment the PAX3-FKHR-specific CTL response (Yun *et al*, 1999).

KLT is a CTL epitope, and DCs loaded with KLT peptide would only be able stimulate $CD8^+$ T cells. However, it is well recognized that stimulation of $CD4^+$ Th cells is important for the induction of effective, long lasting anti-tumour immunity (Banchereau *et al*, 2001b). Research identifying MHC class II motifs in the N-terminus of PAX3 is warranted, as DCs pulsed with a combination of PAX3-FKHR-derived $CD8^+$ and $CD4^+$ peptide motifs would be preferred. Alternatively, we could use a 'helper peptide' known to bind to MHC class II (such as the hepatitis B virus peptide TPPATRPPNAPIL; Lee *et al*, 1996), which would elicit a $CD4^+$ T cell response that is specific for a non-specific antigen, but is sufficient to provide 'help' for emerging PAX3-specific CTL responses. Loading DCs with full length PAX3-FKHR mRNA or protein would allow endogenous processing and presentation of any immunogenic $CD4^+$ peptide epitopes.

4.2.3.1. The specificity of $CD8^+$ T cells present in ARMS patients:

It would be interesting to determine whether peripheral blood lymphocytes isolated from HLA-A*0201^+ ARMS patients contain CTLs that specifically lyse HLA-A*0201^+ PAX3-FKHR-expressing target cells *in vitro*. One potential immunotherapeutic strategy is to use autologous MoDCs pulsed with KLT peptide as APCs to stimulate patient peripheral blood lymphocytes *ex vivo*. Peptide-specific T cell clones could then be isolated and be used for adoptive transfer. Tetramer analysis could be used to investigate whether the peripheral blood or tumour infiltrating lymphocytes of HLA-A*0201^+ ARMS patients contain $CD8^+$ T cells specific for the PAX3-derived KLT epitope.

4.2.3.2. Generation of PAX3-specific CTLs to target ERMS, Ewing's sarcoma and melanoma:

If DCs loaded with KLT peptide are able to induce PAX3-FKHR-specific $CD8^+$ T cell responses, then they should also stimulate CTL responses specific for the wild type PAX3 antigen. In this situation, KLT-peptide-pulsed DC vaccines could be used to treat HLA-A*0201^+ patients with RMS, Ewing's sarcoma or melanoma, in which the tumour cells express PAX3.

Interestingly, the KLT peptide is derived from an amino acid sequence that is conserved between PAX3 and PAX7. In HLA-A*0201^+ patients, CTL responses specific for the KLT peptide might be able to target ERMS cells that over-express PAX7.

4.3. Use of DCs transfected with *PAX3-FKHR* mRNA to initiate tumour-specific immune responses:

We set out to examine the ability of *in vitro* differentiated mouse DCs pulsed with *PAX3-FKHR* mRNA to stimulate antigen-specific immune responses, *in vivo* and *in vitro*. Unfortunately, we were unable to transfect immature or mature mouse DCs with *GFP* mRNA efficiently, using TransMessenger Reagent (Figure 15B). In contrast, Liao and colleagues (unpublished data) were able to transfect up to 93% of immature DCs and up to 53% of mature DCs with *GFP* mRNA using TransMessenger Reagent (Qiagen TransMessenger Reagent data sheet). Unfortunately, the authors did not reply to our correspondence asking for their detailed experimental methodology.

The difficulty of transfecting DCs, compared to cell lines for example, is that DCs are non-proliferating cells. Standard lipofection reagents, such as FuGENE 6 Transfection Reagent (Roche) and Lipofectamine 2000 (Invitrogen), are unable to deliver genetic material into non-proliferating cells with high efficiency. Several studies have analysed the efficiency of different delivery strategies for the transfection of DCs with RNA. Van Tendeloo and colleagues (2001) reported that electroporation is superior to lipofection (using the cationic lipid DMRIE-C; Gibco) at introducing mRNA into DCs, obtaining a transfection efficiency of more than 50%. Numerous groups have subsequently electrotransfected DCs with *in vitro* transcribed mRNA or mRNA isolated from tumour cells (Sæbøe-Larssen *et al*, 2002; Grünebach *et al*, 2003; Milazzo *et al*, 2003). Breckpot and colleagues (2003) transduced DCs with a lentiviral vector, and achieved stable gene expression in nearly 100% of mature DCs. Therefore, future work attempting to

transfect DCs with *PAX3-FKHR* mRNA should use proven transfection methods, such as electroporation or lentiviral transduction.

The findings to date using tumour RNA-transfected DCs are very encouraging. Mouse experiments have shown that DCs pulsed with tumour RNA can cause the regression of pre-established tumours (Ashley *et al*, 1997; Boczkowski *et al*, 2000; Nair *et al*, 2003). Furthermore, human DCs transfected with tumour RNA have been shown to induce tumour-specific T cell responses *in vitro*, in various cancer types including melanoma (Milazzo *et al*, 2003), chronic lymphocytic leukaemia (Müller *et al*, 2004), multiple myeloma (Milazzo *et al*, 2003), and prostate cancer (Heiser *et al*, 2002). Hence, immunisation with autologous DCs pulsed with *PAX3-FKHR* mRNA represents an attractive strategy for the generation of T cell responses that specifically target ARMS.

4.4. Conclusions:

We have established a mouse model of ARMS that is suitable for examining the ability of immunotherapeutic strategies to stimulate PAX3-FKHR-specific anti-tumour immunity. Studies utilizing this mouse ARMS model suggest that vaccination with tumour cell lysate-pulsed DCs is unable to prime PAX3-FKHR-specific T cell responses *in vivo*. Interestingly, C23 lysate-pulsed DCs and non-pulsed DCs did appear to have some non-specific protective effect against a subsequent tumour challenge. We have identified two peptides derived from the PAX3 amino acid sequence retained in PAX3-FKHR that are able to bind to mouse H2-D^b MHC class I molecule. The ability of DCs pulsed with these peptides to induce anti-tumour immune responses shall be determined using our mouse model of ARMS. Furthermore, a peptide from the PAX3 sequence present in human PAX3-FKHR has been identified that binds to human HLA-A*0201 with intermediate affinity. The ability of MoDCs pulsed with this peptide to prime PAX3-FKHR-specific CTLs will be assessed *in vitro*, using HLA-A*0201^+ normal donor samples. Transfection of DCs with *PAX3-FKHR* mRNA is a promising approach and warrants further investigation.

Appendices

Treatment	Day 0	Day 7	Day 11	Day 14	Day 18	Day 20	Day 24
Challenge only	0	11.2	89.7	1402.1	2422.8		
Challenge only	0	2.4	30.8	717.9	831	1402.1	
Challenge only	0	11.2	19.4	155.1	831	1402.1	
Challenge only	0	0	11.2	45.9	523.3	1240.5	
Challenge only	0	5.7	19.4	1240.5	955.5		
Challenge only	0	1.4	65.4	955.5	302.8	831	955.5
Challenge only	0	0.7	19.4	30.8	523.3	523.3	1402.1
Challenge only	0	0	0	1240.5	2422.8		
Challenge only	0	5.7	197.1	1402.1	1577.2		
Challenge only	0	1.4	30.8	155.1	1402.1		
Non-Pulsed DC	0	0	0	5.7	197.1	1091.8	1240.5
Non-Pulsed DC	0	0	2.4	5.7	19.4	89.7	155.1
Non-Pulsed DC	0	0.09	0	0	0	0	0
Non-Pulsed DC	0	0	0	0	0	0	0
Non-Pulsed DC	0	0	0	0	0	0	0
Non-Pulsed DC	0	0	2.4	30.8	615.5	1240.5	
Non-Pulsed DC	0	0	30.8	0	0.7	0	0
Non-Pulsed DC	0	0.7	0	19.4	523.3	1240.5	
Non-Pulsed DC	0	0	19.4	0	0	0	0
Non-Pulsed DC	0	0	0	30.8	19.4	119.4	615.5
Pulsed DC	0	0	2.4	0.09	197.1	955.5	717.9
Pulsed DC	0	0	0.7	0.09	45.9	119.4	302.9
Pulsed DC	0	0	0.7	11.2	0.7	19.4	5.7
Pulsed DC	0	0.09	2.4	19.4	197.1	1091.8	2422.8
Pulsed DC	0	0	0	0	0	0	0
Pulsed DC	0	0	0	0.09	0.7	2.4	30.8
Pulsed DC	0	0	0.7	2.4	11.2	45.9	246.2
Pulsed DC	0	0	0	0	0	0	0
Pulsed DC	0	0	0	5.7	19.4	11.2	119.4
Pulsed DC	0	0					

Appendix 1. Tumour volumes (in mm^3) from the initial C23 lysate-pulsed DC vaccine experiment in wild type C57BL/6 mice. To convert tumour diameter into tumour volume we used the formula: volume = $4/3\pi$ $(diameter/2)^3$. Where the volume is not written the mouse had been culled. Note that one mouse receiving C23 lysate-pulsed DC immunisations was culled day 11 post challenge as a result of trauma, but this was not as a result of habouring a large tumour.

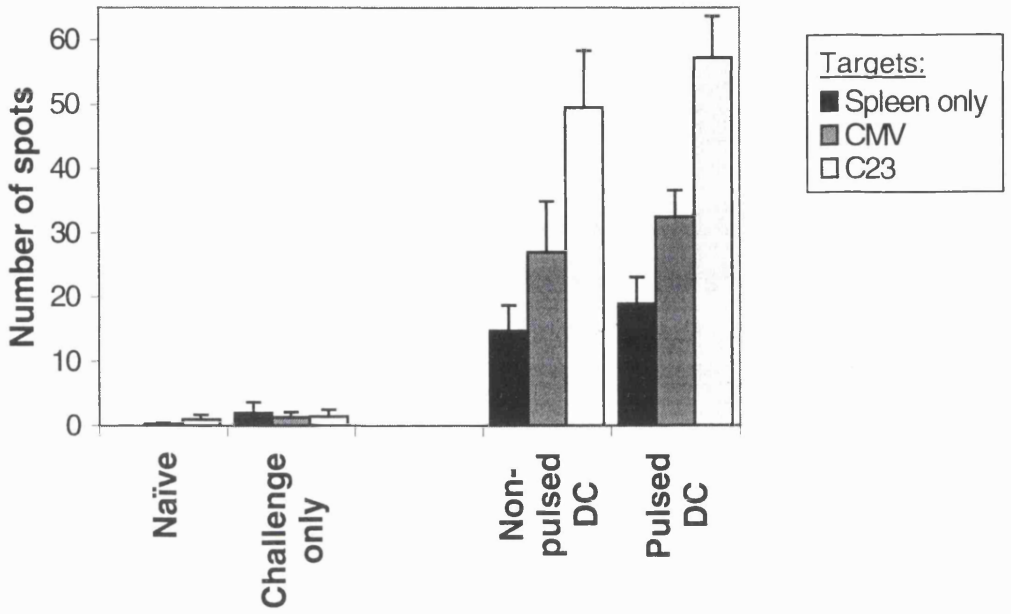

Appendix 2. IFN-γ secretion of splenocytes cultured *in vitro* with CMV or C23 RMS target cells. The filled in bars represent splenocytes cultured alone, and the total number of spots in each sample are plotted. This is in contrast to Figures 5, 9, and 12, where the number of IFN-γ secreting cells in the spleen only wells was subtracted from the values of the test wells. This figure summarises an experiment that was not depicted in any figure in the results section of this chapter. Methodology: splenocytes were isolated from the mice (wild type C57BL/6) from all treatment groups at the end of the *in vivo* tumour growth assay. We measured splenocyte IFN-γ secretion in triplicate wells, and analysed splenocytes from two mice per group. The values plotted are mean ± S.E.M. of each group. In negative control wells, CMV and C23 cells were cultured alone and secreted undetectable levels of IFN-γ.

Treatment	I.D.	Day 0	Day 7	Day 9	Day 12	Day 14	Day 16	Day 19
Challenge only	1 Bl	0	0	0	0	0	0	0
Challenge only	2 Bl	0	0	0	0	4.2	4.2	14.1
Challenge only	1 R	0	0	0	523.6	2144.6	2144.6	2572.4
Challenge only	2 R	0	0	0	0	0	0	0
Challenge only	1 Bl +1R	0	0	0	65.5	33.5	179.6	179.6
Challenge only	Mean	0	0	0	14.1	44.6	65.4	82.4
Non-Pulsed DC	1 Bl	0	0	0	0	0	0	0
Non-Pulsed DC	2 Bl	0	0	0	0	0.5	0.5	4.2
Non-Pulsed DC	1 R	0	0	0	14.1	113.1	179.6	523.6
Non-Pulsed DC	2 R	0	0	0	0	0	0	0
Non-Pulsed DC	1 Bl +1R	0	0	0	0	0	0	0
Non-Pulsed DC	Mean	0	0	0	0.1	1.4	2.1	7.2
Pulsed DC + C23	1 Bl	0	0	0	0	0	0	0
Pulsed DC + C23	2 Bl	0	0	0	0	0	0	268.1
Pulsed DC + C23	1 R	0	0	0	0	0	0	0
Pulsed DC + C23	2 R	0	0	0	0	0	0	0
Pulsed DC + C23	1 Bl +1R	0	0	0	0	0	0	0
Pulsed DC + C23	Mean	0	0	0	0	0	0	2.1
Pulsed DC + CMV	1 Bl	0	0	0	0	0	0	0
Pulsed DC + CMV	2 Bl	0	0	0	0	0	0	0
Pulsed DC + CMV	1 R	0	0	0	0	0	0	4.2
Pulsed DC + CMV	2 R	0	0	0	0	0	0	0
Pulsed DC + CMV	1 Bl +1R	0	0	0	0	0	0	0
Pulsed DC + CMV	None	0	0	0	0	0	0	0
Pulsed DC + CMV	Mean	0	0	0	0	0	0	0.02

Appendix 3. Tumour volumes (in mm^3) from the repeat C23 lysate-pulsed DC vaccine experiment in wild type C57BL/6 mice. The individual mice were identified by the unique stripe pattern painted onto their tail (Key: Bl, black; R, red). The mean tumour volume in each treatment group is also shown at each time point. To convert tumour diameter into tumour volume we used the formula: volume = $4/3\pi$ $(diameter/2)^3$.

Treatment	I.D.	Day 0	Day 7	Day 9	Day 12	Day 14	Day 16	Day 19
Challenge only	1 Bl	0	4.2	179.6	381.7	523.6	904.8	904.8
Challenge only	2 Bl	0	0	0	268.1	1767.2	3053.6	3053.6
Challenge only	1 R	0	0	33.5	65.5	1150.3	1767.2	2572.4
Challenge only	2 R	0	0	14.1	33.5	1436.8	1767.2	2572.4
Challenge only	1 Bl+1R	0	0	4.2	65.5	14.1	179.6	381.7
Challenge only	Mean	0	0.03	33.5	124.8	696.9	1259.8	1629.5
Non-Pulsed DC	1 Bl	0	0	0	0	4.2	4.2	14.1
Non-Pulsed DC	2 Bl	0	0	0	0	0	4.2	14.1
Non-Pulsed DC	1 R	0	0	0	0	0	0	0
Non-Pulsed DC	2 R	0	0	0	0	4.2	4.2	33.5
Non-Pulsed DC	1 Bl+1R	0	0	0	0	0	0	0.5
Non-Pulsed DC	Mean	0	0	0	0	0.3	0.9	5.5
Pulsed DC	1 Bl	0	0	0	0	65.5	179.6	1150.3
Pulsed DC	2 Bl	0	0	0	0	0	0	0
Pulsed DC	1 R	0	0	0	4.2	4.2	179.6	268.1
Pulsed DC	2 R	0	0	0	0	0	0	0
Pulsed DC	1 Bl+1R	0	0	0	0	0	4.2	4.2
Pulsed DC	Mean	0	0	0	0.03	1.4	17.2	51.0

Appendix 4. Tumour volumes (in mm^3) from the C23 lysate-pulsed DC vaccine experiment in beige C57BL/6 mice. The individual mice were identified by the unique stripe pattern painted onto their tail (Key: Bl, black; R, red). The mean tumour volume in each treatment group is also shown at each time point. To convert tumour diameter into tumour volume we used the formula: volume = $4/3\pi$ $(diameter/2)^3$.

Chapter 4:

Generation of Immunostimulatory Dendritic Cells from the Malignant Clone in Patients with Juvenile Myelomonocytic Leukaemia

Abstract

Dendritic cells (DCs) are professional antigen presenting cells and play a central role in the development of anti-leukaemia immune responses. DCs develop from haematopoietic progenitors committed to the lymphoid or myeloid lineages, and in some instances from blood monocytes. We sought to determine whether malignant juvenile myelomonocytic leukaemia (JMML) cells could be differentiated *in vitro* into functionally active DCs, capable of presenting endogenous leukaemic antigens in the context of co-stimulatory signals, as required for the priming of leukaemia-specific T lymphocytes. Using granulocyte macrophage-colony stimulating factor and interleukin (IL)-4, we successfully differentiated peripheral blood mononuclear cells (PBMCs) from three JMML patients into cells that immunophenotypically and morphologically resembled immature DCs. With two of the patient immature DC cultures (JMML-1 and JMML-2), the addition of lipopolysaccharide (LPS) resulted in activation of the DCs, as measured by up-regulation of the co-stimulatory antigen CD86, the major histocompatibility complex (MHC) class II molecule HLA-DR, and the DC activation marker CD83. Additionally, the LPS maturation stimulus induced DCs cultured from normal donor and JMML-2 PBMCs to secrete large amounts of IL-12, an immunostimulatory cytokine important for DC-T cell interactions. Combined, these results provide strong evidence that the mature DCs generated from JMML-2 PBMCs possessed an immunostimulatory phenotype. However, the minimal secretion of IL-12 by JMML-3 DCs following incubation with LPS for 24 hours is consistent with the flow cytometic data, demonstrating that the DCs cultured *in vitro* from this patient were partially resistant to activation using LPS. The variability in the phenotypes of the DCs generated from the 3 JMML patients might reflect the heterogeneity of the disorder. Similarly, it is not possible to culture leukaemic DCs from all chronic and acute leukaemia patients. Interestingly, the leukaemic cells in two of the patients (JMML-2 and JMML-3) displayed monosomy 7, which was used as a marker of malignant origin. Fluorescence *in situ* hybridisation analysis detected monosomy 7 in more than 90% of the $CD86^{+}$-purified DCs generated *in vitro* from these two JMML patients, indicating that the DCs were derived from the malignant clone. In the majority of JMML patients, *in vitro* cultured DCs should therefore express any endogenous leukaemic antigens and possess the MHC molecules, co-stimulatory molecules, and the cytokine production profile required to present these antigens to the immune effector cells. Examining the functional activity of the *in vitro* generated leukaemic DCs, a mixed leukocyte reaction

(MLR) revealed that activated DCs differentiated from JMML-2 PBMCs were potent stimulators of MHC-mismatched allogeneic T cells, as determined by interferon-γ release, and hence functionally active. In a preliminary experiment, leukaemic DCs generated from JMML-1 PBMCs were used to stimulate and expand allogeneic (bone marrow transplant donor-derived) T cells *in vitro*. A cytotoxicity assay revealed that the expanded allogeneic T cells specifically lysed leukaemic JMML-1 cells, with markedly reduced killing of non-leukaemic JMML-1 cells. This result suggests that the graft versus leukaemia effect appears to be at least partially separable from graft versus host disease. These findings demonstrate that functionally active DCs can be generated *in vitro* from JMML cells, providing a possible mechanism for the *in vivo* or *ex vivo* generation of anti-leukaemia immune responses.

1. Introduction

1.1. Clinical features of JMML:

JMML is a rare myeloproliferative disorder (MPD) of early childhood, accounting for approximately 2% of all childhood leukaemias (Arico *et al*, 1997; Niemeyer *et al*, 1997).

1.1.1. Diagnosis of JMML:

Arico and colleagues (1997) published the clinical and laboratory criteria that are currently used to diagnose JMML. Patients commonly present in the first year of life, and 74% of cases occur before the age of 3 years. Clinical features include hepatomegaly, splenomegaly, and lymphadenopathy, which are typical of most proliferative diseases. Additional symptoms at presentation include fever, frequent viral infections, and signs of respiratory involvement, such as tonsillitis or bronchitis (Arico *et al*, 1997; Niemeyer *et al*, 1997). Laboratory analysis of peripheral blood and bone marrow samples typically reveals leukocytosis with an increase in myeloid cells (Matthes-Martin *et al*, 2000).

1.1.2. Link between JMML and neurofibromatosis type 1 (NF1):

JMML is closely associated with NF1, with 10-15% of JMML cases occurring in children with NF1 (Stiller *et al*, 1994; Niemeyer *et al*, 1997; Luna-Fineman *et al*, 1999). NF1 is a common autosomal dominant disorder, caused by the inheritance of a mutated allele of the *NF1* gene. The normal allele of *NF1* is commonly deleted in the NF1 patient's bone marrow (Kalra *et al*, 1994). NF1 patients are predisposed to developing specific cancers, including neurofibroma, astrocytoma, and JMML (Side *et al*, 1998; Gutmann *et al*, 2003). Side and colleagues (1998) suggested that JMML can be the initial presenting feature of NF1.

1.2. Pathobiology of JMML:

1.2.1. Monosomy 7:

Loss of chromosome 7 (-7) or deletion of the long arm of chromosome 7 (7q-) have been detected in 15-35% of JMML patients (Arico *et al*, 1997; Luna-Fineman *et al*, 1999). The association of monosomy 7 with JMML, and other malignant myeloid disorders, has led investigators to postulate that there are several key tumour suppressor genes located on long arm of chromosome 7, and the loss of function of these genes

might contribute to tumour transformation or progression of the disease (Dohner *et al*, 1998). The current consensus is that monosomy 7 does not warrant being classified as a distinct syndrome from JMML (Hasle *et al*, 1999).

1.2.2. Hypersensitive growth response to granulocyte macrophage-colony stimulating factor (GM-CSF):

A major feature of JMML cell behaviour is hypersensitivity to GM-CSF and tumour necrosis factor (TNF)-α induced proliferation and colony growth *in vitro* (Gualtieri *et al*, 1989; Emanuel *et al*, 1991; Iversen and Sioud, 1998). Furthermore, both these cytokines increase the aggressiveness of JMML *in vivo* (Iversen *et al*, 1997; Iversen and Sioud, 1998). Iversen and Sioud (1998) provided evidence indicating that the function of TNF-α in JMML cells is to stimulate GM-CSF gene expression. A hypersensitive growth response to GM-CSF appears to be involved in the pathogenesis of JMML, and has been linked to aberrant cytokine signal transduction through the RAS signalling pathway.

1.2.2.1. Deregulation of the RAS signalling pathway:

The RAS family of proteins plays a key role in relaying exogenous cytokine signals from the cell surface receptor to the nuclear effector mechanisms, resulting in the stimulation of cell proliferation and nuclear differentiation (Bos, 1989; Satoh *et al*, 1991). Signalling is mediated by activated guanosine triphosphate (GTP) bound RAS, called RAS-GTP (Satoh *et al*, 1991). RAS-GTP signals through the protein kinase RAF-1 and the mitogen-activated protein kinase (MAPK) cascade (Muszynski *et al*, 1995). The *NF1* gene encodes neurofibromin, which inhibits RAS activity by accelerating the hydrolysis of GTP linked to RAS proteins (Kalra *et al*, 1994) (Figure 1).

Mutations that result in hyperactive RAS signalling are common in JMML patients. Activating RAS point mutations are found in many human cancers (Bos, 1989; reviewed in Rodenhuis, 1992), and have been detected in 15-30% of JMML patients (Kalra *et al*, 1994; Flotho *et al*, 1999). The RAS point mutations result in an increase in the levels of active RAS-GTP, resulting in constitutive activation of this common signal transduction pathway (Arico *et al*, 1997).

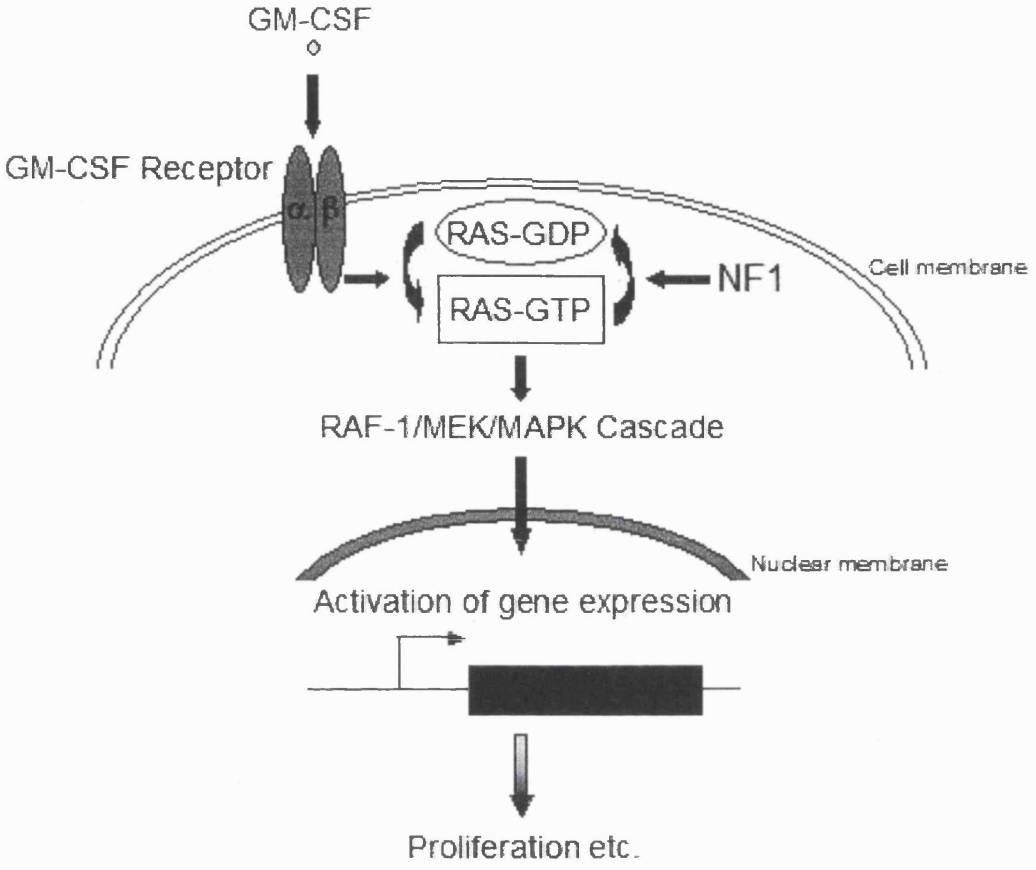

Figure 1. RAS signalling pathway. This common signal pathway transmits the exogenous GM-CSF signal to the nucleus, leading to cell proliferation.

Primary leukaemic cells from patients with NF1, which possess a mutated allele of the *NF1* tumour suppressor gene, commonly exhibit elevated levels of RAS-GTP (Bollag *et al*, 1996). Additionally, Side and colleagues (1998) found mutations of the *NF1* gene in 15% of bone marrow samples collected from JMML patients with no clinical evidence of NF1. Hence, approximately 30% of all JMML cases harbour mutations in the *NF1* gene, causing a loss of the inhibitory actions of *NF1* on RAS-GTP (see *1.2.2.2.*).

The *PTPN11* gene codes for the protein tyrosine phosphatase SHP-2, implicated in transducing signals mediated through the RAS/RAF-1/MAPK cascade. It has recently been reported that mutations in the *PTPN11* gene occur in approximately 30% of JMML cases, leading to a gain of function of SHP-2 and deregulated myeloid growth (Tartaglia *et al*, 2003; Loh *et al*, 2004). *RAS*, *NF1*, and *PTPN11* mutations appear to be mutually exclusive in JMML and all result in hyperactive RAS signalling (Tartaglia *et al*, 2003).

Nevertheless, pathogenic point mutations in the GM-CSF receptor coding sequence have not been identified in primary JMML cells (Freeburn *et al*, 1997). In addition to activating RAS, the GM-CSF receptor can associate with janus kinase (JAK) 2 and initiate intracellular signalling through the JAK-signal transducers and activators of transcription (STAT) cascade (Quelle *et al*, 1994). It is possible that GM-CSF hypersensitivity could be the result of constitutive activation of the JAK-STAT signal pathway.

1.2.2.2. NF1 knock out mice:

Several studies support the hypothesis that *NF1* acts as a tumour suppressor gene in immature myeloid cells by negatively regulating RAS signalling (Bollag *et al*, 1996; Largaespada *et al*, 1996; Side *et al*, 1998). Approximately 10% of heterozygous mutant mice ($NF1^{+/-}$) spontaneously develop a MPD that closely resembles JMML and is associated with the somatic inactivation of the wild type *NF1* allele (Jacks *et al*, 1994). Bollag and colleagues (1996) demonstrated that in NFI-deficient ($NF1^{-/-}$) mouse embryos, haematopoietic cells are hypersensitive to GM-CSF in methylcellulose cultures, similar to primary JMML cells. $NF1^{-/-}$ embryos die *in utero*, however adoptive transfer of $NF1^{-/-}$ fetal liver cells consistently induces a MPD disorder in irradiated recipient mice that models JMML (Largaespada *et al*, 1996; Zhang *et al*, 1998). The

data from this mouse model of JMML provides further evidence that the deregulation of RAS signalling is involved in JMML pathogenesis.

1.2.3. Additional genetic alterations in JMML:

Mutations and/or deletions of the *p53* tumour suppressor gene have been detected in a large proportion of all human cancers (Steele *et al*, 1998). However, Miyauchi and colleagues (1999) found that *p53* mutations are very rare in JMML patients, with only 1 out of the 20 JMML samples examined containing a functionally significant mutation of the *p53* gene. Further studies are required to examine whether other components of the p53 pathway, such as *MDM2*, are mutated in JMML patients. It is possible that the genetic alterations that result in RAS hyperactivity are sufficient to promote proliferation and overcome apoptotic signals during leukaemogenesis in JMML. Further investigation of *p53* mutations in the 10-30% of JMML patients that do not demonstrate deregulation of the RAS signalling pathway is warranted, and may shed light on the molecular mechanism of leukaemogenesis in these patients.

1.2.4. Origins of the JMML progenitor clone:

JMML is characterised by the overproduction of leukaemic cells that increasingly replaces normal haematopoiesis (Emanuel *et al*, 1996; Luna-Fineman *et al*, 1999). Several lines of evidence indicate that the JMML initiating cell may belong to the pool of early pluripotent haematopoietic progenitors, capable to differentiating into both lymphoid and myeloid cell types. Cooper and colleagues (2000) examined an individual who developed both JMML and T cell lymphoma. They found that the malignant JMML and lymphoma cells exhibited the same loss of genetic material (at the *NF1* locus), suggesting that the two cancers originated from the same clone. Similarly, several investigators have observed JMML patients that developed B cell linage acute lymphoblastic leukaemia (ALL), with both leukaemias possessing identical genetic features (such as the same clonal rearrangement of the T cell receptor γ gene) (Lau *et al*, 1994; Scrideli *et al*, 2003). Together these data indicate that JMML is a clonal disease of pluripotent stem cell origin.

1.3. Treatment of JMML:

1.3.1. Conventional therapies:

The treatment of JMML with chemotherapy has been unsuccessful (Arico *et al*, 1997). The probability of 10 years disease-free survival, following single agent chemotherapy

or intensive combination chemotherapy, is less than 10% (Niemeyer *et al*, 1997). Allogeneic bone marrow transplantation (BMT) (also referred to as haematopoietic stem cell transplantation) is the only curative treatment for JMML (Orchard *et al*, 1998). However, allogeneic BMT is associated with high transplant-related mortality, especially in children receiving BMT from unrelated donors, and a large number of patients relapse following treatment (Matthes-Martin *et al*, 2000; Manabe *et al*, 2002). Furthermore, there is currently no effective treatment for JMML patients lacking access to BMT. Therefore, novel alternative therapeutic regimes are required for the treatment of JMML.

1.3.2. Therapy directed against hyperactive RAS signalling:

Hyperactive signal transduction through the RAS pathway is associated with the pathogenesis of JMML (see *1.2.2.1.*), and several treatments that inhibit RAS signalling are now being tested. Iversen and colleagues (2002) examined the feasibility of targeting *RAF-1* gene expression using a specific DNA enzyme as a novel therapeutic option for the treatment of JMML. RAF-1 is downstream of RAS (see Figure 1), and JMML cells typically exhibit elevated levels of activated RAF-1. Iversen and colleagues (2002) designed a DNA enzyme that selectively cleaves *RAF-1* mRNA transcripts. In a xenograft model, immunodeficient mice were engrafted with JMML cells and treated with the DNA enzyme for 4 weeks to examine the efficacy of the enzyme in inhibiting leukaemogenesis. The investigators reported a significant reduction in JMML cell mass in the bone marrow of DNA enzyme-treated individuals relative to non-treated controls. A concern is that the DNA enzyme does not specifically target leukaemic cells, thus the enzyme will also affect normal cells throughout the body that express *RAF-1*, causing non-specific cell death.

RAS initiates the intracellular signal transduction cascade by binding to the inner surface of the GM-CSF receptor. The binding process requires that a farnesyl group is non-covalently bound to RAS, and this is catalysed by farnesyl-transferase enzymes (Gibbs *et al*, 1994). Emanuel *et al* (2000) demonstrated that farnesyltransferase inhibitors are able to block RAS signalling, abrogating JMML cell growth *in vitro*. The investigators concluded that farnesyltransferase inhibitors could be used for the treatment of JMML patients. However, the farnesyltransferase inhibitors also affected RAS signalling in GM-CSF stimulated normal adult bone marrow cells, raising a major concern about the toxicity of the farnesyltransferase inhibitors.

1.3.3. Immunotherapy:

1.3.3.1. Evidence that JMML is susceptible to immune attack:

Long term survival of JMML patients following allogeneic BMT is closely associated with graft-versus-host disease (GVHD) (Orchard *et al*, 1998; Bunin *et al*, 1999). This finding suggests that donor-derived immune cells have the ability to recognise and eliminate residual leukaemic cells in the host following allogeneic BMT, and is referred to as the graft-versus-leukaemia (GVL) effect (Antin, 1993; Matthes-Martin *et al*, 2000). The GVL effect is well documented in chronic and acute leukaemias (see *1.3.3.2.*). Several groups have now successfully treated JMML patients with donor lymphocyte infusions (DLIs) following allogeneic BMT (Matthes-Martin *et al*, 2000; Worth *et al*, 2002), providing strong evidence for a GVL effect in establishing and maintaining prolonged remission. However, the success of DLIs at inducing a GVL effect for the treatment of relapsed myeloid leukaemias is limited by the morbidity and mortality associated with the accompanying GVHD (Kolb *et al*, 1995).

One JMML patient who relapsed following an allogeneic BMT has been successfully treated with interferon (IFN)-α (Ohta *et al*, 2000). IFN-α is an immunostimulatory cytokine (Boehm *et al*, 1997), however the exact mechanism by which IFN-α induced remission is uncertain. Recently, Pulsipher *et al* (2004) successfully treated a JMML patient that had relapsed after an unrelated allogeneic BMT with DLIs and IFN-α. Whether the patient required DLIs or could have responded solely to IFN-α is unknown. Large-scale studies are needed to investigate the effectiveness of using IFN-α to induce leukaemia-specific immune responses and promote prolonged remission.

Hence, unlike most other paediatric leukaemias, JMML appears to be a disorder susceptible to a GVL effect, and is suitable for immuno-based therapy. The major challenge is to isolate the GVL effect from the unwanted GVHD.

1.3.3.2. GVL effect in chronic and acute leukaemias:

There have been several reports suggestive of a GVL effect in chronic and acute leukaemias. Examining the treatment of chronic myeloid leukaemia (CML) with allogeneic BMT, Marmont and colleagues (1991) noted that the depletion of lymphocytes from the BMT, in an attempt to avoid GVHD, resulted in increased relapse rates. The infusion of donor lymphocyte populations into CML patients, who have relapsed after allogeneic BMT, induces prolonged remission in three quarters of patients

(Kolb *et al*, 1990; Kolb *et al*, 1995). Hence, DLIs following allogeneic BMT are common practice in the treatment of relapsed CML patients.

Acute myeloid leukaemia (AML) patients that relapse after allogeneic BMT are also treated with DLIs. However, DLIs appear to be less successful in the treatment of AML relative to CML. This could be because the rapid progression of AML outstrips the clinical benefit of the DLI, or that AML blasts more actively hinder the presentation of leukaemia-associated antigens to the immune effector cells (Antin, 1993).

1.3.3.3. Use of in vitro cultured DCs to induce leukaemia-specific immune responses:

The induction of a strong anti-tumour immune response requires efficient presentation of tumour antigens to the effector cells of the adaptive immune system (Avigan, 1999). DCs, the most potent antigen presenting cells (APCs), are specialized at initiating primary cellular and humoral immune responses (see Chapter 1, **3.**) (Banchereau and Steinman, 1998). This DC function is attributable to their high level expression of major histocompatibility complex (MHC) class I and class II molecules for antigen presentation, coupled with the additional signals required for activating T cells, namely co-stimulation and cytokine production (Steinman, 1991). Hence, there is great interest in utilizing DCs for the development of immunotherapeutic strategies that specifically target leukaemic cells.

Human DCs can be generated *in vitro* from peripheral blood monocytes and $CD34^+$ progenitors in the presence of GM-CSF and IL-4 (Romani *et al*, 1994; Sallusto and Lanzavecchia, 1994). This raises the intriguing possibility of culturing DCs directly from myeloid leukaemic cells, and thereby generating a leukaemic DC that expresses leukaemia-associated antigens and is specialized at presenting these antigens to effector cells of the adaptive immune system.

Several groups working on CML have utilized *in vitro* culturing techniques to generate leukaemic DCs from CML patients' leukaemic blasts, and shown that these Philadelphia chromosome positive (Ph^+) CML-derived DCs initiate specific anti-leukaemia immune responses *in vitro* (Choudhury *et al*, 1997; Eibl *et al*, 1997; Muller *et al*, 2001). Similarly, there is increasing evidence that the majority of AML blasts can be differentiated into functional DCs that are capable of stimulating leukaemia-specific

T cell responses *in vitro* (Charbonnier *et al*, 1999; Choudhury *et al*, 1999; Harrison *et al*, 2001). Choudhury and colleagues (1997) proposed using leukaemic DCs in an *ex vivo* setting to stimulate and expand autologous cytotoxic T lymphocytes (CTLs) that react specifically against leukaemic cells, and can be adoptively transferred into patients with myeloid leukaemia to eliminate residual disease following autologous BMT. Alternatively, leukaemic DCs could be used as a cellular vaccine *in vivo* (Choudhury *et al*, 1999).

However, several investigators have recently shown that DCs generated *in vitro* from CML blasts have phenotypic and functional deficiencies when compared to DCs differentiated *in vitro* from PBMCs of healthy individuals. Dong *et al* (2003) found that CML-derived DCs have a reduced capacity to capture and process exogenous antigen, as well as impaired migratory ability. Eisendle and colleagues (2003) reported that CML-derived DCs show an abnormal maturation response to bacterial LPS, expressing reduced levels of MHC class I, MHC class II and the co-stimulatory molecules CD80 and CD86, along with diminished production of the immunostimulatory cytokines IL-8 and TNF-α. Furthermore, DCs differentiated from CML patients have been shown to display decreased T cell stimulatory activity when cultured *in vitro* with allogeneic responder T cells (Wang *et al*, 1999). Altogether, these findings raise concerns about the suitability of leukaemia-derived DCs for vaccination, and any phenotypic and functional deficiencies of leukaemia-derived DCs must be overcome before they can be used for vaccination. Eisendle *et al* (2003) demonstrated that activation of CML-derived DCs with a cytokine/prostaglandin E_2 mix, including TNF-α, was sufficient to abrogate the DC phenoptyic abnormalities observed using LPS as the maturation signal.

1.4. DC-based immunotherapeutic strategy for JMML:

JMML cells are of monocytic lineage, and potentially can be differentiated into DCs that express any JMML-associated antigens in conjunction with the dendritic phenotype required for initiating an anti-leukaemia immune response. However, the ability to generate malignant-derived DCs from JMML patients and their ability to prime specific anti-JMML immune responses have not yet been reported.

We propose using *ex vivo* generated JMML-derived DCs to stimulate and expand allogeneic (BMT donor-derived) leukaemia-specific CTLs that can be injected into the patient following allogeneic BMT to eliminate any residual disease (Figure 2). This

immunotherapeutic strategy would potentially enable clinicians to harness the powerful GVL effect in isolation from GVHD.

In this study, we have shown for the first time that functional DCs can be generated *in vitro* from the peripheral blood of JMML patients. Further experiments revealed that the DCs expressed the malignant phenotype and were potent stimulators of allogeneic T lymphocytes. These preliminary results support the use of *ex vivo*-generated leukaemic DCs to enroll the adaptive immune system in a novel immunotherapy for JMML.

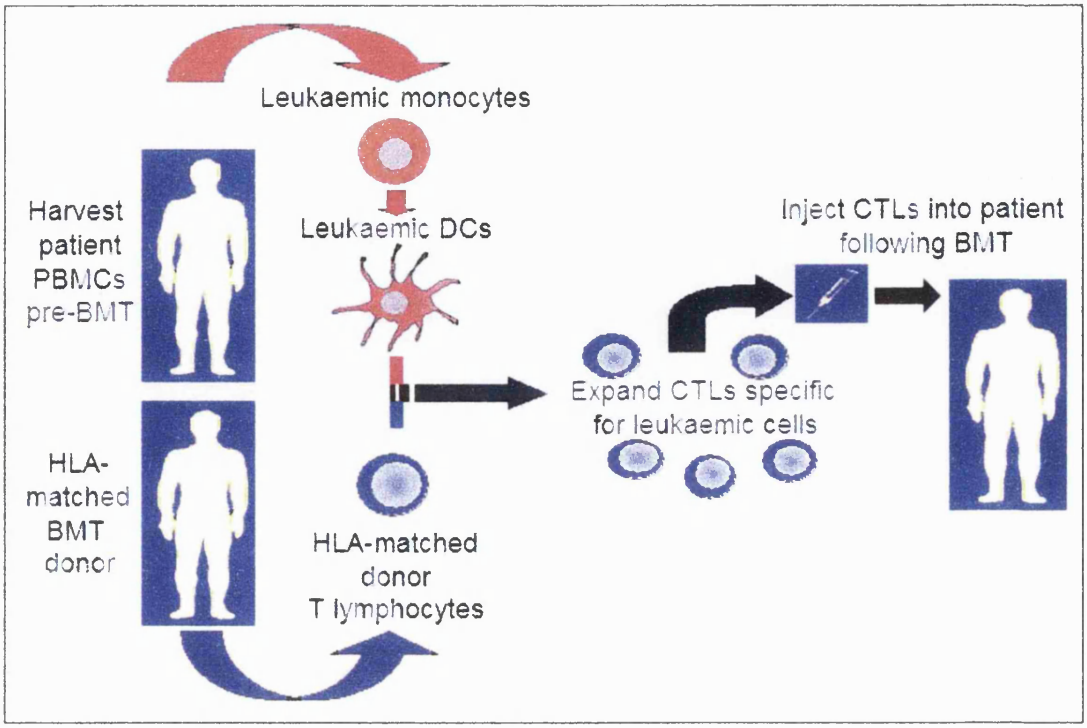

Figure 2. Proposed DC-based therapy for JMML. PBMCs are harvested from the patient prior to allogeneic BMT from a human leukocyte antigen (HLA)-matched donor. The PBMCs are used as a source of leukaemic cells, which are differentiated *ex vivo* into activated functional DCs. These 'leukaemic' DCs are then used to stimulate and expand allogeneic (BMT donor-derived) CTLs that have cytotoxic activity against JMML cells. Finally, the expanded CTLs are injected into the patient following allogeneic BMT to eliminate any residual disease.

2. Methods and Materials

2.1. Patient samples:

Patients were identified as they presented at Great Ormond Street Hospital with JMML, and informed consent was gained. Leukaemia samples were obtained from peripheral blood prior to the administration of chemotherapy. In accordance with our institution's policy, all patients were treated with chemotherapy followed by allogeneic BMT. Peripheral blood was also taken following allogeneic BMT engraftment and used as a source of HLA-matched BMT donor-derived lymphocytes. Patient details are given in Table 1.

2.2. Isolation of PBMCs and generation of DCs:

Mononuclear cells were isolated from heparinized peripheral blood of JMML patients and normal donors by centrifugation over a Ficoll-Hypaque (Lymphoprep; Nycomed Pharma, Norway) density gradient. The mononuclear cell fraction was washed twice in serum free Roswell Park Memorial Institute (RPMI) 1640 media (Gibco, UK), and resuspended in complete media (RPMI 1640 media supplemented with 10% heat-inactivated fetal calf serum (FCS), 2mM glutamine, 100IU/ml penicillin and 100μg/ml streptomycin; all from Gibco). PBMCs were cultured immediately or cryopreserved in complete media plus 10% dimethyl sulphoxide (DMSO; Sigma, UK). Cryopreserved PBMCs were thawed and washed once in complete media prior to culure.

Plastic-adherent monocytes were selected from fresh and cryopreserved PBMCs by plating 4×10^6 cells/ml in 6-well plates (TPP, Switzerland) for 3 hours at 37°C in 5% CO_2 atmosphere. The non-adherent PBMCs were washed off by gentle rinsing, cryopreserved, and later used as a source of T lymphocytes (see **2.6.**). The remaining adherent cells were cultured for 6 days in complete media with 100ng/ml recombinant human (rhu) GM-CSF (Leucomax, Novartis, UK) and 25ng/ml rhuIL-4 (PeproTech, UK). DC maturation was subsequently induced by the addition of 100ng/ml LPS (Sigma) to the cell cultures for 24 hours. If required, DC cultures were replenished with fresh media and cytokines on day 4. On day 6 and 7 of culture, cells were harvested, washed with phosphate buffered saline (PBS; Gibco), and stained for fluorescence activated cell sorter (FACS) analysis, or used in various assays. In some experiments, DCs were purified by depleting $CD3^+$ and $CD19^+$ cells using dynabeads (Dynal,

Patient identification	Sex	Age at presentation	Cytogenetic abnormality
JMML-1	Female	5 months	None
JMML-2	Female	6 months	Monosomy 7
JMML-3	Male	2 years	Monosomy 7

Table 1. Clinical and laboratory data for the 3 JMML patients in the current study.

Norway), following the manufacturer's protocol. The morphology of developing DCs was monitored by phase-contrast microscopy. At the start and end of culture, cell density in each culture was enumerated using a haemocytometer.

LPS contamination was minimised to avoid unwanted activation of immature DC cultures. All culture media and tissue culture reagents were endotoxin-free, and glassware was baked at 180°C for 4 hours to remove LPS.

2.3. Immunophenotypic analysis of DCs by flow cytometry:

2.3.1. FACS staining methodology:

Approximately 5×10^5 cells were resuspended in 30µl of PBS and incubated with a combination of fluorochrome-conjugated monoclonal antibodies, in the dark at 4°C for 30 minutes. To wash off unbound antibody, the samples were centrifuged at 180g for 4 minutes at 4°C, the supernatant was discarded, and the cells were resuspended in cold PBS. This washing step was repeated twice more. The cells were then fixed in 300µl of PBS containing 1% paraformaldehyde, and stored at 4°C in the dark until analysis using a Beckman Coulter Epics FACS machine and Expo 32 software (Beckman Coulter, USA).

2.3.2. Antibodies used to immunophenotype in vitro cultured DCs:

The *in vitro* differentiated DC samples were incubated with optimal concentrations of fluoroscein isothiocyanate (FITC)-, and phycoerythrin (PE)-conjugated mouse monoclonal antibodies specific for CD11c, CD14, CD25, CD45, CD83, CD86, Lineage cocktail 1 (Lin1; cocktail of CD3, CD14, CD16, CD19, CD20, CD56), and HLA-DR (all from Becton Dickinson, USA). Each patient sample was also stained with fluorochrome-conjugated isotype-matched control mouse monoclonal antibodies (Becton Dickinson) to check that the antibodies were not binding non-specifically to the cells.

2.3.3. 3-colour assay to determine peripheral blood DC numbers:

The 3-colour assay was performed on freshly isolated PBMC samples, using the following antibody staining combinations:

- To identify the $Lin1^{-/low}HLA\text{-}DR^{+}CD11c^{+}$ DC subset: Lin1-FITC, anti-HLA-DR peridinin chlorophyll protein (PerCP), and CD11c-PE mouse monoclonal antibodies.

- To identify the Lin1$^{-/low}$HLA-DR^{+}CD123^{+} DC subset: Lin1-FITC, anti-HLA-DR-PerCP, and CD123-PE mouse monoclonal antibodies.

The isotype control antibodies used were mouse IgG_1-FITC, mouse IgG_1-PE, and mouse IgG_{2A}-PE. All the test antibodies and isotype control antibodies were purchased from Becton Dickinson.

Complex FACS analysis was required to determine the number of Lin1$^{-/low}$HLA-DR^{+}CD11c^{+} and Lin1$^{-/low}$HLA-DR^{+}CD123^{+} DCs present in patient and normal control PBMC samples. Initially, cell debris was excluded based on forward scatter (FSC) and side scatter (SSC; gate A). The viable cells were analysed in a HLA-DR versus Lin1 histograms. The Lin1^{Lo} cells were gated (gate B) and further analysed in HLA-DR versus CD11c and HLA-DR versus CD123 histograms.

2.4. Fluorescence *in situ* hybridisation (FISH) analysis:

FISH analysis was performed to confirm the leukaemic origin of DCs generated in culture from PBMCs of patients with leukaemias that exhibited monosomy 7 (JMML-2 and JMML-3). 1×10^6 CD86^{+} mature DCs differentiated *in vitro* from normal donor or JMML PBMCs, as well as CD14^{+} JMML PBMCs, were purified by flow sorting and fixed in 3:1 methanol to acetic acid (BDH Laboratories, UK). Chromosome 7 was identified in interphase nuclei using the following probes: an α-satellite probe for chromosome 7 that displays a yellow hybridisation signal, a Texas red-labelled α-satellite probe specific for the long arm of chromosome 7 (7q31), and a fluorescein-labelled D5386 probe specific for the centromeric region of chromosome 7 (all from Abbott Laboratories, UK). A Texas red-labelled α-satellite probe specific for chromosome X (Abbott Laboratories) was used as a control for JMML-2 samples. FISH was performed in conjunction with H. Kempski, and the probes were used according to the manufacturer's recommendations. To quantify the percentage of cells carrying monosomy 7, at least 100 interphase nuclei were counted and scored in each sample.

2.5. IL-12 enzyme-linked immunosorbent assay (ELISA):

DCs were generated *in vitro* from the adherent PBMCs of normal donors and JMML patients (JMML-2 and JMML-3), as described in **2.2.**. On day 6 of culture, the non-adherent immature DCs were harvested and immunomagnetically purified using dynabeads to remove CD3^{+} and CD19^{+} cells. Purified immature DCs were plated out at

1.5×10^5 cells/well of a 96-well plate, and cultured for 24 hours in 200µl of complete media containing GM-CSF and IL-4, with or without the addition of 100ng/ml LPS. The plates were then centrifuged at 180g for 5 minutes and the supernatants collected. The amount of IL-12 released by the cells into the culture media was determined using a commercial IL-12p70 assay (OptEIA human IL-12 p70 kit, Pharmingen, USA), according to the manufacturer's instructions. Standards were run on each ELISA, allowing the production of a standard curve and the extrapolation of the IL-12 concentration in each sample. Each DC sample was treated with or without LPS in triplicate wells, allowing the mean and standard deviation (S.D.) of the IL-12 concentration values to be calculated, and student *t*-tests to be performed.

2.6. IFN-γ enzyme-linked immunospot (ELISpot) assay:

The ability of mature DCs, cultured *in vitro* from normal donor and JMML-2 PBMCs, to activate allogeneic T lymphocytes was examined in a MLR using an IFN-γ ELISpot assay. The LPS activated DC cultures were harvested, the T and B lymphocytes were immunodepleted using dynabeads, and the immunopurified mature DCs were used as stimulator cells. Non-adherent PBMCs were immunodepleted with anti-CD14 and anti-CD19 dynabeads and used as a source of responder T lymphocytes. 2×10^3 immunopurified mature DC stimulators were cultured with 2×10^4 autologous or allogeneic (third party) T lymphocytes in 96-well plates for 4 days at 37°C. In negative control wells, stimulator cells and responder cells were cultured alone. After 4 days in culture, the cells were washed, resuspended in fresh complete media, and transferred to ELISpot 96-well plates (Millipore, USA) pre-coated with purified monoclonal antibody against human IFN-γ (1-D1K; Mabtech, Sweden). The cells were incubated in the antibody coated ELISpot plates for a further 24 hours at 37°C. The cells were then removed by washing, and a biotinylated monoclonal antibody specific for human IFN-γ (7-B6-1-biotin; Mabtech) was added to the wells. After washing, Extravidin Alkaline Phosphatase Conjugate (Sigma) was added, and finally the plates were developed by the addition of Alkaline Phosphatase Substrate (Bio-Rad, UK). Dark spots occurred at the site of individual IFN-γ secreting T cells, and acted as a measure of T cell activation. The number of spots was counted on a plate reader (BioReader 3000; BioSys, Germany) using BioSys analysis software. Each stimulator cell-responder cell combination was performed in triplicate wells.

2.7. Generation of allogeneic CTLs specific for JMML cells:

2.7.1. Expansion of allogeneic (BMT donor-derived) CTLs:

Non-adherent PBMCs collected from JMML-1 post BMT engraftment were used as a source of allogeneic (BMT donor-derived) T lymphocytes. Mature leukaemic DCs, generated *in vitro* from preBMT JMML-1 PBMCs, were γ-irradiated (30 Gy) and used as stimulator cells. 5×10^6 allogeneic T lymphocytes were plated per well of a 12-well plate, and stimulated with 2.5×10^6 γ-irradiated mature leukaemic DCs in 1.5ml of complete media. The cultures were re-stimulated every 7 days with a fresh aliquot of γ-irradiated leukaemic DCs, and supplemented with 20U/ml of rhuIL-2 (PeproTech) 24 and 96 hours after stimulation. Following three rounds of leukaemic DC stimulation, the T lymphocytes were immunopurified using $CD3^+$ magnetic beads and assayed for anti-leukaemic activity.

2.7.2. Cytotoxicity assay:

The cytotoxicity of the expanded CTLs against leukaemic cells was analysed using an *in vitro* non-radioactive cytotoxicity assay (Cytotox 96; Promega, USA). Various concentrations of the CTL effector cells were co-cultured with constant amounts of target cells (1×10^4 cells/well of a 96-well plate) in phenol red-free RPMI (Gibco) plus 3% FCS for four hours at 37°C. The different target cell populations used were JMML-1 leukaemic preBMT adherent PBMCs, JMML-1 non-leukaemic preBMT $CD3^+$ T cells, and HLA-mismatched normal donor PBMCs. Unfortunately, the low starting cell numbers limited the range of effector to target ratios used. We intended to culture primary fibroblasts, from a JMML-1 skin biopsy, to use as an autologous non-leukaemic target cell population. However, a skin biopsy sample was not available.

After incubating the CTLs with the various target cell populations for 4 hours, the plates were centrifuged at 180g for 5 minutes and the supernatent harvested. Lactate dehydrogenase (LDH) released from lysed cells into the supernatent was measured following the manufacturer's instructions, and used as a measure of target cell killing. To determine the maximum LDH release, triton X-100 detergent (Sigma) was added to wells containing 1×10^4 target cells alone. The LDH spontaneously released by target cells and effector cells cultured alone was also measured. Each sample was performed in triplicate wells. The CTL-mediated killing was calculated from the LDH release values according to the following equation: % cytotoxicity = (experimental – effector spontaneous – target spontaneous)/(target maximum-target spontaneous)) ×100.

3. Results

3.1. *In vitro* generation of DCs from PBMCs of JMML patients:

In this study, we initially assessed whether PBMCs from JMML patients could be cultured into immature DCs and subsequently activated with LPS. After 6 days of culture with GM-CSF and IL-4, cells from all three JMML patients expressed high levels of the myeloid marker CD11c, intermediate levels of the MHC class II molecule HLA-DR and the co-stimulatory molecule CD86 (B7-2), and undetectable levels of the dendritic activation marker CD83 and the monocytic marker CD14 (Figures 3,4, and 5). This represents a typical immature monocyte-derived DC (MoDC) surface phenotype (Banchereau and Steinman, 1998), comparable to that of immature MoDCs cultured from normal donor PBMCs under identical conditions. By day 6 of culture, the cells generated from both normal donors and JMML patients formed non-adherent clusters and possessed short cytoplasmic projections, characteristic of immature DC morphology (Banchereau and Steinman, 1998; Fujii *et al*, 1999).

We next attempted to activate the *in vitro* cultured immature DCs using LPS. Immature DC populations derived from JMML-1, JMML-2, and normal PBMCs up-regulated HLA-DR, CD86, and CD83 expression upon exposure to LPS for 24 hours, acquiring a mature dendritic phenotype (Figures 3 and 4). However, following incubation with LPS, DCs generated from JMML-3 PBMCs expressed elevated levels of CD11c and CD86, but failed to up-regulate HLA-DR and CD83 from the levels observed in the immature DC state (Figure 5). This immunophenotype suggests that JMML-3-derived DCs were sub-optimally activated by LPS.

Typically, 10ml of peripheral blood from a JMML patient yielded approximately 5×10^7 adherent mononuclear cells. The final yield of viable $CD86^+$ DCs was between 25% and 50% of the starting adherent PBMC population.

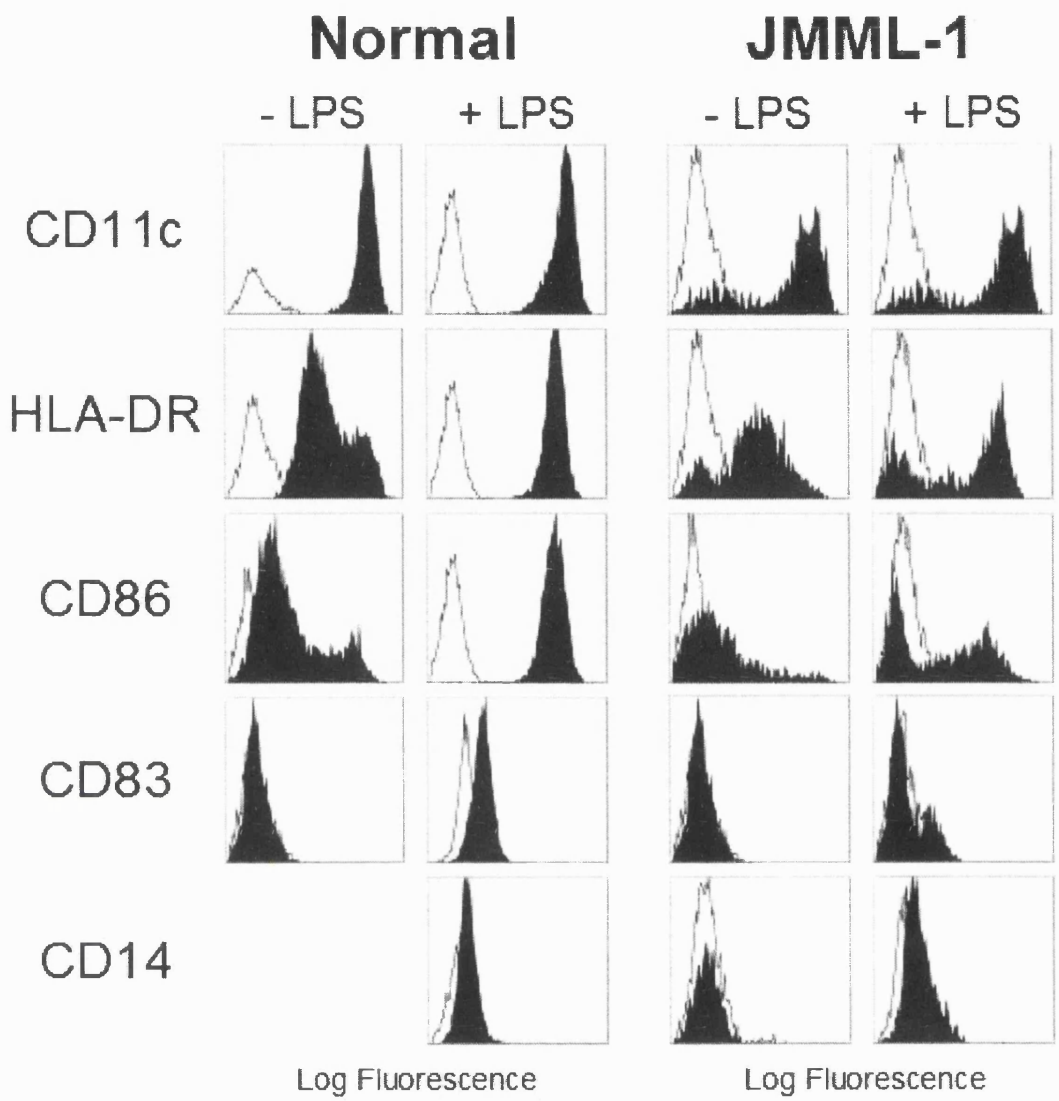

Figure 3. Immunophenotype of DCs cultured *in vitro* from normal donor and JMML-1 PBMCs. Plastic adherent PBMCs were differentiated into immature DCs by culturing the cells in the presence of GM-CSF and IL-4 for 6 days. Immature DCs were harvested on day 6 (labelled -LPS), while mature DCs were collected on day 7 following a subsequent 24 hour incubation with LPS (labelled +LPS). The harvested cells were stained with a panel of immunofluorescent antibodies and analysed by flow cytometry. Large, granular cells were gated and are shown in the histogram plots. The black filled histograms represent staining with the indicated monoclonal antibody, while the unfilled white histograms indicate staining with an appropriate isotype control antibody. The ragged shape of the histograms is a result of only analysing 5,000 cells, rather than the typical 10,000. There were insufficient normal control cells to analyse CD14 expression on the immature DC population.

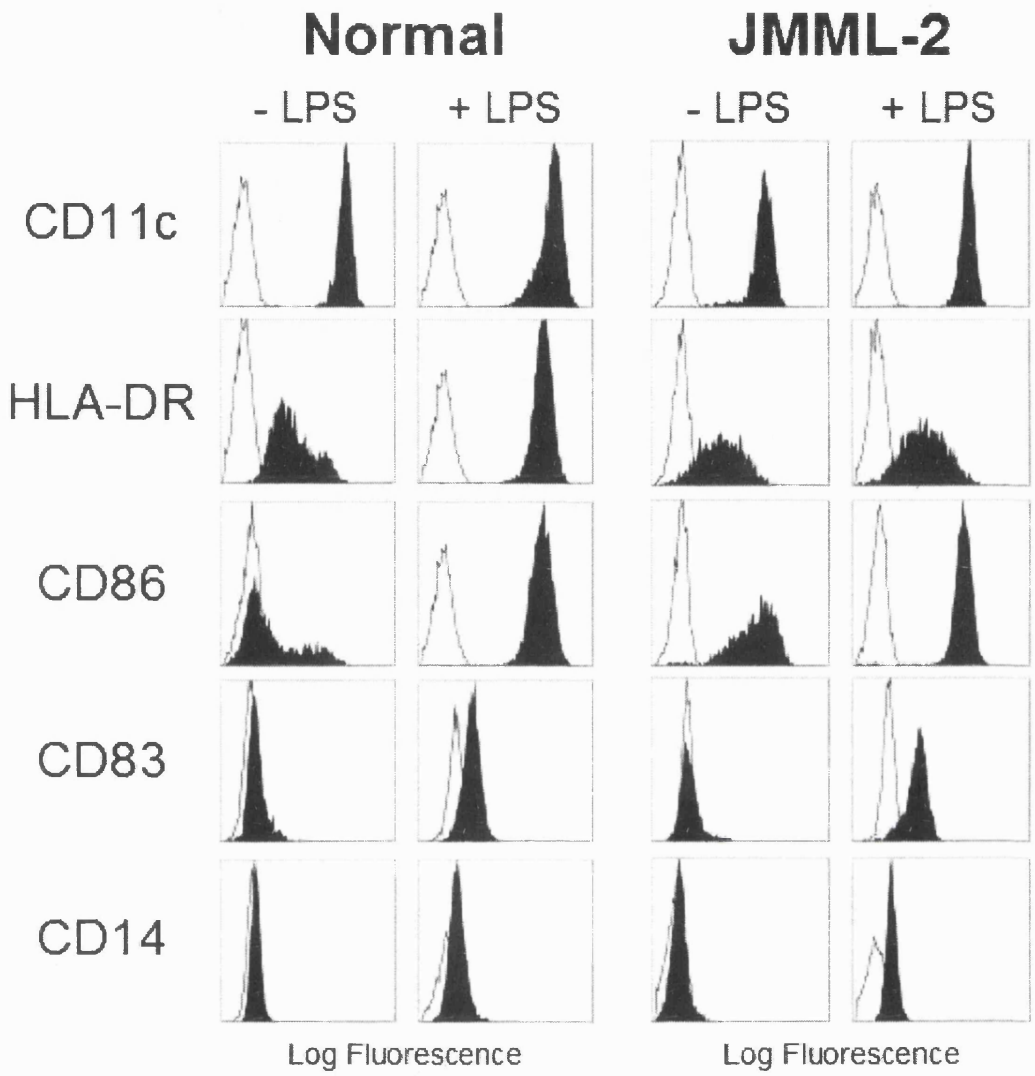

Figure 4. Immunophenotype of DCs cultured *in vitro* from normal donor and JMML-2 PBMCs. See the legend of Figure 3 for detailed methodology on the *in vitro* generation and FACS analysis of DCs.

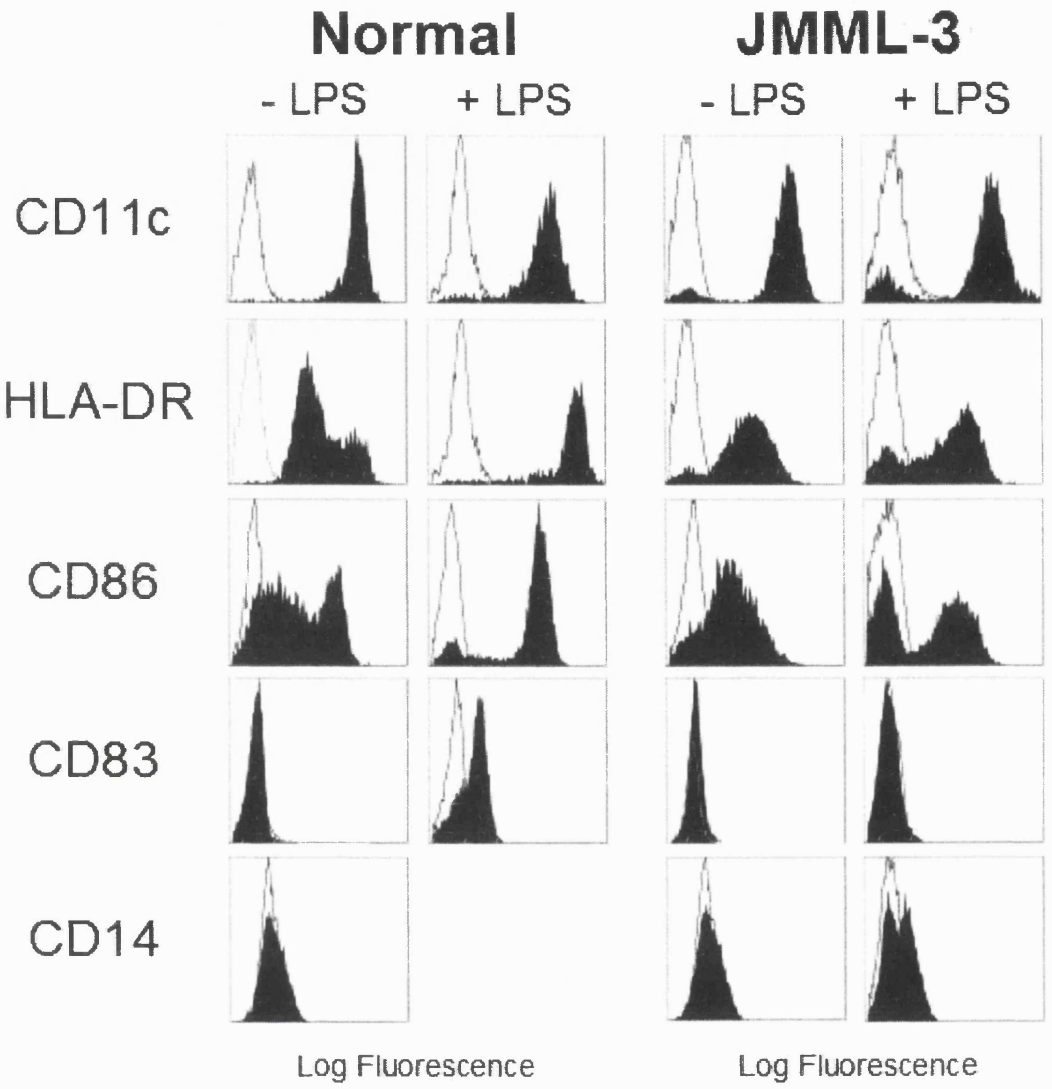

Figure 5. Immunophenotype of DCs cultured *in vitro* from normal donor and JMML-3 PBMCs. See the legend of Figure 3 for detailed methodology on the *in vitro* generation and FACS analysis of DCs. There were insufficient normal control cells to analyse CD14 expression on the mature DC population. The results suggest that the DCs cultured from normal PBMCs were successfully activated by LPS, whereas JMML-3 DCs were sub-optimally activated by LPS, under identical conditions.

3.2. Leukaemic origin of DCs cultured *in vitro* from JMML PBMCs:

The leukaemic cells in two of the patients (JMML-2 and JMML-3) exhibited monosomy 7, a commonly observed chromosomal abnormality in this disease (Hasle *et al*, 1999). We were able to use this as a marker of malignant origin. Interphase FISH analysis revealed that the vast majority of $CD86^+$-purified mature DCs generated *in vitro* from the PBMCs of these patients displayed monosomy 7 (92% of JMML-2 DCs and 98% of JMML-3 DCs; Figures 6 and 7). In contrast, mature DCs cultured *in vitro* from normal donor PBMCs possessed two copies of chromosome 7 (Figure 7). $CD14^+$ cells purified from the peripheral blood of JMML-3 were used as a positive control, and 95% these cells carried only 1 copy of chromosome 7 (Figure 7). These findings confirm that virtually all the DCs cultured *in vitro* from these patients were of leukaemic origin.

3.3. Cytokine production of *in vitro* cultured DCs:

To examine further the ability of *in vitro* differentiated DCs to provide the co-stimulatory signal required to activate naïve T cells, we measured IL-12 production by ELISA. Secretion of IL-12 by mature DCs is required for T cell activation, and is associated with a T helper1 (Th1) response (Banchereau *et al*, 2000). Consistent with published data, immature DCs generated *in vitro* from normal donor, JMML-2, and JMML-3 PBMCs secreted undetectable levels of IL-12 into the supernatant ($\leq$ 7.5 pg/150,000 cells; Figure 8). Following LPS activation, the DCs cultured *in vitro* from normal donor and JMML-2 PBMCs produced large amounts of IL-12 (210pg/150,000 cells and 320pg/150,000 cells, respectively; Figure 8). In contrast, the incubation of JMML-3-derived immature DCs with LPS for 24 hours resulted in the secretion of minimal amounts of IL-12 (15pg/150,000 cells), significantly less than observed in normal mature MoDCs cultures with LPS ($p<0.05$, student *t*-test; Figure 8).

3.4. Ability of leukaemic DCs to stimulate allogeneic T lymphocytes:

The immunostimulatory properties of DCs cultured *in vitro* from normal donor and JMML-2 PBMCs were tested in a MLR using an IFN-γ ELISpot assay. The mature DCs were used as stimulator cells, and cultured with autologous or allogeneic (MHC-mismatched) non-adherent PBMCs responder cell populations at a ratio of 1:10. Figure 9 shows that JMML-2-derived DCs were able to stimulate allogeneic T cells slightly more efficiently than normal MoDCs, as measured by the amount of IFN-γ secreted by

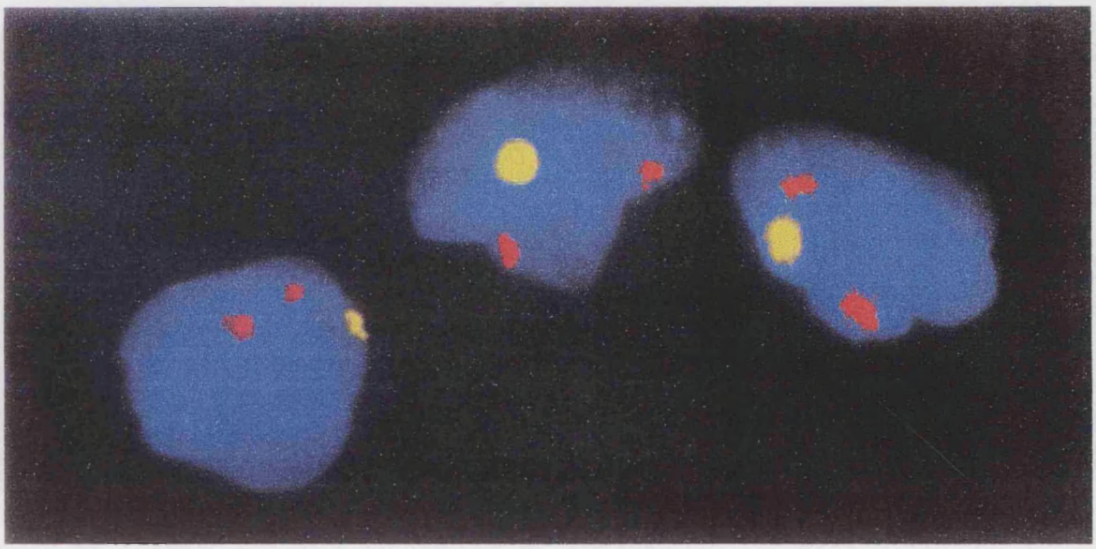

Figure 6. Interphase FISH showing monosomy 7 in the nuclei of DCs cultured *in vitro* from JMML-2 PBMCs. The yellow α-satellite probe is specific for chromosome 7, and the red α-satellite probe is specific for chromosome X. Nuclear DNA appears blue as a result of DAPI staining. 92% of the $CD86^{+}$-purified mature DCs cultured from JMML-2 exhibited monosomy 7. The control probe revealed two X chromosomes in every cell, and acts as a control for detecting both probe signals in this female patient. More than 200 interphase nuclei were counted and scored for monosomy 7.

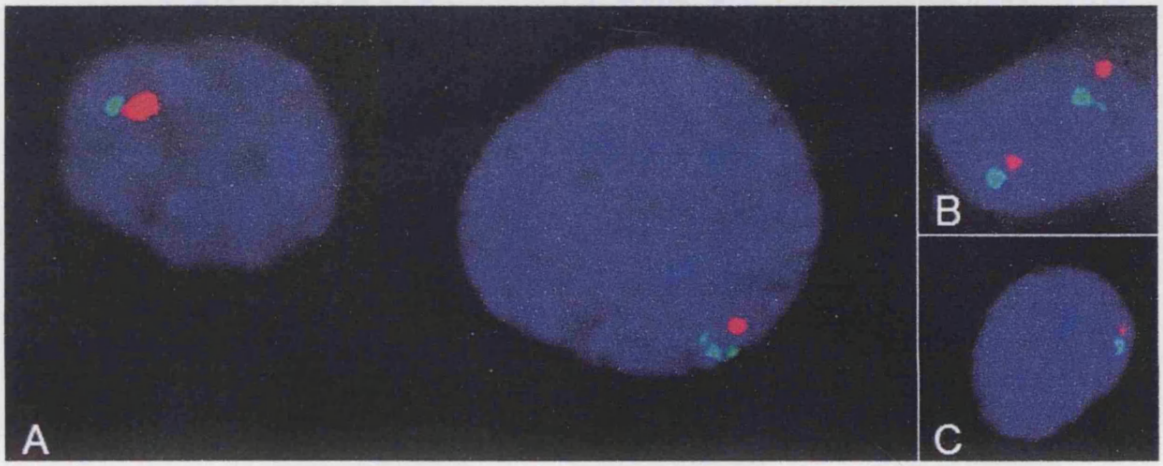

Figure 7. Interphase FISH showing monosomy 7 in the nuclei of DCs cultured *in vitro* from JMML-3 PBMCs. The red α-satellite probe is specific for the long arm of chromosome 7 (7q31), and the green D5386 probe is specific for the centromeric region of chromosome 7. Nuclear DNA appears blue as a result of DAPI staining. **A** Purified $CD86^+$ DCs cultured *in vitro* from JMML-3 PBMCs. 98% of the 100 $CD86^+$ DC nuclei counted displayed monosomy 7. **B** $CD86^+$ DCs cultured *in vitro* from a normal control. 100 nuclei were scored, and two red and two green signals were detected in every nucleus, indicating that the nuclei carry two copies of chromosome 7. **C** Purified $CD14^+$ cells from JMML-3 PBMCs. These monocytic $CD14^+$ cells are known to carry monosomy 7. 95% of the 100 nuclei counted exhibited monsomy 7.

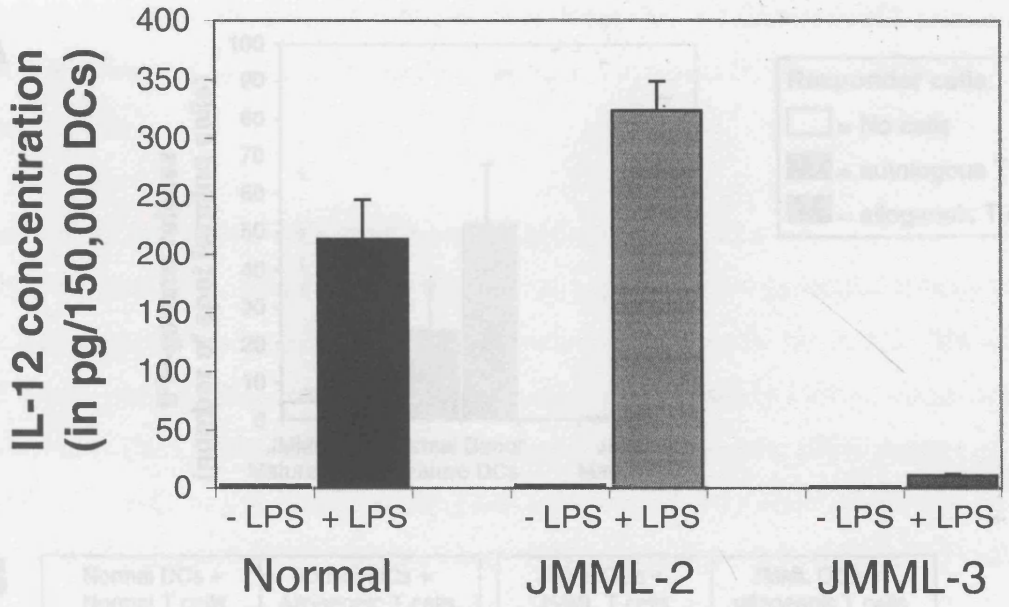

Figure 8. IL-12 secretion profile of DCs cultured *in vitro* from normal donor, JMML-2, and JMML-3 PBMCs. PBMCs from normal donors and JMML patients were cultured in the presence of GM-CSF and IL-4 for 6 days. 150,000 purified immature DCs were plated out into 96-well plates. Half the cells were cultured in the presence of LPS for 24 hours to activate the immature DCs, while the remaining cells were cultured for 24 hours in the absence of LPS in order to retain an immature DC phenotype. After the 24 hour incubation, cell supernatents were collected and tested for their IL-12p70 content by ELISA. Each sample was performed in triplicate, and the error bars depict S.D.. LPS activated JMML-3 DCs secreted very small amounts of IL-12, significantly less than observed in LPS activated normal mature MoDCs ($p<0.05$, student *t*-test).

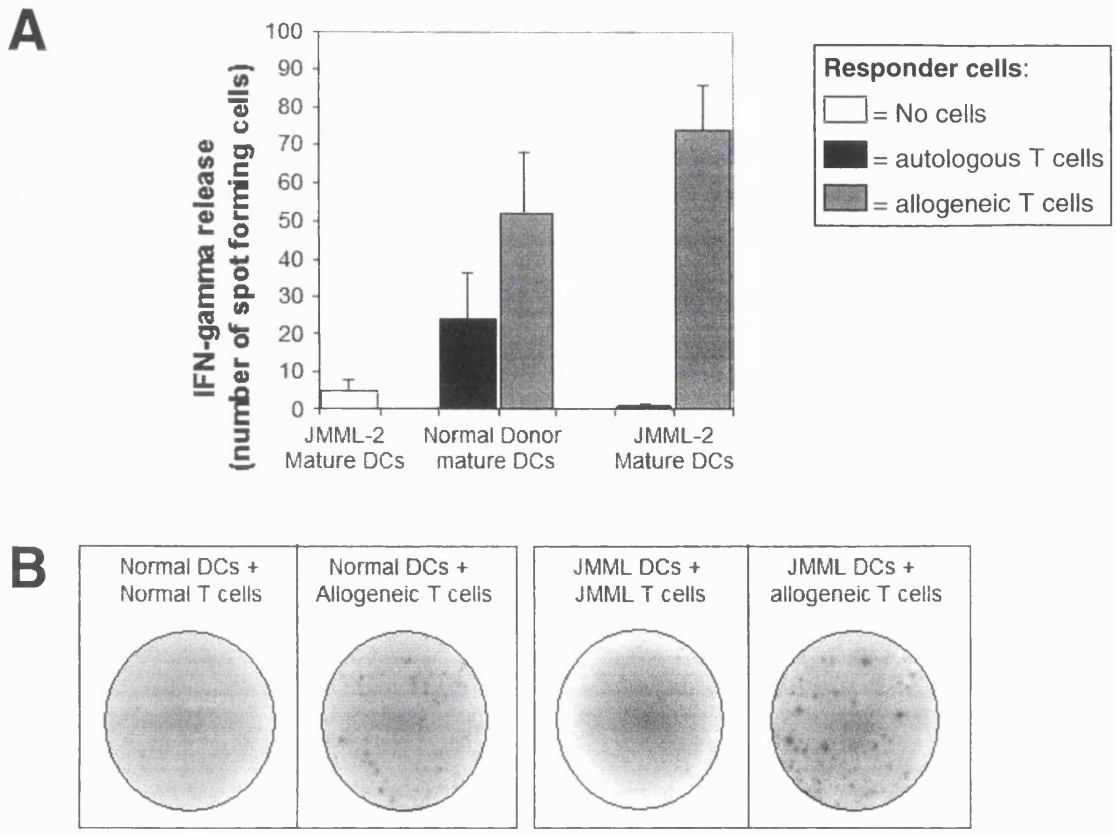

Figure 9. IFN-γ secretion, as a marker of T cell activation, following stimulation with *in vitro* cultured mature DCs. A Graph depicting the IFN-γ ELISpot results from the MLR. The stimulator cells were DCs differentiated *in vitro* from normal donor and JMML-2 PBMCs (indicated on x-axis). Responder cells were: (□) no responder cells; (■) autologous T lymphocytes; (▩) allogeneic (third party) lymphocytes. A total of 2×10^3 $CD86^+$-purified mature DCs were cultured with 2×10^4 responder cells for 4 days, and IFN-γ secretion was subsequently measured using an ELISpot assay. Results represent the mean ± S.D. of triplicate cultures. **B** Pictures of representative ELISpot wells, with the stimulator and effector cell populations indicated.

activated T cells. However, culturing normal donor-derived DCs and JMML-2-derived DCs with autologous T cells caused moderate and minimal IFN-γ secretion, respectively.

3.5. Use of leukaemic DCs to expand JMML-specific CTLs:

We next attempted, with JMML-1 samples, to use the *in vitro* generated leukaemic DCs as stimulator cells to expand allogeneic T lymphocytes specific for JMML. The source of T cells was PBMCs obtained from the patient approximately 1 month following allogeneic BMT. DNA chimerism studies at this stage showed a 100% donor engraftment. Owing to limited starting cell numbers, after 3 rounds of stimulation using irradiated leukaemic DCs in the presence of IL-2, there were only sufficient T cells to perform a basic cytotoxicity assay. This preliminary result shows that the CTLs lysed the leukaemic JMML cells with some degree of specificity (Figure 10). Even at the very low effector:target ratio of 1:1, the CTLs were able to lyse more than 15% of the leukaemic targets. The CTLs lysed the non-leukaemic $CD3^+$ T cells from the JMML patient to a slightly lesser extent, and there was minimal CTL-directed lysis of allogeneic PBMCs from a MHC-mismatched normal donor. However, a student *t*-test revealed that the CTLs did not lyse significantly more JMML-1 leukaemic targets than JMML-1 non-leukaemic targets at the low effector:target ratio of 1:1 ($p=0.09$). Unfortunately, the cytotoxicity assay was associated with high spontaneous LDH release by the effector and target cell populations. This high background level of LDH masked any potential CTL-directed lysis in numerous samples, especially at higher effector:target ratios.

3.6. The number of naturally occurring DCs in the peripheral blood of JMML patients:

3-colour flow cytometry was performed on normal donor and JMML-2 PBMCs to determine whether JMML patients possess a normal number of circulating DCs in their peripheral blood. We were able to identify two main subsets of DCs, identified by their $Lin1^{-/low}HLA\text{-}DR^+CD11c^+$ and $Lin1^{-/low}HLA\text{-}DR^+CD123^+$ expression patterns. The PBMCs obtained from JMML-2 contained a larger number of both $Lin1^{-/low}HLA\text{-}DR^+CD11c^+$ and $Lin1^{-/low}HLA\text{-}DR^+CD123^+$ cells than PBMCs collected from a normal donor (4.1% versus 0.5%, and 1.4% versus 0.6% total PBMC population, respectively; Figure 11).

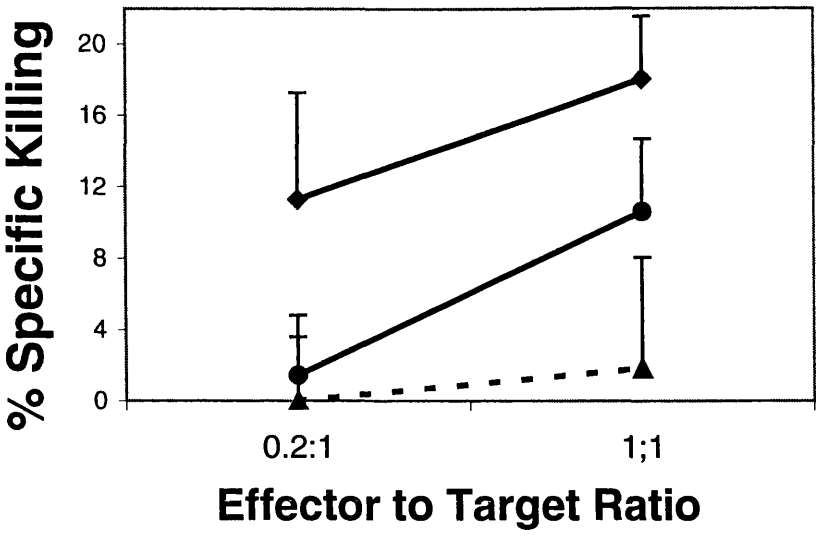

Figure 10. Cytotoxicity of T cells (derived from JMML-1 BMT donor PBMCs post engraftment) stimulated with JMML-1-derived leukaemic DCs. The target cell populations were: (◆) JMML-1 leukaemic preBMT adherent PBMCs; (●) JMML-1 non-leukaemic preBMT $CD3^+$ T cells; (▲) normal donor PBMCs. A total of 1×10^4 target cells were plated with effector cells, at effector to target ratios of 0.2:1 and 1:1. After a 4 hour incubation, LDH enzyme release was calculated and used as a measure of target cell killing. The mean values are plotted and the error bars are S.D. of triplicate LDH release cultures.

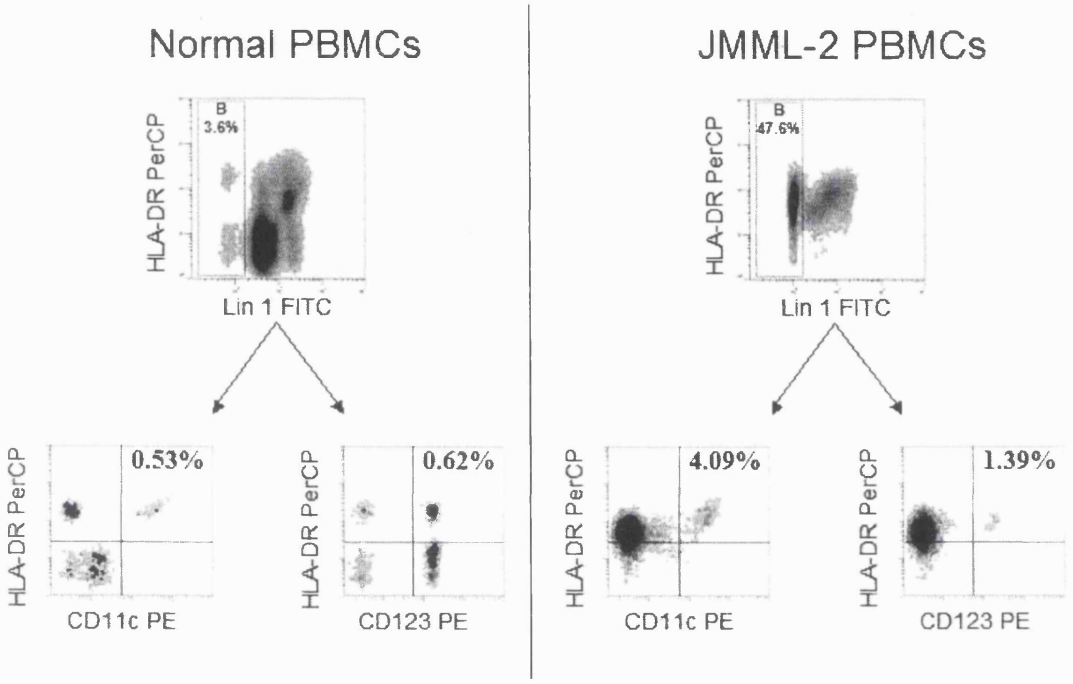

Figure 11. The number of DCs found in normal donor and JMML-2 peripheral blood. Freshly isolated PBMCs were labelled with the appropriate combination of fluorescent monoclonal antibodies, and analysed by flow cytometry. The viable cells are depicted in the HLA-DR versus Lin1 histograms. The $Lin1^{Lo}$ cells were gated (in gate B) and are further analysed in the CD11c and CD123 histograms. It is worth noting that there are significantly more $Lin1^{Lo}HLA\text{-}DR^{+}CD11c^{-}CD123^{-}$ cells in JMML-2 PBMCs than in normal donor PBMCs. It is possible that these cells are monocytes, however monocytes are $Lin1^{+}$, so should be excluded from gate B. Further examining the FSC and SSC of these $HLA\text{-}DR^{+}Lin1^{Lo}$ $CD11c^{-}CD123^{-}$ cells shows that they are the size of monocytes and lymphocytes.

4. Discussion

4.1. *In vitro* differentiation of leukaemic DCs from JMML patient PBMCs:

DCs are professional APCs that are uniquely capable of initiating primary immune responses from naïve T lymphocytes (Cella *et al*, 1997). We have attempted to differentiate JMML cells into immunostimulatory DCs that co-express leukaemia-associated antigens along with the co-stimulatory signals required to initiate JMML-specific immune responses.

4.1.1. Immunophenotype of DCs generated in vitro from JMML patient PBMCs:

In this study we have successfully generated cells with phenotypic and morphological characteristics of immature DCs from adherent PBMCs of three JMML patients (Figures 3, 4, and 5). Immature DCs are specialized at capturing and processing antigens. However, optimal presentation of antigens to T lymphocytes requires that the DCs are in a mature state (Banchereau and Steinman, 1998). Therefore, we next attempted to activate the immature DCs with LPS.

Flow cytometric analysis revealed that LPS successfully activated the immature DCs derived from two of the patients (JMML-1 and JMML-2), and these mature DCs expressed the necessary cell surface molecules for efficient antigen presentation and co-stimulation. T cells recognise antigens as peptide epitopes presented on the cell surface in the peptide-binding groove of MHC molecules (Germain, 1995). Expression of MHC class I and class II molecules on the surface of APCs are required for the presentation of antigenic peptides to $CD8^+$ and $CD4^+$ T lymphocytes, respectively. All nucleated cells express MHC class I antigens (Janeway *et al*, 1999), and flow cytometric analysis demonstrated that the LPS-activated DCs generated from JMML-1 and JMML-2 PBMCs expressed high levels of the MHC class II molecule HLA-DR on their surface (Figures 3 and 4). The activation of naïve T cells also requires the presence of a co-stimulatory signal (see Chapter 1, Figure 1; Harding *et al*, 1992). High level expression of the co-stimulatory antigen CD86, as was detected on the surface of LPS-activated JMML DCs, is able to provide this co-stimulatory signal (referred to as 'signal 2' of T cell activation) (Avigan, 1999). Zhou and Tedder (1995) identified CD83 as a specific antigenic marker of the activated MoDC phenotype, and we found that CD83 was expressed on the surface of LPS-activated DCs differentiated from normal donor, JMML-1, and JMML-2 PBMCs.

4.1.2. Three signal model of CD8$^+$ T cell activation:

Some investigators postulate that in addition to expressing MHC class I and co-stimulatory molecules, APCs need to secrete the immunostimulatory cytokine IL-12 in order to activate naïve CD8$^+$ T cells (Schmidt and Mescher, 2002). This is often referred to as the '3 signal model' of T cell activation. Immature MoDCs do not secrete IL-12 and this reflects their primary function, which is capturing and processing antigens. In contrast, the major role of mature DCs is to present captured antigens to the immune effector cells. Therefore, mature DCs secrete IL-12 to aid the activation of naïve CD8$^+$ T cells. In agreement with published findings, we found that LPS-activated DCs cultured from both normal donor and JMML-2 PBMCs secreted large amounts of IL-12 (Figure 8). This result provides additional evidence for the stimulatory phenotype of mature DCs generated from JMML-2 PBMCs.

4.1.3. Additional properties of DCs cultured in vitro from JMML PBMCs:

We found that DCs generated *in vitro* from both normal donor and JMML PBMCs formed non-adherent clusters. This behaviour is only observed in DCs cultured *in vitro*, and DC clusters have not been observed *in vivo*. Fujii and colleagues (1999) reported that the clustering of MoDCs is vital for DC activation of T cell responses *in vitro*. Therefore, this data is consistent with the normal function of JMML-derived DCs.

Normal mature DCs are terminally differentiated and unable to proliferate (Banchereau and Steinman, 1998). However, it is not known whether DCs generated from JMML blasts retain the ability to proliferate. In future studies, this could be assessed by staining CD86$^+$-purified leukaemic DCs with Ki67, using standard immunohistochemical techniques. It is interesting to note that DCs differentiated *in vitro* from CML and AML blasts do not proliferate (Choudhury *et al*, 1997; Choudhury *et al*, 1999).

A major feature of mature DC behaviour is migration to T cell areas of secondary lymphoid organs (Banchereau *et al*, 2000), and this migration is directed by chemokines such as Mip-3β (Ngo *et al*, 1998). Unfortunately, we did not have sufficient cell numbers to evaluate the chemokine-induced migration of JMML-derived DCs. Longoni *et al* (2002) demonstrated that activated DCs from both normal donors and JMML patients responded to Mip-3β in chemotaxis assays. In contrast, DCs generated *in vitro*

from CML blasts have reduced chemokine-induced migratory ability compared to normal MoDCs (Dong *et al*, 2003).

4.1.4. Leukaemic origin of DCs generated in vitro from PBMCs of JMML patients: The leukaemic cells in two of the patients (JMML-2 and JMML-3) displayed monosomy 7, and we used this distinct cytogenetic feature as a marker of malignant origin. The finding that more than 90% of the $CD86^+$ DCs differentiated *in vitro* from JMML-2 and JMML-3 PBMCs exhibited monosomy 7 conclusively shows that the DCs were derived from the malignant clone (Figures 6 and 7). These leukaemic DCs should therefore express any JMML-specific antigens and possess the MHC molecules, co-stimulatory molecules, and the cytokine production profile required to present these antigens to the immune effector cells. However, it cannot be guaranteed that DCs differentiated from leukaemic blasts retain expression of leukaemia-associated antigens. For example, a leukaemia-associated antigen involved in maintaining the cell's proliferative potential might be down-regulated when the leukaemia cell is differentiated into a terminally differentiated DC.

4.2. Variability in the immunophenotype of DCs cultured from different JMML patients:

The abnormal IL-12 secretion profile of JMML-3-derived DCs (Figure 8) is consistent with the flow cytometric data (Figure 5), demonstrating that the DCs cultured from this patient were partially resistant to activation with LPS. DCs differentiated *in vitro* from neonatal PBMCs have markedly reduced IL-12 synthesis (Goriely *et al*, 2001; Upham *et al*, 2002). However, this evidence does not explain our findings with JMML-3 samples because this JMML patient was 2 years of age at presentation. The variability in the immunophenotype of the DCs generated from the 3 JMML patients probably reflects the heterogeneity of the disorder. Similarly, it is not possible to culture leukaemic DCs from all CML (Chen *et al*, 2000; Paquette *et al*, 2002) and AML patients (Charbonnier *et al*, 1999; Choudhury *et al*, 1999; Harrison *et al*, 2001).

Overall, our results demonstrate that immunostimulatory DCs can be generated from the majority of human JMML patient samples. Our findings are in keeping with previous studies, showing that leukaemic cells from the majority of patients with myeloid stem cell disorders, such as CML (Choudhury *et al*, 1997) and AML (Charbonnier *et al*, 1999; Choudhury *et al*, 1999), maintain their capacity to differentiate into DCs.

4.3. Functional activity of leukaemic DCs:

4.3.1. Allostimulatory capacity of in vitro generated leukaemic DCs:

Activated DCs are significantly better stimulator cells that other APCs, such as monocytes or B cells (Steinman, 1991), and should stimulate proliferation of allogeneic T cells at low DC:T cell ratios. We found that leukaemic DCs derived from JMML-2 PBMCs were potent stimulators of allogeneic T lymphocytes, as determined by IFN-γ release, and hence functionally active (Figure 9). Unfortunately, we did not collect sufficient numbers of PBMCs from this patient to compare the allostimulatory ability of freshly isolated JMML-2 PBMCs with *in vitro* generated JMML-2 DCs. Furthermore, because of the limited material available from any given patient, not all studies shown could be done for every patient's leukaemia.

4.3.2. Use of leukaemic DCs to stimulate JMML-specific T lymphocytes:

We used leukaemic DCs generated from JMML-1 PBMCs to stimulate allogeneic (BMT donor-derived) T cells. A preliminary *in vitro* cytotoxicity assay revealed that the expanded T cells lysed leukaemic JMML-1 target cells with some degree of specificity, however this was not found to be statistically significant (student *t*-test; p=0.08) (Figure 10). The cytotoxicity assay needs to be repeated using higher effector:target ratios to determine whether the CTLs can lyse significantly more leukaemic JMML-1 target cells than non-leukaemic JMML-1 targets. Nonetheless, the percentage cytotoxicity of the expanded T cells against JMML targets was equivalent to that reported for CML DC-stimulated CTLs against CML targets, at the same effector:target ratio (Choudhury *et al*, 1997). Further studies with a larger number of patient samples are warranted to determine whether the JMML-derived DCs can be utilised as stimulators of allogeneic T cell responses against JMML cells, in an *ex vivo* setting following allogeneic BMT.

The BMT donor-derived T cells used in this experiment were collected from the JMML patient following allogeneic BMT and 100% donor engraftment. This was preferred over using T cells collected from the donor. The reasoning behind this was that the donor-derived T cells had had the opportunity to encounter residual leukaemic cells in the patient before being used for *in vitro* expansion of JMML-specific CTLs. Hence we were not having to stimulate a truly primary T cell immune response in an *in vitro* setting, which is more difficult to achieve. Furthermore, using PBMCs obtained from the patient after BMT as the source of allogeneic T cells is feasible for an adoptive immunotherapy strategy to treat minimal residual disease.

In future experiments, cytotoxicity should be measured with a more reliable assay system, such as a standard ^{51}Chromium-release assay. This assay system is associated with low background levels, allowing the investigation of CTL cytotoxicity at higher effector to target ratios than was possible measuring LDH release. Additionally, the number of expanded CTLs could be increased by polyclonal stimulation with anti-CD3 antibody, ensuring that there are sufficient numbers of effector cells for more elaborate cytotoxicity assays.

4.3.2.1. Stimulation of allogeneic T cells rather than autologous T cells:
Despite the encouraging findings that leukaemic DCs generated *ex vivo* from CML blasts can stimulate potent anti-leukaemia responses from autologous T cells *in vitro*, there has been little evidence of *in vivo* efficacy (Pinilla-Ibarz *et al*, 2000). Hence, we have attempted to stimulate and expand allogeneic (BMT donor-derived) T cells that are JMML-specific. The successful treatment of relapsed JMML patients with DLIs (Matthes-Martin *et al*, 2000; Worth *et al*, 2002) suggests that allogeneic responses may be needed to cure patients of the disease. Our results suggest that leukaemic DCs can be used to expand allogeneic T lymphocytes that are specific for JMML cells and only have minimal activity against non-leukaemic patient cells (Figure 10). Allogeneic CTLs expanded *ex vivo* could be used for adoptive immunotherapy to augment the GVL effect in isolation from GVHD.

However, stimulation of BMT donor T cells with HLA-matched allogeneic leukaemic DCs will most likely generate responses directed against multiple minor histocompatability antigens (mHags), in addition to responses against any leukaemia-associated antigens (Goulmy, 1997). A concern is that the adoptive transfer of such CTLs to patients might cause GVHD, since many normal cells of the patient will express multiple mHags. Hence the use of allogeneic T cells for adoptive therapy remains controversial.

A detailed study is required to compare the ability of leukaemic DCs to stimulate JMML-specific responses from autologous CTLs and allogeneic (BMT donor-derived) CTLs *in vitro*. It would be interesting to determine whether JMML induces T cell anergy in autologous T cells, and whether *in vitro* stimulation with leukaemic DCs can overcome this tolerance. It is worth noting that in the MLR (Figure 9) there is reduced

reactivity against autologous PBMCs with JMML-derived DCs compared to normal MoDCs. This might be due to reduced T cell number or function in the JMML patient.

4.3.2.2. CTL-mediated lysis of JMML cells in vivo:

In future studies, we could examine the ability of *ex vivo* expanded CTLs to kill leukaemic cells *in vivo*. NOD/SCID mice would be engrafted with PBMCs from JMML patients, and one group of engrafted mice treated with leukaemic DC-stimulated CTLs. We would be able to determine the number of engrafted myelomonocytic cells within the spleens of treated and untreated mice by flow cytometry. Additionally, we could study the longevity of the CTLs *in vivo*. However, the mouse model would not mimic the human situation sufficiently to study any GVHD, because no other cells in the animal express target antigens for the *ex vivo* generated CTLs.

4.4. Generation of leukaemia-specific immune responses:

There is accumulating evidence from murine models (Tsukada *et al*, 1999) and human studies (Montagna *et al*, 1998; Osman *et al*, 1999; Muller *et al*, 2001) that T cell responses can be mounted that specifically lyse leukaemic cells and avoid targeting normal cells. Our data (Figure 10) corroborates these findings, suggesting that the GVL effect appears to be at least partially separable from GVHD following allogeneic BMT.

4.4.1. Presentation of leukaemia-specific antigens by DCs:

The lack of a T cell response sufficient to prevent the development of primary malignancies *in vivo* might be related to many factors, including a lack of presentation of leukaemic antigens by APCs, failure of tumours to express MHC antigen, or leukaemia-induced T cell anergy (Banchereau and Steinman, 1998). However, some leukaemic antigens might function as leukaemia rejection antigens when presented with the appropriate co-stimulatory signals on the surface of professional APCs.

CML studies illustrate how DCs can be used to initiate an effective anti-leukaemia immune response in situations where the primary malignant cells have failed to do so. CML is characterised by the t(9;22) chromosomal translocation that generates *BCR-ABL* and *ABL-BCR* fusion genes (Deininger *et al*, 2000), and the break points of the corresponding fusion proteins are leukaemia-specific. Osman and colleagues (1999) synthesized immunogenic peptides from the BCR-ABL break point, and found that MoDCs pulsed with the peptides were able to prime autologous CTLs that specifically

lyse CML blasts. The investigators propose using this method to prime donor lymphocytes before DLI for patients with CML.

Unlike CML, no putative leukaemia-specific antigens have been identified for JMML. Nonetheless, the results from our limited cytotoxicity assay suggest that such antigens are likely to exist. Further studies using leukaemic DCs to stimulate and expand JMML-specific T lymphocytes are warranted to identify the individual target antigens responsible for the observed anti-leukaemia response. One approach to identify the leukaemia-specific antigens involves eluting and sequencing the peptides bound to MHC molecules expressed on the surface of the *in vitro* generated leukaemic DCs (Halder *et al*, 2000).

Myeloid malignancies offer the opportunity to differentiate DCs from the malignant cells themselves. An advantage of this approach is that *in vitro* cultured JMML DCs present leukaemic antigens to T cells in conjunction with co-stimulatory signals, and can be used to initiate JMML-specific immune responses without the need of identifying the exact leukaemia antigen(s) involved.

4.4.2. Effector cell types mounting the anti-leukaemia response:

In future cytotoxicity assays, the effector cell types that are producing the anti-JMML response should be determined. For example, it is possible to inhibit CTL and natural killer (NK) cell responses using anti-CD8 and anti-NK1.1 blocking antibodies, respectively.

Muller and colleagues (2001) used leukaemic DCs cultured *in vitro* from CML blasts to stimulate autologous T lymphocytes. They isolated 3 expanded T cell lines that were specifically activated by CML blasts, and immunophenotyping revealed that two were pure $CD4^+$ cells while one was a mixture of $CD8^+$ and $CD4^+$ cells. Montagna and colleagues (1998) detected a high frequency of donor-derived CTLs specific for the leukaemic blasts in the peripheral blood of acute leukaemia patients following allogeneic BMT. Furthermore, the frequency of leukaemia-specific CTLs correlated with maintenance of a state of remission.

Edinger *et al* (2003) identified $CD4^+CD25^+$ regulatory T cells as essential for inhibiting lethal GVHD while preserving the beneficial GVL activity following MHC-mismatched

allogeneic BMT in mice. Regulatory T cells might play an important role during the *ex vivo* stimulation and expansion of allogeneic T lymphocytes specific for JMML blasts. Furthermore, the infusion of regulatory T cells might help prevent/minimise GVHD in JMML patients whilst preserving the GVL responses following allogeneic BMT.

Natural killer T (NKT) cells possess an invariant T cell receptor that specifically recognises α-galactosylceramide antigen bound to CD1d molecules on the surface of target cells (Bendelac *et al*, 1995). Metelitsa and colleagues (2003) found that up to 77% of primary JMML cells express CD1d and can be lysed by NKT cells via the perforin/granzyme-B pathway. Future experiments could examine whether there is an increase in the number of NKT cells (identified as $CD161^+$) in the expanded BMT donor-derived effector cell population following stimulation with JMML DCs, and whether the specific killing of JMML targets can be inhibited by blocking NKT function.

4.5. JMML cells spontaneously differentiate into DCs:

Longoni and colleagues (2002) have recently shown that JMML cells can spontaneously differentiate *in vitro* into DC, but these leukaemic DCs secrete the immunosuppressive cytokine IL-10 that might dampen anti-leukaemia immune responses. However, we have found that JMML cells cultured *in vitro* with GM-CSF, IL-4, and LPS differentiate into immunostimulatory DCs that secrete IL-12 and are capable of inducing allogeneic anti-leukaemia immune responses. DCs differentiated *in vitro* from JMML cells in the presence of GM-CSF and IL-4 are therefore potentially useful for the priming of JMML-specific cytotoxic immune responses.

Longoni *et al* (2002) did not address whether JMML cells differentiate into DCs *in vivo*. The human peripheral blood DC population contains several phenotypically and functionally distinct subtypes. All human peripheral blood DC subpopulations can be identified by their lack of lineage-specific markers ($Lin1^-$) and high level expression of HLA-DR (MacDonald *et al*, 2002). The two main human subsets are 'myeloid' $Lin1^{-/low}HLA\text{-}DR^+CD11c^+$ DCs and 'lymphoid' $Lin1^{-/low}HLA\text{-}DR^+CD123^+$ DCs (Robinson *et al*, 1999). We observed that PBMCs from JMML-2 contained a larger number of $Lin1^{-/low}HLA\text{-}DR^+CD11c^+$ and $Lin1^{-/low}HLA\text{-}DR^+CD123^+$ DC subtypes than normal individuals (4.1% versus 0.5%, and 1.4% versus 0.6% total PBMC population, respectively; Figure 11). This suggests that JMML cells do spontaneously differentiate

into DCs *in vivo*, but it remains to be determined whether the $CD11c^+$ and $CD123^+$ DCs in JMML patients are functionally active and immunostimulatory.

4.6. DC-based vaccine strategies for the treatment of JMML patients:

4.6.1. Clinical use of in vitro cultured DCs:

In the current study, we have not used tissue culture conditions suitable for clinical preparations. However, Ossenkoppele and colleagues (2003) have generated mature DCs from CML blasts *ex vivo*, using clinically approved methodology. LPS cannot be used in clinical preparations, so Ossenkoppele *et al* (2003) used TNF-α along with GM-CSF and IL-4 to culture mature DCs. Other clinically acceptable ligands used to activate human DCs *ex vivo* include prostaglandin E_2, CD40 ligand, Fms-like tyrosine kinase 3 ligand (Holtl *et al*, 2002; Panoskaltsis *et al*, 2002). Additionally, FCS cannot be used in clinical preparations. In one experiment we supplemented the RPMI media with patient serum in place of FCS, and successfully generated MoDCs (data not shown). Future work involves confirming that we can generate activated DCs from JMML blasts using a clinically approved protocol.

4.6.2. Clinical application of our data:

The use of leukaemic DCs to stimulate allogeneic responses against JMML remains problematic because of the wide array of self antigens presented, which are likely to induce potent GVHD responses. However, there are several potential clinical applications of our data.

Firstly, *in vitro* generated leukaemic DCs could be used for the stimulation of autologous PBMCs (in an *ex vivo* setting) to generate anti-leukaemic T cell lines for adoptive immunotherapy to eliminate residual disease. Autologous strategies are attractive because of the reduced risk of GVHD.

Secondly, DC differentiated *in vitro* from JMML cells could potentially be administered as a cellular vaccine to induce anti-leukaemia T cell immunity *in vivo*. Such treatment would be suitable for patients with resistant disease or following BMT failure. In a phase I study, Ossenkoppele and colleagues (2003) intradermally vaccinated CML patients with autologous *in vitro* cultured leukaemic DCs. In one of the three CML patients treated, the investigators detected a leukaemia-specific immune response up to 20 months after the last vaccination.

Thirdly, the data supports the concept of generating allogeneic JMML-specific CTL lines from BMT donor T lymphocytes (T cell source being either donor PBMCs or activated T cells post engraftment). Transduction of the CTL lines with a retroviral vector encoding suicide genes would allow their ablation in cases of graft versus host disease. Qasim *et al* (2003) performed pre-clinical studies, transducing T lymphocytes with a retroviral vector encoding the herpes simplex thymidine kinase gene. Transduction with this vector rendered the T cells sensitive to suicide after administration of the prodrug ganciclovir, while wild-type cells were unaffected.

Lastly, systemic treatment with cytokine therapy could potentially be used to differentiate JMML blasts into immunostimulatory leukaemic DCs *in vivo*, and would be applicable for patients with resistant disease post BMT. Administration of GM-CSF and IFN-α has been shown to induce cytogenetic remission (i.e. 0% Ph^+ nuclei) in some CML patients (Cortes *et al*, 1998). Chen and colleagues (2000) postulated that cytokine therapy drives in the *in vivo* generation of highly stimulatory CML-derived APCs, capable of stimulating a specific anti-leukaemia response.

Publications

• Nabarro, S., Thrasher, A. J., Kempski, H., Amrolia, P., and Anderson, J. (2003) Generation of immunostimulatory dendritic cells from the malignant clone in patients with juvenile myelomonocytic leukemia. Leukemia 17, 1910-1912.

The paper is attached at the end of the thesis.

Chapter 5: Conclusions

1. Summary of thesis:

Tumour cells are genetically very unstable, acquiring numerous mutations (Fenton and Longo, 1995). Cancer progression can be viewed as a balance between the tumour's gain of function from the mutations against the effectiveness of the host immune system at targeting tumour cells expressing the neo antigens created by the mutations. As a result, tumours frequently develop immune evasion mechanisms to avoid detection. In recent years, the critical role of dendritic cells (DCs) at initiating anti-tumour immune responses has become better understood. This raises the possibility of using DC-based immunotherapeutic approaches to manipulate the balance, resulting in effective and long-lasting anti-tumour immunity. Preliminary clinical trials have demonstrated that tumour antigen-pulsed DC vaccines can induce beneficial clinical responses in some patients (Hsu *et al*, 1996; Nestle *et al*, 1998).

The translocation t(2;13)(q35;q14) is a hallmark of alveolar rhabdomyosarcoma (ARMS), and codes for a chimeric PAX3-FKHR fusion protein (Turc-Carel *et al*, 1986; Galili *et al*, 1993; Shapiro *et al*, 1993). We have performed gene expression profiling experiments to identify novel tumour-associated antigens downstream from PAX3-FKHR. Our results suggest that PAX3-FKHR initiates an immune escape mechanism by disrupting normal interferon (IFN)-γ signalling within ARMS cells. Aberrant IFN-γ regulated gene expression is likely to have pleiotropic effects on tumour cell behaviour. We found that one result of PAX3-FKHR-mediated interference of IFN-γ signalling is decreased major histocompatibility complex (MHC) expression on the cell surface, which may help avoid detection by tumour antigen-specific T lymphocytes. Understanding the function of this fusion protein in ARMS cells is important for the development of therapeutic strategies. The finding that PAX3-FKHR down-regulates MHC class I expression suggests that DC vaccines that activate natural killer (NK) and natural killer T (NKT) cells might be successful at eradicating ARMS. Additionally, our results suggest that IFN-γ treatment might be clinically beneficial for the partial correction of these PAX3-FKHR-mediated effects in ARMS patients. This research project has been taken on by Antigoni Papanastasiou, who has recently shown that PAX3-FKHR forms a complex with STAT3 *in vivo*. Further experiments will determine whether the interaction between PAX3-FKHR and STAT3 is responsible for in the aberrant IFN-γ target gene expression observed in RMS cell lines.

There are currently no successful immunotherapeutic approaches in clinical use for the treatment of ARMS. Nevertheless, the N-terminal PAX3 region of PAX3-FKHR is a suitable target for vaccine therapy for several reasons: PAX3-FKHR is highly expressed in ARMS cells (Davis and Barr, 1997), whilst PAX3 is silent in virtually all postnatal tissues (Stoykova and Gruss, 1994; Tsukamoto *et al*, 1994); PAX3-FKHR expression is crucial for the growth and survival of tumour cells (Bernasconi *et al*, 1996; Ayyanathan *et al*, 2000), minimising the risk that PAX3-FKHR expression can be down-regulated to avoid immune detection; any immunotherapeutic approach targeting the fusion protein is widely applicable, thus potentially suitable for the treatment of most ARMS patients. In our mouse model of ARMS, we found that DCs pulsed with tumour lysate are unable to elicit PAX3-FKHR-specific T lymphocyte responses. DCs loaded with PAX3-specific immunogenic peptides or *PAX3-FKHR* RNA might be superior at inducing antigen-specific immune responses, and shall be tested using our established mouse ARMS model. One potential problem is that T lymphocytes that bind to PAX3 peptide epitopes with high avidity might have been inactivated by immunological tolerance mechanisms during development. It is vital that future immunotherapeutic approaches attempt to overcome immunological tolerance in order to elicit antigen-specific responses from high avidity T cells capable of mediating tumour rejection (Morris *et al*, 2003).

In the case of juvenile myelomonocytic leukaemia (JMML), no leukaemia-associated antigens have been identified. However, the evidence of a graft versus leukaemia effect following allogeneic bone marrow transplantation (Matthes-Martin *et al*, 2000) suggests that JMML is susceptible to immune attack and that JMML-associated antigens exist. Myeloid leukaemias are unique in their ability to differentiate into functional DCs that co-express the co-stimulatory signals required to efficiently present any endogenously processed leukaemia-rejection antigens to the adaptive immune system (Choudhury *et al*, 1997). We have shown for the first time that mature DCs can be generated *in vitro* from the malignant JMML clone. These leukaemic DCs possess an immunostimulatory phenotype, and appear to be able to activate cytotoxic T lymphocytes specific for JMML targets *in vitro*. The main advantage of an immunotherapeutic strategy using *ex vivo* differentiated leukaemic DCs is that it bypasses the need to identify JMML-associated antigens. Further pre-clinical studies are required to optimise the immunotherapeutic approach for the treatment of JMML patients.

2. The future of DC-based immunotherapeutic approaches:

DC-based therapies provide the opportunity to manipulate the balance between host immune responses and tumour immune escape mechanisms in favour of the host. In the 8 years since the first published DC vaccination pilot study (Hsu *et al*, 1996), more than 1,000 cancer patients have been treated with DC vaccines and the preliminary findings are encouraging (Ridgway, 2003). Mounting evidence from phase I and II clinical trials suggests that DC vaccination is safe, with very few patients exhibiting adverse side effects. Most clinical trials have treated patients with late stage disease after the failure of standard therapies. The disadvantage of this is that advanced stage tumours are often immunosuppressive, and potentially able to dampen down the immune response initiated by the DC vaccine (Pardoll, 2003). Nonetheless, beneficial clinical responses have been observed in approximately half the DC vaccine trials (Ridgway, 2003). I believe that it is now time to bite the bullet and use DC-based immunotherapies for the treatment of appropriate patients with minimal tumour burden. This would enable us to monitor the clinical benefit of DC vaccinations in the optimal clinical setting for priming anti-tumour immunity.

Bibliography

• Ackerman, A. L., and Cresswell, P. (2004). Cellular mechanisms governing cross-presentation of exogenous antigens. Nat Immunol 5, 678-684.

• Acuto, O., and Michel, F. (2003). CD28-mediated co-stimulation: a quantitative support for TCR signalling. Nat Rev Immunol 3, 939-951.

• Aguanno, S., Bouche, M., Adamo, S., and Molinaro, M. (1990). 12-O-tetradecanoylphorbol-13-acetate-induced differentiation of a human rhabdomyosarcoma cell line. Cancer Res 50, 3377-3382.

• Aiuti, A., Webb, I. J., Bleul, C., Springer, T., and Gutierrez-Ramos, J. C. (1997). The chemokine SDF-1 is a chemoattractant for human CD34+ hematopoietic progenitor cells and provides a new mechanism to explain the mobilization of CD34+ progenitors to peripheral blood. J Exp Med 185, 111-120.

• Albert, M. L., Sauter, B., and Bhardwaj, N. (1998). Dendritic cells acquire antigen from apoptotic cells and induce class I-restricted CTLs. Nature 392, 86-89.

• Alexander, J., Payne, J. A., Murray, R., Frelinger, J. A., and Cresswell, P. (1989). Differential transport requirements of HLA and H-2 class I glycoproteins. Immunogenetics 29, 380-388.

• Alexander-Miller, M. A., Leggatt, G. R., and Berzofsky, J. A. (1996). Selective expansion of high- or low-avidity cytotoxic T lymphocytes and efficacy for adoptive immunotherapy. Proc Natl Acad Sci U S A 93, 4102-4107.

• Alexopoulou, L., Holt, A. C., Medzhitov, R., and Flavell, R. A. (2001). Recognition of double-stranded RNA and activation of NF-kappaB by Toll-like receptor 3. Nature 413, 732-738.

• Andersen, M. H., Keikavoussi, P., Brocker, E. B., Schuler-Thurner, B., Jonassen, M., Sondergaard, I., Straten, P. T., Becker, J. C., and Kampgen, E. (2001). Induction of systemic CTL responses in melanoma patients by dendritic cell vaccination: cessation of CTL responses is associated with disease progression. Int J Cancer 94, 820-824.

• Anderson, J., Gordon, A., Pritchard-Jones, K., and Shipley, J. (1999a). Genes, chromosomes, and rhabdomyosarcoma. Genes Chromosomes Cancer 26, 275-285.

• Anderson, J., Gordon, A., McManus, A., Shipley, J., and Pritchard-Jones, K. (1999b). Disruption of imprinted genes at chromosome region 11p15.5 in paediatric rhabdomyosarcoma. Neoplasia 1, 340-348.

• Anderson, J., Ramsay, A., Gould, S., and Pritchard-Jones, K. (2001a). PAX3-FKHR induces morphological change and enhances cellular proliferation and invasion in rhabdomyosarcoma. Am J Pathol 159, 1089-1096.

• Anderson, M. J., Shelton, G. D., Cavenee, W. K., and Arden, K. C. (2001b). Embryonic expression of the tumor-associated PAX3-FKHR fusion protein interferes with the developmental functions of Pax3. Proc Natl Acad Sci U S A 98, 1589-1594.

• Andre, F., Schartz, N. E., Movassagh, M., Flament, C., Pautier, P., Morice, P., Pomel, C., Lhomme, C., Escudier, B., Le Chevalier, T., et al. (2002). Malignant effusions and immunogenic tumour-derived exosomes. Lancet 360, 295-305.

• Antin, J. H. (1993). Graft-versus-leukemia: no longer an epiphenomenon. Blood 82, 2273-2277.

• Arico, M., Biondi, A., and Pui, C. H. (1997). Juvenile myelomonocytic leukemia. Blood 90, 479-488.

• Ariel, I., Lustig, O., Schneider, T., Pizov, G., Sappir, M., De-Groot, N., and Hochberg, A. (1995). The imprinted H19 gene as a tumor marker in bladder carcinoma. Urology 45, 335-338.

• Arnold, D., Faath, S., Rammensee, H., and Schild, H. (1995). Cross-priming of minor histocompatibility antigen-specific cytotoxic T cells upon immunization with the heat shock protein gp96. J Exp Med 182, 885-889.
• Ashley, D. M., Faiola, B., Nair, S., Hale, L. P., Bigner, D. D., and Gilboa, E. (1997). Bone marrow-generated dendritic cells pulsed with tumor extracts or tumor RNA induce antitumor immunity against central nervous system tumors. J Exp Med 186, 1177-1182.
• Atanackovic, D., Altorki, N. K., Stockert, E., Williamson, B., Jungbluth, A. A., Ritter, E., Santiago, D., Ferrara, C. A., Matsuo, M., Selvakumar, A., et al. (2004). Vaccine-induced CD4+ T cell responses to MAGE-3 protein in lung cancer patients. J Immunol 172, 3289-3296.
• Avigan, D. (1999). Dendritic cells: development, function and potential use for cancer immunotherapy. Blood Rev 13, 51-64.
• Axton, R., Hanson, I., Danes, S., Sellar, G., van Heyningen, V., and Prosser, J. (1997). The incidence of PAX6 mutation in patients with simple aniridia: an evaluation of mutation detection in 12 cases. J Med Genet 34, 279-286.
• Ayyanathan, K., Fredericks, W. J., Berking, C., Herlyn, M., Balakrishnan, C., Gunther, E., and Rauscher, F. J., 3rd (2000). Hormone-dependent tumor regression in vivo by an inducible transcriptional repressor directed at the PAX3-FKHR oncogene. Cancer Res 60, 5803-5814.
• Bajou, K., Noel, A., Gerard, R. D., Masson, V., Brunner, N., Holst-Hansen, C., Skobe, M., Fusenig, N. E., Carmeliet, P., Collen, D., and Foidart, J. M. (1998). Absence of host plasminogen activator inhibitor 1 prevents cancer invasion and vascularization. Nat Med 4, 923-928.
• Baldwin, C. T., Hoth, C. F., Amos, J. A., da-Silva, E. O., and Milunsky, A. (1992). An exonic mutation in the HuP2 paired domain gene causes Waardenburg's syndrome. Nature 355, 637-638.
• Baldwin, C. T., Hoth, C. F., Macina, R. A., and Milunsky, A. (1995). Mutations in PAX3 that cause Waardenburg syndrome type I: ten new mutations and review of the literature. Am J Med Genet 58, 115-122.
• Ballas, Z. K., and Rasmussen, W. (1990). NK1.1+ thymocytes. Adult murine CD4-, CD8- thymocytes contain an NK1.1+, CD3+, CD5hi, CD44hi, TCR-V beta 8+ subset. J Immunol 145, 1039-1045.
• Balsinde, J., Balboa, M. A., Insel, P. A., and Dennis, E. A. (1999). Regulation and inhibition of phospholipase A2. Annu Rev Pharmacol Toxicol 39, 175-189.
• Banchereau, J., and Steinman, R. M. (1998). Dendritic cells and the control of immunity. Nature 392, 245-252.
• Banchereau, J., Briere, F., Caux, C., Davoust, J., Lebecque, S., Liu, Y. J., Pulendran, B., and Palucka, K. (2000). Immunobiology of dendritic cells. Annu Rev Immunol 18, 767-811.
• Banchereau, J., Palucka, A. K., Dhodapkar, M., Burkeholder, S., Taquet, N., Rolland, A., Taquet, S., Coquery, S., Wittkowski, K. M., Bhardwaj, N., et al. (2001a). Immune and clinical responses in patients with metastatic melanoma to CD34(+) progenitor-derived dendritic cell vaccine. Cancer Res 61, 6451-6458.
• Banchereau, J., Schuler-Thurner, B., Palucka, A. K., and Schuler, G. (2001b). Dendritic cells as vectors for therapy. Cell 106, 271-274.
• Bannai, M., Oya, H., Kawamura, T., Naito, T., Shimizu, T., Kawamura, H., Miyaji, C., Watanabe, H., Hatakeyama, K., and Abo, T. (2000). Disparate effect of beige mutation on cytotoxic function between natural killer and natural killer T cells. Immunology 100, 165-169.

• Barber, T. D., Barber, M. C., Tomescu, O., Barr, F. G., Ruben, S., and Friedman, T. B. (2002). Identification of target genes regulated by PAX3 and PAX3-FKHR in embryogenesis and alveolar rhabdomyosarcoma. Genomics 79, 278-284.
• Barr, F. G. (1998). Translocations, cancer and the puzzle of specificity. Nat Genet 19, 121-124.
• Barr, F. G. (2001). Gene fusions involving PAX and FOX family members in alveolar rhabdomyosarcoma. Oncogene 20, 5736-5746.
• Barr, F. G., Qualman, S. J., Macris, M. H., Melnyk, N., Lawlor, E. R., Strzelecki, D. M., Triche, T. J., Bridge, J. A., and Sorensen, P. H. (2002). Genetic heterogeneity in the alveolar rhabdomyosarcoma subset without typical gene fusions. Cancer Res 62, 4704-4710.
• Bassi, P. (2002). BCG (Bacillus of Calmette Guerin) therapy of high-risk superficial bladder cancer. Surg Oncol 11, 77-83.
• Bauer, M., Heeg, K., Wagner, H., and Lipford, G. B. (1999). DNA activates human immune cells through a CpG sequence-dependent manner. Immunology 97, 699-705.
• Bauer, S., Groh, V., Wu, J., Steinle, A., Phillips, J. H., Lanier, L. L., and Spies, T. (1999). Activation of NK cells and T cells by NKG2D, a receptor for stress-inducible MICA. Science 285, 727-729.
• Baumann, P., and West, S. C. (1998). DNA end-joining catalyzed by human cell-free extracts. Proc Natl Acad Sci U S A 95, 14066-14070.
• Bendelac, A., Lantz, O., Quimby, M. E., Yewdell, J. W., Bennink, J. R., and Brutkiewicz, R. R. (1995). CD1 recognition by mouse NK1+ T lymphocytes. Science 268, 863-865.
• Bennett, S. R., Carbone, F. R., Karamalis, F., Flavell, R. A., Miller, J. F., and Heath, W. R. (1998). Help for cytotoxic-T-cell responses is mediated by CD40 signalling. Nature 393, 478-480.
• Bennicelli, J. L., Edwards, R. H., and Barr, F. G. (1996). Mechanism for transcriptional gain of function resulting from chromosomal translocation in alveolar rhabdomyosarcoma. Proc Natl Acad Sci U S A 93, 5455-5459.
• Berard, F., Blanco, P., Davoust, J., Neidhart-Berard, E. M., Nouri-Shirazi, M., Taquet, N., Rimoldi, D., Cerottini, J. C., Banchereau, J., and Palucka, A. K. (2000). Cross-priming of naive CD8 T cells against melanoma antigens using dendritic cells loaded with killed allogeneic melanoma cells. J Exp Med 192, 1535-1544.
• Bernasconi, M., Remppis, A., Fredericks, W. J., Rauscher, F. J., 3rd, and Schafer, B. W. (1996). Induction of apoptosis in rhabdomyosarcoma cells through down-regulation of PAX proteins. Proc Natl Acad Sci U S A 93, 13164-13169.
• Berner, J. M., Forus, A., Elkahloun, A., Meltzer, P. S., Fodstad, O., and Myklebost, O. (1996). Separate amplified regions encompassing CDK4 and MDM2 in human sarcomas. Genes Chromosomes Cancer 17, 254-259.
• Bevan, M. J. (1976). Cross-priming for a secondary cytotoxic response to minor H antigens with H-2 congenic cells which do not cross-react in the cytotoxic assay. J Exp Med 143, 1283-1288.
• Biegel, J. A., Meek, R. S., Parmiter, A. H., Conard, K., and Emanuel, B. S. (1991). Chromosomal translocation t(1;13)(p36;q14) in a case of rhabdomyosarcoma. Genes Chromosomes Cancer 3, 483-484.
• Binder, B. R., Christ, G., Gruber, F., Grubic, N., Hufnagl, P., Krebs, M., Mihaly, J., and Prager, G. W. (2002). Plasminogen activator inhibitor 1: physiological and pathophysiological roles. News Physiol Sci 17, 56-61.

• Biragyn, A., Ruffini, P. A., Leifer, C. A., Klyushnenkova, E., Shakhov, A., Chertov, O., Shirakawa, A. K., Farber, J. M., Segal, D. M., Oppenheim, J. J., and Kwak, L. W. (2002). Toll-like receptor 4-dependent activation of dendritic cells by beta-defensin 2. Science 298, 1025-1029.
• Bladt, F., Riethmacher, D., Isenmann, S., Aguzzi, A., and Birchmeier, C. (1995). Essential role for the c-met receptor in the migration of myogenic precursor cells into the limb bud. Nature 376, 768-771.
• Blaine, S. A., Wick, M., Dessev, C., and Nemenoff, R. A. (2001). Induction of cPLA2 in lung epithelial cells and non-small cell lung cancer is mediated by Sp1 and c-Jun. J Biol Chem 276, 42737-42743.
• Blanck, G. (2002). Components of the IFN-gamma signaling pathway in tumorigenesis. Arch Immunol Ther Exp (Warsz) 50, 151-158.
• Bober, E., Franz, T., Arnold, H. H., Gruss, P., and Tremblay, P. (1994). Pax-3 is required for the development of limb muscles: a possible role for the migration of dermomyotomal muscle progenitor cells. Development 120, 603-612.
• Boczkowski, D., Nair, S. K., Nam, J. H., Lyerly, H. K., and Gilboa, E. (2000). Induction of tumor immunity and cytotoxic T lymphocyte responses using dendritic cells transfected with messenger RNA amplified from tumor cells. Cancer Res 60, 1028-1034.
• Boehm, U., Klamp, T., Groot, M., and Howard, J. C. (1997). Cellular responses to interferon-gamma. Annu Rev Immunol 15, 749-795.
• Bollag, G., Clapp, D. W., Shih, S., Adler, F., Zhang, Y. Y., Thompson, P., Lange, B. J., Freedman, M. H., McCormick, F., Jacks, T., and Shannon, K. (1996). Loss of NF1 results in activation of the Ras signaling pathway and leads to aberrant growth in haematopoietic cells. Nat Genet 12, 144-148.
• Boon, T., Cerottini, J. C., Van den Eynde, B., van der Bruggen, P., and Van Pel, A. (1994). Tumor antigens recognized by T lymphocytes. Annu Rev Immunol 12, 337-365.
• Bos, J. L. (1989). ras oncogenes in human cancer: a review. Cancer Res 49, 4682-4689.
• Bottaro, D. P., Rubin, J. S., Faletto, D. L., Chan, A. M., Kmiecik, T. E., Vande Woude, G. F., and Aaronson, S. A. (1991). Identification of the hepatocyte growth factor receptor as the c-met proto-oncogene product. Science 251, 802-804.
• Braciale, T. J., Morrison, L. A., Sweetser, M. T., Sambrook, J., Gething, M. J., and Braciale, V. L. (1987). Antigen presentation pathways to class I and class II MHC-restricted T lymphocytes. Immunol Rev 98, 95-114.
• Breckpot, K., Dullaers, M., Bonehill, A., van Meirvenne, S., Heirman, C., de Greef, C., van der Bruggen, P., and Thielemans, K. (2003). Lentivirally transduced dendritic cells as a tool for cancer immunotherapy. J Gene Med 5, 654-667.
• Bretscher, P., and Cohn, M. (1970). A theory of self-nonself discrimination. Science 169, 1042-1049.
• Brohmann, H., Jagla, K., and Birchmeier, C. (2000). The role of Lbx1 in migration of muscle precursor cells. Development 127, 437-445.
• Brunet, A., Bonni, A., Zigmond, M. J., Lin, M. Z., Juo, P., Hu, L. S., Anderson, M. J., Arden, K. C., Blenis, J., and Greenberg, M. E. (1999). Akt promotes cell survival by phosphorylating and inhibiting a Forkhead transcription factor. Cell 96, 857-868.
• Brutkiewicz, R. R., and Sriram, V. (2002). Natural killer T (NKT) cells and their role in antitumor immunity. Crit Rev Oncol Hematol 41, 287-298.
• Budhu, A. S., and Noy, N. (2002). Direct channeling of retinoic acid between cellular retinoic acid-binding protein II and retinoic acid receptor sensitizes mammary carcinoma cells to retinoic acid-induced growth arrest. Mol Cell Biol 22, 2632-2641.

• Bukowski, R. M. (1999). Immunotherapy in renal cell carcinoma. Oncology (Huntingt) 13, 801-810; discussion 810, 813.
• Bunin, N., Saunders, F., Leahey, A., Doyle, J., Calderwood, S., and Freedman, M. H. (1999). Alternative donor bone marrow transplantation for children with juvenile myelomonocytic leukemia. J Pediatr Hematol Oncol 21, 479-485.
• Burdelya, L., Catlett-Falcone, R., Levitzki, A., Cheng, F., Mora, L. B., Sotomayor, E., Coppola, D., Sun, J., Sebti, S., Dalton, W. S., et al. (2002). Combination therapy with AG-490 and interleukin 12 achieves greater antitumor effects than either agent alone. Mol Cancer Ther 1, 893-899.
• Burgering, B. M., and Kops, G. J. (2002). Cell cycle and death control: long live Forkheads. Trends Biochem Sci 27, 352-360.
• Burnett, F. (1967). Immunological aspects of malignant disease. Lancet 1, 1171-1174.
Cao, Y., and Wang, C. (2000). The COOH-terminal transactivation domain plays a key role in regulating the in vitro and in vivo function of Pax3 homeodomain. J Biol Chem 275, 9854-9862.
• Byrd, J. C., Kitada, S., Flinn, I. W., Aron, J. L., Pearson, M., Lucas, D., and Reed, J. C. (2002). The mechanism of tumor cell clearance by rituximab in vivo in patients with B-cell chronic lymphocytic leukemia: evidence of caspase activation and apoptosis induction. Blood 99, 1038-1043.
• Capecchi, M. et al. (2003). AACR conference abstract.
• Cartron, G., Dacheux, L., Salles, G., Solal-Celigny, P., Bardos, P., Colombat, P., and Watier, H. (2002). Therapeutic activity of humanized anti-CD20 monoclonal antibody and polymorphism in IgG Fc receptor FcgammaRIIIa gene. Blood 99, 754-758.
• Caspar, C. B., Levy, S., and Levy, R. (1997). Idiotype vaccines for non-Hodgkin's lymphoma induce polyclonal immune responses that cover mutated tumor idiotypes: comparison of different vaccine formulations. Blood 90, 3699-3706.
• Castelli, C., Rivoltini, L., Rini, F., Belli, F., Testori, A., Maio, M., Mazzaferro, V., Coppa, J., Srivastava, P. K., and Parmiani, G. (2004). Heat shock proteins: biological functions and clinical application as personalized vaccines for human cancer. Cancer Immunol Immunother 53, 227-233.
• Cathcart, K., Pinilla-Ibarz, J., Korontsvit, T., Schwartz, J., Zakhaleva, V., Papadopoulos, E. B., and Scheinberg, D. A. (2004). A multivalent bcr-abl fusion peptide vaccination trial in patients with chronic myeloid leukemia. Blood 103, 1037-1042.
• Cebon, J., Jager, E., Shackleton, M. J., Gibbs, P., Davis, I. D., Hopkins, W., Gibbs, S., Chen, Q., Karbach, J., Jackson, H., et al. (2003). Two phase I studies of low dose recombinant human IL-12 with Melan-A and influenza peptides in subjects with advanced malignant melanoma. Cancer Immun 3, 7.
• Cella, M., Sallusto, F., and Lanzavecchia, A. (1997). Origin, maturation and antigen presenting function of dendritic cells. Curr Opin Immunol 9, 10-16.
• Cerundolo, V., Alexander, J., Anderson, K., Lamb, C., Cresswell, P., McMichael, A., Gotch, F., and Townsend, A. (1990). Presentation of viral antigen controlled by a gene in the major histocompatibility complex. Nature 345, 449-452.
• Chace, J. H., Hooker, N. A., Mildenstein, K. L., Krieg, A. M., and Cowdery, J. S. (1997). Bacterial DNA-induced NK cell IFN-gamma production is dependent on macrophage secretion of IL-12. Clin Immunol Immunopathol 84, 185-193.
• Chalepakis, G., and Gruss, P. (1995). Identification of DNA recognition sequences for the Pax3 paired domain. Gene 162, 267-270.

• Chan, S. H., Kobayashi, M., Santoli, D., Perussia, B., and Trinchieri, G. (1992). Mechanisms of IFN-gamma induction by natural killer cell stimulatory factor (NKSF/IL-12). Role of transcription and mRNA stability in the synergistic interaction between NKSF and IL-2. J Immunol 148, 92-98.
• Chang, S. Y., Lee, K. C., Ko, S. Y., Ko, H. J., and Kang, C. Y. (2004). Enhanced efficacy of DNA vaccination against Her-2/neu tumor antigen by genetic adjuvants. Int J Cancer 111, 86-95.
• Chapoval, A. I., Tamada, K., and Chen, L. (2000). In vitro growth inhibition of a broad spectrum of tumor cell lines by activated human dendritic cells. Blood 95, 2346-2351.
• Charbonnier, A., Gaugler, B., Sainty, D., Lafage-Pochitaloff, M., and Olive, D. (1999). Human acute myeloblastic leukemia cells differentiate in vitro into mature dendritic cells and induce the differentiation of cytotoxic T cells against autologous leukemias. Eur J Immunol 29, 2567-2578.
• Chefalo, P. J., and Harding, C. V. (2001). Processing of exogenous antigens for presentation by class I MHC molecules involves post-Golgi peptide exchange influenced by peptide-MHC complex stability and acidic pH. J Immunol 167, 1274-1282.
• Chen, G., and Radominska-Pandya, A. (2000). Direct photoaffinity labeling of cellular retinoic acid-binding protein I (CRABP-I) with all-trans-retinoic acid: identification of amino acids in the ligand binding site. Biochemistry 39, 12568-12574.
• Choudhury, A., Gajewski, J. L., Liang, J. C., Popat, U., Claxton, D. F., Kliche, K. O., Andreeff, M., and Champlin, R. E. (1997). Use of leukemic dendritic cells for the generation of antileukemic cellular cytotoxicity against Philadelphia chromosome-positive chronic myelogenous leukemia. Blood 89, 1133-1142.
• Choudhury, B. A., Liang, J. C., Thomas, E. K., Flores-Romo, L., Xie, Q. S., Agusala, K., Sutaria, S., Sinha, I., Champlin, R. E., and Claxton, D. F. (1999). Dendritic cells derived in vitro from acute myelogenous leukemia cells stimulate autologous, antileukemic T-cell responses. Blood 93, 780-786.
• Christman, J. K. (2002). 5-Azacytidine and 5-aza-2'-deoxycytidine as inhibitors of DNA methylation: mechanistic studies and their implications for cancer therapy. Oncogene 21, 5483-5495.
• Cichy, S. B., Uddin, S., Danilkovich, A., Guo, S., Klippel, A., and Unterman, T. G. (1998). Protein kinase B/Akt mediates effects of insulin on hepatic insulin-like growth factor-binding protein-1 gene expression through a conserved insulin response sequence. J Biol Chem 273, 6482-6487.
• Clark, E. A., Golub, T. R., Lander, E. S., and Hynes, R. O. (2000). Genomic analysis of metastasis reveals an essential role for RhoC. Nature 406, 532-535.
• Clohessy, J. G., Zhuang, J., and Brady, H. J. (2004). Characterisation of Mcl-1 cleavage during apoptosis of haematopoietic cells. Br J Haematol 125, 655-665.
• Coffer, P. J., Geijsen, N., M'Rabet, L., Schweizer, R. C., Maikoe, T., Raaijmakers, J. A., Lammers, J. W., and Koenderman, L. (1998). Comparison of the roles of mitogen-activated protein kinase kinase and phosphatidylinositol 3-kinase signal transduction in neutrophil effector function. Biochem J 329 (Pt 1), 121-130.
• Coiffier, B., Lepage, E., Briere, J., Herbrecht, R., Tilly, H., Bouabdallah, R., Morel, P., Van Den Neste, E., Salles, G., Gaulard, P., et al. (2002). CHOP chemotherapy plus rituximab compared with CHOP alone in elderly patients with diffuse large-B-cell lymphoma. N Engl J Med 346, 235-242.

• Colella, T. A., Bullock, T. N., Russell, L. B., Mullins, D. W., Overwijk, W. W., Luckey, C. J., Pierce, R. A., Restifo, N. P., and Engelhard, V. H. (2000). Self-tolerance to the murine homologue of a tyrosinase-derived melanoma antigen: implications for tumor immunotherapy. J Exp Med 191, 1221-1232.
• Cooper, L. J., Shannon, K. M., Loken, M. R., Weaver, M., Stephens, K., and Sievers, E. L. (2000). Evidence that juvenile myelomonocytic leukemia can arise from a pluripotential stem cell. Blood 96, 2310-2313.
• Cooper, M. A., Fehniger, T. A., and Caligiuri, M. A. (2001). The biology of human natural killer-cell subsets. Trends Immunol 22, 633-640.
• Cordon-Cardo, C., Fuks, Z., Drobnjak, M., Moreno, C., Eisenbach, L., and Feldman, M. (1991). Expression of HLA-A,B,C antigens on primary and metastatic tumor cell populations of human carcinomas. Cancer Res 51, 6372-6380.
• Corr, M., Lee, D. J., Carson, D. A., and Tighe, H. (1996). Gene vaccination with naked plasmid DNA: mechanism of CTL priming. J Exp Med 184, 1555-1560.
• Corr, M., von Damm, A., Lee, D. J., and Tighe, H. (1999). In vivo priming by DNA injection occurs predominantly by antigen transfer. J Immunol 163, 4721-4727.
• Cortes, J., Kantarjian, H., O'Brien, S., Kurzrock, R., Keating, M., and Talpaz, M. (1998). GM-CSF can improve the cytogenetic response obtained with interferon-alpha therapy in patients with chronic myelogenous leukemia. Leukemia 12, 860-864.
• Crouch, G. D., and Helman, L. J. (1991). All-trans-retinoic acid inhibits the growth of human rhabdomyosarcoma cell lines. Cancer Res 51, 4882-4887.
• Cui, J., Shin, T., Kawano, T., Sato, H., Kondo, E., Toura, I., Kaneko, Y., Koseki, H., Kanno, M., and Taniguchi, M. (1997). Requirement for Valpha14 NKT cells in IL-12-mediated rejection of tumors. Science 278, 1623-1626.
• Cullell-Young, M., Barrachina, M., Lopez-Lopez, C., Gonalons, E., Lloberas, J., Soler, C., and Celada, A. (2001). From transcription to cell surface expression, the induction of MHC class II I-A alpha by interferon-gamma in macrophages is regulated at different levels. Immunogenetics 53, 136-144.
• Dagher, R., Long, L. M., Read, E. J., Leitman, S. F., Carter, C. S., Tsokos, M., Goletz, T. J., Avila, N., Berzofsky, J. A., Helman, L. J., and Mackall, C. L. (2002). Pilot trial of tumor-specific peptide vaccination and continuous infusion interleukin-2 in patients with recurrent Ewing sarcoma and alveolar rhabdomyosarcoma: an inter-institute NIH study. Med Pediatr Oncol 38, 158-164.
• Daston, G., Lamar, E., Olivier, M., and Goulding, M. (1996). Pax-3 is necessary for migration but not differentiation of limb muscle precursors in the mouse. Development 122, 1017-1027.
• Davis, H. L., Weeratna, R., Waldschmidt, T. J., Tygrett, L., Schorr, J., Krieg, A. M., and Weeranta, R. (1998). CpG DNA is a potent enhancer of specific immunity in mice immunized with recombinant hepatitis B surface antigen. J Immunol 160, 870-876.
• Davis, I. D. (2000). An overview of cancer immunotherapy. Immunol Cell Biol 78, 179-195.
• Davis, R. J., D'Cruz, C. M., Lovell, M. A., Biegel, J. A., and Barr, F. G. (1994). Fusion of PAX7 to FKHR by the variant t(1;13)(p36;q14) translocation in alveolar rhabdomyosarcoma. Cancer Res 54, 2869-2872.
• Davis, R. J., and Barr, F. G. (1997). Fusion genes resulting from alternative chromosomal translocations are overexpressed by gene-specific mechanisms in alveolar rhabdomyosarcoma. Proc Natl Acad Sci U S A 94, 8047-8051.
• Davis, T. A., Maloney, D. G., Czerwinski, D. K., Liles, T. M., and Levy, R. (1998). Anti-idiotype antibodies can induce long-term complete remissions in non-Hodgkin's lymphoma without eradicating the malignant clone. Blood 92, 1184-1190.

• DeChiara, T. M., Robertson, E. J., and Efstratiadis, A. (1991). Parental imprinting of the mouse insulin-like growth factor II gene. Cell 64, 849-859.
• Deininger, M. W., Goldman, J. M., and Melo, J. V. (2000). The molecular biology of chronic myeloid leukemia. Blood 96, 3343-3356.
• Del Peso, L., Gonzalez, V. M., Hernandez, R., Barr, F. G., and Nunez, G. (1999). Regulation of the forkhead transcription factor FKHR, but not the PAX3-FKHR fusion protein, by the serine/threonine kinase Akt. Oncogene 18, 7328-7333.
• Delp, K., Momburg, F., Hilmes, C., Huber, C., and Seliger, B. (2000). Functional deficiencies of components of the MHC class I antigen pathway in human tumors of epithelial origin. Bone Marrow Transplant 25 Suppl 2, S88-95.
• den Haan, J. M., Lehar, S. M., and Bevan, M. J. (2000). CD8(+) but not CD8(-) dendritic cells cross-prime cytotoxic T cells in vivo. J Exp Med 192, 1685-1696.
• DeRisi, J., Penland, L., Brown, P. O., Bittner, M. L., Meltzer, P. S., Ray, M., Chen, Y., Su, Y. A., and Trent, J. M. (1996). Use of a cDNA microarray to analyse gene expression patterns in human cancer. Nat Genet 14, 457-460.
• DeRisi, J. L., Iyer, V. R., and Brown, P. O. (1997). Exploring the metabolic and genetic control of gene expression on a genomic scale. Science 278, 680-686.
• Devy, L., Blacher, S., Grignet-Debrus, C., Bajou, K., Masson, V., Gerard, R. D., Gils, A., Carmeliet, G., Carmeliet, P., Declerck, P. J., et al. (2002). The pro- or antiangiogenic effect of plasminogen activator inhibitor 1 is dose dependent. Faseb J 16, 147-154.
• Diefenbach, A., Jamieson, A. M., Liu, S. D., Shastri, N., and Raulet, D. H. (2000). Ligands for the murine NKG2D receptor: expression by tumor cells and activation of NK cells and macrophages. Nat Immunol 1, 119-126.
• Dijkers, P. F., Medema, R. H., Lammers, J. W., Koenderman, L., and Coffer, P. J. (2000). Expression of the pro-apoptotic Bcl-2 family member Bim is regulated by the forkhead transcription factor FKHR-L1. Curr Biol 10, 1201-1204.
• Dohner, K., Brown, J., Hehmann, U., Hetzel, C., Stewart, J., Lowther, G., Scholl, C., Frohling, S., Cuneo, A., Tsui, L. C., et al. (1998). Molecular cytogenetic characterization of a critical region in bands 7q35-q36 commonly deleted in malignant myeloid disorders. Blood 92, 4031-4035.
• Dong, R., Cwynarski, K., Entwistle, A., Marelli-Berg, F., Dazzi, F., Simpson, E., Goldman, J. M., Melo, J. V., Lechler, R. I., Bellantuono, I., et al. (2003). Dendritic cells from CML patients have altered actin organization, reduced antigen processing, and impaired migration. Blood 101, 3560-3567.
• Douglass, E. C., Rowe, S. T., Valentine, M., Parham, D. M., Berkow, R., Bowman, W. P., and Maurer, H. M. (1991). Variant translocations of chromosome 13 in alveolar rhabdomyosarcoma. Genes Chromosomes Cancer 3, 480-482.
• Dovhey, S. E., Ghosh, N. S., and Wright, K. L. (2000). Loss of interferon-gamma inducibility of TAP1 and LMP2 in a renal cell carcinoma cell line. Cancer Res 60, 5789-5796.
• Dranoff, G. (2004). Cytokines in cancer pathogenesis and cancer therapy. Nat Rev Cancer 4, 11-22.
• Dressler, G. R., and Douglass, E. C. (1992). Pax-2 is a DNA-binding protein expressed in embryonic kidney and Wilms tumor. Proc Natl Acad Sci U S A 89, 1179-1183.
• Driman, D., Thorner, P. S., Greenberg, M. L., Chilton-MacNeill, S., and Squire, J. (1994). MYCN gene amplification in rhabdomyosarcoma. Cancer 73, 2231-2237.

• Dudley, M. E., Wunderlich, J. R., Robbins, P. F., Yang, J. C., Hwu, P., Schwartzentruber, D. J., Topalian, S. L., Sherry, R., Restifo, N. P., Hubicki, A. M., et al. (2002). Cancer regression and autoimmunity in patients after clonal repopulation with antitumor lymphocytes. Science 298, 850-854.
• Duffy, M. J. (2002). Urokinase-type plasminogen activator: a potent marker of metastatic potential in human cancers. Biochem Soc Trans 30, 207-210.
• Dyall, R., Bowne, W. B., Weber, L. W., LeMaoult, J., Szabo, P., Moroi, Y., Piskun, G., Lewis, J. J., Houghton, A. N., and Nikolic-Zugic, J. (1998). Heteroclitic immunization induces tumor immunity. J Exp Med 188, 1553-1561.
• Edinger, M., Hoffmann, P., Ermann, J., Drago, K., Fathman, C. G., Strober, S., and Negrin, R. S. (2003). CD4+CD25+ regulatory T cells preserve graft-versus-tumor activity while inhibiting graft-versus-host disease after bone marrow transplantation. Nat Med 9, 1144-1150.
• Eibl, B., Ebner, S., Duba, C., Bock, G., Romani, N., Erdel, M., Gachter, A., Niederwieser, D., and Schuler, G. (1997). Dendritic cells generated from blood precursors of chronic myelogenous leukemia patients carry the Philadelphia translocation and can induce a CML-specific primary cytotoxic T-cell response. Genes Chromosomes Cancer 20, 215-223.
• Eisendle, K., Lang, A., Eibl, B., Nachbaur, D., Glassl, H., Fiegl, M., Thaler, J., and Gastl, G. (2003). Phenotypic and functional deficiencies of leukaemic dendritic cells from patients with chronic myeloid leukaemia. Br J Haematol 120, 63-73.
• Elgert, K. D., Alleva, D. G., and Mullins, D. W. (1998). Tumor-induced immune dysfunction: the macrophage connection. J Leukoc Biol 64, 275-290.
• Emanuel, P. D., Bates, L. J., Castleberry, R. P., Gualtieri, R. J., and Zuckerman, K. S. (1991). Selective hypersensitivity to granulocyte-macrophage colony-stimulating factor by juvenile chronic myeloid leukemia hematopoietic progenitors. Blood 77, 925-929.
• Emanuel, P. D., Shannon, K. M., and Castleberry, R. P. (1996). Juvenile myelomonocytic leukemia: molecular understanding and prospects for therapy. Mol Med Today 2, 468-475.
• Emanuel, P. D., Snyder, R. C., Wiley, T., Gopurala, B., and Castleberry, R. P. (2000). Inhibition of juvenile myelomonocytic leukemia cell growth in vitro by farnesyltransferase inhibitors. Blood 95, 639-645.
• Epstein, D. J., Vekemans, M., and Gros, P. (1991). Splotch (Sp2H), a mutation affecting development of the mouse neural tube, shows a deletion within the paired homeodomain of Pax-3. Cell 67, 767-774.
• Epstein, J. A., Lam, P., Jepeal, L., Maas, R. L., and Shapiro, D. N. (1995). Pax3 inhibits myogenic differentiation of cultured myoblast cells. J Biol Chem 270, 11719-11722.
• Epstein, J. A., Shapiro, D. N., Cheng, J., Lam, P. Y., and Maas, R. L. (1996). Pax3 modulates expression of the c-Met receptor during limb muscle development. Proc Natl Acad Sci U S A 93, 4213-4218.
• Epstein, J. A., Song, B., Lakkis, M., and Wang, C. (1998). Tumor-specific PAX3-FKHR transcription factor, but not PAX3, activates the platelet-derived growth factor alpha receptor. Mol Cell Biol 18, 4118-4130.
• Escalier, D., and Garchon, H. J. (2000). XMR is associated with the asynapsed segments of sex chromosomes in the XY body of mouse primary spermatocytes. Chromosoma 109, 259-265.
• Evans, R. (1983). Combination therapy by using cyclophosphamide and tumor-sensitized lymphocytes: a possible mechanism of action. J Immunol 130, 2511-2513.

• Fanger, N. A., Maliszewski, C. R., Schooley, K., and Griffith, T. S. (1999). Human dendritic cells mediate cellular apoptosis via tumor necrosis factor-related apoptosis-inducing ligand (TRAIL). J Exp Med 190, 1155-1164.
• Fenton, R. G., and Longo, D. L. (1995). Genetic instability and tumor cell variation: implications for immunotherapy. J Natl Cancer Inst 87, 241-243.
• Ferlazzo, G., Tsang, M. L., Moretta, L., Melioli, G., Steinman, R. M., and Munz, C. (2002). Human dendritic cells activate resting natural killer (NK) cells and are recognized via the NKp30 receptor by activated NK cells. J Exp Med 195, 343-351.
• Fernandez, N. C., Lozier, A., Flament, C., Ricciardi-Castagnoli, P., Bellet, D., Suter, M., Perricaudet, M., Tursz, T., Maraskovsky, E., and Zitvogel, L. (1999). Dendritic cells directly trigger NK cell functions: cross-talk relevant in innate anti-tumor immune responses in vivo. Nat Med 5, 405-411.
• Ferrone, S., and Marincola, F. M. (1995). Loss of HLA class I antigens by melanoma cells: molecular mechanisms, functional significance and clinical relevance. Immunol Today 16, 487-494.
• Fields, R. C., Shimizu, K., and Mule, J. J. (1998). Murine dendritic cells pulsed with whole tumor lysates mediate potent antitumor immune responses in vitro and in vivo. Proc Natl Acad Sci U S A 95, 9482-9487.
• Finn, O. J. (2003). Cancer vaccines: between the idea and the reality. Nat Rev Immunol 3, 630-641.
• Fisher, C. (1990). The value of electronmicroscopy and immunohistochemistry in the diagnosis of soft tissue sarcomas: a study of 200 cases. Histopathology 16, 441-454.
• Fletcher, C. D. (1995). Immunohistochemistry in diagnosis of soft tissue sarcomas and new techniques in soft tissue tumour pathology. Recent Results Cancer Res 138, 17-24.
• Flotho, C., Valcamonica, S., Mach-Pascual, S., Schmahl, G., Corral, L., Ritterbach, J., Hasle, H., Arico, M., Biondi, A., and Niemeyer, C. M. (1999). RAS mutations and clonality analysis in children with juvenile myelomonocytic leukemia (JMML). Leukemia 13, 32-37.
• Foley, E. J. (1953). Antigenic properties of methylcholanthrene-induced tumors in mice of the strain of origin. Cancer Res 13, 835-837.
• Fong, L., Brockstedt, D., Benike, C., Wu, L., and Engleman, E. G. (2001). Dendritic cells injected via different routes induce immunity in cancer patients. J Immunol 166, 4254-4259.
• Forus, A., Florenes, V. A., Maelandsmo, G. M., Meltzer, P. S., Fodstad, O., and Myklebost, O. (1993). Mapping of amplification units in the q13-14 region of chromosome 12 in human sarcomas: some amplica do not include MDM2. Cell Growth Differ 4, 1065-1070.
• Frascella, E., Toffolatti, L., and Rosolen, A. (1998). Normal and rearranged PAX3 expression in human rhabdomyosarcoma. Cancer Genet Cytogenet 102, 104-109.
• Fredericks, W. J., Galili, N., Mukhopadhyay, S., Rovera, G., Bennicelli, J., Barr, F. G., and Rauscher, F. J., 3rd (1995). The PAX3-FKHR fusion protein created by the t(2;13) translocation in alveolar rhabdomyosarcomas is a more potent transcriptional activator than PAX3. Mol Cell Biol 15, 1522-1535.
• Freeburn, R. W., Gale, R. E., Wagner, H. M., and Linch, D. C. (1997). Analysis of the coding sequence for the GM-CSF receptor alpha and beta chains in patients with juvenile chronic myeloid leukemia (JCML). Exp Hematol 25, 306-311.
• Frolkis, M., Fischer, M. B., Wang, Z., Lebkowski, J. S., Chiu, C. P., and Majumdar, A. S. (2003). Dendritic cells reconstituted with human telomerase gene induce potent cytotoxic T-cell response against different types of tumors. Cancer Gene Ther 10, 239-249.

• Fujii, S., Fujimoto, K., Shimizu, K., Ezaki, T., Kawano, F., Takatsuki, K., Kawakita, M., and Matsuno, K. (1999). Presentation of tumor antigens by phagocytic dendritic cell clusters generated from human CD34+ hematopoietic progenitor cells: induction of autologous cytotoxic T lymphocytes against leukemic cells in acute myelogenous leukemia patients. Cancer Res 59, 2150-2158.
• Furuyama, T., Nakazawa, T., Nakano, I., and Mori, N. (2000). Identification of the differential distribution patterns of mRNAs and consensus binding sequences for mouse DAF-16 homologues. Biochem J 349, 629-634.
• Gagnon, E., Duclos, S., Rondeau, C., Chevet, E., Cameron, P. H., Steele-Mortimer, O., Paiement, J., Bergeron, J. J., and Desjardins, M. (2002). Endoplasmic reticulum-mediated phagocytosis is a mechanism of entry into macrophages. Cell 110, 119-131.
• Galibert, M. D., Yavuzer, U., Dexter, T. J., and Goding, C. R. (1999). Pax3 and regulation of the melanocyte-specific tyrosinase-related protein-1 promoter. J Biol Chem 274, 26894-26900.
• Galili, N., Davis, R. J., Fredericks, W. J., Mukhopadhyay, S., Rauscher, F. J., 3rd, Emanuel, B. S., Rovera, G., and Barr, F. G. (1993). Fusion of a fork head domain gene to PAX3 in the solid tumour alveolar rhabdomyosarcoma. Nat Genet 5, 230-235.
• Gallucci, S., Lolkema, M., and Matzinger, P. (1999). Natural adjuvants: endogenous activators of dendritic cells. Nat Med 5, 1249-1255.
• Gallucci, S., and Matzinger, P. (2001). Danger signals: SOS to the immune system. Curr Opin Immunol 13, 114-119.
• Gao, J. X., Liu, X., Wen, J., Caligiuri, M. A., Stroynowski, I., Zheng, P., and Liu, Y. (2003). Two-signal requirement for activation and effector function of natural killer cell response to allogeneic tumor cells. Blood 102, 4456-4463.
• Garcia-Hernandez, M. L., Hernandez-Pando, R., Gariglio, P., and Berumen, J. (2002). Interleukin-10 promotes B16-melanoma growth by inhibition of macrophage functions and induction of tumour and vascular cell proliferation. Immunology 105, 231-243.
• Garrido, F., Ruiz-Cabello, F., Cabrera, T., Perez-Villar, J. J., Lopez-Botet, M., Duggan-Keen, M., and Stern, P. L. (1997). Implications for immunosurveillance of altered HLA class I phenotypes in human tumours. Immunol Today 18, 89-95.
• Germain, R. N., and Margulies, D. H. (1993). The biochemistry and cell biology of antigen processing and presentation. Annu Rev Immunol 11, 403-450.
• Germain, R. N. (1995). The biochemistry and cell biology of antigen presentation by MHC class I and class II molecules. Implications for development of combination vaccines. Ann N Y Acad Sci 754, 114-125.
• Gerosa, F., Baldani-Guerra, B., Nisii, C., Marchesini, V., Carra, G., and Trinchieri, G. (2002). Reciprocal activating interaction between natural killer cells and dendritic cells. J Exp Med 195, 327-333.
• Gibbs, J. B., Oliff, A., and Kohl, N. E. (1994) Farnesyltransferase inhibitors: Ras research yields a potential cancer therapeutic. Cell 77, 175-178.
• Gil-Benso, R., Lopez-Gines, C., Carda, C., Lopez-Guerrero, J. A., Ferrer, J., Pellin-Perez, A., and Llombart-Bosch, A. (2003). Cytogenetic and molecular findings related to rhabdomyosarcoma. An analysis of seven cases. Cancer Genet Cytogenet 144, 125-133.
• Gilboa, E. (1999). The makings of a tumor rejection antigen. Immunity 11, 263-270.
• Gilley, J., Coffer, P. J., and Ham, J. (2003). FOXO transcription factors directly activate bim gene expression and promote apoptosis in sympathetic neurons. J Cell Biol 162, 613-622.
• Ginsberg, J. P., Davis, R. J., Bennicelli, J. L., Nauta, L. E., and Barr, F. G. (1998). Up-regulation of MET but not neural cell adhesion molecule expression by the PAX3-FKHR fusion protein in alveolar rhabdomyosarcoma. Cancer Res 58, 3542-3546.

• Goldszmid, R. S., Idoyaga, J., Bravo, A. I., Steinman, R., Mordoh, J., and Wainstok, R. (2003). Dendritic cells charged with apoptotic tumor cells induce long-lived protective CD4+ and CD8+ T cell immunity against B16 melanoma. J Immunol 171, 5940-5947.
• Gong, J., Chen, D., Kashiwaba, M., and Kufe, D. (1997). Induction of antitumor activity by immunization with fusions of dendritic and carcinoma cells. Nat Med 3, 558-561.
• Goodnow, C. C. (1997). Balancing immunity, autoimmunity, and self-tolerance. Ann N Y Acad Sci 815, 55-66.
• Goriely, S., Vincart, B., Stordeur, P., Vekemans, J., Willems, F., Goldman, M., and De Wit, D. (2001). Deficient IL-12(p35) gene expression by dendritic cells derived from neonatal monocytes. J Immunol 166, 2141-2146.
• Goulding, M. D., Chalepakis, G., Deutsch, U., Erselius, J. R., and Gruss, P. (1991). Pax-3, a novel murine DNA binding protein expressed during early neurogenesis. Embo J 10, 1135-1147.
• Goulding, M., Sterrer, S., Fleming, J., Balling, R., Nadeau, J., Moore, K. J., Brown, S. D., Steel, K. P., and Gruss, P. (1993). Analysis of the Pax-3 gene in the mouse mutant splotch. Genomics 17, 355-363.
• Goulmy, E. (1997). Human minor histocompatibility antigens: new concepts for marrow transplantation and adoptive immunotherapy. Immunol Rev 157, 125-140.
• Granucci, F., Zanoni, I., Feau, S., and Ricciardi-Castagnoli, P. (2003). Dendritic cell regulation of immune responses: a new role for interleukin 2 at the intersection of innate and adaptive immunity. Embo J 22, 2546-2551.
• Groh, V., Rhinehart, R., Secrist, H., Bauer, S., Grabstein, K. H., and Spies, T. (1999). Broad tumor-associated expression and recognition by tumor-derived gamma delta T cells of MICA and MICB. Proc Natl Acad Sci U S A 96, 6879-6884.
• Gromme, M., Uytdehaag, F. G., Janssen, H., Calafat, J., van Binnendijk, R. S., Kenter, M. J., Tulp, A., Verwoerd, D., and Neefjes, J. (1999). Recycling MHC class I molecules and endosomal peptide loading. Proc Natl Acad Sci U S A 96, 10326-10331.
• Grunebach, F., Muller, M. R., Nencioni, A., and Brossart, P. (2003). Delivery of tumor-derived RNA for the induction of cytotoxic T-lymphocytes. Gene Ther 10, 367-374.
• Gualtieri, R. J., Emanuel, P. D., Zuckerman, K. S., Martin, G., Clark, S. C., Shadduck, R. K., Dracker, R. A., Akabutu, J., Nitschke, R., Hetherington, M. L., and et al. (1989).
• Granulocyte-macrophage colony-stimulating factor is an endogenous regulator of cell proliferation in juvenile chronic myelogenous leukemia. Blood 74, 2360-2367.
• Gunzer, M., Janich, S., Varga, G., and Grabbe, S. (2001). Dendritic cells and tumor immunity. Semin Immunol 13, 291-302.
• Guo, S., Rena, G., Cichy, S., He, X., Cohen, P., and Unterman, T. (1999). Phosphorylation of serine 256 by protein kinase B disrupts transactivation by FKHR and mediates effects of insulin on insulin-like growth factor-binding protein-1 promoter activity through a conserved insulin response sequence. J Biol Chem 274, 17184-17192.
• Gupta, S. K., Lysko, P. G., Pillarisetti, K., Ohlstein, E., and Stadel, J. M. (1998). Chemokine receptors in human endothelial cells. Functional expression of CXCR4 and its transcriptional regulation by inflammatory cytokines. J Biol Chem 273, 4282-4287.
• Gurunathan, S., Wu, C. Y., Freidag, B. L., and Seder, R. A. (2000). DNA vaccines: a key for inducing long-term cellular immunity. Curr Opin Immunol 12, 442-447.
• Gutmann, D. H., James, C. D., Poyhonen, M., Louis, D. N., Ferner, R., Guha, A., Hariharan, S., Viskochil, D., and Perry, A. (2003). Molecular analysis of astrocytomas presenting after age 10 in individuals with NF1. Neurology 61, 1397-1400.

• Haenssle, H. A., Krause, S. W., Emmert, S., Zutt, M., Kretschmer, L., Schmidberger, H., Andreesen, R., and Soruri, A. (2004). Hybrid cell vaccination in metastatic melanoma: clinical and immunologic results of a phase I/II study. J Immunother 27, 147-155.
• Hafner, M., Zawatzky, R., Hirtreiter, C., Buurman, W. A., Echtenacher, B., Hehlgans, T., and Mannel, D. N. (2001). Antimetastatic effect of CpG DNA mediated by type I IFN. Cancer Res 61, 5523-5528.
• Hahn, S., Gehri, R., and Erb, P. (1995). Mechanism and biological significance of CD4-mediated cytotoxicity. Immunol Rev 146, 57-79.
• Halder, T. M., Bluggel, M., Heinzel, S., Pawelec, G., Meyer, H. E., and Kalbacher, H. (2000). Defensins are dominant HLA-DR-associated self-peptides from CD34(-) peripheral blood mononuclear cells of different tumor patients (plasmacytoma, chronic myeloid leukemia). Blood 95, 2890-2896.
• Hallermalm, K., Seki, K., Wei, C., Castelli, C., Rivoltini, L., Kiessling, R., and Levitskaya, J. (2001). Tumor necrosis factor-alpha induces coordinated changes in major histocompatibility class I presentation pathway, resulting in increased stability of class I complexes at the cell surface. Blood 98, 1108-1115.
• Harbeck, N., Kates, R. E., Look, M. P., Meijer-Van Gelder, M. E., Klijn, J. G., Kruger, A., Kiechle, M., Janicke, F., Schmitt, M., and Foekens, J. A. (2002). Enhanced benefit from adjuvant chemotherapy in breast cancer patients classified high-risk according to urokinase-type plasminogen activator (uPA) and plasminogen activator inhibitor type 1 (n = 3424). Cancer Res 62, 4617-4622.
• Harding, F. A., McArthur, J. G., Gross, J. A., Raulet, D. H., and Allison, J. P. (1992). CD28-mediated signalling co-stimulates murine T cells and prevents induction of anergy in T-cell clones. Nature 356, 607-609.
• Harrison, B. D., Adams, J. A., Briggs, M., Brereton, M. L., and Yin, J. A. (2001). Stimulation of autologous proliferative and cytotoxic T-cell responses by "leukemic dendritic cells" derived from blast cells in acute myeloid leukemia. Blood 97, 2764-2771.
• Hasle, H., Arico, M., Basso, G., Biondi, A., Cantu Rajnoldi, A., Creutzig, U., Fenu, S., Fonatsch, C., Haas, O. A., Harbott, J., et al. (1999). Myelodysplastic syndrome, juvenile myelomonocytic leukemia, and acute myeloid leukemia associated with complete or partial monosomy 7. European Working Group on MDS in Childhood (EWOG-MDS). Leukemia 13, 376-385.
• He, L., Feng, H., Raymond, A., Kreeger, M., Zeng, Y., Graner, M., Whitesell, L., and Katsanis, E. (2001). Dendritic-cell-peptide immunization provides immunoprotection against bcr-abl-positive leukemia in mice. Cancer Immunol Immunother 50, 31-40.
• Heiser, A., Coleman, D., Dannull, J., Yancey, D., Maurice, M. A., Lallas, C. D., Dahm, P., Niedzwiecki, D., Gilboa, E., and Vieweg, J. (2002). Autologous dendritic cells transfected with prostate-specific antigen RNA stimulate CTL responses against metastatic prostate tumors. J Clin Invest 109, 409-417.
• Heisterkamp, N., Stam, K., Groffen, J., de Klein, A., and Grosveld, G. (1985). Structural organization of the bcr gene and its role in the Ph' translocation. Nature 315, 758-761.
• Hernandez, L., Kozlov, S., Piras, G., and Stewart, C. L. (2003). Paternal and maternal genomes confer opposite effects on proliferation, cell-cycle length, senescence, and tumor formation. Proc Natl Acad Sci U S A 100, 13344-13349.
• Ho, W. Y., Blattman, J. N., Dossett, M. L., Yee, C., and Greenberg, P. D. (2003). Adoptive immunotherapy: engineering T cell responses as biologic weapons for tumor mass destruction. Cancer Cell 3, 431-437.

• Hollenbach, A. D., Sublett, J. E., McPherson, C. J., and Grosveld, G. (1999). The Pax3-FKHR oncoprotein is unresponsive to the Pax3-associated repressor hDaxx. Embo J 18, 3702-3711.
• Holtl, L., Rieser, C., Papesh, C., Ramoner, R., Herold, M., Klocker, H., Radmayr, C., Stenzl, A., Bartsch, G., and Thurnher, M. (1999). Cellular and humoral immune responses in patients with metastatic renal cell carcinoma after vaccination with antigen pulsed dendritic cells. J Urol 161, 777-782.
• Holtl, L., Zelle-Rieser, C., Gander, H., Papesh, C., Ramoner, R., Bartsch, G., Rogatsch, H., Barsoum, A. L., Coggin, J. H., Jr., and Thurnher, M. (2002). Immunotherapy of metastatic renal cell carcinoma with tumor lysate-pulsed autologous dendritic cells. Clin Cancer Res 8, 3369-3376.
• Hovey, R. C., Harris, J., Hadsell, D. L., Lee, A. V., Ormandy, C. J., and Vonderhaar, B. K. (2003). Local insulin-like growth factor-II mediates prolactin-induced mammary gland development. Mol Endocrinol 17, 460-471.
• Hromas, R., and Costa, R. (1995). The hepatocyte nuclear factor-3/forkhead transcription regulatory family in development, inflammation, and neoplasia. Crit Rev Oncol Hematol 20, 129-140.
• Hsu, F. J., Benike, C., Fagnoni, F., Liles, T. M., Czerwinski, D., Taidi, B., Engleman, E. G., and Levy, R. (1996). Vaccination of patients with B-cell lymphoma using autologous antigen-pulsed dendritic cells. Nat Med 2, 52-58.
• Huang, A. Y., Golumbek, P., Ahmadzadeh, M., Jaffee, E., Pardoll, D., and Levitsky, H. (1994). Role of bone marrow-derived cells in presenting MHC class I-restricted tumor antigens. Science 264, 961-965.
• Huang, A. Y., Gulden, P. H., Woods, A. S., Thomas, M. C., Tong, C. D., Wang, W., Engelhard, V. H., Pasternack, G., Cotter, R., Hunt, D., et al. (1996). The immunodominant major histocompatibility complex class I-restricted antigen of a murine colon tumor derives from an endogenous retroviral gene product. Proc Natl Acad Sci U S A 93, 9730-9735.
• Hung, K., Hayashi, R., Lafond-Walker, A., Lowenstein, C., Pardoll, D., and Levitsky, H. (1998). The central role of CD4(+) T cells in the antitumor immune response. J Exp Med 188, 2357-2368.
• Inaba, K., Inaba, M., Naito, M., and Steinman, R. M. (1993). Dendritic cell progenitors phagocytose particulates, including bacillus Calmette-Guerin organisms, and sensitize mice to mycobacterial antigens in vivo. J Exp Med 178, 479-488.
• Inaba, K., Swiggard, W. J., Inaba, M., Meltzer, J., Mirza, A., Sasagawa, T., Nussenzweig, M. C., and Steinman, R. M. (1995). Tissue distribution of the DEC-205 protein that is detected by the monoclonal antibody NLDC-145. I. Expression on dendritic cells and other subsets of mouse leukocytes. Cell Immunol 163, 148-156.
• Ito, T., Inaba, M., Inaba, K., Toki, J., Sogo, S., Iguchi, T., Adachi, Y., Yamaguchi, K., Amakawa, R., Valladeau, J., et al. (1999). A CD1a+/CD11c+ subset of human blood dendritic cells is a direct precursor of Langerhans cells. J Immunol 163, 1409-1419.
• Iversen, P. O., Lewis, I. D., Turczynowicz, S., Hasle, H., Niemeyer, C., Schmiegelow, K., Bastiras, S., Biondi, A., Hughes, T. P., and Lopez, A. F. (1997). Inhibition of granulocyte-macrophage colony-stimulating factor prevents dissemination and induces remission of juvenile myelomonocytic leukemia in engrafted immunodeficient mice. Blood 90, 4910-4917.
• Iversen, P. O., and Sioud, M. (1998). Modulation of granulocyte-macrophage colony-stimulating factor gene expression by a tumor necrosis factor specific ribozyme in juvenile myelomonocytic leukemic cells. Blood 92, 4263-4268.

• Iversen, P. O., Emanuel, P. D., and Sioud, M. (2002). Targeting Raf-1 gene expression by a DNA enzyme inhibits juvenile myelomonocytic leukemia cell growth. Blood 99, 4147-4153.
• Jacks, T., Shih, T. S., Schmitt, E. M., Bronson, R. T., Bernards, A., and Weinberg, R. A. (1994). Tumour predisposition in mice heterozygous for a targeted mutation in Nf1. Nat Genet 7, 353-361.
• Jackson, J. G., Kreisberg, J. I., Koterba, A. P., Yee, D., and Brattain, M. G. (2000). Phosphorylation and nuclear exclusion of the forkhead transcription factor FKHR after epidermal growth factor treatment in human breast cancer cells. Oncogene 19, 4574-4581.
• Jagla, K., Dolle, P., Mattei, M. G., Jagla, T., Schuhbaur, B., Dretzen, G., Bellard, F., and Bellard, M. (1995). Mouse Lbx1 and human LBX1 define a novel mammalian homeobox gene family related to the Drosophila lady bird genes. Mech Dev 53, 345-356.
• Jakob, T., Walker, P. S., Krieg, A. M., Udey, M. C., and Vogel, J. C. (1998). Activation of cutaneous dendritic cells by CpG-containing oligodeoxynucleotides: a role for dendritic cells in the augmentation of Th1 responses by immunostimulatory DNA. J Immunol 161, 3042-3049.
• Janeway, C. A., Jr. (1992). The immune system evolved to discriminate infectious nonself from noninfectious self. Immunol Today 13, 11-16.
• Janeway, C. A., Jr. et al (1999). Immunobiology, Vol 4 (London, Current Biology Publications).
• Jenne, L., Arrighi, J. F., Jonuleit, H., Saurat, J. H., and Hauser, C. (2000). Dendritic cells containing apoptotic melanoma cells prime human CD8+ T cells for efficient tumor cell lysis. Cancer Res 60, 4446-4452.
• Jiang, Y. Z., Mavroudis, D., Dermime, S., Hensel, N., Couriel, D., Molldrem, J., and Barrett, A. J. (1996). Alloreactive CD4+ T lymphocytes can exert cytotoxicity to chronic myeloid leukaemia cells processing and presenting exogenous antigen. Br J Haematol 93, 606-612.
• Jiang, J., Neubauer, B. L., Graff, J. R., Chedid, M., Thomas, J. E., Roehm, N. W., Zhang, S., Eckert, G. J., Koch, M. O., Eble, J. N., and Cheng, L. (2002). Expression of group IIA secretory phospholipase A2 is elevated in prostatic intraepithelial neoplasia and adenocarcinoma. Am J Pathol 160, 667-671.
• Kagi, D., Vignaux, F., Ledermann, B., Burki, K., Depraetere, V., Nagata, S., Hengartner, H., and Golstein, P. (1994). Fas and perforin pathways as major mechanisms of T cell-mediated cytotoxicity. Science 265, 528-530.
• Kalra, R., Paderanga, D. C., Olson, K., and Shannon, K. M. (1994). Genetic analysis is consistent with the hypothesis that NF1 limits myeloid cell growth through p21ras. Blood 84, 3435-3439.
• Kaplan, D. H., Shankaran, V., Dighe, A. S., Stockert, E., Aguet, M., Old, L. J., and Schreiber, R. D. (1998). Demonstration of an interferon gamma-dependent tumor surveillance system in immunocompetent mice. Proc Natl Acad Sci U S A 95, 7556-7561.
• Karre, K., Ljunggren, H. G., Piontek, G., and Kiessling, R. (1986). Selective rejection of H-2-deficient lymphoma variants suggests alternative immune defence strategy. Nature 319, 675-678.
• Keleti, J., Quezado, M. M., Abaza, M. M., Raffeld, M., and Tsokos, M. (1996). The MDM2 oncoprotein is overexpressed in rhabdomyosarcoma cell lines and stabilizes wild-type p53 protein. Am J Pathol 149, 143-151.

• Kelly, K. M., Womer, R. B., Sorensen, P. H., Xiong, Q. B., and Barr, F. G. (1997). Common and variant gene fusions predict distinct clinical phenotypes in rhabdomyosarcoma. J Clin Oncol 15, 1831-1836.
• Kennedy, R. C., and Shearer, M. H. (2003). A role for antibodies in tumor immunity. Int Rev Immunol 22, 141-172.
• Kerr, I. M., Costa-Pereira, A. P., Lillemeier, B. F., and Strobl, B. (2003). Of JAKs, STATs, blind watchmakers, jeeps and trains. FEBS Lett 546, 1-5.
• Kershaw, M. H., Hsu, C., Mondesire, W., Parker, L. L., Wang, G., Overwijk, W. W., Lapointe, R., Yang, J. C., Wang, R. F., Restifo, N. P., and Hwu, P. (2001). Immunization against endogenous retroviral tumor-associated antigens. Cancer Res 61, 7920-7924.
• Kessels, H. W., Wolkers, M. C., van den Boom, M. D., van der Valk, M. A., and Schumacher, T. N. (2001). Immunotherapy through TCR gene transfer. Nat Immunol 2, 957-961.
• Keyomarsi, K., and Pardee, A. B. (1993). Redundant cyclin overexpression and gene amplification in breast cancer cells. Proc Natl Acad Sci U S A 90, 1112-1116.
• Khan, J., Simon, R., Bittner, M., Chen, Y., Leighton, S. B., Pohida, T., Smith, P. D., Jiang, Y., Gooden, G. C., Trent, J. M., and Meltzer, P. S. (1998). Gene expression profiling of alveolar rhabdomyosarcoma with cDNA microarrays. Cancer Res 58, 5009-5013.
• Khan, J., Bittner, M. L., Saal, L. H., Teichmann, U., Azorsa, D. O., Gooden, G. C., Pavan, W. J., Trent, J. M., and Meltzer, P. S. (1999). cDNA microarrays detect activation of a myogenic transcription program by the PAX3-FKHR fusion oncogene. Proc Natl Acad Sci U S A 96, 13264-13269.
• Kiertscher, S. M., and Roth, M. D. (1996). Human CD14+ leukocytes acquire the phenotype and function of antigen-presenting dendritic cells when cultured in GM-CSF and IL-4. J Leukoc Biol 59, 208-218.
• Kikuchi, T., Akasaki, Y., Irie, M., Homma, S., Abe, T., and Ohno, T. (2001). Results of a phase I clinical trial of vaccination of glioma patients with fusions of dendritic and glioma cells. Cancer Immunol Immunother 50, 337-344.
• Kim, N. W., Piatyszek, M. A., Prowse, K. R., Harley, C. B., West, M. D., Ho, P. L., Coviello, G. M., Wright, W. E., Weinrich, S. L., and Shay, J. W. (1994). Specific association of human telomerase activity with immortal cells and cancer. Science 266, 2011-2015.
• King, C. A., Spellerberg, M. B., Zhu, D., Rice, J., Sahota, S. S., Thompsett, A. R., Hamblin, T. J., Radl, J., and Stevenson, F. K. (1998). DNA vaccines with single-chain Fv fused to fragment C of tetanus toxin induce protective immunity against lymphoma and myeloma. Nat Med 4, 1281-1286.
• Kitamura, H., Iwakabe, K., Yahata, T., Nishimura, S., Ohta, A., Ohmi, Y., Sato, M., Takeda, K., Okumura, K., Van Kaer, L., et al. (1999). The natural killer T (NKT) cell ligand alpha-galactosylceramide demonstrates its immunopotentiating effect by inducing interleukin (IL)-12 production by dendritic cells and IL-12 receptor expression on NKT cells. J Exp Med 189, 1121-1128.
• Kloetzel, P. M. (2004). Generation of major histocompatibility complex class I antigens: functional interplay between proteasomes and TPPII. Nat Immunol 5, 661-669.
• Kokhaei, P., Rezvany, M. R., Virving, L., Choudhury, A., Rabbani, H., Osterborg, A., and Mellstedt, H. (2003). Dendritic cells loaded with apoptotic tumour cells induce a stronger T-cell response than dendritic cell-tumour hybrids in B-CLL. Leukemia 17, 894-899.

• Kolb, H. J., Mittermuller, J., Clemm, C., Holler, E., Ledderose, G., Brehm, G., Heim, M., and Wilmanns, W. (1990). Donor leukocyte transfusions for treatment of recurrent chronic myelogenous leukemia in marrow transplant patients. Blood 76, 2462-2465.
• Kolb, H. J., Schattenberg, A., Goldman, J. M., Hertenstein, B., Jacobsen, N., Arcese, W., Ljungman, P., Ferrant, A., Verdonck, L., Niederwieser, D., and et al. (1995). Graft-versus-leukemia effect of donor lymphocyte transfusions in marrow grafted patients. European Group for Blood and Marrow Transplantation Working Party Chronic Leukemia. Blood 86, 2041-2050.
• Kops, G. J., de Ruiter, N. D., De Vries-Smits, A. M., Powell, D. R., Bos, J. L., and Burgering, B. M. (1999). Direct control of the Forkhead transcription factor AFX by protein kinase B. Nature 398, 630-634.
• Kortylewski, M., Feld, F., Kruger, K. D., Bahrenberg, G., Roth, R. A., Joost, H. G., Heinrich, P. C., Behrmann, I., and Barthel, A. (2003). Akt modulates STAT3-mediated gene expression through a FKHR (FOXO1a)-dependent mechanism. J Biol Chem 278, 5242-5249.
• Krieg, A. M., Yi, A. K., Matson, S., Waldschmidt, T. J., Bishop, G. A., Teasdale, R., Koretzky, G. A., and Klinman, D. M. (1995). CpG motifs in bacterial DNA trigger direct B-cell activation. Nature 374, 546-549.
• Krieg, A. M. (2002). CpG motifs in bacterial DNA and their immune effects. Annu Rev Immunol 20, 709-760.
• Kucharczuk, K. L., Love, C. M., Dougherty, N. M., and Goldhamer, D. J. (1999). Fine-scale transgenic mapping of the MyoD core enhancer: MyoD is regulated by distinct but overlapping mechanisms in myotomal and non-myotomal muscle lineages. Development 126, 1957-1965.
• Kugler, A., Stuhler, G., Walden, P., Zoller, G., Zobywalski, A., Brossart, P., Trefzer, U., Ullrich, S., Muller, C. A., Becker, V., et al. (2000). Regression of human metastatic renal cell carcinoma after vaccination with tumor cell-dendritic cell hybrids. Nat Med 6, 332-336.
• Kulaeva, O. I., Draghici, S., Tang, L., Kraniak, J. M., Land, S. J., and Tainsky, M. A. (2003). Epigenetic silencing of multiple interferon pathway genes after cellular immortalization. Oncogene 22, 4118-4127.
• Kwaan, H. C., Wang, J., Svoboda, K., and Declerck, P. J. (2000). Plasminogen activator inhibitor 1 may promote tumour growth through inhibition of apoptosis. Br J Cancer 82, 1702-1708.
• Labeur, M. S., Roters, B., Pers, B., Mehling, A., Luger, T. A., Schwarz, T., and Grabbe, S. (1999). Generation of tumor immunity by bone marrow-derived dendritic cells correlates with dendritic cell maturation stage. J Immunol 162, 168-175.
• Lafferty, K. J., and Cunningham, A. J. (1975). A new analysis of allogeneic interactions. Aust J Exp Biol Med Sci 53, 27-42.
Lagutina, I., Conway, S. J., Sublett, J., and Grosveld, G. C. (2002). Pax3-FKHR knock-in mice show developmental aberrations but do not develop tumors. Mol Cell Biol 22, 7204-7216.
• Lam, P. Y., Sublett, J. E., Hollenbach, A. D., and Roussel, M. F. (1999). The oncogenic potential of the Pax3-FKHR fusion protein requires the Pax3 homeodomain recognition helix but not the Pax3 paired-box DNA binding domain. Mol Cell Biol 19, 594-601.
• Lambert, L. A., Gibson, G. R., Maloney, M., Durell, B., Noelle, R. J., and Barth, R. J., Jr. (2001). Intranodal immunization with tumor lysate-pulsed dendritic cells enhances protective antitumor immunity. Cancer Res 61, 641-646.
•Lankat-Buttgereit, B., and Tampe, R. (2002). The transporter associated with antigen processing: function and implications in human diseases. Physiol Rev 82, 187-204.

• Largaespada, D. A., Brannan, C. I., Jenkins, N. A., and Copeland, N. G. (1996). Nf1 deficiency causes Ras-mediated granulocyte/macrophage colony stimulating factor hypersensitivity and chronic myeloid leukaemia. Nat Genet 12, 137-143.
• Lau, R. C., Squire, J., Brisson, L., Kamel-Reid, S., Grunberger, T., Dube, I., Letarte, M., Shannon, K., and Freedman, M. H. (1994). Lymphoid blast crisis of B-lineage phenotype with monosomy 7 in a patient with juvenile chronic myelogenous leukemia (JCML). Leukemia 8, 903-908.
• Lau, R., Wang, F., Jeffery, G., Marty, V., Kuniyoshi, J., Bade, E., Ryback, M. E., and Weber, J. (2001). Phase I trial of intravenous peptide-pulsed dendritic cells in patients with metastatic melanoma. J Immunother 24, 66-78.
• Lawlor, M. A., and Alessi, D. R. (2001). PKB/Akt: a key mediator of cell proliferation, survival and insulin responses? J Cell Sci 114, 2903-2910.
Lehmann, S., Paul, C., and Torma, H. (2002). The expression of cellular retinoid binding proteins in non-APL leukemic cells and its association with retinoid sensitivity. Leuk Lymphoma 43, 851-858.
• Lee, Y. I., Hur, G. M., Suh, D. J., and Kim, S. H. (1996). Novel pre-C/C gene mutants of hepatitis B virus in chronic active hepatitis: naturally occurring escape mutants. J Gen Virol 77 (Pt 6), 1129-1138.
• Libura, J., Drukala, J., Majka, M., Tomescu, O., Navenot, J. M., Kucia, M., Marquez, L., Peiper, S. C., Barr, F. G., Janowska-Wieczorek, A., and Ratajczak, M. Z. (2002). CXCR4-SDF-1 signaling is active in rhabdomyosarcoma cells and regulates locomotion, chemotaxis, and adhesion. Blood 100, 2597-2606.
• Lin, C. M., Wang, F. H., and Lee, P. K. (2002). Activated human CD4+ T cells induced by dendritic cell stimulation are most sensitive to transforming growth factor-beta: implications for dendritic cell immunization against cancer. Clin Immunol 102, 96-105.
• Liu, H. M., Newbrough, S. E., Bhatia, S. K., Dahle, C. E., Krieg, A. M., and Weiner, G. J. (1998). Immunostimulatory CpG oligodeoxynucleotides enhance the immune response to vaccine strategies involving granulocyte-macrophage colony-stimulating factor. Blood 92, 3730-3736.
• Liu, Y., and Linsley, P. S. (1992). Costimulation of T-cell growth. Curr Opin Immunol 4, 265-270.
• Liu, Y. J. (2001). Dendritic cell subsets and lineages, and their functions in innate and adaptive immunity. Cell 106, 259-262.
• Loh, M. L., Vattikuti, S., Schubbert, S., Reynolds, M. G., Carlson, E., Lieuw, K. H., Cheng, J. W., Lee, C. M., Stokoe, D., Bonifas, J. M., et al. (2004). Mutations in PTPN11 implicate the SHP-2 phosphatase in leukemogenesis. Blood 103, 2325-2331.
• Long, E. O. (1999). Regulation of immune responses through inhibitory receptors. Annu Rev Immunol 17, 875-904.
• Longoni, D., D'Amico, G., Gaipa, G., Bernasconi, S., Vulcano, M., Onnis, P., Niemeyer, C. M., Allavena, P., and Biondi, A. (2002). Commitment of juvenile myelo-monocytic (JMML) leukemic cells to spontaneously differentiate into dendritic cells. Hematol J 3, 302-310.
• Lower, R., Lower, J., and Kurth, R. (1996). The viruses in all of us: characteristics and biological significance of human endogenous retrovirus sequences. Proc Natl Acad Sci U S A 93, 5177-5184.
• Lu, Y. J., Williamson, D., Clark, J., Wang, R., Tiffin, N., Skelton, L., Gordon, T., Williams, R., Allan, B., Jackman, A., et al. (2001). Comparative expressed sequence hybridization to chromosomes for tumor classification and identification of genomic regions of differential gene expression. Proc Natl Acad Sci U S A 98, 9197-9202.

• Luft, T., Rizkalla, M., Tai, T. Y., Chen, Q., MacFarlan, R. I., Davis, I. D., Maraskovsky, E., and Cebon, J. (2001). Exogenous peptides presented by transporter associated with antigen processing (TAP)-deficient and TAP-competent cells: intracellular loading and kinetics of presentation. J Immunol 167, 2529-2537.
• Luna-Fineman, S., Shannon, K. M., Atwater, S. K., Davis, J., Masterson, M., Ortega, J., Sanders, J., Steinherz, P., Weinberg, V., and Lange, B. J. (1999). Myelodysplastic and myeloproliferative disorders of childhood: a study of 167 patients. Blood 93, 459-466.
• Lynch, R. G., Rohrer, J. W., Odermatt, B., Gebel, H. M., Autry, J. R., and Hoover, R. G. (1979). Immunoregulation of murine myeloma cell growth and differentiation: a monoclonal model of B cell differentiation. Immunol Rev 48, 45-80.
• MacDonald, H. R. (1995). NK1.1+ T cell receptor-alpha/beta+ cells: new clues to their origin, specificity, and function. J Exp Med 182, 633-638.
• MacDonald, K. P., Munster, D. J., Clark, G. J., Dzionek, A., Schmitz, J., and Hart, D. N. (2002). Characterization of human blood dendritic cell subsets. Blood 100, 4512-4520.
• Mackall, C., Berzofsky, J., and Helman, L. J. (2000). Targeting tumor specific translocations in sarcomas in pediatric patients for immunotherapy. Clin Orthop, 25-31.
• Manabe, A., Okamura, J., Yumura-Yagi, K., Akiyama, Y., Sako, M., Uchiyama, H., Kojima, S., Koike, K., Saito, T., and Nakahata, T. (2002). Allogeneic hematopoietic stem cell transplantation for 27 children with juvenile myelomonocytic leukemia diagnosed based on the criteria of the International JMML Working Group. Leukemia 16, 645-649.
• Maniotis, A. J., Folberg, R., Hess, A., Seftor, E. A., Gardner, L. M., Pe'er, J., Trent, J. M., Meltzer, P. S., and Hendrix, M. J. (1999). Vascular channel formation by human melanoma cells in vivo and in vitro: vasculogenic mimicry. Am J Pathol 155, 739-752.
• Marchand, M., Weynants, P., Rankin, E., Arienti, F., Belli, F., Parmiani, G., Cascinelli, N., Bourlond, A., Vanwijck, R., and Humblet, Y. (1995). Tumor regression responses in melanoma patients treated with a peptide encoded by gene MAGE-3. Int J Cancer 63, 883-885.
• Margue, C. M., Bernasconi, M., Barr, F. G., and Schafer, B. W. (2000). Transcriptional modulation of the anti-apoptotic protein BCL-XL by the paired box transcription factors PAX3 and PAX3/FKHR. Oncogene 19, 2921-2929.
• Marmont, A. M., Horowitz, M. M., Gale, R. P., Sobocinski, K., Ash, R. C., van Bekkum, D. W., Champlin, R. E., Dicke, K. A., Goldman, J. M., Good, R. A., and et al. (1991). T-cell depletion of HLA-identical transplants in leukemia. Blood 78, 2120-2130.
• Matthes-Martin, S., Mann, G., Peters, C., Lion, T., Fritsch, G., Haas, O. A., Potschger, U., and Gadner, H. (2000). Allogeneic bone marrow transplantation for juvenile myelomonocytic leukaemia: a single centre experience and review of the literature. Bone Marrow Transplant 26, 377-382.
• Matzinger, P. (1994). Tolerance, danger, and the extended family. Annu Rev Immunol 12, 991-1045.
• Maulbecker, C. C., and Gruss, P. (1993). The oncogenic potential of Pax genes. Embo J 12, 2361-2367.
• Mauro, A., Ciccarelli, C., De Cesaris, P., Scoglio, A., Bouche, M., Molinaro, M., Aquino, A., and Zani, B. M. (2002). PKCalpha-mediated ERK, JNK and p38 activation regulates the myogenic program in human rhabdomyosarcoma cells. J Cell Sci 115, 3587-3599.

• May, W. A., Lessnick, S. L., Braun, B. S., Klemsz, M., Lewis, B. C., Lunsford, L. B., Hromas, R., and Denny, C. T. (1993). The Ewing's sarcoma EWS/FLI-1 fusion gene encodes a more potent transcriptional activator and is a more powerful transforming gene than FLI-1. Mol Cell Biol 13, 7393-7398.
• Mayanil, C. S., George, D., Mania-Farnell, B., Bremer, C. L., McLone, D. G., and Bremer, E. G. (2000). Overexpression of murine Pax3 increases NCAM polysialylation in a human medulloblastoma cell line. J Biol Chem 275, 23259-23266.
• Mayanil, C. S., George, D., Freilich, L., Miljan, E. J., Mania-Farnell, B., McLone, D. G., and Bremer, E. G. (2001). Microarray analysis detects novel Pax3 downstream target genes. J Biol Chem 276, 49299-49309.
• Mayer, M., Lund, L. R., Riccio, A., Skouv, J., Nielsen, L. S., Stacey, S. N., Dano, K., and Andreasen, P. A. (1988). Plasminogen activator inhibitor type-1 protein, mRNA and gene transcription are increased by phorbol esters in human rhabdomyosarcoma cells. J Biol Chem 263, 15688-15693.
• McKenzie, I. F., Apostolopoulos, V., Plebanski, M., Pietersz, G. A., and Loveland, B. E. (2003). Aspects of cancer immunotherapy. Immunol Cell Biol 81, 79-85.
• Medzhitov, R. (2001). Toll-like receptors and innate immunity. Nat Rev Immunol 1, 135-145.
• Melero, I., Vile, R. G., and Colombo, M. P. (2000). Feeding dendritic cells with tumor antigens: self-service buffet or a la carte? Gene Ther 7, 1167-1170.
• Melief, C. J. (2003). Mini-review: Regulation of cytotoxic T lymphocyte responses by dendritic cells: peaceful coexistence of cross-priming and direct priming? Eur J Immunol 33, 2645-2654.
• Mennerich, D., Schafer, K., and Braun, T. (1998). Pax-3 is necessary but not sufficient for lbx1 expression in myogenic precursor cells of the limb. Mech Dev 73, 147-158.
• Mennerich, D., and Braun, T. (2001). Activation of myogenesis by the homeobox gene Lbx1 requires cell proliferation. Embo J 20, 7174-7183.
• Metelitsa, L. S., Weinberg, K. I., Emanuel, P. D., and Seeger, R. C. (2003). Expression of CD1d by myelomonocytic leukemias provides a target for cytotoxic NKT cells. Leukemia 17, 1068-1077.
• Milazzo, C., Reichardt, V. L., Muller, M. R., Grunebach, F., and Brossart, P. (2003). Induction of myeloma-specific cytotoxic T cells using dendritic cells transfected with tumor-derived RNA. Blood 101, 977-982.
• Miller, G., Lahrs, S., Pillarisetty, V. G., Shah, A. B., and DeMatteo, R. P. (2002). Adenovirus infection enhances dendritic cell immunostimulatory properties and induces natural killer and T-cell-mediated tumor protection. Cancer Res 62, 5260-5266.
• Mineo, J. F., Bordron, A., Quintin-Roue, I., Loisel, S., Ster, K. L., Buhe, V., Lagarde, N., and Berthou, C. (2004). Recombinant humanised anti-HER2/neu antibody (Herceptin) induces cellular death of glioblastomas. Br J Cancer 91, 1195-1199.
• Mitchell, M. S. (1998). Perspective on allogeneic melanoma lysates in active specific immunotherapy. Semin Oncol 25, 623-635.
• Miyauchi, J., Asada, M., Tsunematsu, Y., Kaneko, Y., Kojima, S., and Mizutani, S. (1999). Abnormalities of the p53 gene in juvenile myelomonocytic leukaemia. Br J Haematol 106, 980-986.
• Mizoguchi, H., O'Shea, J. J., Longo, D. L., Loeffler, C. M., McVicar, D. W., and Ochoa, A. C. (1992). Alterations in signal transduction molecules in T lymphocytes from tumor-bearing mice. Science 258, 1795-1798.
• Molkentin, J. D., and Olson, E. N. (1996). Defining the regulatory networks for muscle development. Curr Opin Genet Dev 6, 445-453.

• Montagna, D., Locatelli, F., Calcaterra, V., Comoli, P., Moretta, A., Giorgiani, G., Zecca, M., Bonetti, F., Giraldi, E., Rondini, G., and Maccario, R. (1998). Does the emergence and persistence of donor-derived leukaemia-reactive cytotoxic T lymphocytes protect patients given an allogeneic BMT from recurrence? Results of a preliminary study. Bone Marrow Transplant 22, 743-750.
• Moretta, A. (2002). Natural killer cells and dendritic cells: rendezvous in abused tissues. Nat Rev Immunol 2, 957-964.
• Morris, E. C., Bendle, G. M., and Stauss, H. J. (2003). Prospects for immunotherapy of malignant disease. Clin Exp Immunol 131, 1-7.
• Muller, L., Provenzani, C., Faul, C., and Pawelec, G. (2001). Recognition of chronic myelogenous leukaemia cells by autologous T lymphocytes primed in vitro against the patient's dendritic cells. Br J Haematol 112, 740-748.
• Muller, M. R., Tsakou, G., Grunebach, F., Schmidt, S. M., and Brossart, P. (2004). Induction of chronic lymphocytic leukemia (CLL)-specific CD4- and CD8-mediated T-cell responses using RNA-transfected dendritic cells. Blood 103, 1763-1769.
• Mumberg, D., Monach, P. A., Wanderling, S., Philip, M., Toledano, A. Y., Schreiber, R. D., and Schreiber, H. (1999). CD4(+) T cells eliminate MHC class II-negative cancer cells in vivo by indirect effects of IFN-gamma. Proc Natl Acad Sci U S A 96, 8633-8638.
• Muster, T., Waltenberger, A., Grassauer, A., Hirschl, S., Caucig, P., Romirer, I., Fodinger, D., Seppele, H., Schanab, O., Magin-Lachmann, C., et al. (2003). An endogenous retrovirus derived from human melanoma cells. Cancer Res 63, 8735-8741.
• Muszynski, K. W., Ruscetti, F. W., Heidecker, G., Rapp, U., Troppmair, J., Gooya, J. M., and Keller, J. R. (1995). Raf-1 protein is required for growth factor-induced proliferation of hematopoietic cells. J Exp Med 181, 2189-2199.
• Nair, S. K., Snyder, D., Rouse, B. T., and Gilboa, E. (1997). Regression of tumors in mice vaccinated with professional antigen-presenting cells pulsed with tumor extracts. Int J Cancer 70, 706-715.
• Nair, S. K., Hull, S., Coleman, D., Gilboa, E., Lyerly, H. K., and Morse, M. A. (1999). Induction of carcinoembryonic antigen (CEA)-specific cytotoxic T-lymphocyte responses in vitro using autologous dendritic cells loaded with CEA peptide or CEA RNA in patients with metastatic malignancies expressing CEA. Int J Cancer 82, 121-124.
• Nair, S. K., Heiser, A., Boczkowski, D., Majumdar, A., Naoe, M., Lebkowski, J. S., Vieweg, J., and Gilboa, E. (2000). Induction of cytotoxic T cell responses and tumor immunity against unrelated tumors using telomerase reverse transcriptase RNA transfected dendritic cells. Nat Med 6, 1011-1017.
• Nair, S., Boczkowski, D., Moeller, B., Dewhirst, M., Vieweg, J., and Gilboa, E. (2003). Synergy between tumor immunotherapy and antiangiogenic therapy. Blood 102, 964-971.
• Nestle, F. O., Alijagic, S., Gilliet, M., Sun, Y., Grabbe, S., Dummer, R., Burg, G., and Schadendorf, D. (1998). Vaccination of melanoma patients with peptide- or tumor lysate-pulsed dendritic cells. Nat Med 4, 328-332.
• Nestle, F. O., Banchereau, J., and Hart, D. (2001). Dendritic cells: On the move from bench to bedside. Nat Med 7, 761-765.
• Newton, W. A., Jr. (1995). Classification of rhabdomyosarcoma. Curr Top Pathol 89, 241-259.

• Newton, W. A., Jr., Gehan, E. A., Webber, B. L., Marsden, H. B., van Unnik, A. J., Hamoudi, A. B., Tsokos, M. G., Shimada, H., Harms, D., Schmidt, D., and et al. (1995). Classification of rhabdomyosarcomas and related sarcomas. Pathologic aspects and proposal for a new classification--an Intergroup Rhabdomyosarcoma Study. Cancer 76, 1073-1085.
• Ngo, V. N., Tang, H. L., and Cyster, J. G. (1998). Epstein-Barr virus-induced molecule 1 ligand chemokine is expressed by dendritic cells in lymphoid tissues and strongly attracts naive T cells and activated B cells. J Exp Med 188, 181-191.
• Nieda, M., Nicol, A., Kikuchi, A., Kashiwase, K., Taylor, K., Suzuki, K., Tadokoro, K., and Juji, T. (1998). Dendritic cells stimulate the expansion of bcr-abl specific CD8+ T cells with cytotoxic activity against leukemic cells from patients with chronic myeloid leukemia. Blood 91, 977-983.
• Niemeyer, C. M., Arico, M., Basso, G., Biondi, A., Cantu Rajnoldi, A., Creutzig, U., Haas, O., Harbott, J., Hasle, H., Kerndrup, G., et al. (1997). Chronic myelomonocytic leukemia in childhood: a retrospective analysis of 110 cases. European Working Group on Myelodysplastic Syndromes in Childhood (EWOG-MDS). Blood 89, 3534-3543.
• Nishioka, Y., Nishimura, N., Suzuki, Y., and Sone, S. (2001). Human monocyte-derived and CD83(+) blood dendritic cells enhance NK cell-mediated cytotoxicity. Eur J Immunol 31, 2633-2641.
• Noessner, E., Gastpar, R., Milani, V., Brandl, A., Hutzler, P. J., Kuppner, M. C., Roos, M., Kremmer, E., Asea, A., Calderwood, S. K., and Issels, R. D. (2002). Tumor-derived heat shock protein 70 peptide complexes are cross-presented by human dendritic cells. J Immunol 169, 5424-5432.
• Ogawa, O., Eccles, M. R., Szeto, J., McNoe, L. A., Yun, K., Maw, M. A., Smith, P. J., and Reeve, A. E. (1993). Relaxation of insulin-like growth factor II gene imprinting implicated in Wilms' tumour. Nature 362, 749-751.
• Ohta, H., Kawai, M., Sawada, A., Tokimasa, S., Fujisaki, H., Matsuda, Y., Osugi, Y., Okada, S., and Hara, J. (2000). Juvenile myelomonocytic leukemia relapsing after allogeneic bone marrow transplantation successfully treated with interferon-alpha. Bone Marrow Transplant 26, 681-683.
• Orchard, P. J., Miller, J. S., McGlennen, R., Davies, S. M., and Ramsay, N. K. (1998). Graft-versus-leukemia is sufficient to induce remission in juvenile myelomonocytic leukemia. Bone Marrow Transplant 22, 201-203.
• Osman, Y., Takahashi, M., Zheng, Z., Koike, T., Toba, K., Liu, A., Furukawa, T., Aoki, S., and Aizawa, Y. (1999). Generation of bcr-abl specific cytotoxic T-lymphocytes by using dendritic cells pulsed with bcr-abl (b3a2) peptide: its applicability for donor leukocyte transfusions in marrow grafted CML patients. Leukemia 13, 166-174.
• Ossenkoppele, G. J., Stam, A. G., Westers, T. M., de Gruijl, T. D., Janssen, J. J., van de Loosdrecht, A. A., and Scheper, R. J. (2003). Vaccination of chronic myeloid leukemia patients with autologous in vitro cultured leukemic dendritic cells. Leukemia 17, 1424-1426.
• Panoskaltsis, N., Belanger, T. J., Liesveld, J. L., and Abboud, C. N. (2002). Optimal cytokine stimulation for the enhanced generation of leukemic dendritic cells in short-term culture. Leuk Res 26, 191-201.
• Pappo, A. S., Shapiro, D. N., Crist, W. M., and Maurer, H. M. (1995). Biology and therapy of pediatric rhabdomyosarcoma. J Clin Oncol 13, 2123-2139.
• Paquette, R. L., Hsu, N., Said, J., Mohammed, M., Rao, N. P., Shih, G., Schiller, G., Sawyers, C., and Glaspy, J. A. (2002). Interferon-alpha induces dendritic cell differentiation of CML mononuclear cells in vitro and in vivo. Leukemia 16, 1484-1489.

• Pardoll, D. M., and Topalian, S. L. (1998). The role of CD4+ T cell responses in antitumor immunity. Curr Opin Immunol 10, 588-594.
• Pardoll, D. M. (2002). Spinning molecular immunology into successful immunotherapy. Nat Rev Immunol 2, 227-238.
• Pardoll, D. M. (2003). Does the immune system see tumors as foreign or self? Annu Rev Immunol 21, 807-839.
• Pardoll, D., and Allison, J. (2004). Cancer immunotherapy: breaking the barriers to harvest the crop. Nat Med 10, 887-892.
• Parihar, R., Dierksheide, J., Hu, Y., and Carson, W. E. (2002). IL-12 enhances the natural killer cell cytokine response to Ab-coated tumor cells. J Clin Invest 110, 983-992.
• Parish, C. R. (2003). Cancer immunotherapy: the past, the present and the future. Immunol Cell Biol 81, 106-113.
• Parkhurst, M. R., Salgaller, M. L., Southwood, S., Robbins, P. F., Sette, A., Rosenberg, S. A., and Kawakami, Y. (1996). Improved induction of melanoma-reactive CTL with peptides from the melanoma antigen gp100 modified at HLA-A*0201-binding residues. J Immunol 157, 2539-2548.
• Pfreundschuh, M. (2000). Exploitation of the B cell repertoire for the identification of human tumor antigens. Cancer Chemother Pharmacol 46 Suppl, S3-7.
• Phan, G. Q., Yang, J. C., Sherry, R. M., Hwu, P., Topalian, S. L., Schwartzentruber, D. J., Restifo, N. P., Haworth, L. R., Seipp, C. A., Freezer, L. J., et al. (2003). Cancer regression and autoimmunity induced by cytotoxic T lymphocyte-associated antigen 4 blockade in patients with metastatic melanoma. Proc Natl Acad Sci U S A 100, 8372-8377.
• Piccioli, D., Sbrana, S., Melandri, E., and Valiante, N. M. (2002). Contact-dependent stimulation and inhibition of dendritic cells by natural killer cells. J Exp Med 195, 335-341.
• Pinilla-Ibarz, J., Cathcart, K., Korontsvit, T., Soignet, S., Bocchia, M., Caggiano, J., Lai, L., Jimenez, J., Kolitz, J., and Scheinberg, D. A. (2000). Vaccination of patients with chronic myelogenous leukemia with bcr-abl oncogene breakpoint fusion peptides generates specific immune responses. Blood 95, 1781-1787.
• Poltorak, A., He, X., Smirnova, I., Liu, M. Y., Van Huffel, C., Du, X., Birdwell, D., Alejos, E., Silva, M., Galanos, C., et al. (1998). Defective LPS signaling in C3H/HeJ and C57BL/10ScCr mice: mutations in Tlr4 gene. Science 282, 2085-2088.
• Praus, M., Collen, D., and Gerard, R. D. (2002). Both u-PA inhibition and vitronectin binding by plasminogen activator inhibitor 1 regulate HT1080 fibrosarcoma cell metastasis. Int J Cancer 102, 584-591.
• Pulendran, B., Banchereau, J., Maraskovsky, E., and Maliszewski, C. (2001). Modulating the immune response with dendritic cells and their growth factors. Trends Immunol 22, 41-47.
• Pulsipher, M. A., Adams, R. H., Asch, J., and Petersen, F. B. (2004). Successful treatment of JMML relapsed after unrelated allogeneic transplant with cytoreduction followed by DLI and interferon-alpha: evidence for a graft-versus-leukemia effect in non-monosomy-7 JMML. Bone Marrow Transplant 33, 113-115.
• Qasim, W., King, D., Buddle, J., Verfuerth, S., Kinnon, C., Thrasher, A. J., and Gaspar, H. B. (2003). The impact of retroviral suicide gene transduction procedures on T cells. Br J Haematol 123, 712-719.
• Quelle, F. W., Sato, N., Witthuhn, B. A., Inhorn, R. C., Eder, M., Miyajima, A., Griffin, J. D., and Ihle, J. N. (1994). JAK2 associates with the beta c chain of the receptor for granulocyte-macrophage colony-stimulating factor, and its activation requires the membrane-proximal region. Mol Cell Biol 14, 4335-4341.

• Rabbitts, T. H. (1994). Chromosomal translocations in human cancer. Nature 372, 143-149.
• Ramana, C. V., Gil, M. P., Schreiber, R. D., and Stark, G. R. (2002). Stat1-dependent and -independent pathways in IFN-gamma-dependent signaling. Trends Immunol 23, 96-101.
• Ramaswamy, S., Ross, K. N., Lander, E. S., and Golub, T. R. (2003). A molecular signature of metastasis in primary solid tumors. Nat Genet 33, 49-54.
• Rammensee, H. G., Falk, K., and Rotzschke, O. (1993). Peptides naturally presented by MHC class I molecules. Annu Rev Immunol 11, 213-244.
• Rammensee, H., Bachmann, J., Emmerich, N. P., Bachor, O. A., and Stevanovic, S. (1999). SYFPEITHI: database for MHC ligands and peptide motifs. Immunogenetics 50, 213-219.
• Read, A. P. (1995). Pax genes--paired feet in three camps. Nat Genet 9, 333-334.
Reis e Sousa, C., Stahl, P. D., and Austyn, J. M. (1993). Phagocytosis of antigens by Langerhans cells in vitro. J Exp Med 178, 509-519.
• Relaix, F., Polimeni, M., Rocancourt, D., Ponzetto, C., Schafer, B. W., and Buckingham, M. (2003). The transcriptional activator PAX3-FKHR rescues the defects of Pax3 mutant mice but induces a myogenic gain-of-function phenotype with ligand-independent activation of Met signaling in vivo. Genes Dev 17, 2950-2965.
• Rendon-Mitchell, B., Ochani, M., Li, J., Han, J., Wang, H., Yang, H., Susarla, S., Czura, C., Mitchell, R. A., Chen, G., et al. (2003). IFN-gamma induces high mobility group box 1 protein release partly through a TNF-dependent mechanism. J Immunol 170, 3890-3897.
• Rescigno, M., Granucci, F., Citterio, S., Foti, M., and Ricciardi-Castagnoli, P. (1999). Coordinated events during bacteria-induced DC maturation. Immunol Today 20, 200-203.
• Rice, J., Buchan, S., and Stevenson, F. K. (2002). Critical components of a DNA fusion vaccine able to induce protective cytotoxic T cells against a single epitope of a tumor antigen. J Immunol 169, 3908-3913.
• Rickinson, A. B., and Moss, D. J. (1997). Human cytotoxic T lymphocyte responses to Epstein-Barr virus infection. Annu Rev Immunol 15, 405-431.
• Ridge, J. P., Di Rosa, F., and Matzinger, P. (1998). A conditioned dendritic cell can be a temporal bridge between a CD4+ T-helper and a T-killer cell. Nature 393, 474-478.
• Ridgeway, A. G., and Skerjanc, I. S. (2001). Pax3 is essential for skeletal myogenesis and the expression of Six1 and Eya2. J Biol Chem 276, 19033-19039.
• Ridgway, D. (2003). The first 1000 dendritic cell vaccinees. Cancer Invest 21, 873-886.
• Riethmuller, G., Schneider-Gadicke, E., Schlimok, G., Schmiegel, W., Raab, R., Hoffken, K., Gruber, R., Pichlmaier, H., Hirche, H., Pichlmayr, R., and et al. (1994).
• Randomised trial of monoclonal antibody for adjuvant therapy of resected Dukes' C colorectal carcinoma. German Cancer Aid 17-1A Study Group. Lancet 343, 1177-1183.
• Robertson, M. J., and Ritz, J. (1990). Biology and clinical relevance of human natural killer cells. Blood 76, 2421-2438.
• Robertson, M. J. (2002). Role of chemokines in the biology of natural killer cells. J Leukoc Biol 71, 173-183.
• Robinson, S. P., Patterson, S., English, N., Davies, D., Knight, S. C., and Reid, C. D. (1999). Human peripheral blood contains two distinct lineages of dendritic cells. Eur J Immunol 29, 2769-2778.
• Rodenhuis, S. (1992). ras and human tumors. Semin Cancer Biol 3, 241-247.
• Roder, J. C. (1979). The beige mutation in the mouse. I. A stem cell predetermined impairment in natural killer cell function. J Immunol 123, 2168-2173.

• Romana, S. P., Le Coniat, M., and Berger, R. (1994). t(12;21): a new recurrent translocation in acute lymphoblastic leukemia. Genes Chromosomes Cancer 9, 186-191.
• Romani, N., Gruner, S., Brang, D., Kampgen, E., Lenz, A., Trockenbacher, B., Konwalinka, G., Fritsch, P. O., Steinman, R. M., and Schuler, G. (1994). Proliferating dendritic cell progenitors in human blood. J Exp Med 180, 83-93.
• Rosato, A., Santa, S. D., Zoso, A., Giacomelli, S., Milan, G., Macino, B., Tosello, V., Dellabona, P., Lollini, P. L., De Giovanni, C., and Zanovello, P. (2003). The cytotoxic T-lymphocyte response against a poorly immunogenic mammary adenocarcinoma is focused on a single immunodominant class I epitope derived from the gp70 Env product of an endogenous retrovirus. Cancer Res 63, 2158-2163.
• Rosenberg, S. A. (1997). Cancer vaccines based on the identification of genes encoding cancer regression antigens. Immunol Today 18, 175-182.
• Rosenberg, S. A., Packard, B. S., Aebersold, P. M., Solomon, D., Topalian, S. L., Toy, S. T., Simon, P., Lotze, M. T., Yang, J. C., and Seipp, C. A. (1988). Use of tumor-infiltrating lymphocytes and interleukin-2 in the immunotherapy of patients with metastatic melanoma. A preliminary report. N Engl J Med 319, 1676-1680.
• Rosenberg, S. A., Yang, J. C., and Restifo, N. P. (2004). Cancer immunotherapy: moving beyond current vaccines. Nat Med 10, 909-915.
• Rowley, J. D. (1994). 1993 Robert R. deVilliers Lecture. Chromosome translocations: dangerous liaisons. Leukemia 8 Suppl 1, S1-6.
• Ruchatz, H., Coluccia, A. M., Stano, P., Marchesi, E., and Gambacorti-Passerini, C. (2003). Constitutive activation of Jak2 contributes to proliferation and resistance to apoptosis in NPM/ALK-transformed cells. Exp Hematol 31, 309-315.
• Sadanaga, N., Nagashima, H., Mashino, K., Tahara, K., Yamaguchi, H., Ohta, M., Fujie, T., Tanaka, F., Inoue, H., Takesako, K., et al. (2001). Dendritic cell vaccination with MAGE peptide is a novel therapeutic approach for gastrointestinal carcinomas. Clin Cancer Res 7, 2277-2284.
• Saeboe-Larssen, S., Fossberg, E., and Gaudernack, G. (2002). mRNA-based electrotransfection of human dendritic cells and induction of cytotoxic T lymphocyte responses against the telomerase catalytic subunit (hTERT). J Immunol Methods 259, 191-203.
• Saeki, H., Moore, A. M., Brown, M. J., and Hwang, S. T. (1999). Cutting edge: secondary lymphoid-tissue chemokine (SLC) and CC chemokine receptor 7 (CCR7) participate in the emigration pathway of mature dendritic cells from the skin to regional lymph nodes. J Immunol 162, 2472-2475.
• Salgaller, M. L., Marincola, F. M., Cormier, J. N., and Rosenberg, S. A. (1996). Immunization against epitopes in the human melanoma antigen gp100 following patient immunization with synthetic peptides. Cancer Res 56, 4749-4757.
• Salgaller, M. L., and Lodge, P. A. (1998). Use of cellular and cytokine adjuvants in the immunotherapy of cancer. J Surg Oncol 68, 122-138.
• Sallusto, F., and Lanzavecchia, A. (1994). Efficient presentation of soluble antigen by cultured human dendritic cells is maintained by granulocyte/macrophage colony-stimulating factor plus interleukin 4 and downregulated by tumor necrosis factor alpha. J Exp Med 179, 1109-1118.
• Sallusto, F., Cella, M., Danieli, C., and Lanzavecchia, A. (1995). Dendritic cells use macropinocytosis and the mannose receptor to concentrate macromolecules in the major histocompatibility complex class II compartment: downregulation by cytokines and bacterial products. J Exp Med 182, 389-400.

• Sallusto, F., Palermo, B., Lenig, D., Miettinen, M., Matikainen, S., Julkunen, I., Forster, R., Burgstahler, R., Lipp, M., and Lanzavecchia, A. (1999). Distinct patterns and kinetics of chemokine production regulate dendritic cell function. Eur J Immunol 29, 1617-1625.
• Sallusto, F., Mackay, C. R., and Lanzavecchia, A. (2000). The role of chemokine receptors in primary, effector, and memory immune responses. Annu Rev Immunol 18, 593-620.
• Sambrook, Fritsch, and Maniatis (1989). Molecular Cloning: A Laboratory Manual, Second edn, Cold Spring Harbour Laboratory Press).
• Satoh, T., Nakafuku, M., Miyajima, A., and Kaziro, Y. (1991). Involvement of ras p21 protein in signal-transduction pathways from interleukin 2, interleukin 3, and granulocyte/macrophage colony-stimulating factor, but not from interleukin 4. Proc Natl Acad Sci U S A 88, 3314-3318.
• Schafer, B. W., Czerny, T., Bernasconi, M., Genini, M., and Busslinger, M. (1994). Molecular cloning and characterization of a human PAX-7 cDNA expressed in normal and neoplastic myocytes. Nucleic Acids Res 22, 4574-4582.
• Scheidler, S., Fredericks, W. J., Rauscher, F. J., 3rd, Barr, F. G., and Vogt, P. K. (1996). The hybrid PAX3-FKHR fusion protein of alveolar rhabdomyosarcoma transforms fibroblasts in culture. Proc Natl Acad Sci U S A 93, 9805-9809.
• Schiavetti, F., Thonnard, J., Colau, D., Boon, T., and Coulie, P. G. (2002). A human endogenous retroviral sequence encoding an antigen recognized on melanoma by cytolytic T lymphocytes. Cancer Res 62, 5510-5516.
• Schmidt, C. S., and Mescher, M. F. (2002). Peptide antigen priming of naive, but not memory, CD8 T cells requires a third signal that can be provided by IL-12. J Immunol 168, 5521-5529.
• Schmidt, M., Fernandez de Mattos, S., van der Horst, A., Klompmaker, R., Kops, G. J., Lam, E. W., Burgering, B. M., and Medema, R. H. (2002). Cell cycle inhibition by FoxO forkhead transcription factors involves downregulation of cyclin D. Mol Cell Biol 22, 7842-7852.
• Scholl, F. A., Kamarashev, J., Murmann, O. V., Geertsen, R., Dummer, R., and Schafer, B. W. (2001). PAX3 is expressed in human melanomas and contributes to tumor cell survival. Cancer Res 61, 823-826.
• Schuler-Thurner, B., Schultz, E. S., Berger, T. G., Weinlich, G., Ebner, S., Woerl, P., Bender, A., Feuerstein, B., Fritsch, P. O., Romani, N., and Schuler, G. (2002). Rapid induction of tumor-specific type 1 T helper cells in metastatic melanoma patients by vaccination with mature, cryopreserved, peptide-loaded monocyte-derived dendritic cells. J Exp Med 195, 1279-1288.
• Schulte, T. W., Toretsky, J. A., Ress, E., Helman, L., and Neckers, L. M. (1997). Expression of PAX3 in Ewing's sarcoma family of tumors. Biochem Mol Med 60, 121-126.
• Schumacher, T. N., Heemels, M. T., Neefjes, J. J., Kast, W. M., Melief, C. J., and Ploegh, H. L. (1990). Direct binding of peptide to empty MHC class I molecules on intact cells and in vitro. Cell 62, 563-567.
• Scrideli, C. A., Baruffi, M. R., Rogatto, S. R., Valera, E. T., Defavery, R., and Tone, L. G. (2003). B lineage acute lymphoblastic leukemia transformation in a child with juvenile myelomonocytic leukemia, type 1 neurofibromatosis and monosomy of chromosome 7. Possible implications in the leukemogenesis. Leuk Res 27, 371-374.
• Seliger, B., Wollscheid, U., Momburg, F., Blankenstein, T., and Huber, C. (2000). Coordinate downregulation of multiple MHC class I antigen processing genes in chemical-induced murine tumor cell lines of distinct origin. Tissue Antigens 56, 327-336.

• SenGupta, D., Norris, P. J., Suscovich, T. J., Hassan-Zahraee, M., Moffett, H. F., Trocha, A., Draenert, R., Goulder, P. J., Binder, R. J., Levey, D. L., et al. (2004). Heat shock protein-mediated cross-presentation of exogenous HIV antigen on HLA class I and class II. J Immunol 173, 1987-1993.
• Shankaran, V., Ikeda, H., Bruce, A. T., White, J. M., Swanson, P. E., Old, L. J., and Schreiber, R. D. (2001). IFNgamma and lymphocytes prevent primary tumour development and shape tumour immunogenicity. Nature 410, 1107-1111.
• Shapiro, D. N., Sublett, J. E., Li, B., Downing, J. R., and Naeve, C. W. (1993). Fusion of PAX3 to a member of the forkhead family of transcription factors in human alveolar rhabdomyosarcoma. Cancer Res 53, 5108-5112.
• Sharp, R., Recio, J. A., Jhappan, C., Otsuka, T., Liu, S., Yu, Y., Liu, W., Anver, M., Navid, F., Helman, L. J., *et al.* (2002). Synergism between INK4a/ARF inactivation and aberrant HGF/SF signaling in rhabdomyosarcomagenesis. Nat Med 8, 1276-1280.
• Shi, Y., Evans, J. E., and Rock, K. L. (2003). Molecular identification of a danger signal that alerts the immune system to dying cells. Nature 425, 516-521.
• Shimizu, K., Thomas, E. K., Giedlin, M., and Mule, J. J. (2001). Enhancement of tumor lysate- and peptide-pulsed dendritic cell-based vaccines by the addition of foreign helper protein. Cancer Res 61, 2618-2624.
• Side, L. E., Emanuel, P. D., Taylor, B., Franklin, J., Thompson, P., Castleberry, R. P., and Shannon, K. M. (1998). Mutations of the NF1 gene in children with juvenile myelomonocytic leukemia without clinical evidence of neurofibromatosis, type 1. Blood 92, 267-272.
• Slamon, D. J., Clark, G. M., Wong, S. G., Levin, W. J., Ullrich, A., and McGuire, W. L. (1987). Human breast cancer: correlation of relapse and survival with amplification of the HER-2/neu oncogene. Science 235, 177-182.
• Slamon, D. J., Leyland-Jones, B., Shak, S., Fuchs, H., Paton, V., Bajamonde, A., Fleming, T., Eiermann, W., Wolter, J., Pegram, M., et al. (2001). Use of chemotherapy plus a monoclonal antibody against HER2 for metastatic breast cancer that overexpresses HER2. N Engl J Med 344, 783-792.
• Slansky, J. E., Rattis, F. M., Boyd, L. F., Fahmy, T., Jaffee, E. M., Schneck, J. P., Margulies, D. H., and Pardoll, D. M. (2000). Enhanced antigen-specific antitumor immunity with altered peptide ligands that stabilize the MHC-peptide-TCR complex. Immunity 13, 529-538.
• Slingluff, C. L., Jr., Hunt, D. F., and Engelhard, V. H. (1994). Direct analysis of tumor-associated peptide antigens. Curr Opin Immunol 6, 733-740.
• Small, E. J., Fratesi, P., Reese, D. M., Strang, G., Laus, R., Peshwa, M. V., and Valone, F. H. (2000). Immunotherapy of hormone-refractory prostate cancer with antigen-loaded dendritic cells. J Clin Oncol 18, 3894-3903.
• Song, W., Kong, H. L., Carpenter, H., Torii, H., Granstein, R., Rafii, S., Moore, M. A., and Crystal, R. G. (1997). Dendritic cells genetically modified with an adenovirus vector encoding the cDNA for a model antigen induce protective and therapeutic antitumor immunity. J Exp Med 186, 1247-1256.
• Sorensen, P. H., Lynch, J. C., Qualman, S. J., Tirabosco, R., Lim, J. F., Maurer, H. M., Bridge, J. A., Crist, W. M., Triche, T. J., and Barr, F. G. (2002). PAX3-FKHR and PAX7-FKHR gene fusions are prognostic indicators in alveolar rhabdomyosarcoma: a report from the children's oncology group. J Clin Oncol 20, 2672-2679.
• Specht, J. M., Wang, G., Do, M. T., Lam, J. S., Royal, R. E., Reeves, M. E., Rosenberg, S. A., and Hwu, P. (1997). Dendritic cells retrovirally transduced with a model antigen gene are therapeutically effective against established pulmonary metastases. J Exp Med 186, 1213-1221.

• Spellerberg, M. B., Zhu, D., Thompsett, A., King, C. A., Hamblin, T. J., and Stevenson, F. K. (1997). DNA vaccines against lymphoma: promotion of anti-idiotypic antibody responses induced by single chain Fv genes by fusion to tetanus toxin fragment C. J Immunol 159, 1885-1892.
• Spits, H., Couwenberg, F., Bakker, A. Q., Weijer, K., and Uittenbogaart, C. H. (2000). Id2 and Id3 inhibit development of CD34(+) stem cells into predendritic cell (pre-DC)2 but not into pre-DC1. Evidence for a lymphoid origin of pre-DC2. J Exp Med 192, 1775-1784.
• Starnes, C. O. (1992). Coley's toxins in perspective. Nature 357, 11-12.
• Steele, R. J., Thompson, A. M., Hall, P. A., and Lane, D. P. (1998). The p53 tumour suppressor gene. Br J Surg 85, 1460-1467.
• Steinman, R. M. (1991). The dendritic cell system and its role in immunogenicity. Annu Rev Immunol 9, 271-296.
• Steinman, R. M., Hawiger, D., and Nussenzweig, M. C. (2003). Tolerogenic dendritic cells. Annu Rev Immunol 21, 685-711.
• Stevenson, F. K., Rice, J., Ottensmeier, C. H., Thirdborough, S. M., and Zhu, D. (2004a). DNA fusion gene vaccines against cancer: from the laboratory to the clinic. Immunol Rev 199, 156-180.
• Stevenson, F. K., Ottensmeier, C. H., Johnson, P., Zhu, D., Buchan, S. L., McCann, K. J., Roddick, J. S., King, A. T., McNicholl, F., Savelyeva, N., and Rice, J. (2004b). DNA vaccines to attack cancer. Proc Natl Acad Sci U S A 101 Suppl 2, 14646-14652.
• Stiller, C. A., Chessells, J. M., and Fitchett, M. (1994). Neurofibromatosis and childhood leukaemia/lymphoma: a population-based UKCCSG study. Br J Cancer 70, 969-972.
• Storni, T., and Bachmann, M. F. (2004). Loading of MHC class I and II presentation pathways by exogenous antigens: a quantitative in vivo comparison. J Immunol 172, 6129-6135.
• Stoykova, A., and Gruss, P. (1994). Roles of Pax-genes in developing and adult brain as suggested by expression patterns. J Neurosci 14, 1395-1412.
• Strong, L. C., Williams, W. R., and Tainsky, M. A. (1992). The Li-Fraumeni syndrome: from clinical epidemiology to molecular genetics. Am J Epidemiol 135, 190-199.
• Stuart, E. T., and Gruss, P. (1995). PAX genes: what's new in developmental biology and cancer? Hum Mol Genet 4 Spec No, 1717-1720.
• Stuart, E. T., Kioussi, C., Aguzzi, A., and Gruss, P. (1995). PAX5 expression correlates with increasing malignancy in human astrocytomas. Clin Cancer Res 1, 207-214.
• Sublett, J. E., Jeon, I. S., and Shapiro, D. N. (1995). The alveolar rhabdomyosarcoma PAX3/FKHR fusion protein is a transcriptional activator. Oncogene 11, 545-552.
•Tajbakhsh, S., Rocancourt, D., Cossu, G., and Buckingham, M. (1997). Redefining the genetic hierarchies controlling skeletal myogenesis: Pax-3 and Myf-5 act upstream of MyoD. Cell 89, 127-138.
• Takayama, H., LaRochelle, W. J., Sharp, R., Otsuka, T., Kriebel, P., Anver, M., Aaronson, S. A., and Merlino, G. (1997). Diverse tumorigenesis associated with aberrant development in mice overexpressing hepatocyte growth factor/scatter factor. Proc Natl Acad Sci U S A 94, 701-706.
• Takeda, K., Hayakawa, Y., Smyth, M. J., Kayagaki, N., Yamaguchi, N., Kakuta, S., Iwakura, Y., Yagita, H., and Okumura, K. (2001). Involvement of tumor necrosis factor-related apoptosis-inducing ligand in surveillance of tumor metastasis by liver natural killer cells. Nat Med 7, 94-100.

• Tallman, M. S., Nabhan, C., Feusner, J. H., and Rowe, J. M. (2002). Acute promyelocytic leukemia: evolving therapeutic strategies. Blood 99, 759-767.
• Tartaglia, M., Niemeyer, C. M., Fragale, A., Song, X., Buechner, J., Jung, A., Hahlen, K., Hasle, H., Licht, J. D., and Gelb, B. D. (2003). Somatic mutations in PTPN11 in juvenile myelomonocytic leukemia, myelodysplastic syndromes and acute myeloid leukemia. Nat Genet 34, 148-150.
• Tassabehji, M., Read, A. P., Newton, V. E., Patton, M., Gruss, P., Harris, R., and Strachan, T. (1993). Mutations in the PAX3 gene causing Waardenburg syndrome type 1 and type 2. Nat Genet 3, 26-30.
• Teeling, J. L., French, R. R., Cragg, M. S., van den Brakel, J., Pluyter, M., Huang, H., Chan, C., Parren, P. W., Hack, C. E., Dechant, M., et al. (2004). Characterization of new human CD20 monoclonal antibodies with potent cytolytic activity against non-Hodgkin lymphomas. Blood 104, 1793-1800.
• Thimmaiah, K. N., Easton, J., Huang, S., Veverka, K. A., Germain, G. S., Harwood, F. C., and Houghton, P. J. (2003). Insulin-like growth factor I-mediated protection from rapamycin-induced apoptosis is independent of Ras-Erk1-Erk2 and phosphatidylinositol 3'-kinase-Akt signaling pathways. Cancer Res 63, 364-374.
• Thomas, A. M., Santarsiero, L. M., Lutz, E. R., Armstrong, T. D., Chen, Y. C., Huang, L. Q., Laheru, D. A., Goggins, M., Hruban, R. H., and Jaffee, E. M. (2004). Mesothelin-specific CD8(+) T cell responses provide evidence of in vivo cross-priming by antigen-presenting cells in vaccinated pancreatic cancer patients. J Exp Med 200, 297-306.
• Tiffin, N., Williams, R. D., Shipley, J., and Pritchard-Jones, K. (2003). PAX7 expression in embryonal rhabdomyosarcoma suggests an origin in muscle satellite cells. Br J Cancer 89, 327-332.
• Topalian, S. L., Solomon, D., Avis, F. P., Chang, A. E., Freerksen, D. L., Linehan, W. M., Lotze, M. T., Robertson, C. N., Seipp, C. A., and Simon, P. (1988). Immunotherapy of patients with advanced cancer using tumor-infiltrating lymphocytes and recombinant interleukin-2: a pilot study. J Clin Oncol 6, 839-853.
• Trefzer, U., Herberth, G., Wohlan, K., Milling, A., Thiemann, M., Sherev, T., Sparbier, K., Sterry, W., and Walden, P. (2004). Vaccination with hybrids of tumor and dendritic cells induces tumor-specific T-cell and clinical responses in melanoma stage III and IV patients. Int J Cancer 110, 730-740.
• Trinchieri, G. (2003). Interleukin-12 and the regulation of innate resistance and adaptive immunity. Nat Rev Immunol 3, 133-146.
• Tsokos, M., Webber, B. L., Parham, D. M., Wesley, R. A., Miser, A., Miser, J. S., Etcubanas, E., Kinsella, T., Grayson, J., Glatstein, E., and et al. (1992). Rhabdomyosarcoma. A new classification scheme related to prognosis. Arch Pathol Lab Med 116, 847-855.
• Tsukamoto, K., Nakamura, Y., and Niikawa, N. (1994). Isolation of two isoforms of the PAX3 gene transcripts and their tissue-specific alternative expression in human adult tissues. Hum Genet 93, 270-274.
• Turc-Carel, C., Lizard-Nacol, S., Justrabo, E., Favrot, M., Philip, T., and Tabone, E. (1986). Consistent chromosomal translocation in alveolar rhabdomyosarcoma. Cancer Genet Cytogenet 19, 361-362.
• Tuting, T., Wilson, C. C., Martin, D. M., Kasamon, Y. L., Rowles, J., Ma, D. I., Slingluff, C. L., Jr., Wagner, S. N., van der Bruggen, P., Baar, J., et al. (1998). Autologous human monocyte-derived dendritic cells genetically modified to express melanoma antigens elicit primary cytotoxic T cell responses in vitro: enhancement by cotransfection of genes encoding the Th1-biasing cytokines IL-12 and IFN-alpha. J Immunol 160, 1139-1147.

• Underhill, D. M., and Ozinsky, A. (2002). Toll-like receptors: key mediators of microbe detection. Curr Opin Immunol 14, 103-110.
• Upham, J. W., Lee, P. T., Holt, B. J., Heaton, T., Prescott, S. L., Sharp, M. J., Sly, P. D., and Holt, P. G. (2002). Development of interleukin-12-producing capacity throughout childhood. Infect Immun 70, 6583-6588.
• van Kooyk, Y., and Geijtenbeek, T. B. (2003). DC-SIGN: escape mechanism for pathogens. Nat Rev Immunol 3, 697-709.
• van Rossum, G. S., Bijvelt, J. J., van den Bosch, H., Verkleij, A. J., and Boonstra, J. (2002). Cytosolic phospholipase A2 and lipoxygenase are involved in cell cycle progression in neuroblastoma cells. Cell Mol Life Sci 59, 181-188.
• van Tendeloo, V. F., Ponsaerts, P., Lardon, F., Nijs, G., Lenjou, M., Van Broeckhoven, C., Van Bockstaele, D. R., and Berneman, Z. N. (2001). Highly efficient gene delivery by mRNA electroporation in human hematopoietic cells: superiority to lipofection and passive pulsing of mRNA and to electroporation of plasmid cDNA for tumor antigen loading of dendritic cells. Blood 98, 49-56.
• Verhasselt, V., Buelens, C., Willems, F., De Groote, D., Haeffner-Cavaillon, N., and Goldman, M. (1997). Bacterial lipopolysaccharide stimulates the production of cytokines and the expression of costimulatory molecules by human peripheral blood dendritic cells: evidence for a soluble CD14-dependent pathway. J Immunol 158, 2919-2925.
• Vogel, C., Cobleigh, M. A., Tripathy, D., Gutheil, J. C., Harris, L. N., Fehrenbacher, L., Slamon, D. J., Murphy, M., Novotny, W. F., Burchmore, M., et al. (2001). First-line, single-agent Herceptin(R) (trastuzumab) in metastatic breast cancer. a preliminary report. Eur J Cancer 37 Suppl 1, 25-29.
• Vulin, A. I., and Stanley, F. M. (2002). A Forkhead/winged helix-related transcription factor mediates insulin-increased plasminogen activator inhibitor-1 gene transcription. J Biol Chem 277, 20169-20176.
• Wang, C., Al-Omar, H. M., Radvanyi, L., Banerjee, A., Bouman, D., Squire, J., and Messner, H. A. (1999). Clonal heterogeneity of dendritic cells derived from patients with chronic myeloid leukemia and enhancement of their T-cells stimulatory activity by IFN-alpha. Exp Hematol 27, 1176-1184.
• Wang, T., Niu, G., Kortylewski, M., Burdelya, L., Shain, K., Zhang, S., Bhattacharya, R., Gabrilovich, D., Heller, R., Coppola, D., et al. (2004). Regulation of the innate and adaptive immune responses by Stat-3 signaling in tumor cells. Nat Med 10, 48-54.
• Wang, W., Kumar, P., Epstein, J., Helman, L., Moore, J. V., and Kumar, S. (1998). Insulin-like growth factor II and PAX3-FKHR cooperate in the oncogenesis of rhabdomyosarcoma. Cancer Res 58, 4426-4433.
• Wang, Y., Selden, C., Farnaud, S., Calnan, D., and Hodgson, H. J. (1994). Hepatocyte growth factor (HGF/SF) is expressed in human epithelial cells during embryonic development; studies by in situ hybridisation and northern blot analysis. J Anat 185 (Pt 3), 543-551.
• Wang, Y., Holland, J. F., Bleiweiss, I. J., Melana, S., Liu, X., Pelisson, I., Cantarella, A., Stellrecht, K., Mani, S., and Pogo, B. G. (1995). Detection of mammary tumor virus env gene-like sequences in human breast cancer. Cancer Res 55, 5173-5179.
• Wang, Z. Y., and Chen, Z. (2000). Differentiation and apoptosis induction therapy in acute promyelocytic leukaemia. Lancet Oncol 1, 101-106.
• Watanabe, A., Takeda, K., Ploplis, B., and Tachibana, M. (1998). Epistatic relationship between Waardenburg syndrome genes MITF and PAX3. Nat Genet 18, 283-286.
• Watts, T. H., and DeBenedette, M. A. (1999). T cell co-stimulatory molecules other than CD28. Curr Opin Immunol 11, 286-293.

• Weber-Hall, S., Anderson, J., McManus, A., Abe, S., Nojima, T., Pinkerton, R., Pritchard-Jones, K., and Shipley, J. (1996). Gains, losses, and amplification of genomic material in rhabdomyosarcoma analyzed by comparative genomic hybridization. Cancer Res 56, 3220-3224.
• Weigel, D., Jurgens, G., Kuttner, F., Seifert, E., and Jackle, H. (1989). The homeotic gene fork head encodes a nuclear protein and is expressed in the terminal regions of the Drosophila embryo. Cell 57, 645-658.
• Whiteside, T. L., and Herberman, R. B. (1995). The role of natural killer cells in immune surveillance of cancer. Curr Opin Immunol 7, 704-710.
• Williams, O., Tanaka, Y., Bix, M., Murdjeva, M., Littman, D. R., and Kioussis, D. (1996). Inhibition of thymocyte negative selection by T cell receptor antagonist peptides. Eur J Immunol 26, 532-538.
• Wilson, J. L., Heffler, L. C., Charo, J., Scheynius, A., Bejarano, M. T., and Ljunggren, H. G. (1999). Targeting of human dendritic cells by autologous NK cells. J Immunol 163, 6365-6370.
• Windbichler, G. H., Hausmaninger, H., Stummvoll, W., Graf, A. H., Kainz, C., Lahodny, J., Denison, U., Muller-Holzner, E., and Marth, C. (2000). Interferon-gamma in the first-line therapy of ovarian cancer: a randomized phase III trial. Br J Cancer 82, 1138-1144.
• Winter, G., and Harris, W. J. (1993). Humanized antibodies. Immunol Today 14, 243-246.
• Witzig, T. E. (2004). Yttrium-90-ibritumomab tiuxetan radioimmunotherapy: a new treatment approach for B-cell non-Hodgkin's lymphoma. Drugs Today (Barc) 40, 111-119.
• Wodarz, D., and Jansen, V. A. (2001). The role of T cell help for anti-viral CTL responses. J Theor Biol 211, 419-432.
• Woglom, W. (1929). Immunity to transplantable tumours. Cancer Research 4, 129-138; Cited by Parish, C. R. (2003).
• Wolfers, J., Lozier, A., Raposo, G., Regnault, A., Thery, C., Masurier, C., Flament, C., Pouzieux, S., Faure, F., Tursz, T., et al. (2001). Tumor-derived exosomes are a source of shared tumor rejection antigens for CTL cross-priming. Nat Med 7, 297-303.
• Woodson, E. M., Chianese-Bullock, K. A., Wiernasz, C. J., Bissonette, E. A., Grosh, W. W., Neese, P. Y., Merrill, P. K., Barnd, D. L., Petroni, G. R., and Slingluff, C. L., Jr. (2004). Assessment of the toxicities of systemic low-dose interleukin-2 administered in conjunction with a melanoma peptide vaccine. J Immunother 27, 380-388.
• Worth, A., Rao, K., Webb, D., Chessells, J., Passmore, J., and Veys, P. (2003). Successful treatment of juvenile myelomonocytic leukemia relapsing after stem cell transplantation using donor lymphocyte infusion. Blood 101, 1713-1714.
• Wu, R. S., Kobie, J. J., Besselsen, D. G., Fong, T. C., Mack, V. D., McEarchern, J. A., and Akporiaye, E. T. (2001). Comparative analysis of IFN-gamma B7.1 and antisense TGF-beta gene transfer on the tumorigenicity of a poorly immunogenic metastatic mammary carcinoma. Cancer Immunol Immunother 50, 229-240.
• Wykes, M., Pombo, A., Jenkins, C., and MacPherson, G. G. (1998). Dendritic cells interact directly with naive B lymphocytes to transfer antigen and initiate class switching in a primary T-dependent response. J Immunol 161, 1313-1319.
• Yang, J. C., and Perry-Lalley, D. (2000). The envelope protein of an endogenous murine retrovirus is a tumor-associated T-cell antigen for multiple murine tumors. J Immunother 23, 177-183.

• Ye, J., Chen, G. S., Song, H. P., Li, Z. S., Huang, Y. Y., Qu, P., Sun, Y. J., Zhang, X. M., and Sui, Y. F. (2004). Heat shock protein 70 / MAGE-1 tumor vaccine can enhance the potency of MAGE-1-specific cellular immune responses in vivo. Cancer Immunol Immunother 53, 825-834.
• Yee, C., Thompson, J. A., Byrd, D., Riddell, S. R., Roche, P., Celis, E., and Greenberg, P. D. (2002). Adoptive T cell therapy using antigen-specific CD8+ T cell clones for the treatment of patients with metastatic melanoma: in vivo persistence, migration, and antitumor effect of transferred T cells. Proc Natl Acad Sci U S A 99, 16168-16173.
• Yotnda, P., Garcia, F., Peuchmaur, M., Grandchamp, B., Duval, M., Lemonnier, F., Vilmer, E., and Langlade-Demoyen, P. (1998). Cytotoxic T cell response against the chimeric ETV6-AML1 protein in childhood acute lymphoblastic leukemia. J Clin Invest 102, 455-462.
• Yu, Z., Theoret, M. R., Touloukian, C. E., Surman, D. R., Garman, S. C., Feigenbaum, L., Baxter, T. K., Baker, B. M., and Restifo, N. P. (2004). Poor immunogenicity of a self/tumor antigen derives from peptide-MHC-I instability and is independent of tolerance. J Clin Invest 114, 551-559.
• Yun, C., Senju, S., Fujita, H., Tsuji, Y., Irie, A., Matsushita, S., and Nishimura, Y. (1999). Augmentation of immune response by altered peptide ligands of the antigenic peptide in a human CD4+ T-cell clone reacting to TEL/AML1 fusion protein. Tissue Antigens 54, 153-161.
• Yun, K. (1992). A new marker for rhabdomyosarcoma. Insulin-like growth factor II. Lab Invest 67, 653-664.
• Zeh, H. J., 3rd, Perry-Lalley, D., Dudley, M. E., Rosenberg, S. A., and Yang, J. C. (1999). High avidity CTLs for two self-antigens demonstrate superior in vitro and in vivo antitumor efficacy. J Immunol 162, 989-994.
• Zhang, L., Zhou, W., Velculescu, V. E., Kern, S. E., Hruban, R. H., Hamilton, S. R., Vogelstein, B., and Kinzler, K. W. (1997). Gene expression profiles in normal and cancer cells. Science 276, 1268-1272.
• Zhang, L., Kim, M., Choi, Y. H., Goemans, B., Yeung, C., Hu, Z., Zhan, S., Seth, P., and Helman, L. J. (1999). Diminished G1 checkpoint after gamma-irradiation and altered cell cycle regulation by insulin-like growth factor II overexpression. J Biol Chem 274, 13118-13126.
• Zhang, L., and Wang, C. (2003). PAX3-FKHR transformation increases 26 S proteasome-dependent degradation of p27Kip1, a potential role for elevated Skp2 expression. J Biol Chem 278, 27-36.
• Zhang, Y. Y., Vik, T. A., Ryder, J. W., Srour, E. F., Jacks, T., Shannon, K., and Clapp, D. W. (1998). Nf1 regulates hematopoietic progenitor cell growth and ras signaling in response to multiple cytokines. J Exp Med 187, 1893-1902.
• Zhou, L. J., and Tedder, T. F. (1995). Human blood dendritic cells selectively express CD83, a member of the immunoglobulin superfamily. J Immunol 154, 3821-3835.
• Zhu, D., and Stevenson, F. K. (2002). DNA gene fusion vaccines against cancer. Curr Opin Mol Ther 4, 41-48.
• Ziegler, S. F., Ramsdell, F., and Alderson, M. R. (1994). The activation antigen CD69. Stem Cells 12, 456-465.

results of a prospective investigation. *Br J Haematol* 1997; **98**: 969–972.
5 Rowe D, Cotterill SJ, Ross FM, Bunyan DJ, Vickers SJ, Bryon J *et al.* Cytogenetically cryptic AML1-ETO and CBF beta-MYH11 gene rearrangements: incidence in 412 cases of acute myeloid leukaemia. *Br J Haematol* 2000; **111**: 1051–1056.
6 Poirel H, Radford-Weiss I, Rack K, Troussard X, Veil A, Valensi F *et al.* Detection of the chromosome 16 CBF beta-MYH11 fusion transcript in myelomonocytic leukemias. *Blood* 1995; **85**: 1313–1322.
7 Mitterbauer M, Laczika K, Novak M, Mitterbauer G, Hilgarth B, Pirc-Danoewinata H *et al.* High concordance of karyotype analysis and RT-PCR for CBF beta/MYH11 in unselected patients with acute myeloid leukemia. A single center study. *Am J Clin Pathol* 2000; **113**: 406–410.
8 Grimwade D. Screening for core binding factor gene rearrangements in acute myeloid leukemia. *Leukemia* 2002; **16**: 964–969.
9 van der Reijden BA, Lombardo M, Dauwerse HG, Giles RH, Muhlematter D, Bellomo MJ *et al.* RT-PCR diagnosis of patients with acute nonlymphocytic leukemia and inv(16)(p13q22) and identification of new alternative splicing in CBFB-MYH11 transcripts. *Blood* 1995; **86**: 277–282.
10 Mancini M, Cedrone M, Diverio D, Emanuel B, Stul M, Vranckx H *et al.* Use of dual-color interphase FISH for the detection of inv(16) in acute myeloid leukemia at diagnosis, relapse and during follow-up: a study of 23 patients. *Leukemia* 2000; **14**: 364–368.
11 Guerrasio A, Pilatrino C, De Micheli D, Cilloni D, Serra A, Gottardi E *et al.* Assessment of minimal residual disease (MRD) in CBFbeta/MYH11-positive acute myeloid leukemias by qualitative and quantitative RT-PCR amplification of fusion transcripts. *Leukemia.* 2002; **16**: 1176–1181.

Generation of immunostimulatory dendritic cells from the malignant clone in patients with juvenile myelomonocytic leukemia

Leukemia (2003) **17**, 1910–1912. doi:10.1038/sj.leu.2403059

TO THE EDITOR

A unique property of myeloid lineage leukemia cells is their potential to be differentiated into dendritic cells (DC), both *in vitro* and *in vivo*. These leukemic DC have potential therapeutic applications, such as stimulation of autologous anti leukemia T-cell responses in leukemia patients, or allogeneic responses in the post bone marrow transplantation (BMT) setting. Several studies have demonstrated that leukemic cells from a proportion of patients with acute myeloid leukemia (AML)[1] or chronic myeloid leukemia (CML)[2] can be differentiated into functionally active DC capable of inducing antileukemia T-cell responses.[3,4]

We were interested in the utilization of such an immunotherapeutic approach for patients with juvenile myelomonocytic leukemia (JMML), a rare condition with poor prognosis. This approach is attractive because allogeneic BMT is considered necessary for cure, and the graft-versus-leukemia (GVL) effect is critically important.[5,6]

We initially assessed whether immature DC could be generated *in vitro* from plastic adherent peripheral blood mononuclear cells (PBMC) from three JMML patients (JMML-1, -2, -3). After 6 days of culture with granulocyte–macrophage colony-stimulating factor (GM-CSF) and interleukin-4 (IL-4) in the presence of 10% fetal calf serum, cells from normal donors and all three JMML patients demonstrated a typical immature monocyte-derived DC (MoDC) surface phenotype. This was inferred from their high expression levels of the myeloid marker CD11c, intermediate levels of the MHC class II molecule HLA-DR and the costimulatory molecule CD86 (B7-2), and undetectable levels of the dendritic activation marker CD83 and the monocytic marker CD14 (Figure 1). Typically, 10 ml of peripheral blood from JMML patients yielded about 5×10^7 adherent cells and the final yield of viable MoDC was between 25 and 50% of this starting population. The cells generated from normal donors and JMML patients formed nonadherent clusters and possessed short cytoplasmic projections, characteristic of immature DC morphology.[7]

Immature DC are specialized at capturing and processing antigens; however, optimal presentation of potential leukemia-specific antigens to T lymphocytes requires that the DC are in an activated, mature state.[7] Therefore, we next attempted to activate the *in vitro* cultured immature DC with lipopolysaccharide (LPS). Immature DC populations generated from normal, JMML-1, and JMML-2 PBMC upregulated HLA-DR, CD83 and CD86 expression following 24-h exposure to LPS, acquiring a mature dendritic phenotype (Figure 1). These mature DC therefore expressed the necessary cell surface molecules required for efficient antigen presentation and costimulation. However, the DC cultured from JMML-3 PBMC failed to upregulate HLA-DR and CD83 following addition of LPS (data not shown).

The leukemic cells in two of the patients (JMML-2 and -3) exhibited monosomy 7, a commonly observed chromosomal abnormality of this disease. We were able to use this as a marker of malignant origin, and interphase fluorescence *in situ* hybridization (FISH) analysis revealed that the vast majority of $CD86^+$-purifed mature DC generated from these patients displayed monosomy 7 (98% of JMML-2 DC and 91% of JMML-3 DC). In contrast, DC cultured from PBMC from a normal donor all possessed two copies of chromosome 7. This finding confirmed that virtually all the DC cultured *in vitro* from these JMML patients were of leukemic origin.

Several experiments were performed to investigate the functional activity of these leukemic DC. Limited sample sizes prevented us from examining the functional activity of DC cultured from all three JMML patients in each assay. To examine further the ability of *in vitro* cultured DC to provide the costimulatory signal required to activate naïve T cells, we measured DC production of IL-12 by ELISA (Becton Dickinson, San Diego, CA, USA). Secretion of IL-12 by mature DC is required for T-cell activation, and is associated with a Th-1 response. Consistent with published data, immature DC generated *in vitro* from normal donor and JMML-2 PBMC did not secrete IL-12 (<7.5 pg/150 000 cells). However, LPS-matured MoDC from a normal donor and LPS-matured DC from JMML-2 produced large amounts of IL-12 (210 pg/150 000 cells and 320 pg/150 000 cells, respectively). These results provide additional evidence for the stimulatory phenotype of mature DC generated from JMML-2 PBMC. In contrast, incubation of immature DC cultured from JMML-3 PBMC with LPS for 24 h resulted in the secretion of minimal amounts of IL-12 (15 pg/150 000 cells), significantly less than that observed in normal mature MoDC ($P<0.05$, Student's *t*-test). This abnormal secretion of IL-12 by JMML-3 DC following incubation with LPS is consistent with the flow cytometric data, demonstrating that the DC cultured from this patient were resistant to activation with LPS. The variability in the phenotypes of the DC generated from the three JMML patients might reflect the heterogeneity of this disorder.

Correspondence: Dr J Anderson, Molecular Haematology and Cancer Biology Unit, Institute of Child Health, 30 Guilford Street, London WC1N 1EH, UK; Fax: +44 20 8813 8100
Received 10 April 2003; accepted 13 May 2003

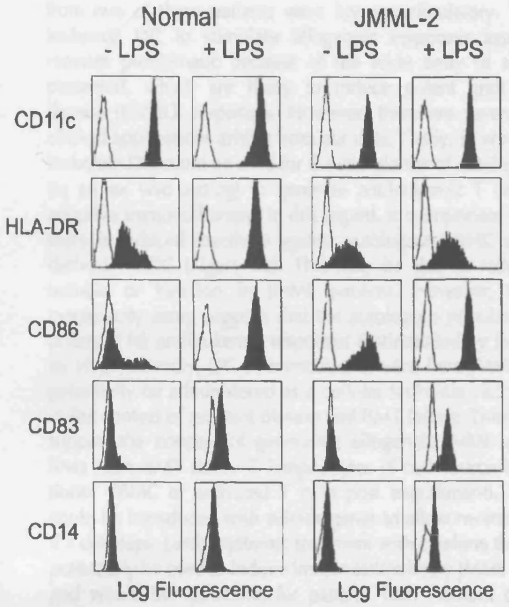

Figure 1 Immunophenotype of DC cultured *in vitro* from normal control and JMML-2 PBMC. Plastic adherent PBMC were differentiated into immature DC with GM-CSF and IL-4 for 6 days. DC maturation was subsequently induced with LPS for 24 h. DC were harvested on day 6 (immature DC) or on day 7 following incubation with LPS (mature DC), stained with a panel of immunofluorescent antibodies and analyzed by flow cytometry. Cells were gated on large, granular cells, and gated cells are shown in the histogram plots. The black filled areas in histograms represent staining with the indicated monoclonal antibody, the unfilled white histograms indicate staining with an appropriate isotype control antibody.

The immunostimulatory properties of DC cultured *in vitro* from JMML-2 PBMC were examined in a mixed leukocyte reaction using an IFN-γ ELISpot assay. Responder PBMC were cultured with different DC stimulator cell populations at a ratio of 10:1, JMML-2-derived DC were able to stimulate allogeneic T cells as efficiently as normal MoDC, as measured by IFN-γ secreted by activated T cells. However, culturing normal MoDC and leukemic DC with autologous T cells caused moderate and minimal IFN-γ secretion, respectively (Figure 2a). These data demonstrate that leukemic DC generated from JMML-2 PBMC were potent stimulators of allogeneic T lymphocytes.

We next attempted, with JMML-1 samples, to use the *in vitro* generated leukemic DC as stimulator cells to expand allogeneic JMML-specific T lymphocytes. The source of T cells was PBMC obtained approximately 1 month following allogeneic BMT. DNA chimerism studies had at this stage shown a 100% donor engraftment. Owing to limited starting cell numbers, after three rounds of stimulation using irradiated leukemic DC in the presence of IL-2, there were only sufficient T cells to perform a basic cytotoxicity assay. Cell killing by the expanded cytotoxic T lymphocytes (CTL) was determined using a lactate dehydrogenase (LDH) release assay (Promega, Madison, WI, USA). These preliminary results show that the CTL specifically lysed the leukemic JMML cells (Figure 2b). Even at the very low effector:target ratio of 1:1, the CTL were able to lyse more than 15% of the leukemic targets. The CTL lysed the nonleukemic $CD3^+$ T cells from the JMML patient to a lesser extent, and there was minimal CTL-directed lysis of allogeneic PBMC from an MHC-mismatched normal donor. The data are consistent with a role for leukemic DC as stimulators of allogeneic T-cell responses against JMML cells, in an *ex vivo* setting following allogeneic BMT.

Longoni *et al*[8] have recently shown that JMML cells can spontaneously differentiate *in vitro* into DC, but these leukemic DC secrete the immunosuppressive cytokine IL-10 that might dampen autologous antileukemia responses. However, we have found that adherent JMML cells cultured *in vitro* with GM-CSF and IL-4 differentiate into stimulatory DC capable of inducing allogeneic antileukemia immune responses. Longoni *et al*[8] did not address whether JMML cells differentiate into DC *in vivo*. We observed that PBMC from JMML-2 contain a larger number of $Lin1^{-/low}HLA\text{-}DR^+CD11c^+$ and $Lin1^{-/low}HLA\text{-}DR^+CD123^+$ DC subtypes than normal individuals (4.1 *vs* 0.5%, and 1.4 *vs* 0.6% total PBMC population, respectively). This suggests that JMML cells do spontaneously differentiate into DC *in vivo*, but it remains to be determined whether these $CD11c^+$ and $CD123^+$ DC in JMML patients are functionally active immunostimulatory DC.

Our findings are in keeping with previous studies showing that monocytes from the majority of patients with the myeloid stem cell disorders AML[1] and CML[2] maintain their capacity to differentiate into phenotypic and functional DC. We had only three patients available for study and although results are rather heterogeneous, we have demonstrated that *ex vivo* generated leukemic DC derived

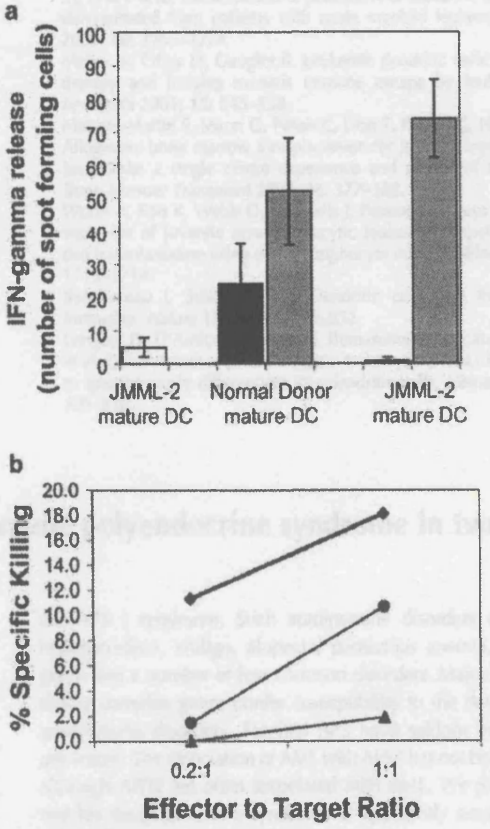

Figure 2 Functional activity of DC generated from JMML patient PBMC (a) IFN-γ secretion, as a marker of T-cell activation, following stimulation with *in vitro* generated DC. Responder cells were: (□)no responder cells; (■) autologous T lymphocytes; (■) allogeneic (third party) T lymphocytes. Results represent mean ± standard deviation of triplicate cultures. A total of 2×10^3 immunopurified mature DC were cultured with 2×10^4 responder cells for 4 days, and IFN-γ secretion was subsequently measured using an ELISpot assay. (b) Cytotoxicity of T cells (derived from JMML-1 BMT donor PBMC post engraftment) stimulated with JMML-1 leukemic DC. Targets were: (◆) JMML-1 leukemic cells; (●) JMML-1 nonleukemic T cells; (▲) control MHC-mismatched PBMC. A total of 1×10^4 target cells were plated with effector cells at 0.2:1 and 1:1 ratios, and incubated for 4 h before LDH release was calculated and used as the measure of target cell killing.

from two of these patients were immunostimulatory. The use of leukemic DC to stimulate allogeneic responses against JMML remains problematic because of the wide array of self-antigens presented, which are likely to induce potent graft-versus-host disease (GVHD) responses. However, there are several potential clinical applications arising from our data. Firstly, *in vitro* generated leukemic DC could be used for the stimulation of autologous PBMC (in an *ex vivo* setting) to generate antileukemic T cell lines for adoptive immunotherapy. In this regard, it is important to note that there is reduced reactivity against autologous PBMC with JMML-derived MoDC (Figure 2a). This may be due to reduced T-cell number or function in JMML patients. However, the limited cytotoxicity assay suggests that the autologous population has the potential for antileukemic responses if stimulated by JMML-MoDC *ex vivo*. Secondly, DC differentiated *in vitro* from JMML cells may potentially be administered as a cellular leukemia vaccine *in vivo*, in the context of resistant disease and BMT failure. Thirdly, the data support the concept of generating allogeneic JMML-specific CTL lines from BMT donor T lymphocytes (T-cell source being either donor PBMC or activated T cells post engraftment). The T cells could be transduced with suicide genes to allow reversal of GVHD if it develops. Lastly, systemic treatment with cytokine therapy could potentially be used to induce immunostimulatory JMML DC *in vivo*, and would be applicable for patients with resistant disease post BMT. Further studies in a larger number of patients are warranted to confirm the immunostimulatory properties of JMML-derived DC.

Acknowledgements

We thank the patients who provided blood samples as well as Dr P Veys, Dr D Webb and Netty Hewitt for sample collection and advice. This work was supported by the Research into Childhood Cancer (RICC), Gibraltar, The Wellcome Trust, The Medical Research Council and Cancer Research UK. Research at the Institute of Child Health and Great Ormond Street Hospital for Children National Health Service trust benefits from Research and Development funding received from the NHS executive.

The views expressed in this publication are those of the authors and are not necessarily those of the NHS executive.

S Nabarro[1]
AJ Thrasher[2]
H Kempski[1]
P Amrolia[2]
J Anderson[1]

[1]*Molecular Haematology and Cancer Biology Unit, Institute of Child Health, London, UK;*
[2]*Molecular Immunology Unit, Institute of Child Health, London, UK*

References

1 Harrison BD, Adams JA, Briggs M, Brereton ML, Yin JA. Stimulation of autologous proliferative and cytotoxic T-cell responses by 'leukemic dendritic cells' derived from blast cells in acute myeloid leukemia. *Blood* 2001; **97**: 2764–2771.
2 Choudhury A, Gajewski JL, Liang JC, Popat U, Claxton DF, Kliche KO *et al.* Use of leukemic dendritic cells for the generation of antileukemic cellular cytotoxicity against Philadelphia chromosome-positive chronic myelogenous leukemia. *Blood* 1997; **89**: 1133–1142.
3 Mohty M, Isnardon D, Blaise D, Mozziconacci MJ, Lafage-Pochitaloff M, Briere *et al.* Identification of precursors of leukemic dendritic cells differentiated from patients with acute myeloid leukemia. *Leukemia* 2002; **16**: 2267–2274.
4 Mohty M, Olive D, Gaugler B. Leukemic dendritic cells: potential for therapy and insights towards immune escape by leukemic blasts. *Leukemia* 2001; **15**: 545–558.
5 Matthes-Martin S, Mann G, Peters C, Lion T, Fritsch G, Haas OA *et al.* Allogeneic bone marrow transplantation for juvenile myelomonocytic leukaemia: a single centre experience and review of the literature. *Bone Marrow Transplant* 2000; **26**: 377–382.
6 Worth A, Rao K, Webb D, Chessells J, Passmore J, Veys P. Successful treatment of juvenile myelomonocytic leukemia relapsing after stem cell transplantation using donor lymphocyte infusion. *Blood* 2003; **101**: 1713–1714.
7 Banchereau J, Steinman RM. Dendritic cells and the control of immunity. *Nature* 1998; **392**: 245–252.
8 Longoni D, D'Amico G, Gaipa G, Bernasconi S, Vulcano M, Onnis P *et al.* Commitment of juvenile myelo-monocytic (JMML) leukemic cells to spontaneously differentiate into dendritic cells. *Hematol J* 2002; **3**: 302–310.

Association of acute leukemia and autoimmune polyendocrine syndrome in two kindreds

Leukemia (2003) **17**, 1912–1914. doi:10.1038/sj.leu.2403064

TO THE EDITOR

Acute myeloid leukemia (AML) has an incidence of 2/100 000 inhabitants. Familial AML is a rare syndrome and its occurrence in two kindreds is less than $4/10^9$ inhabitants. A few pedigrees have been reported, underlying potential but as yet unidentified genetic mechanisms predisposing to AML. On the other hand, the autoimmune polyendocrine syndrome (APS) is defined as the occurrence of several autoimmune diseases of the endocrine system in the same patient.[1] Two types of APS have been described. The autoimmune polyendocrine syndrome type II (APS II) syndrome most frequently associates with autoimmune thyroid disorders (AITD), Addison's disease and Type I diabetes. In this syndrome, AITD encompasses a spectrum of thyroid disorders, including Hashimoto's disease and Graves' disease. For most of the APS II component disorders, the incidence of multiple affected members in a given family is common. Such autoimmune events may be subclinical and detected only by serological tests. 'Nonclassic' APS II is a group of autoimmune disorders with neither Addison's disease nor APS I syndrome. Such autoimmune disorders may include hypogonadism, vitiligo, alopecia, pernicious anemia, myasthenia gravis and a number of less common disorders. Major histocompatibility complex genes confer susceptibility to the development of autoimmune disorders. Familial APS have seldom been reported previously. The association of AML with APSII has not been described, although AITD are often associated with AML. We present a man and his daughter with a syndrome of apparently autosomal adult-onset APSII and AML (Figure 1).

A 40-year-old man was first admitted to the hospital in 1978. A transient ischemic attack, hypercholesterolemia, high blood pressure and polyarthritis of unknown cause were noticed in his medical history. He had developed an AML 2 with 97.6% blasts plus promyelocytes in the bone marrow. Cytogenetics were unsuccessful. He achieved a complete remission after induction chemo-therapy (Daunorubicine, Vincristine, Cytarabine). He then received two courses of consolidation (Daunorubicine, Vincristine, Cytarabine) and 13 courses of maintenance (MethylGAG, Cyclophosphamide, Cytarabine) chemotherapy. The treatment was completed 2 years after diagnosis by two final courses of chemotherapy (Daunorubicine, Vincristine, Mercaptopurine). After chemotherapy, he developed impotence because of testicular

Y Beguin is a Research Director of the National Fund for Scientific Research (FNRS, Belgium)

The Bo
020 72